

**Synthesis, characterization and ^{59}Co NMR study of novel
Co(III) complexes with selected N-acyl-N',N'-dialkylthiourea
ligands: an assessment of spontaneous metathesis by
multinuclear NMR spectroscopy and *rp*-HPLC**

A thesis submitted to

STELLENBOSCH UNIVERSITY



In fulfilment of the requirements for the degree of

MASTER OF SCIENCE

By

Ilse Barnard

Supervisor: Prof. Klaus Koch

December 2016

DECLARATION

By submitting this thesis electronically, I declare that the entirety of the work contained herein is my own, original work, that I am the owner of the copyright therefore (unless to the extent of explicitly otherwise states) and that I have not previously in its entirety or in part submitted it for obtaining any qualification.

Ilse Barnard

Copyright © 2016 Stellenbosch University

All rights reserved

Abstract

A number of ligands of the type *N,N*-dialkyl-*N'*-acyl(aryl)thiourea as well as their corresponding complexes with cobalt(III) have been synthesized and characterized by means of various spectroscopic techniques including ^1H NMR, ^{13}C NMR, mass spectrometry and infrared spectroscopy. These ligands have been found to form relatively stable complexes of the type *fac*-[Co(L-S,O)₃]. X-ray diffraction results supported the assumption that these complexes favour the *facial* conformation and coordination of the ligands occurs by means of the bidentate mode *via* the S and O donor atoms.

Considering some of the more favourable properties of ^{59}Co NMR spectroscopy, which include its high receptivity and chemical shift sensitivity, the technique was thus utilized for studying the effect of varying the structure of the acylthiourea ligands on the octahedral- d^6 cobalt(III) complexes. By selecting one of the compounds under consideration as an external reference, the extent with which the shielding of the ^{59}Co nucleus is effected by various factors such as concentration, temperature, solvent and ligand structure could be determined. The sensitivity of the ^{59}Co nucleus would also prove to be beneficial for the identification and separation of possible isomers present in the complex. This includes not only various possible *E/Z* configurational isomers, but also the separation of more than one possible diastereomer present in solution.

The possibility of ligand exchange occurring amongst these relatively inert Co(III) complexes was also investigated. A brief study followed on the extent and relative rate of ligand exchange occurring amongst two different homoleptic [Co(Lⁿ-S,O)₃] and [Co(L^m-S,O)₃] complexes. The reaction was monitored by means of ^{59}Co NMR spectroscopy as well as *rp*-HPLC.

For the ligand exchange reaction study by means of ^{59}Co NMR spectroscopy, the reactivity of two different sets of complexes was compared in a solution of chloroform. The ligand exchange reactions were very slow and both sets of complexes reached equilibrium after only approximately 30 days, at room temperature. The spectra initially gave two peaks corresponding to the two homoleptic complexes initially added in the solution. Two new peaks began to appear, after about 24h, which over time grew in intensity whilst that of the first mentioned complexes decreased in overall intensity. These new peaks were attributed to the formation of the heteroleptic species, and the four peaks in the ^{59}Co NMR spectra was assigned as: [Co(Lⁿ-S,O)₃], [Co(Lⁿ-S,O)₂(L^m-S,O)], [Co(Lⁿ-S,O)(L^m-S,O)₂] and [Co(L^m-S,O)₃].

The reaction between two different homoleptic $[\text{Co}(\text{L}^{\text{n}}-\text{S},\text{O})_3]$ and $[\text{Co}(\text{L}^{\text{m}}-\text{S},\text{O})_3]$ complexes were also monitored by means of liquid chromatography in a solution of acetonitrile. The same trend could be seen as for the ^{59}Co NMR investigation, wherein a state of equilibrium would eventually be achieved between the homoleptic complexes initially added in the solution and the newly formed heteroleptic complexes. The relative rate of ligand exchange in acetonitrile on the other hand was reduced by almost half the time compared to the ^{59}Co NMR study in chloroform, with the only differences between subsequent experiments being the reaction medium and concentration used. Unambiguous identification of the various peaks in the chromatogram was done by means of Liquid Chromatography-Mass Spectrometry.

In conclusion, it was found by means of ^{59}Co NMR and *rp*-HPLC that complexes of the type *fac*- $[\text{Co}(\text{L}-\text{S},\text{O})_3]$ could be well characterized with these techniques. The ^{59}Co NMR chemical shift proved a good and sensitive tool for the study of complexes under investigation, whereby the most significant finding showed the possibility of ligand exchange occurring upon mixing two different homoleptic *fac*- $[\text{Co}(\text{L}-\text{S},\text{O})_3]$ complexes together in solution. The result was the formation of a mixture of heteroleptic complexes and occurred in a solution of chloroform and acetonitrile respectively. To our knowledge, no such ligand exchange regarding *fac*- $[\text{Co}(\text{L}-\text{S},\text{O})_3]$ complexes have previously been demonstrated.

Opsomming

Verskeie ligande van die soort *N,N*-dialkyl-*N'*-acyl(aryl)thioureas sowel as hul ooreenstemmende komplekse met kobalt(III) was gesintetiseer en gekarakteriseer deur middel van verskeie spektroskopiese tegnieke insluitend ^1H KMR, ^{13}C KMR, massa spektrometrie en infrarooi spektroskopie. Hierdie ligande was gevind om relatiewe stabiele komplekse te vorm van die soort *fac*-[Co(L-S,O)₃]. Die resultate van X-straaldiffraksie-analise het die idee ondersteun dat hierdie komplekse die '*facial*' konformasie begunstig en dat koördinasie van hierdie ligande vind plaas deur middel van die 'bidentate' wyse deur die S- en O-donoratome.

Aangesien van die meer gunstige eienskappe van ^{59}Co KMR spektroskopie, wat insluit sy h e ontvanklikheid en chemiese verskuiwing sensitiviteit, was die tegniek dus aangewend om die effek van die struktuur te wissel van die 'acylthiourea' ligande op die oktahedriese- d^6 kobalt(III) komplekse te bestudeer. Deur een van die komplekse onder oorweging te gebruik as 'n eksterne verwysing, kon daar vasgetel word tot watter mate die 'shielding' van die ^{59}Co kern geaffekteer word deur verskeie faktore te bestudeer insluitend konsentrasie, temperatuur, oplosmiddel en ligand struktuur. Die sensitiviteit van die ^{59}Co kern was ook voordelig in die identifisering en skeiding van moontlike isomere teenwoordig in die kompleks. Dit sluit nie net verskeie moontlike *E/Z* konfigurasie isomere in nie, maar ook die skeiding van meer as een moontlike diastereomeer teenwoordig in die oplossing.

Die moontlikheid van ligand uitreiling wat voorkom onder hierdie kobalt(III) komplekse was ook ondersoek. 'n Vlugtige studie volg, gebaseer op die mate en relatiewe tempo van ligand uitreiling wat plaasvind tussen twee verskillende 'homoleptic' [Co(Lⁿ-S,O)₃] en [Co(L^m-S,O)₃] komplekse. Die reaksie was gemonitor deur middel van ^{59}Co KMR spektroskopie sowel as *rp*-HPLC.

Vir die ligand uitreiling studie deur middel van ^{59}Co KMR spektroskopie, was die reaktiwiteit van twee verskillende stelle komplekse vergelyk in 'n oplossing van chloroform. Die ligand uitreiling reaksies was baie stadig en albei stelle komplekse het slegs na ongeveer 30 dae ewewig bereik, in kamer temperatuur. Die spektra het aanvanklik twee pieke gewys wat ooreengestem het met die twee 'homoleptic' komplekse wat aan die begin bymekaar gevoeg is in dieselfde oplossing. Later het twee nuwe pieke verskyn, na ongeveer 24h, wat met tyd in intensiteit gegroei het terwyl die eersgenoemde komplekse in intensiteit afgeneem het. Hierdie nuwe pieke was toegeskryf aan die vorming van die 'heteroleptic' spesies, en die vier pieke in die ^{59}Co KMR

spektra was toegewys as: $[\text{Co}(\text{L}^{\text{n}}-\text{S},\text{O})_3]$, $[\text{Co}(\text{L}^{\text{n}}-\text{S},\text{O})_2(\text{L}^{\text{m}}-\text{S},\text{O})]$, $[\text{Co}(\text{L}^{\text{n}}-\text{S},\text{O})(\text{L}^{\text{m}}-\text{S},\text{O})_2]$ en $[\text{Co}(\text{L}^{\text{m}}-\text{S},\text{O})_3]$.

Die reaksie tussen twee verskillende ‘homoleptic’ $[\text{Co}(\text{L}^{\text{n}}-\text{S},\text{O})_3]$ en $[\text{Co}(\text{L}^{\text{m}}-\text{S},\text{O})_3]$ komplekse was ook deur middel van vloeistof kromatografie ondersoek in ‘n oplossing van asetoniitril. Dieselfde tendens was gesien as vir die ^{59}Co KMR studie, waar die ewewigs toestand uiteindelik bereik word tussen die oorspronklike ‘homoleptic’ komplekse bygevoeg in dieselfde oplossing en die nuut gevormde ‘heteroleptic’ komplekse. Die relatiewe tempo van die ligand uitreiling in asetoniitril aan die ander kant was verminder met amper helfte die tyd as vir die ^{59}Co KMR studie in chloroform, met die enigste verskil tussen daaropvolgende eksperimente die reaksie medium en konsentrasie wat gebruik is. Ondubbelsinnige identifikasie van die verskeie pieke in die chromatogramme was gedoen deur middel van vloeistof kromatografie-massa spektrometrie (LC-MS).

Om af te sluit, dit was ontdek deur middel van ^{59}Co KMR en *rp*-HPLC dat komplekse van die tipe *fac*- $[\text{Co}(\text{L}-\text{S},\text{O})_3]$ goed gekarakteriseer kan word met hierdie tegnieke. Die ^{59}Co KMR chemiese verskuiwing was bewys as ‘n goeie en sensitiewe gereedskap vir die studie van komplekse wat hier ondersoek is, waarby die mees betekenisvolle bevinding die moontlikheid van ligand uitreiling getoon het wanneer twee verskillende ‘homoleptic’ *fac*- $[\text{Co}(\text{L}-\text{S},\text{O})_3]$ komplekse bygevoeg word in dieselfde oplossing. Die gevolg van hierdie reaksie was die vormasie van ‘n mengsel van ‘heteroleptic’ komplekse en vind plaas in ‘n oplossing van chloroform en asetoniitril onderskeidelik. Tot ons wete, is geen ligand uitreiling reaksie met betrekking tot *fac*- $[\text{Co}(\text{L}-\text{S},\text{O})_3]$ komplekse voorheen gedemonstreer nie.

Acknowledgements

I would hereby like to sincerely thank the following for both their support and financial aid through the course of my study

- I give my deepest and most sincere appreciation to my supervisor, Professor Klaus Koch, for his continuous guidance, mentoring and encouragement and for providing financial aid throughout my studies.
- To some members of the PGM research group for all their contributions, especially Henry Nkabyo for his advice and ongoing encouragement.
- Stellenbosch University for support and use of facilities.
- To my Lord God from whom I obtained my strength to keep carrying on and who continues to bless me.
- My wonderful parents, Esta and Deon, for providing continuous love and moral support.
- To Ms Elsa Malherbe and Dr Jaco Brand for any and all advice as well as assistance provided in acquiring as well as interpreting NMR data.
- To family and friends, especially my dearest friend, whom I consider a sister, Stefani du Toit, for standing behind me even through the hardest times.

List of Abbreviations

DRC	Democratic Republic of the Congo
LA-ICP-MS	Laser-ablation inductively coupled plasma mass spectroscopy
ESR	Electron Spin Resonance
UV-Vis	Ultraviolet visible
HPLC	High Performance Liquid Chromatography
GC	Gas Chromatography
NMR	Nuclear Magnetic Resonance
^{59}Co	Cobalt-59
hfs	Hartree-Fock Slater
HL	<i>N,N</i> -dialkyl- <i>N'</i> -aroyl(acyl)thiourea
H ₂ L	<i>N</i> -alkyl- <i>N'</i> -acyl(aroyl)thiourea
IR	Infrared spectroscopy
NaCOOCH ₃	Sodium Acetate
MeOH	Methanol
DCM	Dichloromethane
CDCl ₃	Chloroform
TMS	Tetramethylsilane
COSY	H-H Correlation Spectroscopy
GHSQC	Gradient Heteronuclear Single Quantum Coherence
XRD	X-ray diffraction
Å	Angstrom; 10 ⁻¹⁰ meters
ppm	parts per million
δ	NMR chemical shift in ppm
TMAP	Tetramethylammonium phosphate
LC-MS	Liquid chromatography-Mass spectrometry
ESI	Electrospray ionization

TABLE OF CONTENTS

Declaration	i
Abstract	ii
Opsomming	iv
Acknowledgements	vi
List of Abbreviations	vii
Table of contents	viii
List of Figures	xi
List of Tables and Schemes	xv
 CHAPTER ONE	 1
LITERATURE REVIEW	1
1.1. COBALT	2
1.2. <i>N,N</i> -DIALKYL- <i>N'</i> -AROYL(ACYL)THIOUREAS	5
1.2.1. General information and application	5
1.2.2. Coordination chemistry of acylthioureas with some transition metals	7
1.2.3. Coordination chemistry of acylthioureas to Co(II) and Co(III)	9
1.3. ⁵⁹ Co NMR SPECTROSCOPY	15
1.4. THE METATHESIS (I.E. LIGAND EXCHANGE) REACTION	18
1.4.1. Metathesis in organic chemistry	18
1.4.2. Metathesis in inorganic reactions	19
1.5. LIGAND EXCHANGE IN METAL COMPLEXES	20
1.5.1. Earliest studies and methods of detection	20
1.5.2. High Performance Liquid Chromatography studies of ligand exchange	21
1.5.3. Ligand exchange in six-coordinate metal complexes	23
1.5.4. Ligand exchange of Co(III) complexes	24
1.6. AIMS AND OBJECTIVES	26

CHAPTER TWO	27
SYNTHESIS AND CHARACTERIZATION	27
2.1. SYNTHESIS OF ACYLTHIOUREA LIGANDS AND THE CORRESPONDING Co(III) COMPLEXES	28
2.1.1. Synthesis of <i>N,N</i> -dialkyl- <i>N'</i> -aroyl(acyl)thioureas	28
2.1.2. Spectroscopic characterization of synthesized acylthiourea ligands	33
2.1.3. Synthesis of tris(<i>N,N</i> -dialkyl- <i>N'</i> -aroyl(acyl)thioureato)Co(III) complexes: [Co(L-S, O) ₃]	35
2.1.4. Spectroscopic characterization of synthesized Co(III) complexes.....	37
CHAPTER THREE	46
NMR AND OTHER SPECTROSCOPIC CHARACTERIZATION OF ACYLTHIOUREA LIGANDS AND Co(III) COMPLEXES.....	46
3.1. SPECTROSCOPIC RESULTS	47
3.1.1. Spectroscopic discussion of the Co(III) complexes coordinated to symmetrical acylthiourea ligands.....	47
3.1.2. Spectroscopic discussion of the Co(III) complex coordinated to an unsymmetrical acylthiourea ligand	57
3.1.3. Spectroscopic discussion of the Co(III) complex coordinated to a chiral acylthiourea ligand	61
3.2. MOLECULAR STRUCTURE DISCUSSION OF SELECTED ACYLTHIOUREA COBALT(III) COMPLEXES BY MEANS OF X-RAY DIFFRACTION ANALYSIS.....	68
3.2.1. Molecular structure of <i>fac</i> -tris(<i>N,N</i> -diethyl- <i>N'</i> -4-methoxybenzoylthioureato)cobalt(III): <i>fac</i> -[Co(L ² -S, O) ₃]	69
3.2.2. Molecular structure of <i>fac</i> -tris(<i>N</i> -methyl- <i>N</i> -ethyl- <i>N'</i> -benzoylthioureato)cobalt(III): <i>fac</i> -[Co(L ¹¹ -S, O) ₃].....	70
3.2.3. Molecular structure of <i>fac</i> -tris(<i>N,N</i> -diethyl- <i>N'</i> -camphanoylthioureato)cobalt(III): <i>fac</i> -[Co(L ¹² -S, O) ₃].....	72
3.3. ⁵⁹ Co NMR SPECTROSCOPY	74
3.3.1. Introduction	74
3.3.2. Referencing in ⁵⁹ Co NMR.....	74
3.4. FACTORS WHICH EFFECT THE SHIELDING OF THE ⁵⁹ Co NUCLEUS	76

3.4.1. Effect of concentration on ^{59}Co NMR shielding.....	77
3.4.2. Effect of temperature on ^{59}Co NMR shielding.....	78
3.4.3. Effect of solvent on ^{59}Co NMR shielding.....	83
3.4.4. Effect of ligand structure on ^{59}Co NMR shielding.....	86
3.5. CONCLUSION	91
CHAPTER FOUR	93
A STUDY OF THE LIGAND EXCHANGE REACTION BY ^{59}Co NMR SPECTROSCOPY AND RP-HPLC.....	93
4.1. INVESTIGATE THE LIGAND EXCHANGE REACTION BY ^{59}Co NMR SPECTROSCOPY AND RP-HPLC	94
4.1.1. Introduction	94
4.1.2. Investigate ligand exchange by ^{59}Co NMR spectroscopy.....	95
4.1.3. Investigate the ligand exchange reaction by <i>rp</i> -HPLC and UV/Vis.....	99
4.1.4. Identification of mixed-ligand species <i>via</i> Liquid-Chromatography Mass-Spectrometry.....	104
4.2. CONCLUDING REMARKS CONCERNING THE SPONTANEOUS LIGAND EXCHANGE REACTION IN <i>fac</i> -[Co(L-S,O) ₃] COMPLEXES IN SOLUTION.....	109
CHAPTER FIVE.....	112
CONCLUSIONS AND FUTURE WORK	112
5.1. CONCLUSION	113
5.1.1. Spectroscopic findings	113
5.1.2 ^{59}Co NMR spectroscopy studies.....	114
5.1.3. The ligand exchange study between homoleptic complexes of type <i>fac</i> -[Co(L-S,O) ₃]	116
5.2. REMARKS AND FUTURE WORK.....	117
REFERENCES	119
ADDENDUM A	123
ADDENDUM B	135

List of Figures

Figure 1.1. Various forms of consumption of cobalt for the year 2012 (adapted from reference 3).

Figure 1.2. A generic Copper/Cobalt/Nickel Recovery Flowsheet (taken from reference 6).

Figure 1.3. General representation of *N,N*-dialkyl-*N'*-aroyl(acyl)thiourea as well as the formation of the acylthioureate anion in the presence of a suitable base.

Figure 1.4. The two possible isomers *cis* and *trans* observed for square planar bis(chelate) complexes coordinated to two acylthiourea ligands (adapted from reference 25).

Figure 1.5. The only crystal structure available in the literature of the neutral monodentate coordination mode showing Pd(II) coordinated to two acylthiourea ligands by means of the S atom (taken from reference 56).

Figure 1.6. The two geometric isomers *cis*- and *trans* of tetraamminedichlorocobalt(III).

Figure 1.7. The two possible geometric isomers *fac*- and *mer* of triamminetrichlorocobalt(III).

Figure 1.8. The two pairs of enantiomers possible for each geometric isomer (a) *fac* and (b) *mer* of the Co(III) complexes coordinated to three acylthiourea ligands.

Figure 1.9. One of six crystal structures available in the literature of a Co(III) complex coordinated to three acylthiourea ligands, showing the tendency for coordinating as the *fac* isomer (taken from reference 45).

Figure 1.10. The two different isomers namely *fac* and *mer* of $M(\text{trifluoroacetylacetonates})_3$ (where $M = \text{Cr(III)}, \text{Co(III)}, \text{Rh(III)}, \text{Al(III)}, \text{Ga(III)}, \text{In(III)}, \text{Mn(III)}$ or Fe(III)) (adapted from reference 70).

Figure 1.11. The two different possible forms of charge distribution found around a nucleus.

Figure 1.12. General metathesis reaction scheme between two a) olefins and b) alkynes.

Figure 1.13. A schematic representation of the ligand exchange reaction between two different homoleptic square planar metal complexes of type *cis*- $[M(L-S, O)_2]$, where $M = \text{Pd(II)}$ (adapted from reference 92).

Figure 2.1. General structure of tris(*N,N*-dialkyl-*N'*-aroyl(acyl)thioureate)Co(III) complexes.

Figure 2.2. Reaction scheme for the coordination reaction of the acylthiourea derivative to Co(III).

Figure 3.1. The 400 MHz ^1H spectra in CDCl_3 at 25°C showing differences and similarities between free ligand *N,N*-diethyl-*N*-benzoylthiourea and its corresponding complex tris(*N,N*-diethyl-*N*-benzoylthioureate)cobalt(III).

Figure 3.2. All possible resonance structure resulting from the partial double bond character of the [C(X)-N] bond^{107,108}

Figure 3.3. Example of non-equivalent fluorine atoms in certain *gem*-difluoro compounds (adapted from reference 112).

Figure 3.4. A demonstration of diastereotopic protons present in a compound with no asymmetric centers.

Figure 3.5. A schematic representation of how the dihedral angle (α) between the two methylene protons is decreased as a result of the repulsive forces from the electron density present upon coordination of the ligand to the metal.

Figure 3.6. 400 MHz ^{13}C NMR spectra of *N,N*-diethyl-*N'*-4-tertbutylbenzoylthiourea and tris(*N,N*-diethyl-*N'*-4-tertbutylbenzoylthioureato)Co(III) in CDCl_3 at 25 °C.

Figure 3.7. The IR spectra of the acylthiourea ligand (HL^1) and its corresponding Co(III) complex.

Figure 3.8. Assignment of the two possible configurational isomers of *N*-methyl-*N*-ethyl-*N'*-benzoylthiourea as a result of the restricted rotation about the C-N bond. The sulphur atom and the ethyl groups are assigned as the two highest priority groups on each side of the C-N bond.

Figure 3.9. The four possible configurational isomers namely *EEE*, *EZE*, *ZZZ*, and *ZEZ* of the complex *fac*-tris(*N*-methyl-*N*-ethyl-*N'*-benzoylthioureato)cobalt(III).

Figure 3.10. A comparison of the 400 MHz ^1H spectra of the *N*-alkyl section of the symmetrical a) *N,N*-diethyl-*N'*-benzoylthiourea ligand and b) *N*-methyl-*N*-ethyl-*N'*-benzoylthiourea ligand showing *E*, *Z* configurational isomers. All spectra were obtained in CDCl_3 at 25 °C.

Figure 3.11. a) The two possible enantiomers of 2-butanol and an b) illustration by means of a Newman Projection how the two methylene protons are chemically different.

Figure 3.12. The 400 MHz ^1H spectrum in CDCl_3 at 25 °C of tris(*N,N*-diethyl-*N'*-camphanoylthioureato)cobalt(III).

Figure 3.13. The 400 MHz ^{13}C spectrum in CDCl_3 at 25 °C of tris(*N,N*-diethyl-*N'*-camphanoylthioureato)cobalt(III).

Figure 3.14. The 600 MHz COSY spectrum in CDCl_3 at 25 °C of tris(*N,N*-diethyl-*N'*-camphanoylthioureato)cobalt(III).

Figure 3.15. The 600 MHz GHSQC spectrum in CDCl_3 at 25 °C of tris(*N,N*-diethyl-*N'*-camphanoylthioureato)cobalt(III).

Figure 3.16. The molecular structure of *fac*-[Co(L^2 -S,O) $_3$] with selected bond lengths (Å) and angles (°) as follows; Co-O 1.923(1), Co-S 2.216(1), O(1)-C(4) 1.264(3), C(4)-N(3) 1.329(3), N(3)-C(15) 1.342(3), C(15)-S 1.742(2), O-Co-S 95.24, O-Co-S 176.56, S-Co-S 88.13, O-Co-O 84.48.

Figure 3.17. Molecular structure of *fac*-[Co(L¹¹-S,O)₃] with selected bond lengths (Å) and angles (°) as follows: Co-O 1.9238(1), Co-S 2.1949(1), O(1)-C(1) 1.2296(1), C(1)-N(1) 1.3473, C(2)-N(1) 1.3473(1), C(2)-S(2) 1.6867(1), S(2)-Co(1)-S(2) 87.79, O(1)-Co(1)-O(1) 85.38, S(2)-Co(1)-O(1) 178.19, O(1)-Co(2)-S(1) 178.19, O(1)-Co(1)-S(2) 93.19.

Figure 3.18. Molecular structure of *fac*-[Co(L¹²-S,O)₃] with selected bond lengths (Å) and angles (°) as follows: Co(2)-O(7) 1.9197(1), Co(2)-S(1) 2.2255(1), O(7)-C(31) 1.2632(1), C(31)-N(10) 1.3158, C(26)-N(10) 1.3511(1), C(26)-S(1) 1.7372(1), S(1)-Co(2)-S(5) 89.05, O(7)-Co(2)-O(5) 84.35, S(1)-Co(2)-O(5) 176.54, O(7)-Co(2)-S(5) 175.26, O(7)-Co(2)-S(1) 95.19.

Figure 3.19. The ⁵⁹Co NMR spectrum of *fac*-tris(*N,N*-diethyl-*N*-benzoylthioureato)Co(III) in CDCl₃ at 25°C.

Figure 3.20. A schematic representation of how the external reference, containing the *fac*-tris(*N,N*-diethyl-*N*-benzoylthioureato)Co(III) complex, is axially inserted inside the NMR tube.

Figure 3.21. A 600 MHz ⁵⁹Co NMR experiment in which the spectra of *fac*-tris(*N,N*-diethyl-*N*'-4-tertbutylbenzoylthioureato)Co(III) at five different concentrations in CDCl₃ at 25 °C are overlaid and their δ(⁵⁹Co) compared.

Figure 3.22. The two complexes used for the temperature dependence study namely a) *fac*-tris(*N,N*-diethyl-*N*'-4-chlorobenzoylthioureato)Co(III) and b) *fac*-tris(*N,N*-diethyl-*N*'-4-tertbutylbenzoylthioureato)Co(III).

Figure 3.23. The 600 MHz ⁵⁹Co NMR temperature dependent experiment of *fac*-tris(*N,N*-diethyl-*N*'-4-tertbutylbenzoylthioureato)Co(III) in CDCl₃.

Figure 3.24. The 600 MHz ⁵⁹Co NMR temperature dependent experiment of *fac*-tris(*N,N*-diethyl-*N*'-4-chlorobenzoylthioureato)Co(III) in CDCl₃.

Figure 3.25. ⁵⁹Co NMR spectra of *fac*-tris(*N,N*-diethyl-*N*'-4-methoxybenzoylthioureato)Co(III) at different volume ratios of chloroform:acetonitrile (v/v) at 25 °C.

Figure 3.26. Graphic illustration of change in δ(⁵⁹Co) and half-height line widths (Δ_{1/2}) of *fac*-tris(*N,N*-diethyl-*N*'-4-methoxybenzoylthioureato)Co(III) with a change in % v/v (CDCl₃/CH₃CN).

Figure 3.27. The 600 MHz ⁵⁹Co NMR spectra of complexes [Co(L¹-S,O)₃] - [Co(L¹⁰-S,O)₃] at 25 °C in CDCl₃ showing their respective ligands next to every peak, illustrating how ligand structure effects δ(⁵⁹Co) upon coordination to Co(III).

Figure 3.28. 600 MHz ⁵⁹Co NMR spectrum of *fac*-tris(*N*-methyl-*N*-ethyl-*N*'-benzoylthioureato)cobalt(III) in CDCl₃ at 25 °C, illustrating four peaks representative of four different configurational isomers.

Figure 3.29. 600 MHz ⁵⁹Co NMR spectra of *fac*-tris(*N,N*-diethyl-*N*'-camphanoylthioureato)cobalt(III) in CDCl₃ at 25 °C.

Figure 4.1. The ligand exchange reaction between tris(*N,N*-diethyl-*N*'-4-chlorobenzoylthioureato)Co(III) (**A**) and tris(*N,N*-diethyl-*N*'-4-tertbutylbenzoylthioureato)Co(III) (**B**) resulting in two new heteroleptic complexes **C** and **D**.

Figure 4.2. 600 MHz ^{59}Co NMR spectra in CDCl_3 at 25 °C of the ligand exchange reaction between tris(*N,N*-diethyl-*N'*-4-chlorobenzoylthioureato)Co(III) (**A**) and tris(*N,N*-diethyl-*N'*-4-tertbutylbenzoylthioureato)Co(III) (**B**) resulting in two new heteroleptic complexes **C** and **D**.

Figure 4.3. The ligand exchange reaction between tris(*N,N*-diethyl-*N'*-4-chlorobenzoylthioureato)Co(III) (**A**) and tris(*N,N*-diethyl-*N'*-4-methoxybenzoylthioureato)Co(III) (**B**) resulting in two new heteroleptic complexes **C** and **D**.

Figure 4.4. 600 MHz ^{59}Co NMR spectra in CDCl_3 at 25 °C of the ligand exchange reaction between tris(*N,N*-diethyl-*N'*-4-chlorobenzoylthioureato)Co(III) (**A**) and tris(*N,N*-diethyl-*N'*-4-methoxybenzoylthioureato)Co(III) (**B**) resulting in two new heteroleptic complexes **C** and **D**.

Figure 4.5. Schematic representations of chromatograms during two different states in the ligand exchange reaction.

Figure 4.6. A schematic representation of how peak separation could be influenced when a) the rate of ligand exchange is faster than separation or b) when rate of separation is faster than the ligand exchange reaction.

Figure 4.7. UV/Vis absorbance spectra of tris(*N,N*-diethyl-*N'*-4-methoxybenzoylthioureato)Co(III) (**A**) and tris(*N,N*-diethyl-*N'*-3,4,5-trimethoxybenzoylthioureato)Co(III) (**B**)

Figure 4.8. The ligand exchange reaction between two homoleptic complexes tris(*N,N*-diethyl-*N'*-4-methoxybenzoylthioureato)Co(III) (**A**) and tris(*N,N*-diethyl-*N'*-3,4,5-trimethoxybenzoylthioureato)Co(III) (**B**) resulting in two new heteroleptic complexes **C** and **D**.

Figure 4.9. A GEMINI C_{18} ODS (5 μm , 150 x 4.6 mm) chromatogram at 20 °C, flow rate of 1 ml min^{-1} , and 90:10 (% v/v) acetonitrile:water of the ligand exchange reaction between a mixture of two homoleptic cobalt complexes tris(*N,N*-diethyl-*N'*-4-methoxybenzoylthioureato)Co(III) (**A**) and tris(*N,N*-diethyl-*N'*-3,4,5-trimethoxybenzoylthioureato)Co(III) (**B**) which results in the formation of the heteroleptic complexes **C** and **D**.

Figure 4.10. Suggested mechanism for the formation of the various molecular ions as seen in the mass spectrum of the $[\text{Co}(\text{L}^1\text{-S}, \text{O})_3]$ complex.

Figure 4.11. LC chromatogram with specifications: Waters BEH C18, 2.1 x 100 mm, 1.7 μm at 35 °C, flow rate 0.3 ml/min, isocratic, 10% aq; illustrating the four species present in the sample as a result of ligand exchange after 13 days between tris(*N,N*-diethyl-*N'*-benzoylthioureato)Co(III) ($[\text{Co}(\text{L}^1\text{-S}, \text{O})_3]$) and tris(*N,N*-diethyl-*N'*-3,4,5-trimethoxybenzoylthioureato)Co(III) ($[\text{Co}(\text{L}^3\text{-S}, \text{O})_3]$) forming two new heteroleptic complexes $[\text{Co}(\text{L}^3\text{-S}, \text{O})(\text{L}^1\text{-S}, \text{O})_2]$ and $[\text{Co}(\text{L}^1\text{-S}, \text{O})(\text{L}^3\text{-S}, \text{O})_2]$.

Figure 4.12. Liquid-chromatography mass spectra of homoleptic complexes a) $[\text{Co}(\text{L}^3\text{-S}, \text{O})_3]$ and d) $[\text{Co}(\text{L}^1\text{-S}, \text{O})_3]$ as well as heteroleptic species b) $[\text{Co}(\text{L}^3\text{-S}, \text{O})_2(\text{L}^1\text{-S}, \text{O})]$ and c) $[\text{Co}(\text{L}^1\text{-S}, \text{O})_2(\text{L}^3\text{-S}, \text{O})]$.

List of Tables and Schemes

Table 1.1. A breakdown of the production of refined cobalt 2012 (taken from reference 3).

Table 2.1. Summary of all acylthiourea ligands used for coordination to Co(III).

Table 3.1. 400 MHz ^1H NMR chemical shifts of *N,N*-diethyl-*N'*-benzoylthiourea (HL^1) and its corresponding complex tris(*N,N*-diethyl-*N'*-benzoylthioureato)cobalt(III) ($[\text{Co}(\text{L}^1\text{-S}, \text{O})_3]$) in CDCl_3 at 25 °C.

Table 3.2. 400 MHz ^{13}C chemical shift values from the spectra of the free ligand *N,N*-diethyl-*N'*-benzoylthiourea and its corresponding complex tris(*N,N*-diethyl-*N'*-benzoylthioureato)cobalt(III) obtained in CDCl_3 at 25 °C.

Table 3.3. The crystal data collection and structure refinement parameters for complexes *fac*- $[\text{Co}(\text{L}^2\text{-S}, \text{O})_3]$, *fac*- $[\text{Co}(\text{L}^{11}\text{-S}, \text{O})_3]$ and *fac*- $[\text{Co}(\text{L}^{12}\text{-S}, \text{O})_3]$.

Table 3.4. Temperature dependence of $\delta(^{59}\text{Co})$ and half-height line widths ($\Delta_{1/2}$) from the 600 MHz ^{59}Co NMR spectrum of *fac*-tris(*N,N*-diethyl-*N'*-4-tertbutylbenzoylthioureato)cobalt(III) and *fac*-tris(*N,N*-diethyl-*N'*-4-chlorobenzoylthioureato)cobalt(III) respectively.

Table 3.5. ^{59}Co chemical shift and half-height line widths ($\Delta_{1/2}$) values of *fac*-tris(*N,N*-diethyl-*N'*-4-methoxybenzoylthioureato)cobalt(III) at different volume ratios of chloroform:acetonitrile (v/v) at 25 °C.

Table 3.6. ^{59}Co chemical shifts and half-height line widths ($\Delta_{1/2}$) values of complexes $[\text{Co}(\text{L}^1\text{-S}, \text{O})_3]$ - $[\text{Co}(\text{L}^{10}\text{-S}, \text{O})_3]$ at 25 °C all measured in CDCl_3 .

Table 4.1. Assignment of the four different peaks, at chemical equilibrium, as a result of the ligand exchange reactions studied by ^{59}Co NMR in CDCl_3 at 25 °C.

Table 4.2. Summary of techniques, conditions and time to reach equilibrium for all ligand exchange reactions investigated.

Scheme 1.1. The exchange of ions as one of the simplest examples of metathesis.

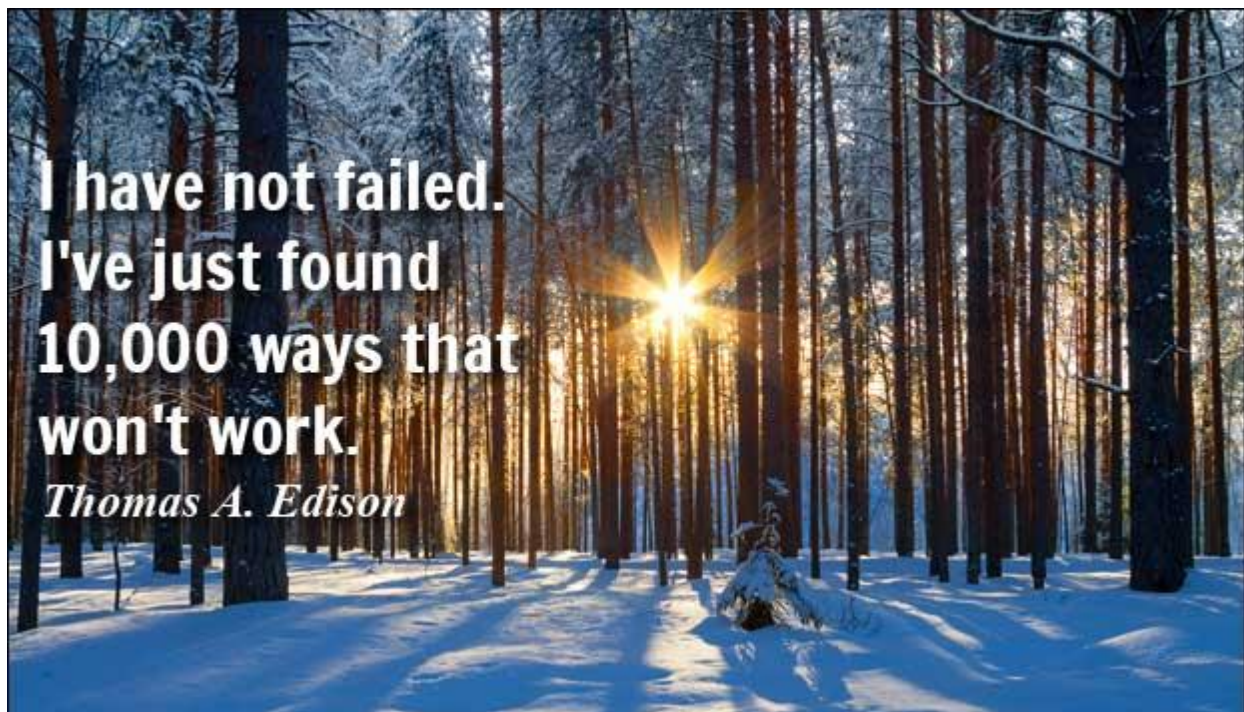
Scheme 2.1. General reaction scheme for the synthesis of *N,N*-dialkyl-*N'*-aroyl(acyl)thiourea ligands.

Scheme 2.2. The two possible means of nucleophilic attack of the thiocyanate ion resulting in either a) S-acylation or b) *N*-acylation although last mentioned is generally favored.

Scheme 2.3. Nucleophilic attack of the amine group at the a) thiocarbonyl carbon or b) carbonyl carbon.

Scheme 2.4. The by-product H_2L is formed upon addition of a primary amine to the second step of the reaction in scheme 2.1.

Scheme 4.1. Suggested mechanism for the ligand exchange reaction between two different homoleptic cobalt(III) complexes, showing a solvent stabilised intermediate.



**I have not failed.
I've just found
10,000 ways that
won't work.**

Thomas A. Edison

CHAPTER ONE

LITERATURE REVIEW

Chapter 1 | Literature Review

1.1. Cobalt

For the largest part of its history, the ores of cobalt were used for imparting a blue colour to glass and pottery. It was only until the twentieth century when metallic cobalt was first used. The term 'kobold' was given to certain ores that appeared in the Hartz Mountains during the sixteenth century. On roasting the cobalt, a blue glass called *smalt* was formed when fused with sand, which was initially attributed to arsenic or bismuth. It was only until 1735 that a Swedish chemist, G. Brandt, discovered the colour was due to a 'demi-metal' he called *cobalt-rer*.¹ In 1780, T.O Bergman, established cobalt as a new element implementing further studies on its properties and elemental characteristics. There are over 150 ores currently known to contain cobalt although only a few contain high enough concentrations to be commercially beneficial.² Cobalt is obtained in South Africa during the recovery process of metals such as nickel, copper and lead as either a by- or co-product. Although the Democratic Republic of the Congo is currently the largest ore reserve and supplier of cobalt in the world, only a small amount is refined in the country itself. The DRC exports unrefined cobalt ores largely to countries such as China, Finland and Zambia where the ores are ultimately refined into cobalt metal, downstream chemical products or speciality materials.³ For the year 2012, the output for refined cobalt was roughly 77 000 MT globally, with China contributing to 40% of the global cobalt market, becoming the largest producing country of refined cobalt in the world (**Table 1.1**).³

Table 1.1. A breakdown of the production of refined cobalt 2012 (taken from reference 3).

2012 Refined cobalt sources (metal, cobalt chemicals and powders)			
Producer / refiner:	Country	Products	2012
Various	China	Chemical, Metal, Powders	30,200
OMG	Finland	Chemical, Powders	10,547
Chambishi	Zambia	Metal	5,435
Umicore ⁽¹⁾	Belgium	Chemical, Powders	4,200
ICCI / Sherritt	Canada	Metal	3,792
Xstrata	Norway	Metal	2,969
Sumitomo	Japan	Metal	2,542
Minara	Australia	Metal	2,400
QNPL	Australia	Chemical	2,369
Norilsk	Russia	Metal	2,186
Katanga Mining	DRC	Metal	2,129
Vale	Canada	Metal	1,890
Votorantim	Brazil	Metal	1,750
CTT	Morocco	Metal	1,314
Various	South Africa	Powders	1,100
Kasere	Uganda	Metal	556
Various	India	Chemical	600
Eramet	France	Chemical	326
Mopani Copper	Zambia	Metal	230
Ambatovy	Madagascar	Metal	450
Total Refined Cobalt:			76,985

Chapter 1 | Literature Review

Cobalt has important properties in metallurgy and thus several chemical uses; in fact there are very few base metals that display the same diversity as cobalt specifically in regards to metallurgical operations. Cobalt is practically utilized in various ways including in aircraft engines, rechargeable batteries as well as in industrial chemical processes, where its distinctive catalytic properties are of particular value. Characteristics such as high temperature resistance, hardness and wear, specifically when alloyed with other metals, also make cobalt ideal for various applications in the hard metal industry.³ Other applications of cobalt include its use in the colouring of pigments or as colouring agents, electroplating, vehicle tyre manufacturing, paint driers, permanent magnets, synthetic diamonds and animal feed.^{3,4} One of the more recent and significant applications of cobalt is demonstrated by the work of Nocera⁵ in his design of the so called 'artificial leaf' wherein he utilizes cobalt in order to create an artificial oxygen evolving complex (OEC) catalyst, which is the driving force for the water-splitting reaction that takes place in photosynthesis. The consequence of such a synthetic material being a cost-effective means of generating hydrogen, a fuel with highly useful and remarkable properties, through solar energy. The diverse applicability of cobalt in various industries suggests this metal will continue to remain in strong demand for the foreseeable future with prices corresponding to specific supply and demand events.

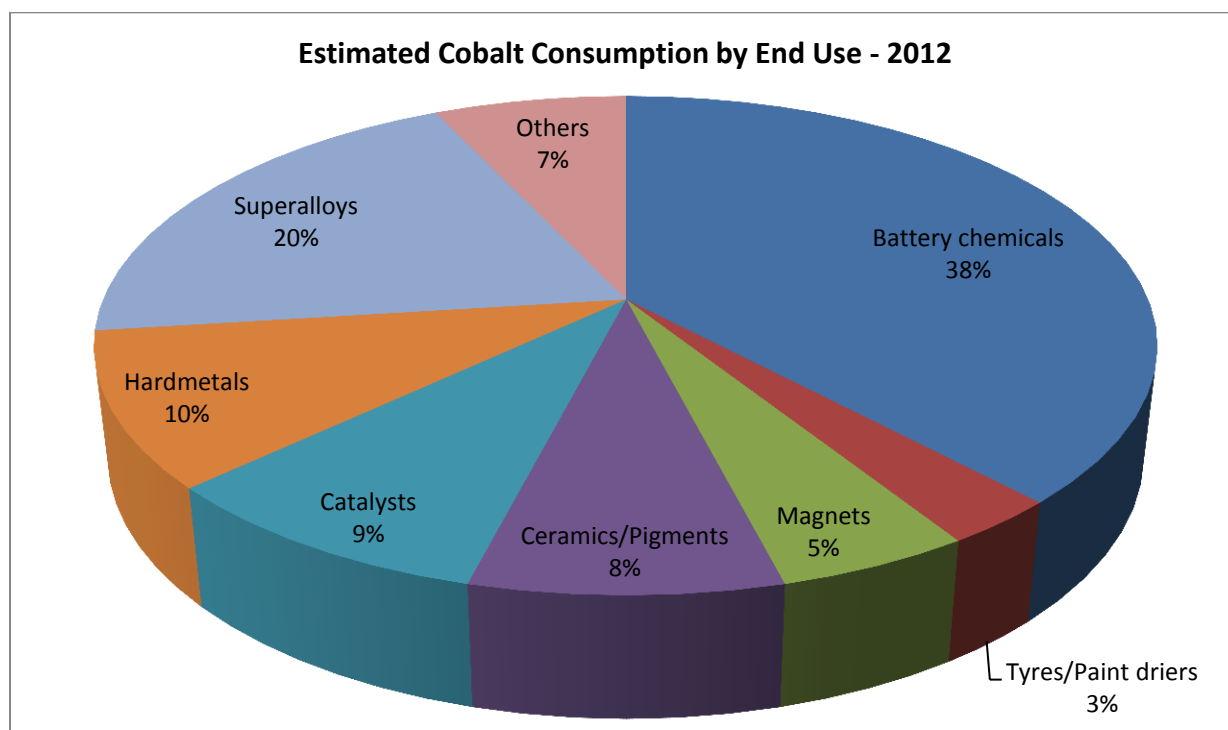


Figure 1.1. Various forms of consumption of cobalt for the year 2012 (adapted from reference 3).

Chapter 1 | Literature Review

The production of cobalt is achieved *via* a recovery process where cobalt is seen as a by-product considering its association with other metals such as nickel and copper, with the nickel and platinum group metal (PGM) industry being the current largest producer of cobalt. A general process flow sheet (**Figure 1.2**) shows a leach, followed firstly by the recovery of copper, then removal of impurities and recovery of cobalt and lastly the recovery of nickel.

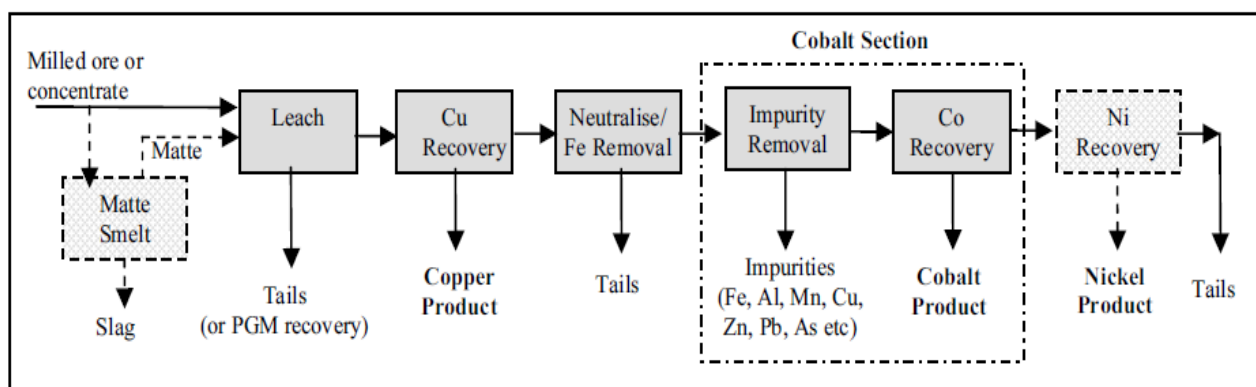


Figure 1.2. A generic Copper/Cobalt/Nickel Recovery Flowsheet (taken from reference 6).

Although the recovery processes of nickel and copper are generally established in advance, the cobalt section needs to be confirmed prior to production depending on the specific type of cobalt required. Since there are various forms in which cobalt can be produced and traded, including as either concentrates or high purity metal, the product to be made needs to be carefully considered before the above-mentioned flowsheet can be finalised.⁶

Various methods are available for recovering cobalt, but the most popular method is by means of solvent extraction. The first commercial application of solvent extraction took place at Xstrata Nikkelverk in Norway in 1968, specifically for the separation of cobalt and nickel.⁶ Since then South Africa became the first site for one of the largest solvent extraction plants and were the first to implement solvent extraction for the recovery of platinum group metals and later on base metals, precious metals as well as speciality metals.⁷ Cobalt solvent extraction generally involves three important steps. The first step is extraction by means of an organic phase containing Cyanex 272 which allows the cobalt concentration in the aqueous phase to be steadily reduced. The second step involves scrubbing of the magnesium, calcium and nickel in the loaded organic phase by means of dilute cobalt sulphate and finally the stripping of the organic phase *via* dilute sulphuric acid for the removal of some final impurities such as zinc. Extraction of metals is a particularly significant field of study considering the continuous need to

Chapter 1 | Literature Review

find both efficient and cost-effective means for recovering said metals. Various ligands have been investigated for their ability to sufficiently extract a variety of metals, where success in extracting transition metals⁸⁻¹⁰ has been found using ligands by means of chelation. A long known ligand known as *N,N*-dialkyl-*N'*-aroylthioureas was first explored for its extraction abilities by Beyer and Hoyer¹¹ and their work was followed by a number of studies interested in their extractability of a variety of metal ions¹²⁻¹⁵. Considering the vast coordination chemistry of these ligands, the aim of the current work is to pay special attention to the synthesis and chemistry as well as spectroscopic aspects of the acylthiourea ligands upon coordination to cobalt.

1.2. *N,N*-dialkyl-*N'*-aroyl(acyl)thioureas

1.2.1. General information and application

The deceptively simple yet versatile series of ligands with the generic name *N,N*-dialkyl-*N'*-aroyl(acyl)thiourea, have been a focus of study since their discovery and first synthesis more than a century ago in 1873¹⁶. Recent studies have shown these ligands to have interesting biological activities including antifungal, insecticidal, fungicide, antibacterial and herbicidal properties.¹⁷⁻²³ Furthermore, these compounds display an extensive coordination chemistry due to the presence of both “hard” and “soft” donor atoms²⁴, making them particularly interesting with regards to metal coordination chemistry²⁵.

Regarding nomenclature, “acyl” refers to the alkyl substituent attached to the carbonyl carbon (i.e. R_1) with “aroyl” referring to the aromatic substituent on the same position. Therefore the conventional name used for these compounds is given as *N,N*-dialkyl-*N'*-acylthiourea and *N*-alkyl-*N'*-acylthiourea (also sometimes more correctly designated as 1-(acyl/aroyl)-3-(alkyl)- and 1-(acyl/aroyl)-3,3-(dialkyl)-thiourea) and will be implemented accordingly for the remainder of this report. Although a few stable conformations are possible for this particular compound, as seen from the work of Woldu and Dillen²⁶, the *anticlinal* geometry (the *U* form), displayed in **Figure 1.3**, is largely preferred. Upon deprotonation with a suitable base, the electrons are delocalized around the central thioureato group and it is this anionic form that ultimately allows for coordination by means of the sulphur and oxygen atoms.

Chapter 1 | Literature Review

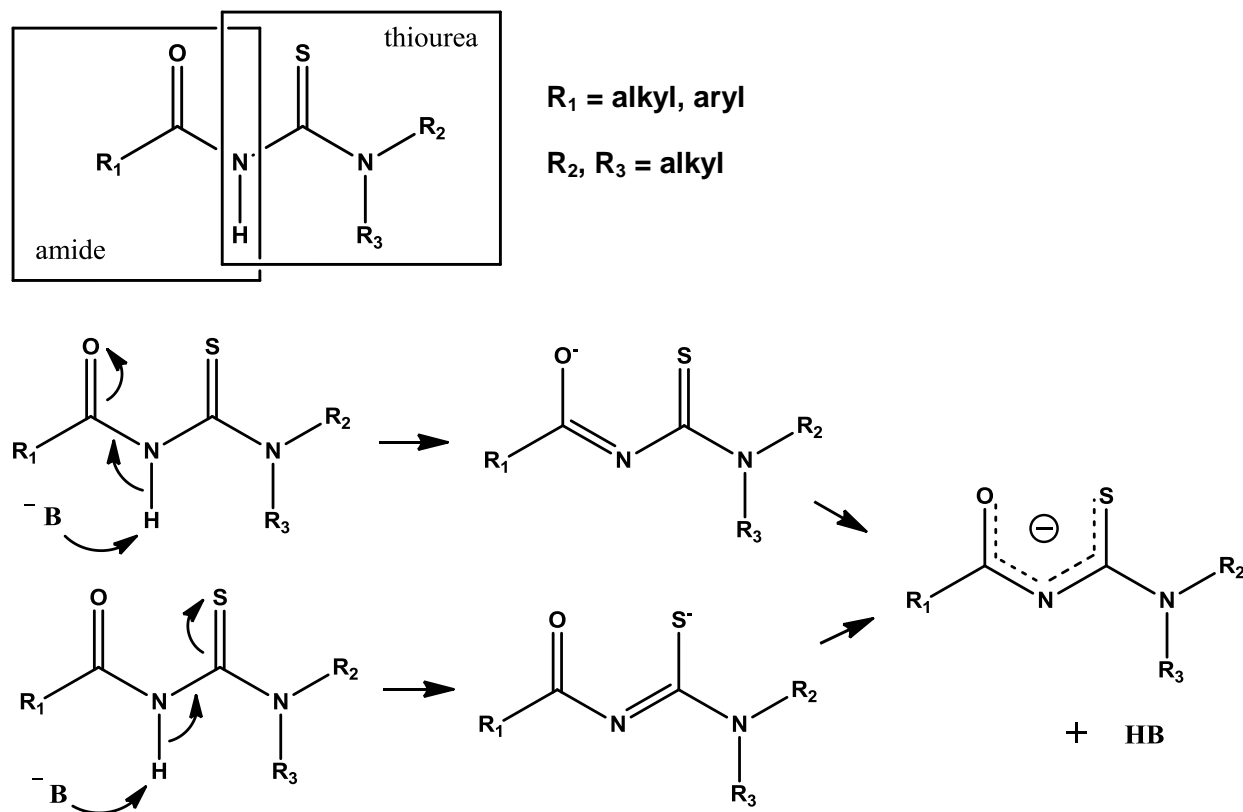


Figure 1.3. General representation of *N,N*-dialkyl-*N'*-aroyl(acyl)thiourea as well as the formation of the acylthiourea anion in the presence of a suitable base.

Systematic studies of the coordination chemistry of *N,N*-dialkyl-*N'*-aroyl(acyl)thioureas with transition metal ions only began in the 1960's^{27,28}, after which numerous studies followed. The most widespread work available regarding these compounds focused mainly on the manner in which these ligands coordinate to transition metal ions such as Ni(II), Pd(II), Cu(II), Rh(III) and Pt(II).^{29-31,36} Some of the research focused on their potential applications in separation of some of these metals, by for example reversed-phase HPLC³², extraction^{14,15,33} as well as trace determination experiments of platinum and palladium³⁴. Merdivan *et al.*³⁵ studied the extraction behavior of transition metals such as Cu(II), Co(II), Ni(II), Cd(II) and Pd(II) by means of *N,N*-dibutyl-*N'*-benzoylthiourea as an extractant in kerosene and was able to determine the extraction efficiency of the various metals using this particular compound.

Hydrophilic acylthiourea ligands, for example *N,N*-di(2-hydroxyethyl)-*N'*-benzoylthiourea, have furthermore been used for the pre-concentration of Pt(II), Pd(II) and Rh(III) *in situ* where determination of their respective concentrations were obtained by means of Laser-ablation

Chapter 1 | Literature Review

inductively coupled plasma mass spectroscopy (LA-ICP-MS).³⁶ The most notable finding regarding this particular method was related to the remarkable linear-response-concentration curves attained, with a greater than 99% recovery of the above-mentioned metals. In addition, the ligands proved to be extremely successful for the on-line pre-concentration of these target precious metals at ultra trace level, where electrothermal atomic absorption spectroscopy was utilized for PGM determination.

Further application of acylthioureas were initially revealed by Zhang and co-workers^{37,38} who illustrated the capability of the compounds to be used as anion receptors, after which Fabrizzi and co-workers^{39,40} utilized the hydrogen bonding ability of the acylthiourea component to ultimately produce a variety of anion receptors. Other studies have also shown certain acylthioureas to be useful as ionophores in ion-selective electrodes for their use in environmental control.^{41,42}

Another significant application of acylthioureas is in their potential as catalysts when coordinated to metal centers.⁴³⁻⁴⁶ This was illustrated by the work of Gunasekaran and co-workers^{43,44} where complexes of Ru(III) and Ru(II) coordinated to *N*-[di(alkyl/aryl)carbamothioyl]benzamide ligands were previously prepared and exhibited catalytic activity for the oxidation of primary, secondary, cyclic, allylic, aliphatic and benzylic alcohols to the corresponding carbonyl compounds. The combination of [RuCl(L)(CO)(PPh₃)₂] and *N*-methylmorpholine-*N*-oxide proved a sufficient active catalyst for the oxidation of some primary and secondary alcohols to their corresponding aldehydes and ketones at room temperature. Similar ligands in combination with six coordinate ruthenium(III) complexes also proved efficient catalysts for oxidation of a variety of alcohols.

1.2.2. Coordination chemistry of acylthioureas with some transition metals

The coordination chemistry of acylthiourea ligands to a variety of transition metals have been extensively reviewed by Koch³⁶ and recently Flörke *et al*²⁵. There are three different modes of coordination that have been previously identified for these ligands including the chelating mode (O,S)⁴⁷, neutral monodentate (S)⁴⁸ and neutral bidentate (O,N)⁴⁹ mode. Upon deprotonation of the amidic proton, the negative charge becomes delocalized on the central thioureato group (illustrated in **Figure 1.3**). Hence, the most commonly occurring coordination seen for these compounds occurs *via* the chelate mode, forming mostly square planar complexes as the *cis* isomer to the specific metal center (**Figure 1.4**).

Chapter 1 | Literature Review

A previous study illustrated that the predominantly formed *cis*-[Pt(L-S,O)₂] and *cis*-[Pd(L-S,O)₂] complexes can be photochemically isomerized to the *trans* complexes in solution, reverting back to the *cis* complexes in the dark.⁵⁰ Regardless of the overwhelming affinity for acylthiourea ligands of type HL to form stable *cis* complexes, a study by Koch *et al.*⁵¹ illustrated that in certain acidic conditions in the presence of some coordinating halide anions, *cis*-[Pt(L-S,O)₂] complexes become deprotonated in order to form a variety of different complex species including some *trans*-[Pt(HL-S)₂I₂] complexes. In retrospect, the preference for the square planar coordination has been seen for d⁸ and d⁹ metals including Ni(II), Cu(II), Pd(II), Ru(II) and Pt(II).⁵²⁻⁵⁵

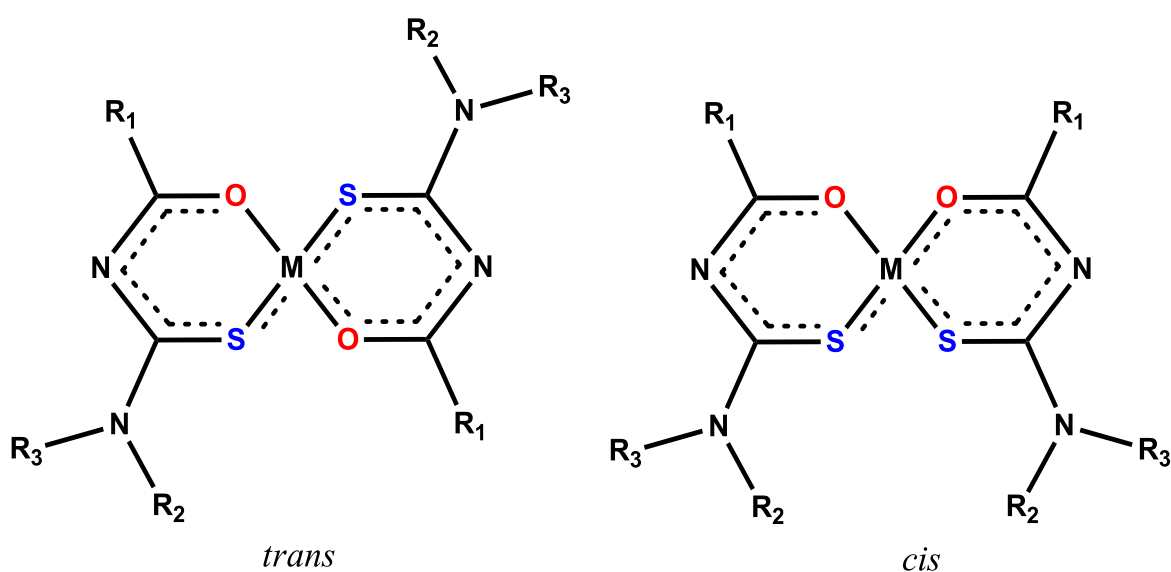


Figure 1.4. The two possible isomers *cis* and *trans* observed for square planar bis(chelate) complexes coordinated to two acylthiourea ligands (adapted from reference 25).

Although coordination of acylthiourea ligands to transition metals primarily occurs by means of the chelating (S,O) mode of coordination, this is not the only mode previously observed and reported. Karvembu *et al.*⁵⁶ were able to synthesize a complex in which they observed the seldom seen neutral monodentate (S) mode upon reacting Pd(II) salt with *N,N*-di(alkyl/aryl)-*N'*-benzoylthiourea (**Figure 1.5**).

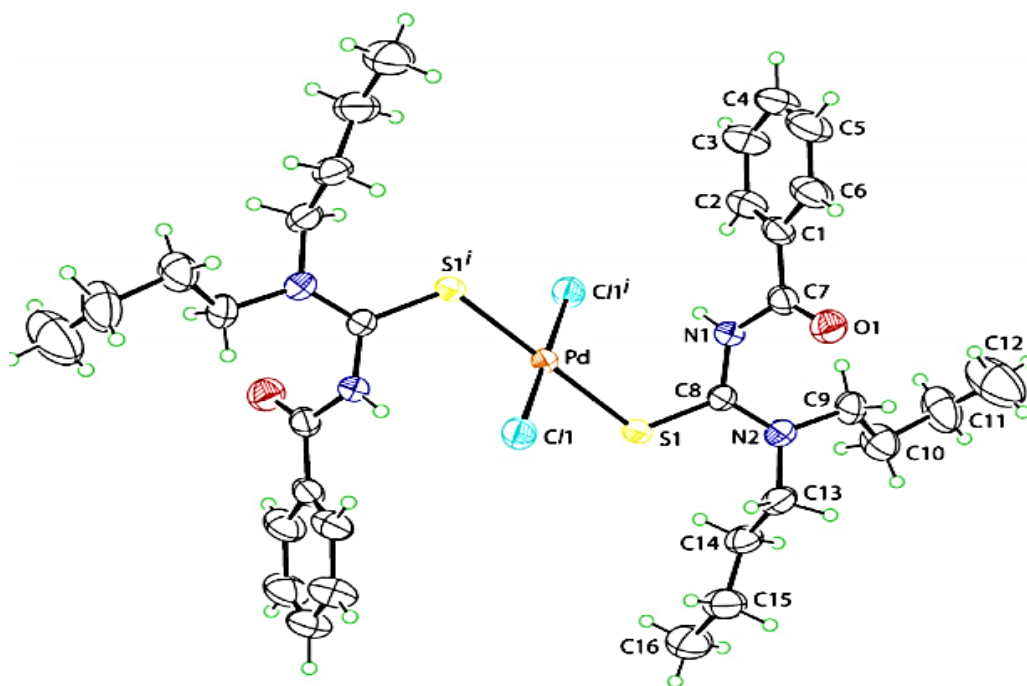


Figure 1.5. The only crystal structure available in the literature of the neutral monodentate coordination mode showing Pd(II) coordinated to two acylthiourea ligands by means of the S atom (taken from reference 56).

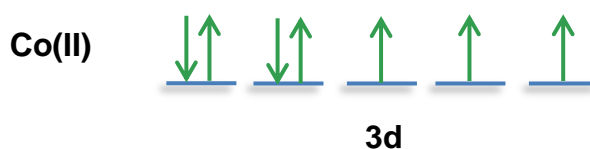
1.2.3. Coordination chemistry of acylthioureas to Co(II) and Co(III)

Cobalt ions in solution generally has two stable oxidation states namely Co(II) and Co(III), both of which dominate its coordination chemistry. The simple cobalt salts generally have the metal in its +2 oxidation state where synthesis of most cobalt complexes makes use of the commercially available $\text{CoX}_2 \cdot 4\text{H}_2\text{O}$ or $\text{CoX}_2 \cdot 6\text{H}_2\text{O}$ (where $\text{X} = \text{F}, \text{Cl}, \text{NO}_3, \text{ClO}_4$) salts. The Co(II) oxidation state is able to form a number of complexes and generally adopts the octahedral or tetrahedral geometry, although some five-coordinate square planar cobalt(II) complexes are available^{57,58}, and these two are often in equilibrium with one another in solution. It is particularly noteworthy that these complexes frequently have a d^7 electron configuration and are thus considered paramagnetic. The tetrahedral configuration is formed more readily for cobalt(II) than any other metal ion largely because the crystal field stabilization energy difference between the two common occurring geometries is small for a high spin d^7 electron configuration.⁵⁹

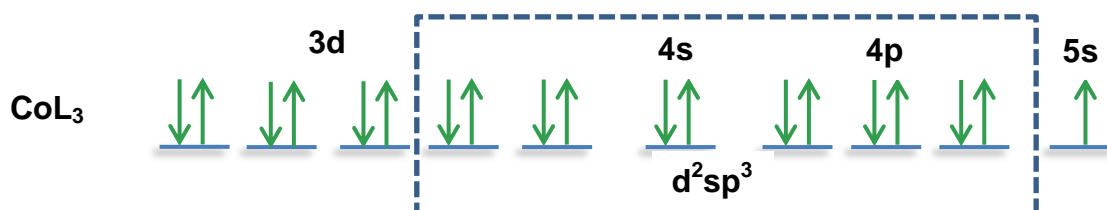
By contrast, the majority of Co(III) complexes have a low-spin d^6 electronic configuration forming almost exclusively six-coordinate octahedral complexes, although some tetrahedral and square-

Chapter 1 | Literature Review

antiprismatic Co(III) complexes are known⁶⁰⁻⁶². Although Co(II) and Co(III) complexes are readily synthesized from a Co(II) salt with an appropriate ligand, there is an important prerequisite for the synthesis of Co(III) complexes. The oxidation of Co(II) to Co(III) during complex formation in aqueous solutions containing no complexing agents is not favored. This can be explained by means of the valence bond theory which describes the ease with which an electron from an octahedral Co(III) complex is lost.²⁴ Consider hereby the electronic arrangement in the 3d orbital of Co(II), shown as follows:



Upon coordination of ligands to the cobalt metal ion by means of the octahedral geometry, the d^2sp^3 hybridization requires use of two of the 3d orbitals consequently resulting in one of the 3d electrons being promoted to the nearest vacant higher energy orbital, i.e. 5s.



This single electron in the higher energy 5s orbital is now easily lost to oxidation of Co(II) to Co(III) which is favored by means of stabilizing ligands.

The focus of this particular study is the coordination chemistry of cobalt to a series of ligands of the type *N,N*-dialkyl-*N'*-aroyl(acyl)thiourea. Considering the paramagnetic nature of the Co(II) d^7 ion does not allow for subsequent NMR study, the primary focus will be to prepare diamagnetic Co(III) complexes coordinated to acylthiourea ligands. To our knowledge, only one paper is currently available on Co(II) complexes coordinated to an acylthiourea ligand by O'Reilly *et al.*⁵² who were able to show the preference of the acylthiourea moiety for coordinating as the *cis* isomer to Co(II), in the square planar geometry. The coordination of *N,N*-dialkyl-*N'*-aroyl(acyl)thioureas to the Co(II) precursor salts results spontaneously in [Co(L-S,O)₃] type complexes when the stoichiometry of Co(II) relative to HL is 1:3 (i.e. oxidation by atmospheric oxygen).

Chapter 1 | Literature Review

There are only a few examples available in the literature showing the coordination of acylthioureas to the Co(III) oxidation state, shown to coordinate *via* the octahedral geometry.^{45,63-67} Many base metals are known to adopt the octahedral geometry whereby Co(III) octahedral complexes coordinated to acylthioureas can be defined by the O_3S_3 donor set. The stereochemistry for Co(III) complexes is relatively vast, considering it not only has a number of possible coordination units but also able to compromise one, two or even three bidentate ligands. The result is a variety of constitutions possible with each constitution able to yield various possible stereoisomers. In the case of a Co(III) complex with a MA_4B_2 composition, the two possible geometric isomers are known as *cis* and *trans*. An example of this can be seen in the complex tetraamminedichlorocobalt(III) which coordinates as either one of the two isomers, shown in **Figure 1.6**.

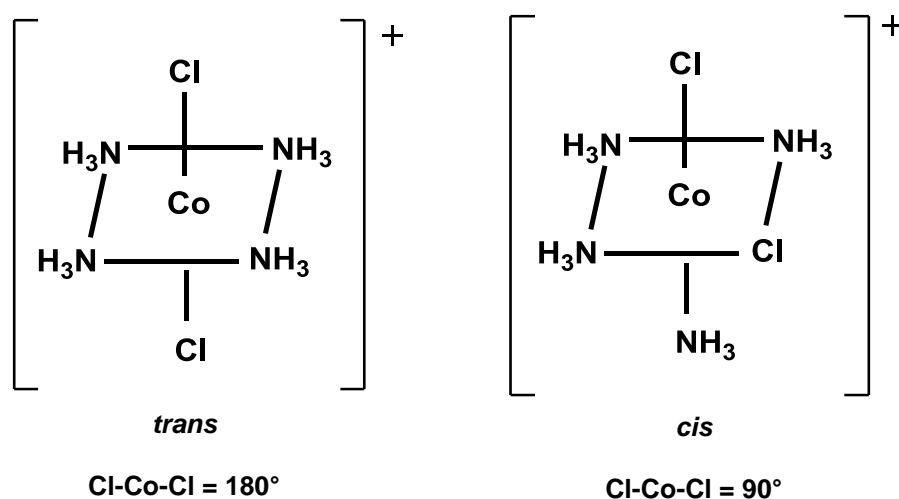


Figure 1.6. The two geometric isomers *cis*- and *trans* of tetraamminedichlorocobalt(III).

Another well-known composition for octahedral complexes is MA_3B_3 which also has two geometric isomers, in this instance known as *fac* and *mer*. Looking at triamminetrichlorocobalt(III) as an example, the *mer* isomer (short for “meridional”) will have the three chloride atoms coordinated in a plane which will include the metal ion, as shown in **Figure 1.7**. This relates to the meridian of a sphere, i.e. the plane through a sphere that contains its center. On the other hand, the *fac*-isomer (short for “facial”) will have all the chloride atoms coordinated on one face of the octahedron.

Chapter 1 | Literature Review

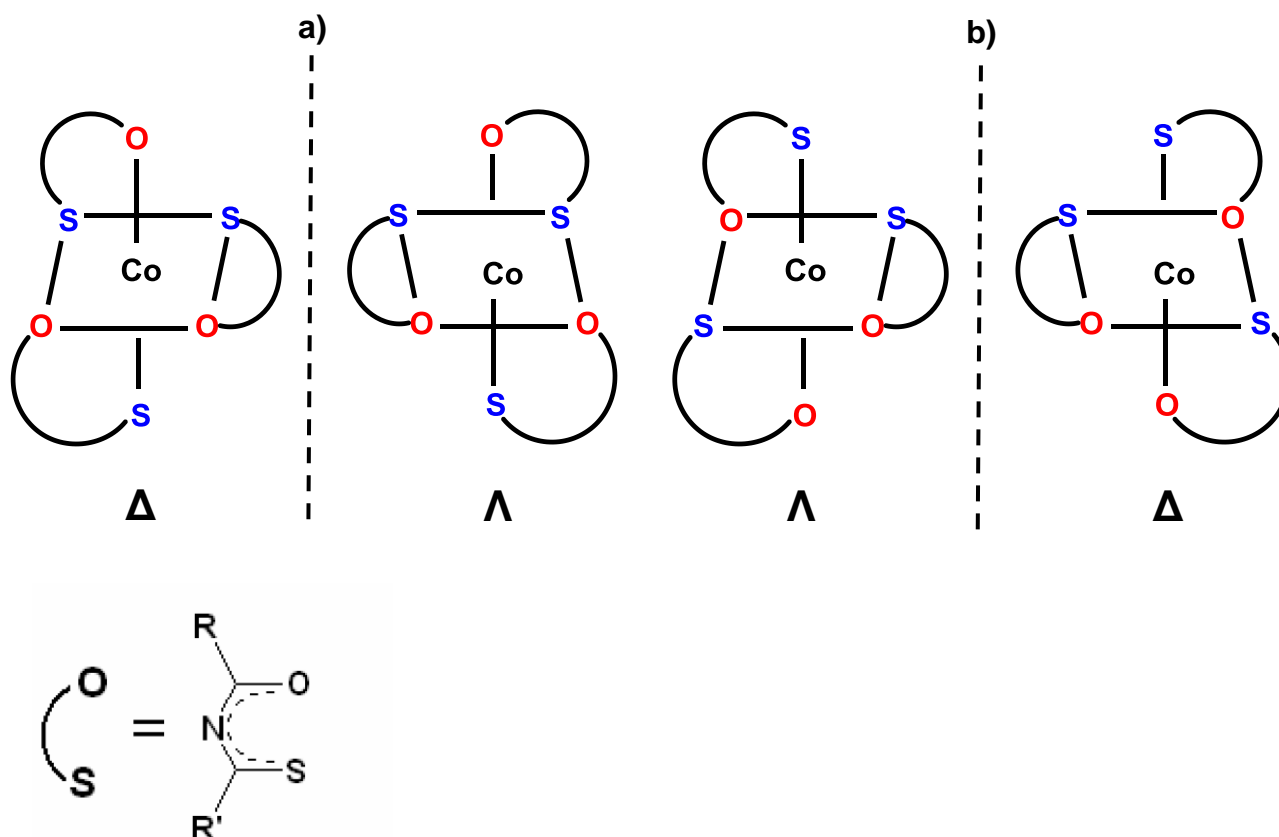


Figure 1.8. The two pairs of enantiomers possible for each geometric isomer (a) *fac* and (b) *mer* of the Co(III) complexes coordinated to three acylthiourea ligands.

Only six crystal structures are available in the literature with respect to Co(III) complexes coordinated to acylthiourea ligands, all of which indicate the preference of the ligands to coordinate to Co(III) by means of the *facial* isomer.^{45,63-67} One of these crystal structures are shown in **Figure 1.9**.

A study by Fay and Piper⁷⁰ revealed a simple method in which NMR can be used in order to distinguish between the two different configurations (i.e. *fac* and *mer*), specifically for trivalent metals including Cr(III), Co(III), Rh(III), Al(III), Ga(III), In(III), Mn(III) and Fe(III) coordinated to unsymmetrical bidentate ligands namely trifluoroacetylacetonates (**Figure 1.10**). It was found that for the *facial* isomer the three chelate rings are present in identical environments, because of the three-fold rotational axis, hence only one signal appears for every proton.

Chapter 1 | Literature Review

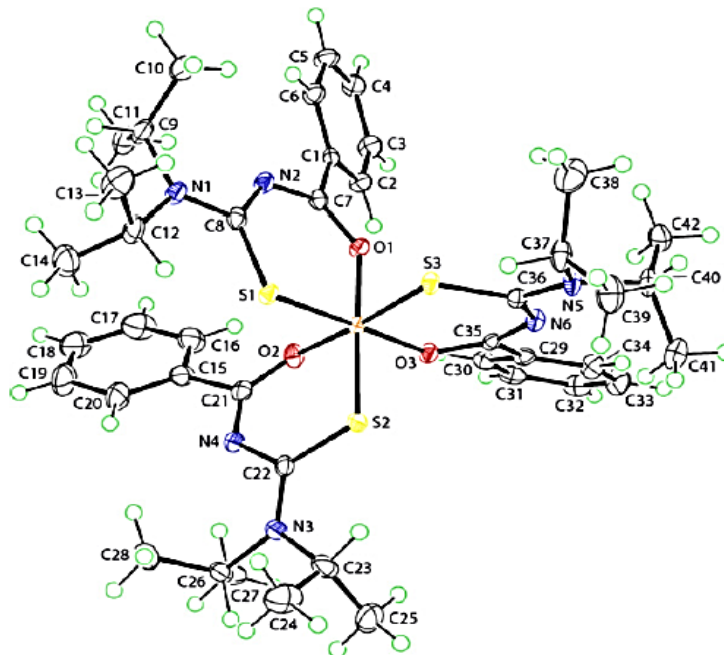


Figure 1.9. One of six crystal structures available in the literature of a Co(III) complex coordinated to three acylthiourea ligands, showing the tendency for coordinating as the *fac* isomer (taken from reference 45).

The opposite is true for the *meridional* isomer, so considering the lack of symmetry, this results in protons being in magnetically inequivalent positions causing additional fine structure visible in the ^1H NMR spectrum of the *mer* isomer.⁷⁰

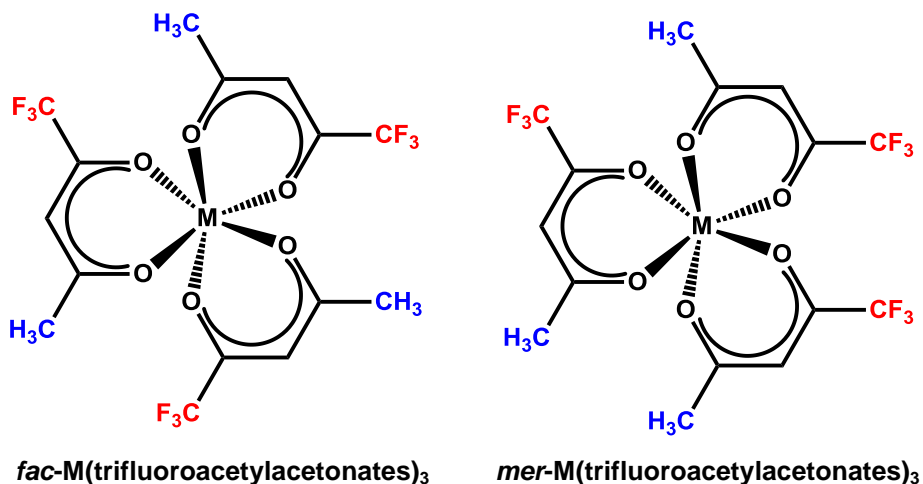


Figure 1.10. The two different isomers namely *fac* and *mer* of $\text{M}(\text{trifluoroacetylacetonates})_3$ (where M = Cr(III), Co(III), Rh(III), Al(III), Ga(III), In(III), Mn(III) or Fe(III)) (adapted from reference 70).

Chapter 1 | Literature Review

Mohamadou *et al.*⁷¹ used this last mentioned concept to show *via* the NMR spectra that Co(III) complexes of *N,N*-disubstituted-*N'*-benzoylthioureas favor the *facial* isomer. In this study, they showed that different substituents of the tertiary amine does not result in different isomers of these complexes, nor affecting the electrochemical properties of these complexes in any way. A similar study of the coordination of cobalt(III) with *N,N*-diethyl or *N*-morpholine, *N'*-substituted benzoyl thioureas repeated the effect of varying the substituents on the benzoyl group of the *fac*-[Co(L-S,O)₃] complexes in order to determine their influence on the NMR and electronic spectra.⁷²

An interesting application of Co(III) complexes coordinated to acylthioureas was illustrated by Kassim *et al.*⁶⁷ who considered the kinetically inertness of Co(III) complexes to make them ideal for spectroscopic study. They used *N,N*-dialkyl-*N'*-benzoylthiourea derivatives and varied the alkyl and aryl groups attached to the nitrogen atom of the tertiary amine in order to determine the effect on both the chemistry and structural properties of these complexes. By means of single crystal X-ray diffraction these compounds were found to coordinate in the octahedral geometry as the *fac* isomer.

Other examples are available in the literature of some biological applications of Co(III) complexes coordinated to acylthioureas. In 2004 derivatives of the acylthiourea compounds, *N*-butylmethylamine and *N*-ethylisopropylamine, were complexed with Ni(II), Co(III) and Pt(II) in order to determine their antifungal activity against the fungus *Penicillium digitatum* in comparison to their uncomplexed compounds.⁷³ The *N*-butylmethylamine compound and its complexes proved to inhibit fungal growth more sufficiently than *N*-ethylisopropyl and its complexes, except for the Co(III) complex. Antifungal activity using *N*-benzoyl-*N'*-thiourea derivatives and their Co(III) complexes have also previously been reported.⁶³

1.3. ⁵⁹Co NMR spectroscopy

The Co(III) complexes coordinated to acylthioureas have previously been investigated by a number of techniques including IR, UV-Vis, MS, ¹H and ¹³C NMR as well as X-ray crystallography.^{67,70-72} Although ⁵⁹Co NMR spectroscopy has been utilized for the study of a variety of different Co(III) complexes, the only study currently available in the literature of complexes of type *fac*-[Co(L-S,O)₃] investigated by ⁵⁹Co NMR spectroscopy, could be seen by

Chapter 1 | Literature Review

the work of Juranic *et al.*⁷⁴ The authors used ^{59}Co NMR spectroscopy in order to determine the effect of oxygen-by-sulfur and sulfur-by-selenium donor atom replacement on the ^{59}Co NMR chemical shifts in Co(III) Tris-chelates of acylchalcogenoureaates. This study proved that well resolved spectra could be obtained of *fac*-[Co(L-S,O)₃] complexes.

Cobalt exists naturally as only one isotope, Cobalt-59, although thermal neutrons can be used to convert this to the radioactive Cobalt-60 isotope mainly used for medicinal research considering it is an easy and concentrated source of gamma rays. ^{59}Co is a unique isotope in that it not only was the first to display a resonance frequency dependent on the compound, but can also experience considerable paramagnetic deshielding (>18 000 ppm) resulting in the ability to reveal even the smallest of changes in the chemical environment.⁷⁵ The chemical shift subsequently varies widely with the hexacyanocobaltate(III) complex appearing at 0 ppm all the way up to carbonatocobaltate(III) appearing at 14 130 ppm. There is also a linear relationship between the chemical shift and $\beta\nu_1$ (where β = nephelauxetic ratio and ν_1 = frequency of the first d-d transition).⁵⁹ ^{59}Co NMR spectroscopy has been widely used for its sensitivity to even the smallest of changes in the electric field gradient at the metal center. This sensitivity can be partly attributed to the 100% natural abundance of the nucleus and its high receptivity of 1572 relative to ^{13}C .⁷⁶ ^{59}Co has a spin of 7/2 which was formerly determined by Kopfermann and Rasmussen⁷⁷ via the hfs method, and this value was later on confirmed by More⁷⁸. Nuclei with spin $\frac{1}{2}$ are generally easier to understand in terms of their NMR behaviour, because of the spherical distribution of their charge and only two energy states.

Nuclei with a spin greater than 1 on the other hand possess what is known as an electric quadrupole moment, because of the non-spherical distribution of charge as illustrated in **Figure 1.11**. Moreover, since ^{59}Co has a spin of $I = 7/2$, in a magnetic field this will have $(2I + 1)$, i.e eight, energy states.

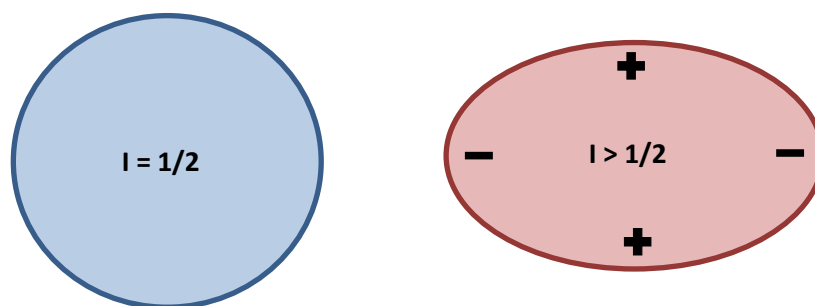


Figure 1.11. The two different possible forms of charge distribution found around a nucleus.

Chapter 1 | Literature Review

The consequence of a quadrupolar nucleus is that the anisotropic electric field gradient present in the molecule can lead to transitions between the 8 spin states, resulting in efficient nuclear relaxation which depends greatly on the degree of quadrupolar coupling. Consequently, with nuclei where the electric quadrupole moment is large, it causes the spin-lattice relaxation time (T_2) to be shorter, thereby resulting in broad lines. Considering now the ^{59}Co nucleus, the signal width for these compounds will increase as the asymmetry of the environment increases, making characterization of such complexes increasingly difficult. Although it should be noted that in tetrahedral or octahedral molecules, the T_2 can be long enough to obtain well resolved spectra considering that the symmetry in these molecules result in a smaller to almost non existing electric field gradient.

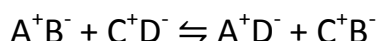
As mentioned in **section 1.2.3**, the most common oxidation state that cobalt salt occurs in is Co(II), a d^7 ion, which is paramagnetic thus leading to very broad ^{59}Co NMR spectra. Thus for Co(II) complexes of the type $[\text{Co}(\text{L-S},\text{O})_2]$ one might expect a ^{59}Co NMR spectrum with broad peaks making it impracticable to obtain any useful information from such a spectrum. Therefore the most commonly studied complexes by ^{59}Co NMR are Co(III) complexes, which are generally diamagnetic. The d^6 Co(III) ion can be expected to give relatively narrow ^{59}Co NMR peaks with well-defined chemical shifts due to the symmetrical ligand field, so that little quadrupolar broadening is observed.

^{59}Co NMR spectroscopy has been shown to be a sensitive technique for investigating the structures, stereochemistry and the reactivity of Co(III) complexes. Some of the earliest studies utilized the high NMR sensitivity and chemical shift range of the ^{59}Co nucleus in order to study solute-solvent interactions in the outer sphere.⁷⁹ Considering the large chemical shift range, ^{59}Co NMR is a sensitive probe for studying subtle differences in the Co(III) coordination sphere and thus allows for in depth study of the effect of ligand structure, solvent effects, temperature and pressure on the $\delta(^{59}\text{Co})$ of the complexes under consideration. More detail about the practical aspects of ^{59}Co NMR are given in chapter 3 **section 3.3 - 3.4**. It is also of interest to utilize this technique for investigating the ligand exchange reaction when two of the homoleptic Co(III) complexes coordinated to the acylthiureas are mixed together in the same solution.

Chapter 1 | Literature Review

1.4. The metathesis (i.e. ligand exchange) reaction

It is well known that in reactions between two compounds in an aqueous solution there occurs an exchange of partners between that of the positive and negative ions in order to form two new compounds in solution, without a change in oxidation numbers. This is what is known as a metathesis reaction, which comes from the Greek word 'μετάθεσις', meaning transposition.⁸⁰ Thus, there is no rearrangement of electrons occurring in this reaction, only the rearrangement of atoms. This can be demonstrated in its simplest form as shown in **scheme 1.1**.



Scheme 1.1. The exchange of ions as one of the simplest examples of metathesis.

1.4.1. Metathesis in organic chemistry

Some of the most well-known examples of metathesis can be seen in the field of organic chemistry. As early as 1931 the first non-catalytic metathesis reaction was observed upon decomposing propene by means of extremely high temperatures⁸¹, after which the first catalyzed metathesis reaction would be implemented in the 1960's when a couple of industrial chemists observed the formation of ethylene and 2-butenes when heating propene with molybdenum⁸². It was during this time that the concept of organometallocatalyzed olefin chemistry became of significant interest especially in the field of organic and polymer synthesis. The term olefin metathesis would although first be used in 1967 during the synthesis of 2-butene and 3-hexene from 2-pentene by means of a specific catalytic system consisting of tungsten hexachloride, ethanol and ethyl-aluminium dichloride.⁸³

The exchange that takes place in olefin metathesis ultimately occurs between two olefins when the carbenes attached differ, leading to a recombination and finally the formation of two new olefins. This can also occur between the carbynes of an alkyne. These two types of reactions are illustrated in **Figure 1.12**. It is clear to see the double bonds are broken in such a way which ultimately causes the atoms in the two groups to change places, and this reaction is eventually assisted by special catalyst molecules.

Chapter 1 | Literature Review

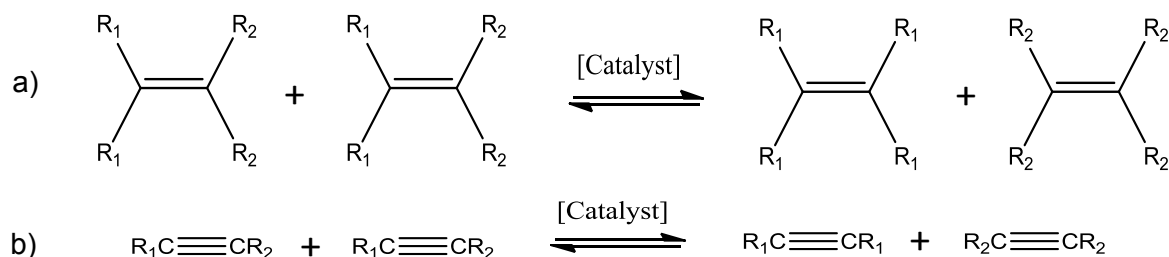


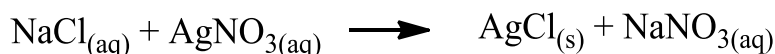
Figure 1.12. General metathesis reaction scheme between two a) olefins and b) alkynes.

A proposed sort of chain mechanism for the catalyzed metathesis reaction as well as ring opening polymerization would be published in 1971 by Chauvin and Herisson⁸⁴. This mechanism proved vital and established metal-carbenes as worthy initiators of the catalysis of the metathesis reactions. This work continued to inspire further research into finding even more efficient catalysts for this reaction and eventually lead to the three pioneers in this field, Yves Chauvin, Robert H. Grubbs and Richard R. Schrock, to win the Nobel Prize for chemistry in 2005.⁸⁵

1.4.2. Metathesis in inorganic reactions

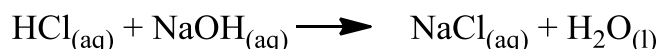
Where metathesis in organic chemistry involves the breaking of multiple bonds in order to yield different products, for inorganic chemistry metathesis comprises the exchange of ions or ligands in solution. The metathesis involving the exchange of ions can be divided into three different categories.

1) **Precipitation reaction:** Here an insoluble compound is formed known as the precipitate and is a technique most often used in gravimetric analysis. An example of this reaction can be seen upon addition of sodium chloride and silver nitrate in the same solution.

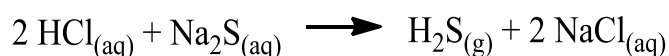


Chapter 1 | Literature Review

2) **Neutralization reaction:** This type of reaction is where an acid and a base react in order to form a salt and water. Equivalence points can generally be easily identified in these types of reactions with proper use of indicators or pH monitoring, and is thus largely used for volumetric analysis. An example can be seen below where the salt, sodium chloride, is formed *via* the addition of hydrochloric acid and sodium hydroxide into the same solution.



3) **Gas formation reaction:** The product formed in this reaction has both a low boiling point and low solubility in water, thus producing a gas as shown below.



The ligand exchange reaction is also a form of metathesis that occurs in inorganic chemistry, but is a type of metathesis that occurs primarily between coordination compounds.

1.5. Ligand exchange in metal complexes

1.5.1. Earliest studies and methods of detection

Chelate metathesis, or more simply known as ligand exchange, is a process that involves the substitution of one or more ligand in a particular complex with that of a ligand from a different complex. This can occur between four-, six- or eight- coordinate metals, although research has focused predominantly on the more labile four-coordinate metals including Cu(II) and Ni(II).⁸⁶⁻⁹¹

Ligand exchange studies can be divided into one of two categories; (1) Arrangement of four- or five- membered rings with sulphur or selenium donor sets or (2) arrangement of six-membered chelate rings with nitrogen or oxygen donor sets. Regarding ligand exchange occurring amongst *N*-alkyl- or *N,N*-dialkyl-*N*-aroyl(acyl)thioureato complexes, previous work currently available can be seen in Lyndall van der Molens masters thesis⁹².

Some early work regarding ligand exchange reactions were illustrated by Davison *et al.*⁹³ between some homoleptic Ni(II) complexes coordinated to a series of 1,2-disubstituted ethylene-1,2-dithiolato ligands and made use of polarography for detecting the occurrence and extent of ligand exchange. A significant finding of this study was the effect of solvent on ligand

Chapter 1 | Literature Review

exchange, where in acetonitrile a greater percentage mixed ligand (i.e. heteroleptic) complex formed compared to in less polar dichloromethane. These authors developed a suitable synthetic route for synthesizing heteroleptic complexes, with differences in solubility at equilibrium allowing for sufficient separation of the complexes using the information gathered from polarography. Similar ligand-exchange reactions was done by Balch⁹⁴ with these dithiolene ligands using a variety of metals including Cu(II), Au(II), Ni(II), Pd(II) and Pt(II), tabulating equilibrium times and percentage heteroleptic complexes formed. The more labile Cu(II) complexes first reached equilibrium forming 61% heteroleptic complexes in approximately 15 days, followed by the Pd(II) complexes which reached equilibrium after 27 days. Complexes of Au(II) and Pt(II) did not result in any discernible heteroleptic complexes for the entire 74 and 99 days, suggesting substitutional inertness. A more surprising result came from the reaction between the same Ni(II) complexes studied by Davison *et al.*⁹³ which in contrast to the work by Balch did not result in any heteroleptic complex formation.

Various techniques have been used for studying ligand exchange, which depend largely on the nature of the complex of interest. This is illustrated by a study implemented by Olk *et al.*⁹⁰ in which exchange reactions between Cu(II), Ni(II) and Pd(II) chelates containing unsaturated sulphur and/or selenium donor ligands were monitored. ESR spectroscopy was used to confirm the formation of Cu(II) mixed ligand complexes. It was found that for the copper complexes both the isotropic g values and intensity of the ^{77}Se ligand-hyperfine satellite lines depend on the S/Se ratio. Thus, considering that the homoleptic and heteroleptic chelates do not contain the same donor atom sets, this resulted in ESR characterization of the different heteroleptic complexes. For the nickel complexes, UV-Vis spectroscopy was used to monitor the formation of the heteroleptic complexes, based on their characteristic spectral changes and therefore indicating the ligand exchange reaction as it occurred. Finally, ^{13}C and ^{77}Se NMR was used to characterize the palladium complexes, in which shielding differences as a result of either steric or electronic effects, allowed for differentiating between the heteroleptic chelates formed.

1.5.2. High Performance Liquid Chromatography studies of ligand exchange

Research has shown that chelating ligands play an important role in the separation of metals, especially regarding metal distribution between an organic and aqueous phase. Whether considering the different phases or types of ligand, each of these have shown to significantly affect the manner in which selective extraction takes place. For these reasons, column

Chapter 1 | Literature Review

chromatography was selected for achieving efficient separation of metal chelates. Huber and Kraak⁹⁵ demonstrated this potential using liquid-liquid partition chromatography for separating as many as six metal complexes coordinated to β -diketonates.

A unique ability of high performance liquid chromatography was demonstrated later on in 1979 by Liška and co-workers^{96,97} when a study focusing on the separation of two Ni(II) bisdialkylthiocarbamates, by normal phase HPLC, observed an additional peak in the chromatogram when different *N*-alkyl substituents were used. It was shown that the third complex was formed as a result of ligand exchange, substantiated by two-dimensional thin-layer chromatography, molecular weight determinations and elemental analysis. This study proved HPLC to be an effective technique for determining the relative stability of homoleptic complexes, as well as allowing factors which effect ligand exchange to be studied.

Moriyasu and Hashimoto⁹⁸ used HPLC to study Ni(II) chelates of *N*-disubstituted dithiocarbamic acids, and carried out a kinetic study of the ligand exchange reaction using normal phase HPLC. They designed a *np*-HPLC system for obtaining well resolved chromatograms of the *N,N*-dialkylthiocarbamic acid complexes using different metals. Focusing finally on the Ni(II) complexes, they could follow the ligand exchange reaction by injecting small amounts of a sample of a chelate mixture into the HPLC at specific time intervals. Initially the heteroleptic mixed-chelate peaks were absent, but after some time a peak appeared between the two homoleptic peaks, corresponding to the heteroleptic complex formed. Peak heights decreased for the homoleptic complexes while increasing for the heteroleptic complex until equilibrium was reached.

A more recent unpublished study using *rp*-HPLC for monitoring ligand exchange can be seen in Lynndal van der Molens masters thesis⁹². The author showed by means of reversed-phase HPLC that Pd(II) complexes of a variety of *N,N*-dialkyl-*N*-acyl(aryl)thiourea ligands, at room temperature, readily undergo facile metathesis in a range of different solvents. After addition of two different Pd(II) complexes of type *cis*-[Pd(L^A-S,O)₂] and *cis*-[Pd(L^B-S,O)₂], two new complexes would be formed as a result of ligand exchange with the reaction reaching equilibrium after a few days. van der Molen noted that even with a ten-fold excess of one of the initial homoleptic complexes, all three homo- and heteroleptic complexes, namely *cis*-[Pd(L^A-S,O)₂], *cis*-[Pd(L^B-S,O)₂] and *cis*-[Pd(L^A-S,O)(L^B-S,O)], could still be found in solution.

Chapter 1 | Literature Review

The work of van der Molen resulted in clear evidence of ligand exchange, according to the general reaction scheme illustrated in **Figure 1.13**. The ligand exchange reaction was also investigated between that of an acylthiourea Pd(II) complex and an unbound ligand in a variety of solvents, which illustrated the same results could be achieved as for the reaction between two different coordinated complexes regardless of unbound ligand to complex ratio.⁹²

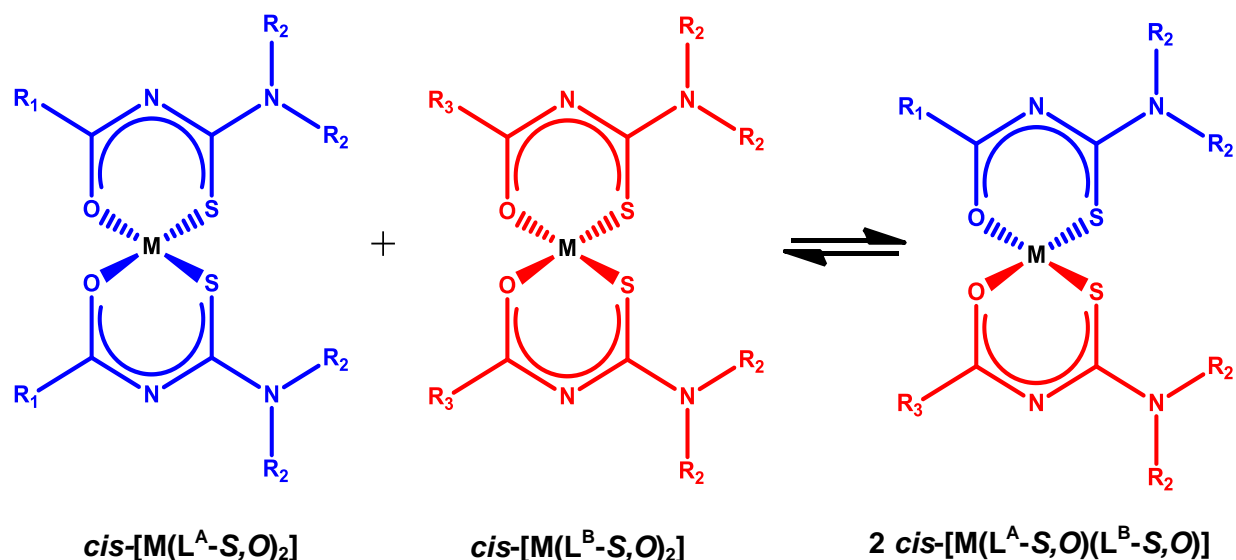


Figure 1.13. A schematic representation of the ligand exchange reaction between two different homoleptic square planar metal complexes of type $cis-[M(L-S,O)_2]$, where $M = Pd(II)$ (adapted from reference 92).

1.5.3. Ligand exchange in six-coordinate metal complexes

The emphasis of the current research project, specifically in regard to possible ligand exchange, is focused on the study of octahedral tris(*N,N*-dialkyl-*N*-aroyl(acyl)thioureato)Co(III) complexes, i.e. $[Co(L-S,O)_3]$. Almost no research is available on the ligand exchange reaction between six-coordinate metal complexes although such reactions have been suggested with more labile non-transition metal chelates such as aluminum(III), gallium(III) and indium(III).

Uden and Wang⁹⁹ studied ligand exchange by means of gas chromatography of Ga(III) complexes namely tris(1,1,1-trifluoropentane-2,4-dione)gallium(III) $[Ga(TFA)_3]$ and tris(1,1,1-trifluoro-6-methylheptane-2,4-dione)gallium(III) $[Ga(TIB)_3]$. After addition of each of the homoleptic chelates in chloroform the mixture was heated to 80°C for 1 hour in order to encourage the re-distribution reaction. The gallium specific chromatogram indicated the

Chapter 1 | Literature Review

presence of four peaks which could be identified as the homoleptic complexes $[\text{Ga}(\text{TFA})_3]$ and $[\text{Ga}(\text{TIB})_3]$ as well as the heteroleptic complexes $[\text{Ga}(\text{TFA})_2(\text{TIB})]$ and $[\text{Ga}(\text{TFA})(\text{TIB})_2]$ with peak areas consistent of a 1:3:3:1 statistical redistribution of the ligands. Different experiments in which the ligands were added in equimolar amounts to a gallium(III) solution, treated similarly above, gave chromatograms similar to those obtained for the ligand exchange reaction between homoleptic complexes.

Further investigation focused on ligand exchange between two different metal chelates of Ga(III) and Al(III) as well as Ga(III) and In(III). These results unexpectedly showed, for the chelates $\text{Al}(\text{TFA})_3$ and $\text{Ga}(\text{TIB})_3$, eight heteroleptic chelates formed in solution. This suggested complete ligand-redistribution occurred, considering each metal center would produce four different chelates in a solution of chloroform after 24h at 25 °C. Gas chromatographic separations were obtained with a carbon-specific microwave-induced plasma detection of gallium at 247.9 nm and 294.3 nm and aluminium detection at 396.1 nm. The results show a bias toward higher molecular mass chelates during the exchange reaction. Interestingly the ligand exchange reaction between $\text{In}(\text{TFA})_3$ and $\text{Ga}(\text{TIB})_3$ gave rise to gallium only products, producing the four peaks corresponding to complete redistribution. No heteroleptic In(III) complexes could be identified, the reasons for which could not be formerly explained.

In 1990, two years after their investigations of ligand exchange by GC, Uden and Wang¹⁰⁰ demonstrated the ability of High performance Liquid chromatography to be a better tool for studying ligand exchange, considering it could be applied to more inert metal chelates at room temperature. By studying the ligand redistribution reactions between gallium, indium, copper and nickel fluorinated β -diketonates, these authors concluded that separations by *np*-HPLC is largely dependent on the specific metal atom with ligand exchange reactions taking place in the liquid phase when employing the specific ambient temperature reaction conditions.

1.5.4. Ligand exchange of Co(III) complexes

Early findings of ligand exchange occurring between Co(III) complexes were reported by Ellis, Wilkins and Williams¹⁰¹ in 1957, who expressed surprise by the ease of exchange occurring in a *neutral aqueous solution* of tris(1:10-phenanthroline)- and tris(2:2'-dipyridyl)-cobalt(III) (*i.e.* $[\text{Co}(\text{phen})_3]$ and $[\text{Co}(\text{dipy})_3]$ respectively) with the corresponding free ligands, compared to that in an acidic solution. This puts into perspective the question of the lability of the ligands in such complexes which are often considered relatively inert to exchange, in view of the low rates of

Chapter 1 | Literature Review

substitution found for Co(III) complexes. $[\text{Co}(\text{dipy})_3](\text{ClO}_4)_3$ was found to undergo a reasonable exchange rate in neutral solution whereas the $[\text{Co}(\text{phen})_3]^{3+}$ ion proved to be very labile to exchange. Further purification of $[\text{Co}(\text{phen})_3](\text{ClO}_4)_3 \cdot 2\text{H}_2\text{O}$, as well as different methods of preparation resulted in slower and inconsistent rates of exchange. Similar irregular results were seen for a fresh sample of $[\text{Co}(\text{dipy})_3](\text{ClO}_4)_3 \cdot 3\text{H}_2\text{O}$, although to a lesser extent. The ligand exchange reaction studied under acidic conditions was found to be considerably slower than in neutral solution. The acid and base forms of the ligand rapidly achieve equilibrium, hence excluded the notion that a decreased ligand exchange rate could be a result of the free base form of the ligands being present in trace amounts under acidic conditions. Instead, these authors suggested that the observed ligand exchange arose due to the presence of a catalyst, more specifically a small amount of cobalt(II) present as either the aquated or complexed ion. Thus in neutral conditions the cobalt(II) impurity could exist as $[\text{CoA}_3]^{2+}$, whereas in acidic conditions it was completely dissociated, thereby possibly accounting for the difference in the rate of ligand exchange in neutral or acidic solutions.

Although this study showed Co(III) complexes to be more labile to exchange than initially assumed, very little research could generally be found in the literature focusing predominantly on ligand exchange of similar Co(III) complexes. Lehotay *et al.*¹⁰² claimed that ligand exchange would not occur between Co(III) complexes, although in 1980 Moriyasu and Hashimoto⁹⁸ observed slow exchange of *N*-disubstituted dithiocarbamic acid of Co(III) chelates by means of high-performance liquid chromatography. Little detail was given on this discovery at the time, until 1984, when Cardwell and Caridi¹⁰³ observed the ease of exchange between two dialkyldithiophosphate chelates of Co(III). The *rp*-HPLC chromatograms from a mixture of two Co(III) dialkyldithiophosphates in solution presented four peaks, each of which identified by means of mass spectrometry as the homoleptic precursor and heteroleptic complex. Minor peaks appeared during the addition of two or more homoleptic Co(III) complexes, with retention times between that of the major components, which eventually grew in intensity as the peaks of the homoleptic complexes decreased in intensity. It was concluded that these results are the consequence of ligand exchange occurring between the Co(III) complexes of interest, which takes place more readily than previously expected for Co(III) complexes. In 1986 a follow-up study found Co(III) dialkyldithiophosphates to undergo rapid ligand exchange, upon mixing homoleptic Co(III) chelates in solution, proving these to be more labile than initially assumed.¹⁰⁴

Chapter 1 | Literature Review

1.6. Aims and Objectives

Reports from previous studies have shown the possibility of ligand exchange to occur between the more labile Co(III) complexes. Although no previous studies are available of ligand exchange occurring amongst cobalt complexes coordinated to ligands of type *N,N*-dialkyl-*N'*-aroyl(acyl)thiourea. One of the more commonly used techniques for monitoring ligand exchange is HPLC and will henceforth be one of the techniques utilized during this study for the same purpose.

Considering the large chemical shift range for ^{59}Co NMR spectroscopy as well as the high receptivity of the nucleus it is hence expected to be a proxy technique for gaining an understanding of the effects of ligand structure, solvent, temperature and concentration on the diamagnetic, octahedral- d^6 cobalt(III) complexes of type $[\text{Co}(\text{L}-\text{S}, \text{O})_3]$. The sensitivity of the ^{59}Co nucleus has made this technique a primary choice for monitoring the ligand exchange reaction between two homoleptic $[\text{Co}(\text{L}^n-\text{S}, \text{O})_3]$ and $[\text{Co}(\text{L}^m-\text{S}, \text{O})_3]$ complexes.

The objectives for the study can be summarized as follows:

1. To synthesize and characterize a variety of Co(III) complexes with several chelating *N,N*-dialkyl-*N'*-aroyl(acyl)thioureas.
2. To investigate the ^{59}Co NMR spectra of these complexes with reference to the effect of ligand structure, solvent, temperature and concentration on octahedral- d^6 cobalt(III) complexes of type $[\text{Co}(\text{L}-\text{S}, \text{O})_3]$.
3. Additionally investigate the effect of ligand asymmetry and chirality on Co(III) complexes by means of ^{59}Co NMR.
4. Monitor by means of ^{59}Co NMR the ligand exchange reaction between two different homoleptic $[\text{Co}(\text{L}^n-\text{S}, \text{O})_3]$ and $[\text{Co}(\text{L}^m-\text{S}, \text{O})_3]$ complexes.
5. Study the potential ligand exchange reaction in this species of complexes by reverse phase HPLC spectroscopy.

CHAPTER TWO

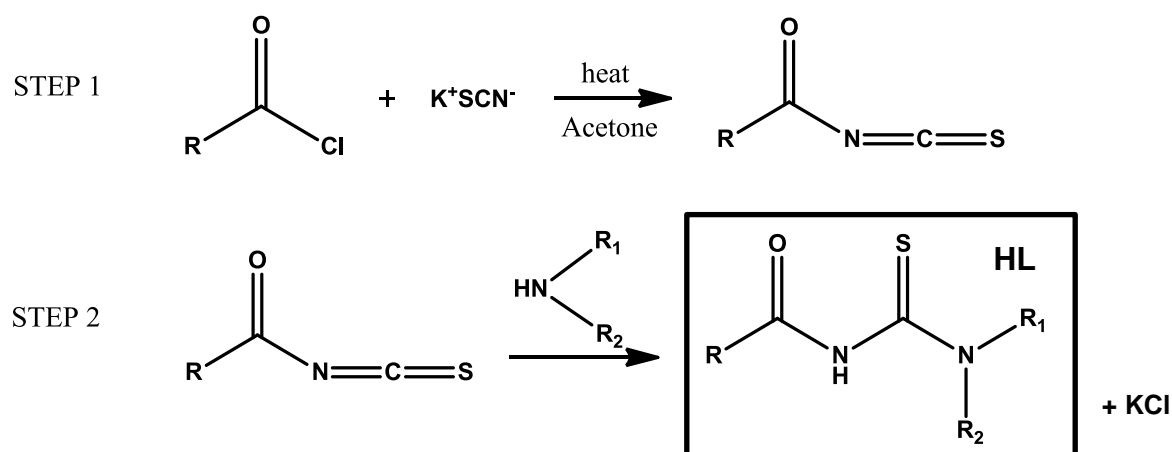
SYNTHESIS AND CHARACTERIZATION

Chapter 2 | Synthesis and Characterization

2.1. Synthesis of acylthiourea ligands and the corresponding Co(III) complexes

2.1.1. Synthesis of *N,N*-dialkyl-*N'*-aroyl(acyl)thioureas

The ligand synthesis reaction was implemented according to the Douglas and Dains¹⁰⁵ method which was described more than 8 decades ago. This involves the formation of an acyl isothiocyanate under anhydrous conditions in acetone. This is produced by the reaction of a corresponding acid chloride with potassium thiocyanate. The step is then followed by treatment with a suitable aliphatic or aromatic amino-compound. The reaction is carried out in dry acetone and results in the acylthiourea derivative of interest. The ligand is varied by using different substituted amino compounds as well as different acid chloride derivatives. The two step general synthetic route for the preparation of acylthiourea ligands is shown in **scheme 2.1**.

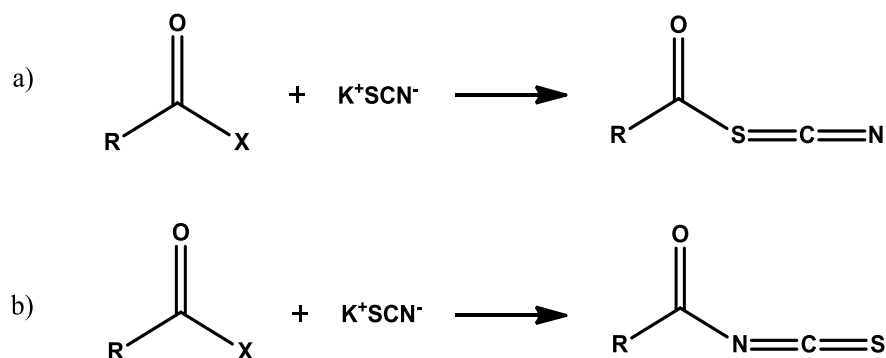


Scheme 2.1. General reaction scheme for the synthesis of *N,N*-dialkyl-*N'*-aroyl(acyl)thiourea ligands.

Careful control of moisture is vital during this synthesis, for acid chloride can easily be converted back to the carboxylic acid in the presence of water. Thus the reaction was maintained under constant nitrogen atmosphere. Potassium thiocyanate was also dried prior to the reaction for approximately two hours in a vacuum oven. All reagents were dissolved in 50 ml anhydrous acetone prior to addition to the reaction mixture. The acid chloride was initially added drop wise to the potassium thiocyanate and allowed to stir for 45 minutes. This was followed by the drop wise addition of the specific amino compound maintaining continuous stirring for another 45 minutes. After completion of the reaction the product is transferred to approximately 50 ml water after which the acetone would be allowed to evaporate overnight. The precipitate is collected *via* filtration and ultimately dried overnight in a desiccator.

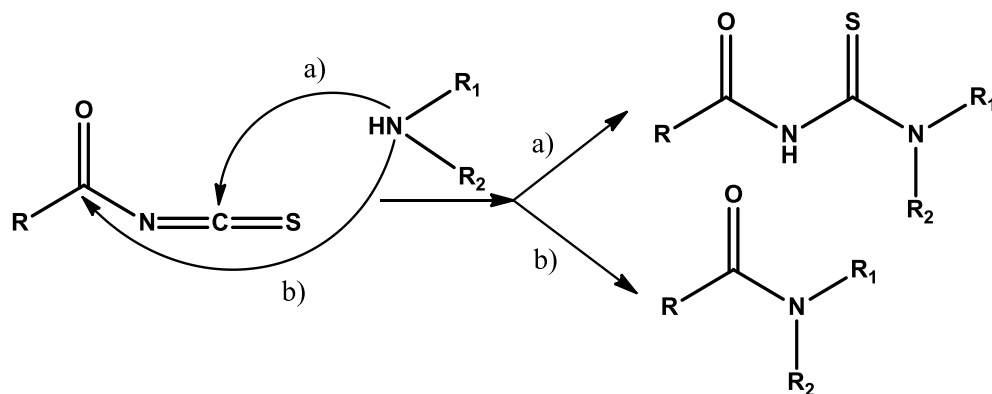
Chapter 2 | Synthesis and Characterization

Some side reactions are unavoidable in the synthesis of the acylthiourea ligands. The more common side reaction occurs for the thiocyanate ion especially in the presence of an acyl/aroyl halide resulting in S-acylation, although *N*-acylation is exclusively favoured.¹⁰⁶ The two possible reactions are shown in **scheme 2.2**.



Scheme 2.2. The two possible means of nucleophilic attack of the thiocyanate ion resulting in either a) S-acylation or b) *N*-acylation although last mentioned is generally favored.

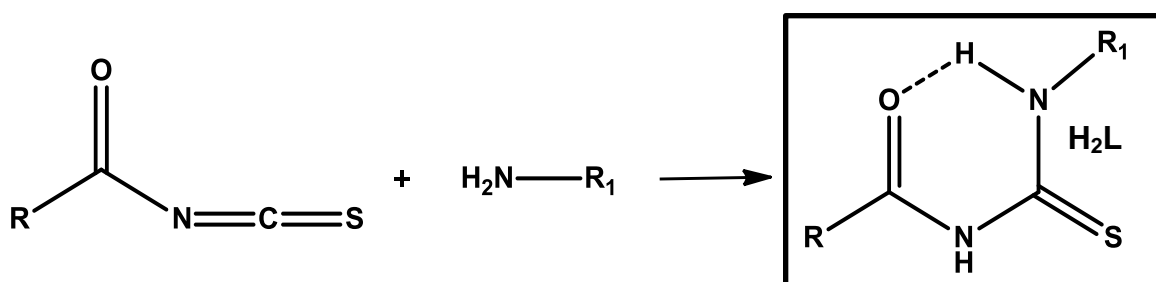
The second step of the reaction shown in **scheme 2.1** is also prone to side reactions, where the nucleophilic amine group reacts with the carbonyl carbon instead of the thiocarbonyl carbon. The likelihood of this side reaction depends on the electrophilic nature of the carbonyl carbon, which can either increase or decrease depending on the electron withdrawing or releasing ability of the R group respectively. This is illustrated in **scheme 2.3**. The reaction route a) is thereby favored in the presence of bulky alkyl/aryl R groups directing nucleophilic attack towards the thiocarbonyl carbon.



Scheme 2.3. Nucleophilic attack of the amine group at the a) thiocarbonyl carbon or b) carbonyl carbon.

Chapter 2 | Synthesis and Characterization

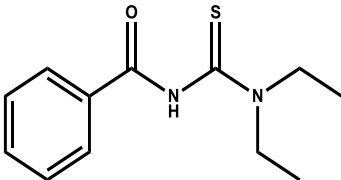
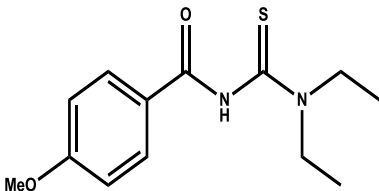
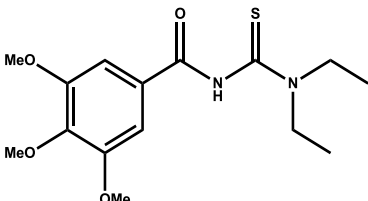
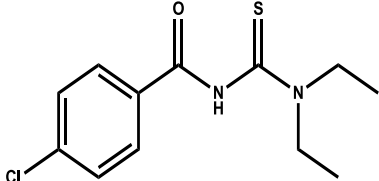
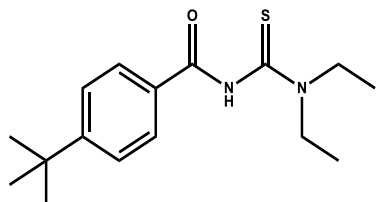
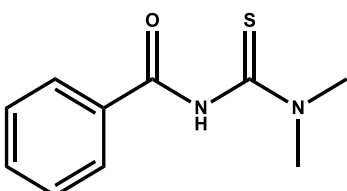
The general reaction scheme as shown in **scheme 2.1** can be employed for both mono- or dialkyl substituted (HL and H₂L) thiourea ligands, although the mono substituted ligands adopt a structural conformation considerably different from that of the disubstituted ligands. In the case of the former, the C=O and C=S are in an antiperiplanar orientation which allows for intramolecular interaction between the proton of the secondary amine and the oxygen of the carbonyl group, thereby forming a pseudo-six membered ring (**Scheme 2.4**). This conformation effects the manner in which these ligands will resultantly coordinate to the metal center, where the disubstituted ligands coordinate *via* the chelating mode (O,S) and the mono substituted ligands coordinate *via* the neutral monodentate mode (S). An example of this type of coordination is available in the literature⁵⁶, but for the purpose of this project, only the former type of coordination will be of interest.



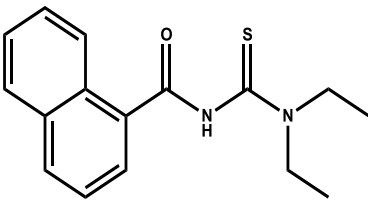
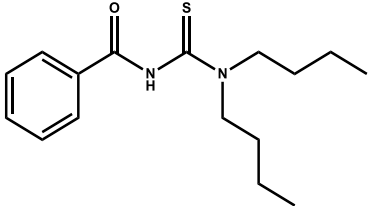
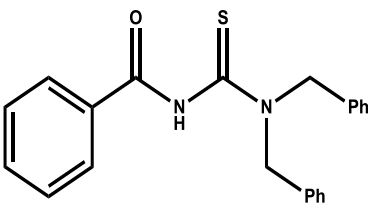
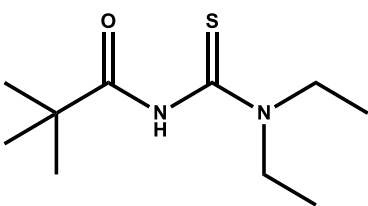
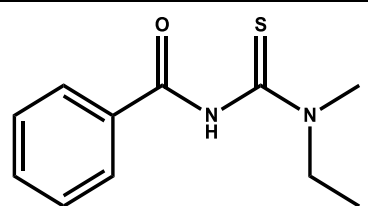
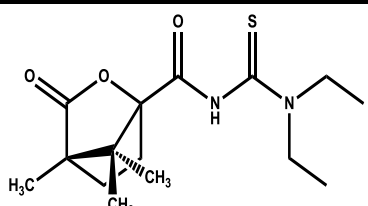
Scheme 2.4. The by-product H₂L is formed upon addition of a primary amine to the second step of the reaction in scheme 2.1.

Chapter 2 | Synthesis and Characterization

Table 2.1. Summary of all acylthiourea ligands used for coordination to Co(III).

Ligand Name	Structure	Chemical Formula and some elemental analysis results	Abbreviation and some melting points
<i>N,N</i> -diethyl- <i>N'</i> -benzoylthiourea		$C_{12}H_{16}OSN_2$	HL ¹ *
<i>N,N</i> -diethyl- <i>N'</i> -4-methoxybenzoylthiourea		$C_{13}H_{18}O_2SN_2$	HL ² *
<i>N,N</i> -diethyl- <i>N'</i> -3,4,5-trimethoxybenzoylthiourea		$C_{15}H_{22}O_4SN_2$	HL ³ *
<i>N,N</i> -diethyl- <i>N'</i> -4-chlorobenzoylthiourea		$C_{12}H_{15}OSN_2Cl$	HL ⁴ *
<i>N,N</i> -diethyl- <i>N'</i> -4-tertbutylbenzoylthiourea		$C_{16}H_{24}OSN_2$ % C: 65.03 % H: 8.2 % N: 9.42 % S: 10.6	HL ⁵ 90.3-91.5 °C.
<i>N,N</i> -dimethyl- <i>N'</i> -benzoylthiourea		$C_{10}H_{12}OSN_2$	HL ⁶ *

Chapter 2 | Synthesis and Characterization

<i>N,N</i> -diethyl- <i>N'</i> -naphthoylthiourea		$C_{16}H_{18}OSN_2$	HL ⁷ *
<i>N,N</i> -dibutyl- <i>N'</i> -benzoylthiourea		$C_{16}H_{24}OSN_2$	HL ⁸ *
<i>N,N</i> -dimethylphenyl- <i>N'</i> -benzoylthiourea		$C_{22}H_{20}OSN_2$	HL ⁹ *
<i>N,N</i> -diethyl- <i>N'</i> -pivaloylthiourea		$C_{10}H_{20}OSN_2$	HL ¹⁰ *
<i>N</i> -methyl- <i>N</i> -ethyl- <i>N'</i> -benzoylthiourea		$C_{11}H_{14}OSN_2$ % C: 59.6 % H: 6.18 % N: 12.46 % S: 13.81	HL ¹¹ 83.2-84.9 °C
(1 <i>S</i>)-(-)- <i>N,N</i> -diethyl- <i>N'</i> -camphanoylthiourea		$C_{15}H_{24}O_3SN_2$ % C: 57.2 % H: 7.19 % N: 9.02 % S: 10.41	HL ¹² 142-143 °C

*ligands synthesized by previous students

Most of the ligands were available for the coordination reaction, considering they were synthesized by previous students from the PGM group of Stellenbosch University and therefore only a selected few acylthiourea ligands were synthesized (HL⁵, HL¹¹ and HL¹²) in this study and furthermore characterized by means of ¹H NMR, ¹³C NMR, elemental analysis and melting point determinations.

Chapter 2 | Synthesis and Characterization

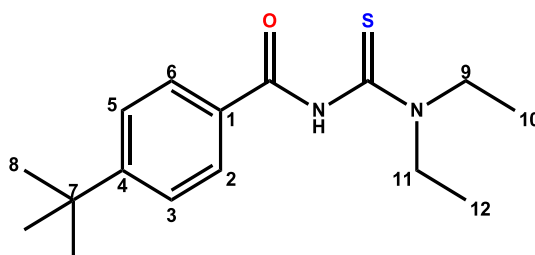
2.1.2. Spectroscopic characterization of synthesized acylthiourea ligands

By means of Nuclear Magnetic Resonance Spectroscopy, one dimensional ^1H and ^{13}C NMR spectra were obtained of the ligands synthesized as well as corresponding Co(III) complexes. All compounds were dissolved in CDCl_3 and placed in 5 mm NMR tubes with temperature kept constant at 25°C . All chemical shift values obtained were referenced relative to the internal standard tetramethylsilane (TMS) and samples were run on a Varian Unity INOVA 600 MHz, Varian INOVA 400 MHz or a Varian VXR 300 MHz spectrometer. These instruments were operating respectively at 600, 400 or 300 MHz for ^1H and 150, 100 or 75 MHz for ^{13}C spectra.

Spectra obtained from infrared spectroscopy were measured on a NEXUS FT-IR, custom-made by Thermo Nicolet Instruments. In order to run infrared spectra of all compounds, Potassium bromide pellets was used and the range kept consistent at $4000\text{--}400\text{ cm}^{-1}$. The standard resolution used was 4 cm^{-1} and represented data point spacing of slightly less than 2 cm^{-1} . The instrument was fitted with a Ge-on-KBr beamsplitter and made use of a DTSG/CsI detector. Nitrogen gas was purged through the instrument during recording of data, and made use of the OMNIC package for data manipulation.

All elemental analyses data were obtained *via* a Carlo Erba EA 1108 Elemental Analyser which was available in the microanalytical laboratory from the University of Cape Town. All melting points determined were attained by an Electrothermal 9300 Digital Melting point Apparatus.

1. *N,N*-diethyl-*N'*-4-tertbutylbenzoylthiourea: HL⁵

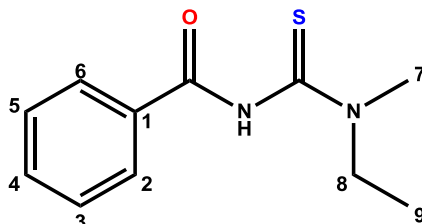


Recrystallised yield 85%; Melting Point: $90.3\text{--}91.5^\circ\text{C}$. Found: C, 65.03; H, 8.2; N, 9.42; S, 10.6 %. $\text{C}_{16}\text{H}_{24}\text{OSN}_2$ requires C, 65.7; H, 8.3; N, 9.6; S, 11.0. ^1H NMR δ_{H} (400 MHz, CDCl_3/ppm): 1.27–1.40 (m, 15H, C(8)H, C(10)H & C(12)H), 3.61 (s, 2H, C(9)H), 4.04 (s, 2H, C(11)H), 7.49 (d, 2H, $^3J_{\text{HH}} = 8.6$, C(2)H & C(6)H), 7.78 (d, 2H, $^3J_{\text{HH}} = 8.6$, C(3)H & C(5)H), 8.18

Chapter 2 | Synthesis and Characterization

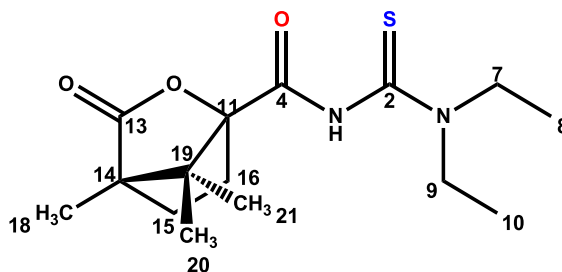
(s, 1H, N(H)). $^{13}\text{C}\{^1\text{H}\}$ NMR δ_{C} (400 MHz, CDCl_3 /ppm): 179.49 (C(S)), 163.70 (C(O)), 156.84 (C1), 129.91 (C3 & C5), 127.77 (C2 & C6), 125.91 (C4), 48.11 (C9), 47.85 (C11), 35.26 (C7), 31.09 (C8), 13.48 (C10), 11.50 (C12).

2. *N*-methyl-*N*-ethyl-*N'*-benzoylthiourea: HL¹¹



Recrystallised yield 90%; Melting Point: 83.2-84.9 °C. Found: C, 59.6; H, 6.18; N, 12.46; S, 13.81 %. $\text{C}_{11}\text{H}_{14}\text{OSN}_2$ requires C, 59.4; H, 6.3; N, 12.6; S, 14.4. ^1H NMR δ_{H} (400 MHz, CDCl_3 /ppm): 1.29 and 1.36 (t, 3H, $^3J_{\text{HH}} = 6.9$, C(7)H), 3.21 and 3.45 (s, 3H, C(9)H), 3.63 and 4.0 (quartet, 2H, C(8)H), 7.48 (t, 2H, $^3J_{\text{HH}} = 7.8$, C(3)H & C(5)H), 7.58 (t, 1H, $^3J_{\text{HH}} = 7.6$, C(4)H), 7.84 (d, 2H, $^3J_{\text{HH}} = 7.4$, C(2)H & C(6)H), 8.37 (s, 1H, N(H)). $^{13}\text{C}\{^1\text{H}\}$ NMR δ_{C} (400 MHz, CDCl_3 /ppm): 179.20 (C(S)), 163.11 (C(O)), 132.81 (C1), 132.36 (C4), 128.72 (C3 & C5), 127.63 (C2 & C6), 51.08 and 50.23 (C8), 40.89 and 39.91 (C7), 12.80 and 10.71 (C9).

3. (1*S*)-(-)-*N,N*-diethyl-*N'*-camphanoylthiourea: HL¹²



Recrystallised yield 81%; Melting Point: 142-143 °C. Found: C, 57.2; H, 7.19; N, 9.02; S, 10.41 %. $\text{C}_{15}\text{H}_{24}\text{O}_3\text{SN}_2$ requires C, 57.7; H, 7.7; N, 9.0; S, 10.3. ^1H NMR δ_{H} (400 MHz, CDCl_3 /ppm): 1.01 (s, 3H, C(21)H), 1.10 – 1.12 (m, 6H, C(20)H and C(18)H), 1.29 (s, 6H, C(8)H and C(10)H), 1.68 – 1.75 (m, 1H, C(15a)H), 1.93 – 2.02 (m, 2H, C(16a)H and C(15b)H), 2.46 – 2.53 (m, 1H, C(16b)H), 3.54 (s, 2H, C(7)H), 3.96 (s, 2H, C(9)H), 8.36 (s, 1H, N(H)). $^{13}\text{C}\{^1\text{H}\}$ NMR δ_{C} (400 MHz, CDCl_3 /ppm): 177.45 (C(S)), 177.42 (C13), 164.23 (C(O)), 92.04 (C11), 55.68 (C14), 55.22 (C19), 48.24 (C7), 47.77 (C9), 30.51 (C15), 29.14 (C16), 16.90 (C20), 16.85 (C21), 13.51 (C8), 11.57 (C10), 9.86 (C18).

Chapter 2 | Synthesis and Characterization

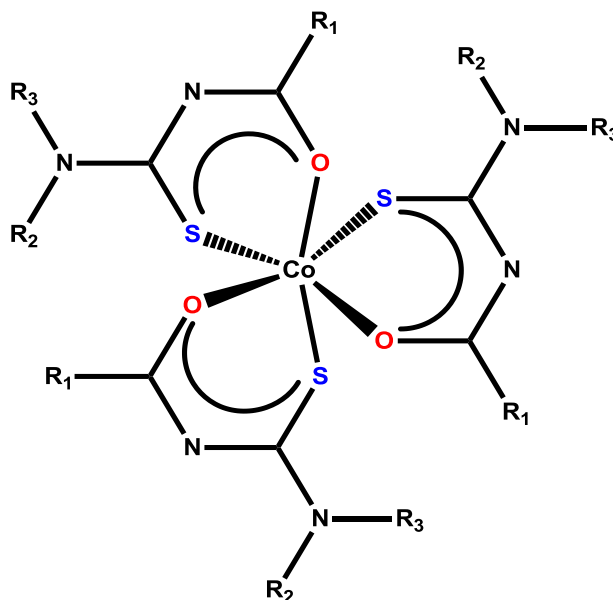
2.1.3. Synthesis of tris(*N,N*-dialkyl-*N'*-aroyl(acyl)thioureato)Co(III) complexes: [Co(L-S,O)₃]

Figure 2.1. General structure of tris(*N,N*-dialkyl-*N'*-aroyl(acyl)thioureato)Co(III) complexes.

The synthetic method used for the Co(III) complexes (illustrated in **Figure 2.2**) are similar to those previously used in literature with minor variations in methodology.⁶⁷ A solution of Cobalt(II) Chloride hexahydrate dissolved in ethanol is added dropwise to the specific acylthiourea derivative, in a 1:3 ratio, which could be dissolved in either ethanol or acetonitrile. The choice of solvent for the acylthiourea derivative depended on the solubility of the ligand. Sodium acetate dissolved in a small amount of water is then added to the ligand solution prior to addition of the Co(II) chloride, with the purpose of deprotonating the amidic proton. The solution is then stirred for approximately 30 min to 1 hour after which a dark green precipitate is visible. This is transferred to a beaker, where DCM would be used to wash out any leftover product still in the reaction flask. The solvents are allowed to evaporate overnight, after which the crude product would be recrystallized by means of a non-polar mixture such as dichloromethane/ethanol in a 1:1 ratio. The recrystallization procedure is in certain cases repeated until a pure product is obtained.

Chapter 2 | Synthesis and Characterization

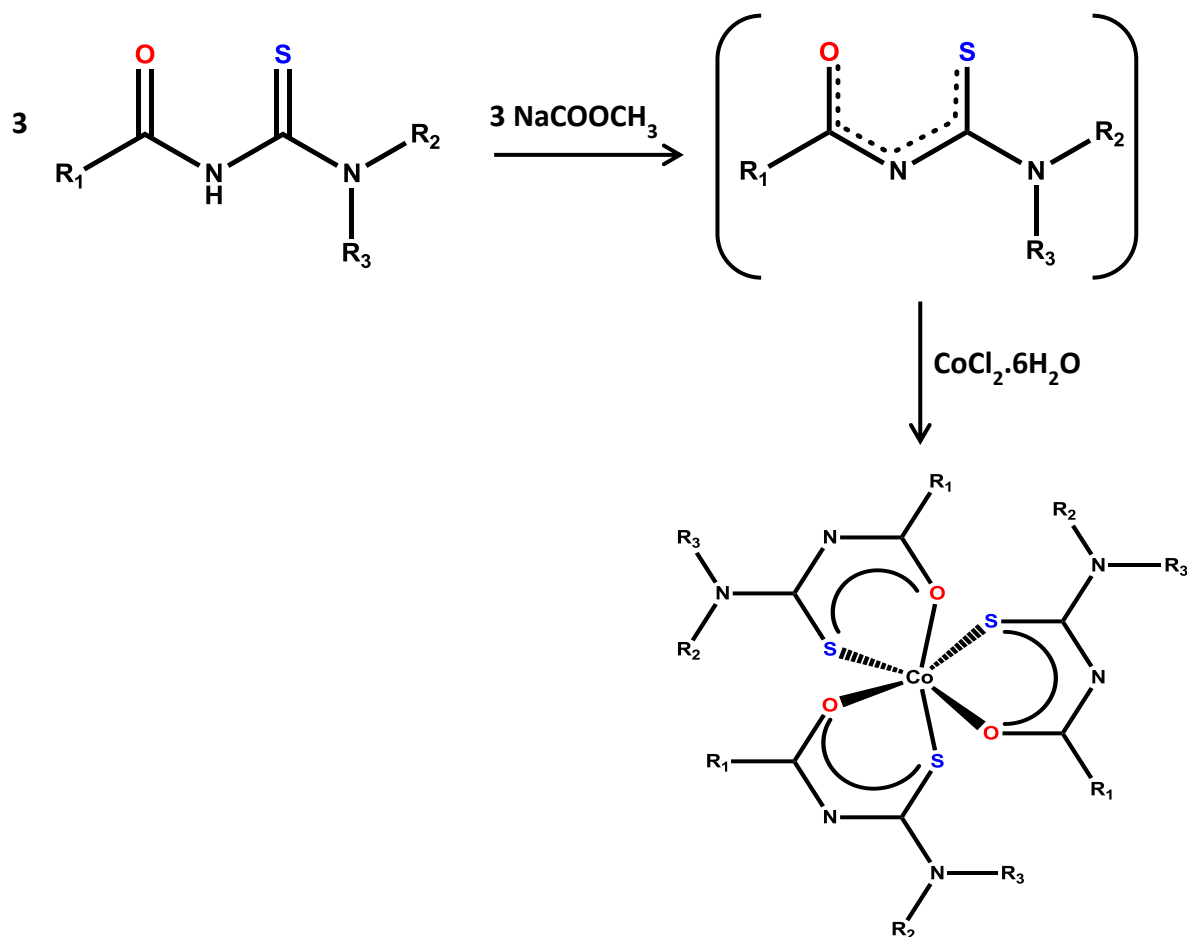


Figure 2.2. Reaction scheme for the coordination reaction of the acylthiourea derivative to Co(III).

During deprotonation of the amidic proton, the negative charge of the thioureato anion intermediate becomes delocalised onto the central thioureato group, shown in brackets in **Figure 2.2**. This step is crucial for the coordination of the ligand to the Co(III) ion. Due to the presence of hard and soft donor atoms in the ligands, it allows for a large bonding variety and thus different modes of coordination. For Co(III), coordination occurs according to the monobasic bidentate mode *via* the sulphur and oxygen donor atoms.

The addition of the Co(II) salt to the ligand solution can consequently be summarized by two important events namely; the oxidation of Co(II) to Co(III) by means of atmospheric O_2 and then finally chelation of three ligand anions to the Co(III) center with each coordinating in the bidentate (S,O) anion mode. This mode of coordination gives rise to the octahedral geometry in which the S and O atoms occupy the same face of the octahedron, i.e. the *fac* isomer, respectively. This is later on verified by means of X-ray crystallography (see Chapter 3).

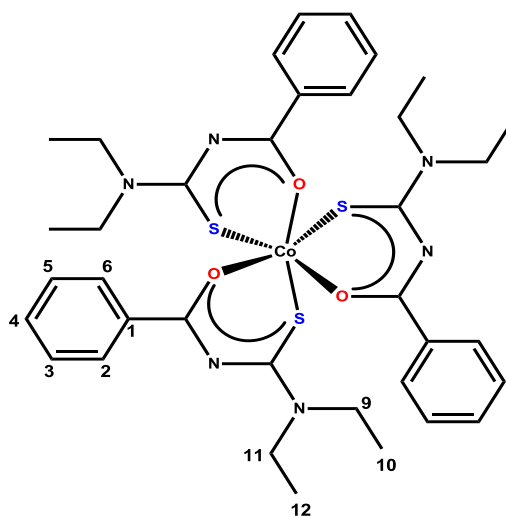
Chapter 2 | Synthesis and Characterization

2.2.4. Spectroscopic characterization of synthesized Co(III) complexes

Characterization of the complexes were done by means of ^1H and ^{13}C nuclear magnetic resonance spectroscopy, infrared spectroscopy, elemental analysis, melting point analysis and in some cases X-ray crystallographic images were obtained from suitable single crystals.

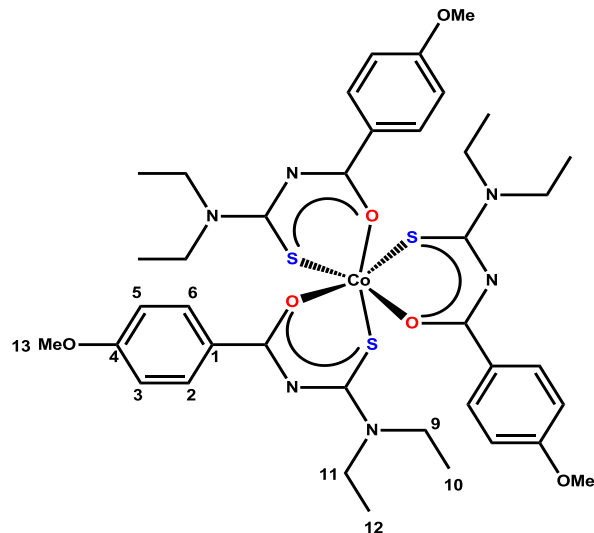
All necessary information regarding how characterization of Co(III) complexes were achieved are mentioned in **section 2.2.2**.

1. *fac*-tris(*N,N*-diethyl-*N'*-benzoylthioureato)cobalt(III): *fac*-[Co(L¹-S,O)₃]



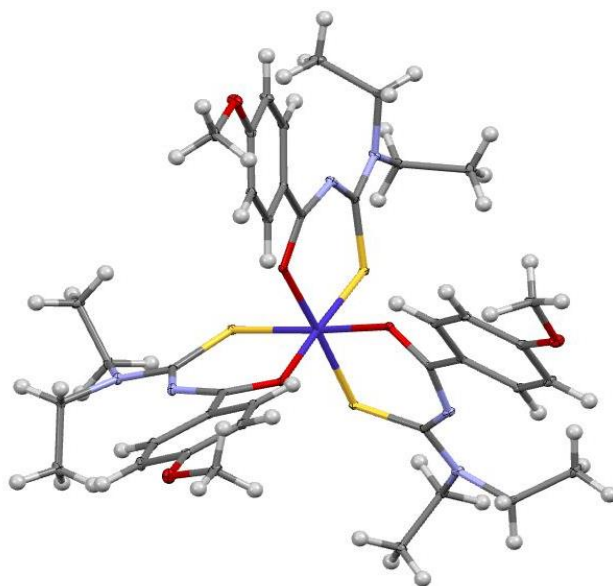
Recrystallised yield 84%; Melting Point: 173.2-174.9 °C. Found: C, 53.2; H, 5.89; N, 9.68; S, 11.01 %. $\text{CoC}_{36}\text{H}_{45}\text{O}_3\text{S}_3\text{N}_6 \cdot \text{H}_2\text{O}$ requires C, 54.2; H, 5.81; N, 10.5; S, 12.1. ^1H NMR δ_{H} (400 MHz, CDCl_3/ppm): 1.18 (t, 3H, $^3J_{\text{HH}} = 6.9$, C(12)H), 1.25 (t, 3H, $^3J_{\text{HH}} = 6.9$, C(10)H), 3.70 - 3.94 (m, 4H, C(9)H & C(11)H), 7.28 (t, 2H, $^3J_{\text{HH}} = 7.14$, C(3)H & C(5)H), 7.39 (t, 1H, $^3J_{\text{HH}} = 7.7$, C(4)H), 8.16 (d, 2H, $^3J_{\text{HH}} = 7.8$, C(2)H & C(6)H). $^{13}\text{C}\{^1\text{H}\}$ NMR δ_{C} (400 MHz, CDCl_3/ppm): 175.61 (C(S)), 175.15 (C(O)), 139.22 (C1), 131.32 (C4), 129.96 (C2 & C6), 127.92 (C3 & C5), 46.07 (C9), 45.87 (C11), 13.70 (C10), 13.42 (C12).

Chapter 2 | Synthesis and Characterization

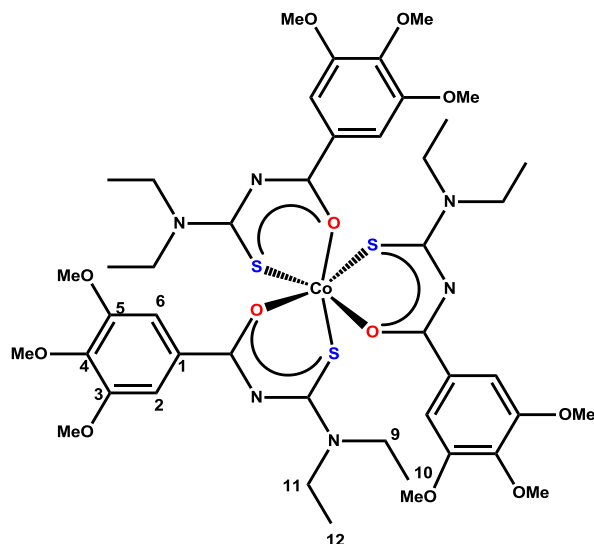
2. *fac*-tris(*N,N*-diethyl-*N'*-4-methoxybenzoylthioureato)cobalt(III): *fac*-[Co(L²-S,O)₃]

Recrystallised yield 75%; Melting Point: 181.5-182.5 °C. Found: C, 55.52; H, 6.65; N, 9.35; S, 10.09 %. $\text{CoC}_{39}\text{H}_{51}\text{O}_6\text{S}_3\text{N}_6$ requires C, 54.78; H, 6.0; N, 9.83; S, 11.3. ^1H NMR δ_{H} (400 MHz, CDCl_3/ppm): 1.17 (t, 3H, $^3J_{\text{HH}} = 7.0$, C(12)H), 1.24 (t, 3H, $^3J_{\text{HH}} = 7.13$, C(10)H), 3.82 (m, 7H, C(9)H, C(11)H & C(13)H), 6.78 (d, 2H, $^3J_{\text{HH}} = 9.14$, C(2)H & C(6)H), 8.13 (d, 2H, $^3J_{\text{HH}} = 8.89$, C(3)H & C(5)H). $^{13}\text{C}\{^1\text{H}\}$ NMR δ_{C} (400 MHz, CDCl_3/ppm): 174.71 (C(S)), 174.14 (C(O)), 161.74 (C4), 131.90 (C1), 131.22 (C3 and C5), 112.43 (C2 and C6), 45.31 (C9), 45.07 (C11), 13.14 (C10), 12.84 (C12).

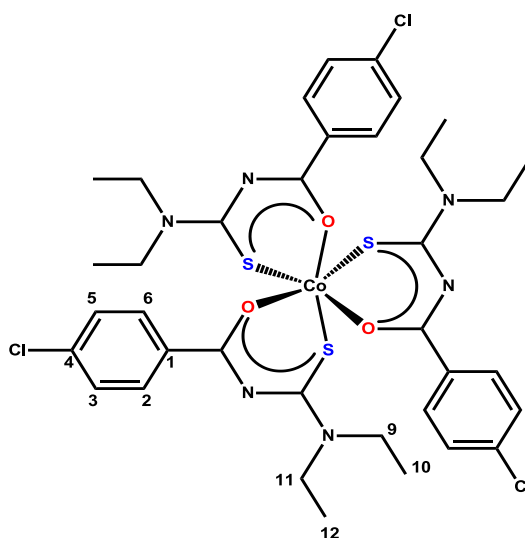
Crystal Structure (See Chapter 3 for further discussion)



Chapter 2 | Synthesis and Characterization

3. *fac*-tris(*N,N*-diethyl-*N'*-3,4,5-trimethoxybenzoylthioureato)cobalt(III): *fac*-[Co(L³-S,O)₃]

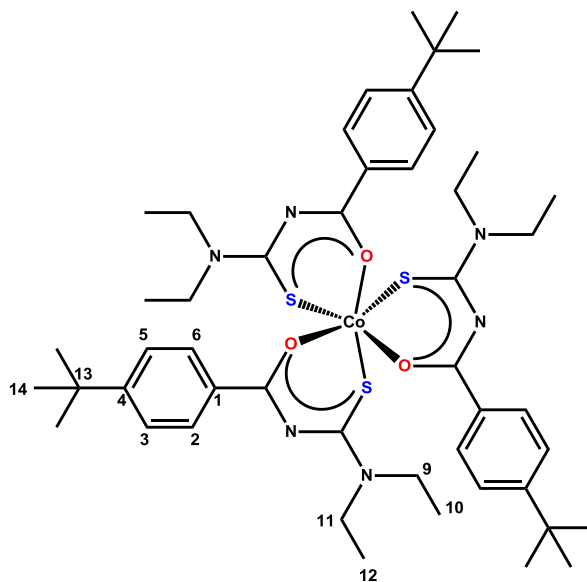
Recrystallised yield 69%; Melting Point: 189.1-191.4 °C. Found: C, 51.95; H, 6.7; N, 7.8; S, 8.67 %. $\text{CoC}_{45}\text{H}_{63}\text{O}_{12}\text{S}_3\text{N}_6$ requires C, 52.2; H, 6.1; N, 8.1; S, 9.3. ^1H NMR δ_{H} (400 MHz, CDCl_3 /ppm): 1.27 (m, 6H, C(10)H & C(12)H), 3.61 (s, 6H, C(3)OCH₃ & C(5)OCH₃), 3.84-3.91 (m, 7H, C(9)H, C(11)H & C(4)OCH₃), 7.50 (s, 2H, C(2)H & C(6)H). $^{13}\text{C}\{^1\text{H}\}$ NMR δ_{C} (400 MHz, CDCl_3 /ppm): 174.62 (C(S)), 174.31 (C(O)), 152.22 (C3 & C5), 140.67 (C4), 134.12 (C1), 106.45 (C2 & C6), 60.73 (C(4)OCH₃), 55.53 (C(3)OCH₃ & C(5)OCH₃), 45.70 (C9), 45.50 (C11), 13.19(C10), 12.90 (C12).

4. *fac*-tris(*N,N*-diethyl-*N'*-4-chlorobenzoylthioureato)cobalt(III): *fac*-[Co(L⁴-S,O)₃]

Chapter 2 | Synthesis and Characterization

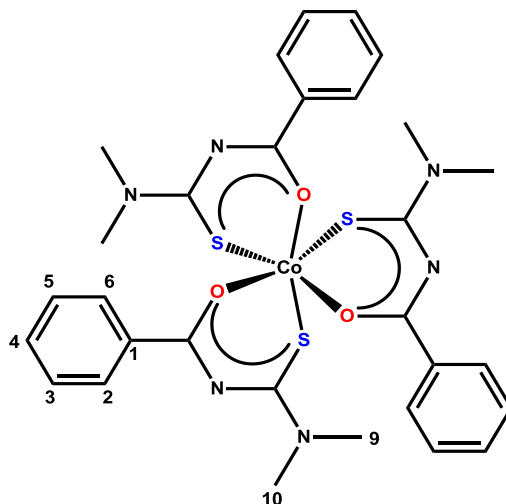
Recrystallised yield 79%; Melting Point: 184.3-186.6 °C. Found: C, 48.92; H, 4.82; N, 8.88; S, 9.9 %. $\text{CoC}_{36}\text{H}_{42}\text{O}_3\text{S}_3\text{N}_6\text{Cl}_3$ requires C, 49.8; H, 4.9; N, 9.7; S, 11.1. ^1H NMR δ_{H} (400 MHz, CDCl_3/ppm): 1.10 (t, 3H, $^3J_{\text{HH}} = 7.3$, C(12)H), 1.17 (t, 3H, $^3J_{\text{HH}} = 7.1$, C(10)H), 3.63-3.83 (m, 4H, C(9)H & C(11)H), 7.24 (d, 2H, $^3J_{\text{HH}} = 8.2$, C(2)H & C(6)H), 8.05 (d, 2H, $^3J_{\text{HH}} = 8.34$, C(3)H & C(5)H). $^{13}\text{C}\{^1\text{H}\}$ NMR δ_{C} (400 MHz, CDCl_3/ppm): 174.51 (C(S)), 173.97 (C(O)), 137 (C4), 136.92 (C1), 130.59 (C3 and C5), 127.59 (C2 and C6), 45.31(C9), 45.07 (C11), 13.14(C10), 12.84 (C12).

5. *fac*-tris(*N,N*-diethyl-*N'*-4-tertbutylbenzoylthioureato)cobalt(III): *fac*-[Co(L⁵-S,O)₃]

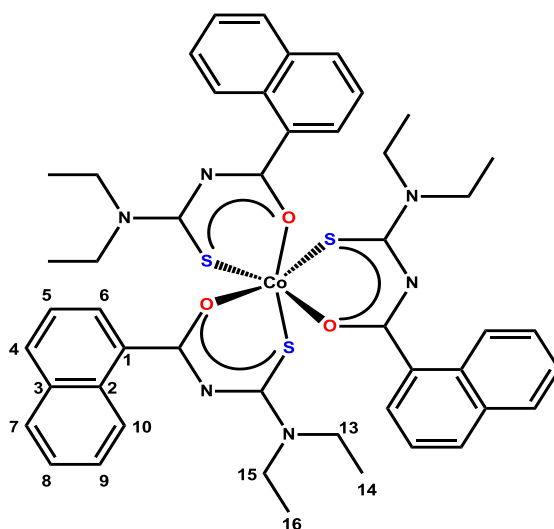


Recrystallised yield 89%; Melting Point: 201.1-201.6 °C. Found: C, 60.85; H, 8.24; N, 8.42; S, 9.6 %. $\text{CoC}_{48}\text{H}_{69}\text{O}_3\text{S}_3\text{N}_6$ requires C, 61.8; H, 7.5; N, 9.0; S, 10.3. ^1H NMR δ_{H} (400 MHz, CDCl_3/ppm): 1.17 (t, 3H, $^3J_{\text{HH}} = 7.1$, C(12)H), 1.22 (t, 3H, $^3J_{\text{HH}} = 7.1$, C(10)H), 1.31 (s, 9H, C(14)H), 3.7 - 3.89 (m, 4H, C(9)H & C(11)H), 7.3 (d, 2H, $^3J_{\text{HH}} = 8.5$, C(2)H & C(6)H), 8.09 (d, 2H, $^3J_{\text{HH}} = 8.5$, C(3)H & C(5)H). $^{13}\text{C}\{^1\text{H}\}$ NMR δ_{C} (400 MHz, CDCl_3/ppm): 175.47 (C(S)), 174.61 (C(O)), 154.21 (C1), 136.36 (C3 & C5), 129.49 (C2 & C6), 124.53 (C4), 45.62 (C9), 45.38 (C11), 34.87 (C13), 31.41 (C14), 13.38 (C10), 13.13 (C12).

Chapter 2 | Synthesis and Characterization

6. *fac*-tris(*N,N*-dimethyl-*N'*-benzoylthioureato)cobalt(III): *fac*-[Co(L⁶-S,O)₃]

Recrystallised yield 65%; Melting Point: 161.5-162.5 °C. Found: C, 53.26; H, 5.14; N, 12.3; S, 12.94 %. CoC₃₀H₃₃O₃S₃N₆ requires C, 52.9; H, 4.9; N, 12.3; S, 14.1. ¹H NMR δ_H(400 MHz, CDCl₃/ppm): 3.32 (s, 3H, C(10)H), 3.56 (s, 3H, C(9)H), 7.29 (t, 2H, ³J_{HH} = 7.29, C(3)H & C(5)H), 7.40 (t, 1H, ³J_{HH} = 7.2, C(4)H), 8.19 (t, 2H, ³J_{HH} = 6.8, C(2)H & C(6)H). ¹³C{¹H} NMR δ_C(400 MHz, CDCl₃/ppm): 174.73 (C(S)), 174.31 (C(O)), 137.66 (C1), 130.55 (C4), 128.5 (C2 and C6), 126.53 (C3 and C5), 39.57 (C9), 39.36 (C10).

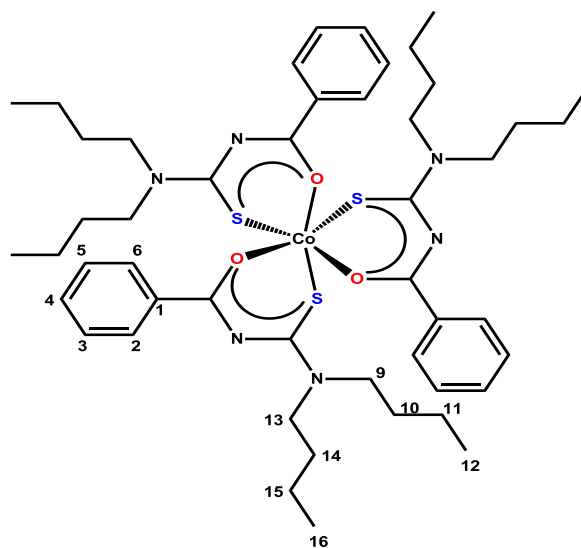
7. *fac*-tris(*N,N*-diethyl-*N'*-naphthoylthioureato)cobalt(III): *fac*-[Co(L⁷-S,O)₃]

Recrystallised yield 72%; Melting Point: 223.2-223.9 °C. Found: C, 63.92; H, 5.71; N, 8.77; S, 9.81 %. CoC₄₈H₅₁O₃S₃N₆ requires C, 63; H, 5.6; N, 9.2; S, 10.51. ¹H NMR δ_H(400 MHz,

Chapter 2 | Synthesis and Characterization

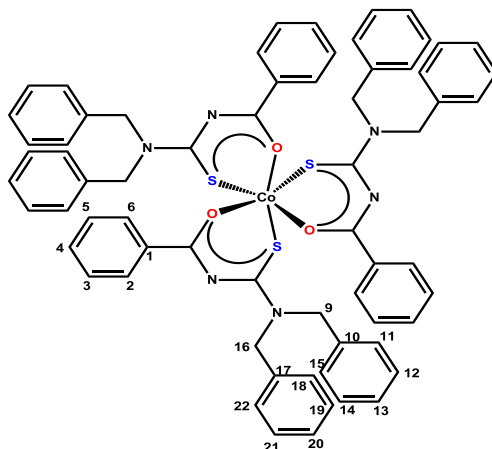
CDCl₃/ppm): 1.02-1.39 (m, 6H, C(14)H & C(16)H), 3.24-4.12 (m, 4H, C(13)H & C(15)H), 6.88 (t, 1H, ³J_{HH} = 6.9, C(5)H), 7.24 (m, 1H, C(8)H), 7.30 (m, 1H, C(9)H), 7.71 (d, 1H, ³J_{HH} = 7.9, C(7)H), 7.80 (d, 1H, ³J_{HH} = 8.5, C(6)H), 8.00 (m, 1H, C(4)H), 8.98 (d, 1H, ³J_{HH} = 7.9, C(10)H). ¹³C{¹H} NMR δ_C(400 MHz, CDCl₃/ppm): 177.21 (C(S)), 176.52 (C(O)), 133.79 (C1), 131.57 (C9), 130.84 (C4), 130.21 (C3), 127.65 (C7), 126.19 (C2), 125.32 (C6), 124.53 (C5), 123.07 (C8), 110 (C10), 51.29 (C13), 49.21 (C15), 13.37 (C14), 13.09 (C16).

8. *fac*-tris(*N,N*-dibutyl-*N'*-benzoylthioureato)cobalt(III): *fac*-[Co(L⁸-S,O)₃]

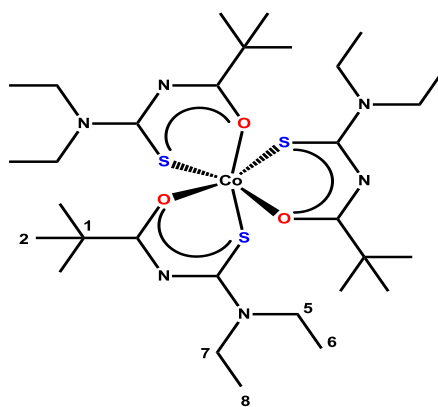


Recrystallised yield 71%; Melting Point: 216.5-217.2 °C. Found: C, 62.57; H, 6.59; N, 8.28; S, 11.88 %. CoC₄₈H₆₉O₃S₃N₆ requires C, 61.8; H, 7.45; N, 9.0; S, 10.3. ¹H NMR δ_H(400 MHz, CDCl₃/ppm): 0.85 (t, 3H, ³J_{HH} = 7.1, C(16)H), 0.94 (t, 3H, ³J_{HH} = 7.1, C(12)H), 1.26 (sextet, 2H, ³J_{HH} = 7.6, C(15)H), 1.38 (sextet, 2H, ³J_{HH} = 7.4, C(11)H), 1.56-1.75 (m, 4H, C(10)H & C(14)H), 3.82 (m, 4H, C(9)H & C(13)H), 7.28 (t, 2H, ³J_{HH} = 7.3, C(3)H & C(5)H), 7.39 (t, 1H, ³J_{HH} = 7.1, C(4)H), 8.17 (d, 2H, ³J_{HH} = 7.3, C(2)H & C(6)H). ¹³C{¹H} NMR δ_C(400 MHz, CDCl₃/ppm): 175.22 (C(S)), 175.11 (C(O)), 138.94 (C1), 130.92 (C4), 129.66 (C2 and C6), 127.58 (C3 and C5), 51.31 (C9), 51.10 (C13), 30.28 (C10), 30.00 (C14), 20.52 (C11), 20.39 (C15), 14.19 (C12), 13.96 (C16).

Chapter 2 | Synthesis and Characterization

9. *fac*-tris(*N,N*-dimethylphenyl-*N'*-benzoylthioureato)cobalt(III): *fac*-[Co(L⁹-S,O)₃]

Recrystallised yield 62%; Melting Point: 233.2-233.9 °C. Found: C, 68.75; H, 5.33; N, 7.22; S, 7.96 %. CoC₆₆H₅₇O₃S₃N₆ requires C, 69.7; H, 5.1; N, 7.39; S, 8.46. ¹H NMR δ_H(400 MHz, CDCl₃/ppm): 5.02 (m, 2H, C(16)H), 5.21 (m, 2H, C(9)H), 7.11-7.48 (m, 13H, C(3)H-C(5)H, C(11)H-C(15)H & C(18)H-C(22)H), 8.25 (d, 2H, ³J_{HH} = 6.72, C(2)H & C(6)H). ¹³C{¹H} NMR δ_C(400 MHz, CDCl₃/ppm): 177.23 (C(S)), 176.56 (C(O)), 138.42 (C1), 136.86 (C10 & C17), 136.11 (C3 & C5), 131.52 (C11 & C15), 129.90 (C18 & C22), 128.73 (C2 & C6), 128.07 (C12 & C14), 127.94 (C19 & C21), 127.59 (C4), 127.44 (C13 and C20), 52.64 (C9), 51.47 (C16).

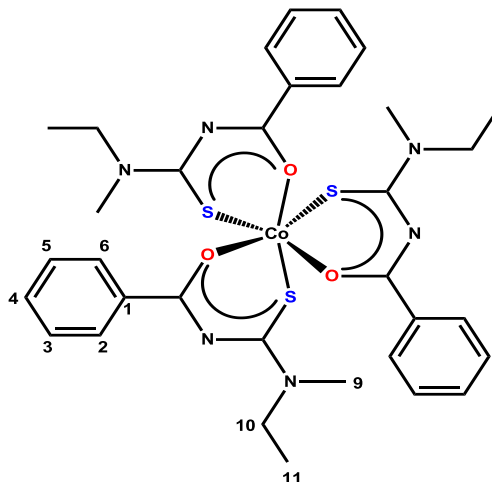
10. *fac*-tris(*N,N*-diethyl-*N'*-pivaloylthioureato)cobalt(III): *fac*-[Co(L¹⁰-S,O)₃]

Recrystallised yield 75%; Melting Point: 191.5-192.8 °C. Found: C, 55.14; H, 5.14; N, 11.6; S, 13.31 %. CoC₃₀H₅₇O₃S₃N₆ requires C, 54.5; H, 5.4; N, 11.6; S, 13.3. ¹H NMR δ_H(400 MHz, CDCl₃/ppm): 1.14 (m, 12H, C(2)H & C(8)H), 1.25 (t, 3H, ³J_{HH} = 7.1, C(6)H), 3.77 (m, 2H, ³J_{HH} = 7.1, C(7)H), 3.92 (m, 2H, ³J_{HH} = 7.1, C(5)H). ¹³C{¹H} NMR δ_C(400 MHz, CDCl₃/ppm):

Chapter 2 | Synthesis and Characterization

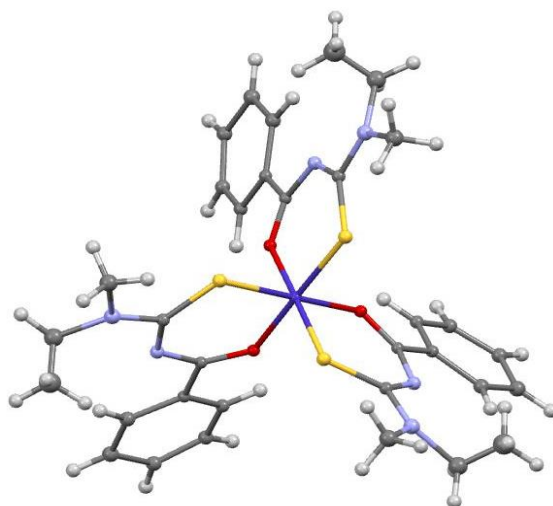
189.31 (C(S)), 174.65 (C(O)), 45.64 (C5), 45.24 (C7), 42.47 (C1), 28.92 (C2), 13.67 (C6), 13.53 (C8).

11. *fac*-tris(*N*-methyl-*N*-ethyl-*N'*-benzoylthioureato)cobalt(III): *fac*-[Co(L¹¹-S,O)₃]

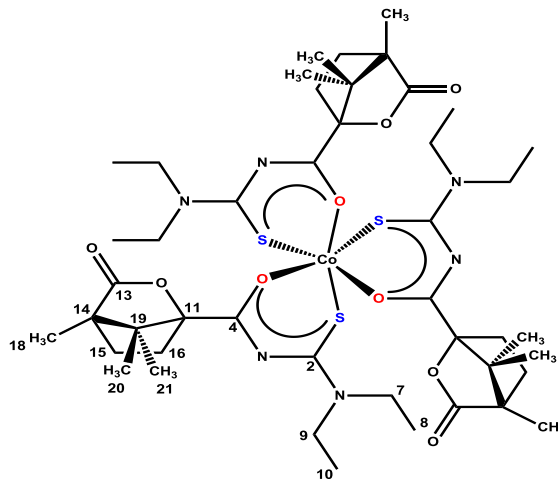


Recrystallised yield 82%; Melting Point: 163.2-164.9 °C. Found: C, 54.2; H, 4.62; N, 12.38; S, 13.72 %. CoC₃₃H₃₉O₃S₃N₆ requires C, 54.8; H, 5.4; N, 11.6; S, 13.3. ¹H NMR δ_H(400 MHz, CDCl₃/ppm): 1.13-1.26 (m, 3H, ³J_{HH} = 6.9, C(11)H), 3.30-3.36 (m, 3H, C(9)H), 3.80 - 4.10 (m, 2H, C(10)H), 7.29 (t, 2H, ³J_{HH} = 7.8, C(3)H & C(5)H), 7.40 (t, 1H, ³J_{HH} = 7.4, C(4)H), 8.18 (m, 2H, ³J_{HH} = 7.8, C(2)H & C(6)H). ¹³C{¹H} NMR δ_C(400 MHz, CDCl₃/ppm): 175.61 (C(S)), 175.15 (C(O)), 139.22 (C1), 132.21 & 131.14 (C2 & C6), 129.75 & 129.72 (C3 & C5), 127.72 & 127.70 (C4), 47.96 & 47.76 (C10), 38.64 & 37.88 (C9), 12.87 & 12.51 (C11).

Crystal Structure (See Chapter 3 for further discussion)

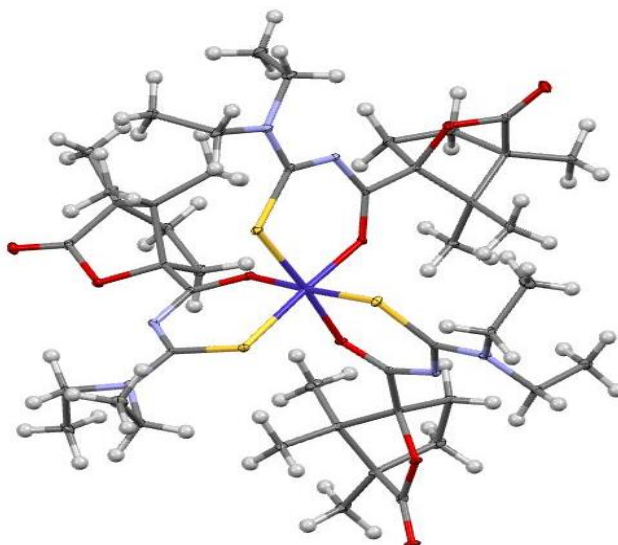


Chapter 2 | Synthesis and Characterization

12. *fac*-tris((1*S*)-(-)-*N,N*-diethyl-*N'*-camphanoylthioureato)cobalt(III): *fac*-[Co(L¹²-S,O)₃]

Recrystallised yield 87%; Melting Point: 226.2-226.9 °C. Found: C, 54.61; H, 7.89; N, 7.75; S, 8.41 %. CoC₄₅H₆₉O₉S₃N₆ requires C, 54.4; H, 7.0; N, 8.5; S, 9.69. ¹H NMR δ_H(400 MHz, CDCl₃/ppm): 0.88 – 1.05 (3, 6H, C(21)H & C(20)H), 1.06 (m, 3H, C(18)H), 1.14 (m, 3H, C(10)H), 1.27 (m, 3H, C(8)H), 1.56 – 1.64 (m, 1H, C(15a)H), 1.78 – 1.92 (m, 2H, C(16a)H & C(15b)H), 2.32 – 2.52 (m, 1H, C(16b)H), 3.51 – 4.01 (m, 4H, C(7)H & C(9)H). ¹³C{¹H} NMR δ_C(400 MHz, CDCl₃/ppm): 179.92 (C13), 175.01 (C(S)), 173.73 (C(O)), 94.36 & 93.96 (C11), 55.38 & 55.36 (C14), 54.41 & 54.31 (C19), 45.73 (C7), 45.59 (C9), 31.46 & 31.13 (C15), 29.58 & 29.43 (C16), 17.37 & 17.32 (C20), 17.00 & 17.82 (C21), 13.22 & 13.19 (C8), 12.94 & 12.90 (C10), 9.98 & 9.94 (C18).

Crystal Structure (See Chapter 3 for further discussion)



CHAPTER THREE

NMR AND OTHER SPECTROSCOPIC CHARACTERIZATION OF ACYLTHIOUREA LIGANDS AND Co(III) COMPLEXES

Chapter 3 | Spectroscopic results

3.1. Spectroscopic results

3.1.1. Spectroscopic discussion of the Co(III) complexes coordinated to symmetrical acylthiourea ligands

¹H NMR spectra of [Co(L-S,O)₃] complexes

When comparing the ¹H NMR spectra of a free ligand with that of a Co(III) complex (**Figure 3.1**), the first noticeable difference is the disappearance of the N-H peak, as seen for the ligand at 8.23 ppm. This occurs during the synthesis by deprotonation of the amidic proton on addition of a suitable base. It can also be identified as the peak with the highest chemical shift attached to an N-atom between the carbonyl and thiocarbonyl groups. All chemical shift values and coupling constants for the free ligand *N,N*-diethyl-*N'*-benzoylthiourea (HL¹) and its corresponding complex tris(*N,N*-diethyl-*N'*-benzoylthioureato)cobalt(III) ([Co(L¹-S,O)₃]) are summarized in **Table 3.1**.

Table 3.1. 400 MHz ¹H NMR chemical shifts of *N,N*-diethyl-*N'*-benzoylthiourea (HL¹) and its corresponding complex tris(*N,N*-diethyl-*N'*-benzoylthioureato)cobalt(III) ([Co(L¹-S,O)₃]) in CDCl₃ at 25 °C.

Compound	¹ H NMR chemical shifts (ppm)										
	N-H	H1	H2	H3	H4	H5	H6	H9	H10	H11	H12
HL ¹	8.23	-	7.84	7.47	7.58	7.47	7.84	4.03	1.37	3.62	1.30
J/Hz (spin coupling)	-	-	7.2	7.9, 7.5	7.4, 7.5	7.9, 7.5	7.2	-	6.0	-	6.0
Multiplicity	S*	-	D*	T*	T	T	D	S	S	S	S
Co(L ¹ -S,O) ₃	-	-	8.16	7.28	7.39	7.28	8.16	3.83	1.25	3.83	1.18
J/Hz (spin coupling)	-	-	7.10	7.7	7.2, 7.1	7.7	7.10	-	7.1, 7.0	-	7.0, 7.0
Multiplicity	-	-	D	T	T	T	D	M*	T	M	T

* D, T, S and M short for doublet, triplet, singlet and multiplet respectively

Chapter 3 | Spectroscopic results

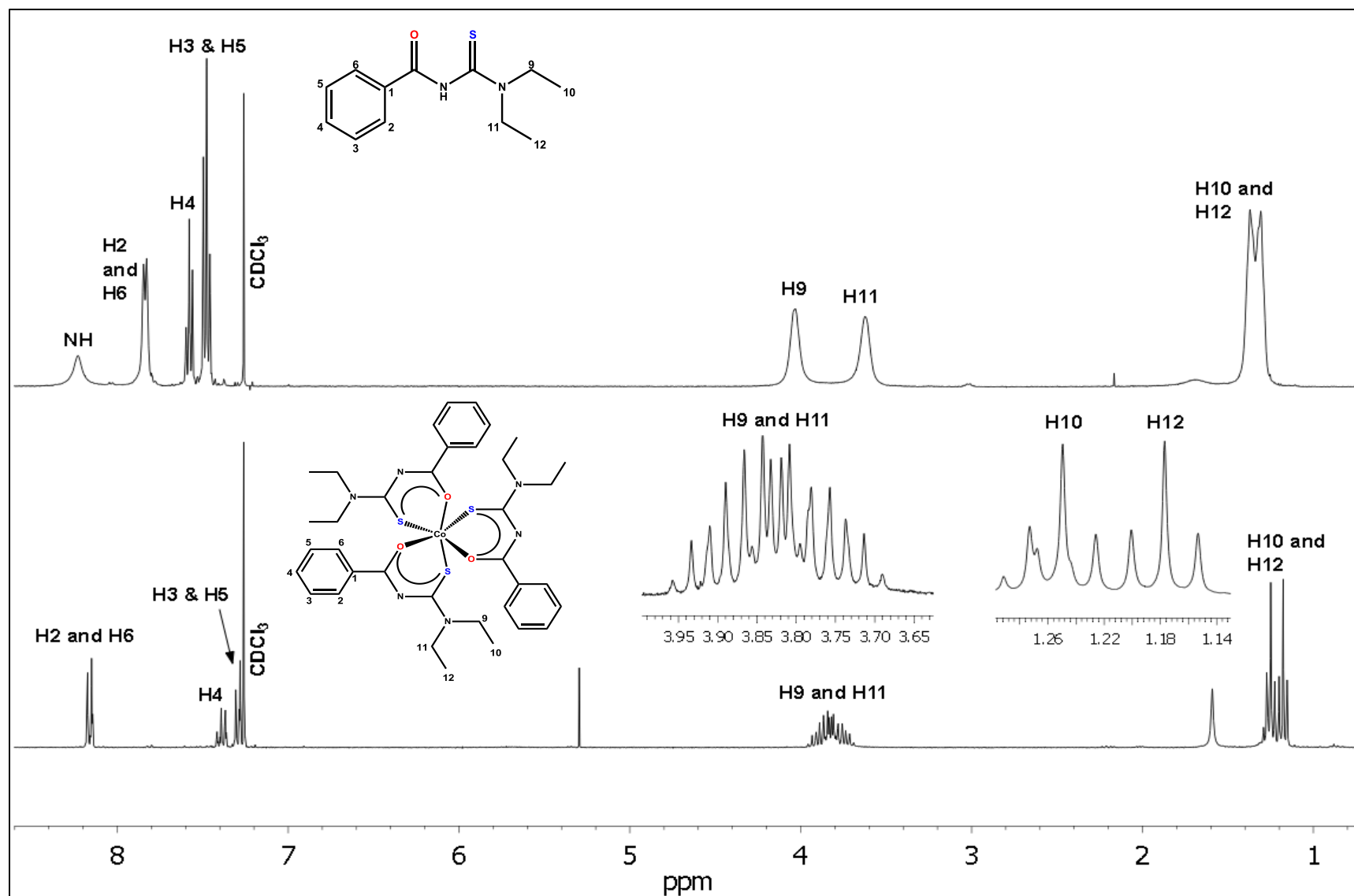


Figure 3.1. The 400 MHz ^1H spectra in CDCl_3 at 25 °C showing differences and similarities between the free ligand *N,N*-diethyl-*N'*-benzoylthiourea and its corresponding complex *tris*(*N,N*-diethyl-*N'*-benzoylthiourea)cobalt(III).

Chapter 3 | Spectroscopic results

In **Figure 3.1**, the methyl and methylene protons (H9-H12) of the thioamide group appear as two separate peaks in the spectra instead of one. This is a consequence of the ‘restricted’ rotation about the partial double bond between the thiocarbonyl carbon and tertiary nitrogen, resulting in separate signals in the ^1H and ^{13}C NMR spectra. The restricted rotation around this bond is brought on by the delocalization of electrons from the amine into the thiocarbonyl functionality of the thiourea group. The lone pair of electrons from the nitrogen atom is partially delocalised into the thiourea moiety as shown in **Figure 3.2**

The ligand can be thought as two resonance structures. Assignment of the ^1H NMR peaks is based on the assumption that protons nearest to sulphur is less shielded compared to those protons antiperiplanar to the sulphur. Hence the protons H9 and H10 were assigned as the peaks with higher chemical shift values than protons H11 and H12 respectively (**Figure 3.1**).

The phenomenon of restricted rotation and its consequence on NMR signals is not a recent concept and requires careful consideration when justifying the spectra of some of these acylthiourea ligands and their corresponding Co(III) complexes. The concept was previously discussed by Stewart and Siddall¹⁰⁷ in 1970, who conducted an extensive review on the consequence of restricted rotation on the resonance signals of amides. This study focused on the partial double bond character and subsequent restricted rotation present in an amide bond $[\text{C}(\text{O})\text{-N}]$, suggested in this review to be as a consequence of the two resonance structures I and II shown in **Figure 3.2**. The significance of this restricted rotation being: (1) the geometric and magnetic non-equivalence of the nitrogen substituents even where $\text{R}_1 = \text{R}_2$, and (2) secondly long-range coupling from R to R_1 or R_2 ; (3) a large rotational barrier about the amidic bond.

A later theoretical study by Wiberg *et al.*¹⁰⁸ showed that such two resonance structures do not sufficiently account for the nature of electronic interactions, which ultimately determines the rotational barrier in amides. Therefore the inclusion of a third resonance structure, III in **Figure 3.2**, was suggested which involves a charge transfer between the carbon and nitrogen atoms. Thioamides were shown by Wiberg *et al.* to have a higher rotational barrier than amides which is thought to be dominated by the charge transfer from nitrogen to sulphur (as opposed to oxygen), substantiated by a number of studies¹⁰⁹⁻¹¹¹. The higher rotational barrier for thioamides consequently enhances any effects of restricted rotation seen in the ^1H NMR spectra of such molecules.

Chapter 3 | Spectroscopic results

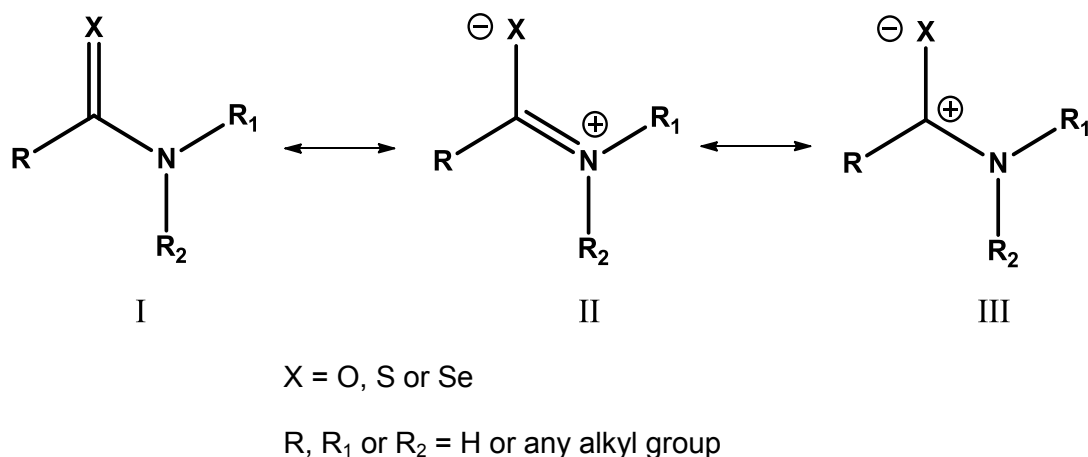


Figure 3.2. All possible resonance structures resulting from the partial double bond character of the [C(X)-N] bond^{107,108}

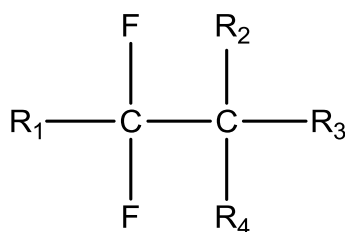
Coordination of the acylthiourea ligand to Co(III) leads to various subtle and distinct differences between the resultant ^1H NMR spectra of the two compound, attributed to a number of factors. One of these factors considers the lowering of the rotational barrier between the thiocarbonyl carbon and tertiary amine upon coordination. It is speculated that this is because electron density from this bond is drawn away due to donation of electron density to the metal centre, slightly decreasing the double bond character about this bond. The consequence is a difference in the relative broadness of the exchanging ^1H NMR peaks observed for the free ligand compared to the coordinated Co(III) complex, although restricted rotation is maintained in both. In the Co(III) complexes, the ^1H peaks of the H10 and H12 triplets and the overlapping multiplets of the H9 and H11 protons, **Figure 3.1**, are much better resolved compared to the ligands.

The sharpness of the ^1H NMR spectrum furthermore confirms that the Co(III) complex is in a low spin electron configuration, considering there are no evidence of peak broadening brought on by unpaired electrons. The sterically crowded environment of the ligand in the octahedral geometry of the Co(III) complex also inhibits molecular motion, placing the phenyl rings close to the thioamide group, $N\text{-CH}_2\text{CH}_3$, resulting in a clear ^1H NMR spectrum. This probably inhibits rotation about the thioamide group, leaving it in the limit of slow exchange by lack of rotation. Also, some protons are shielded either more or less in the complex than in the free ligand. This will depend on the specific orientation of the protons as they appear in the complex, where protons of the phenyl group H2 and H6 are less shielded, but protons H3, H4 and H5 are more shielded when compared to the same peaks for the free ligand. These ^1H NMR trends are

Chapter 3 | Spectroscopic results

similar for these protons in the ^1H NMR spectra of other complexes $\text{fac}[\text{Co}(\text{L}^2\text{-S},\text{O})_3]$, $\text{fac}[\text{Co}(\text{L}^4\text{-S},\text{O})_3]$ and $\text{fac}[\text{Co}(\text{L}^5\text{-S},\text{O})_3]$ when compared to their respective unbound ligands. In the case of $\text{fac}[\text{Co}(\text{L}^3\text{-S},\text{O})_3]$, the peak that represents the two phenyl protons has a higher chemical shift upon coordination, attributed to the magnetic anisotropy present in the coordination sphere (see Appendix A).

Another factor to be considered is that of diastereotopicity, which is used to justify the peculiar multiplicity seen for the methylene protons of the Co(III) complex at 3.83 ppm in **Figure 3.1**, not seen for the free ligand. Nair and Roberts¹¹² were the first to observe the effect of diastereotopicity in Nuclear Magnetic Resonance spectrometry when studying the resonance spectra of *gem*-difluoro compounds (**Figure 3.3**).



Difluoro compound nr.	R ₁	R ₂	R ₃	R ₄
1	Br	H	Cl	Br
2	Br	F	Cl	Br
3	Br	H	Br	C ₆ H ₆
4	Cl	H	Cl	C ₆ H ₆

Figure 3.3. Example of non-equivalent fluorine atoms in certain *gem*-difluoro compounds (adapted from reference 112).

The authors observed diastereotopicity in the presence of restricted rotation about the C-C bond, the *gem*-fluorines being non-equivalent, contrary to what was seen for the freely rotating compounds. They concluded that as a result of restricted rotation, the residence time, i.e. the average amount of time the compound will spend in a particular spacial orientation, of each configuration are not equal and will ultimately lead to different chemical shift values for the two fluorines. Such chemical shift differences do not occur for sterically uncrowded symmetrical compounds, since rapid rotation around these bonds result in similar residence times for the different configurations. This is one of the more common examples where diastereotopic atoms are present as a result of asymmetry in the compound.

There are more subtle examples of diastereotopicity, which appear when you have a compound with no asymmetric centers, but diastereotopic protons are present nonetheless. A good

Chapter 3 | Spectroscopic results

example of this would be diethyl acetal, **Figure 3.4**. In order to simplify the explanation, the substitution method is used by subsequently replacing one of the hydrogens with deuterium. When comparing the two new compounds A and B, note two chiral centers are now visible. The only difference between the two centers being that the chirality of A2 and B2 remain unchanged whereas A1 and B1 are of opposite chirality, i.e. the two compounds are diastereomeric. Therefore, although the molecule is asymmetric with a plane of symmetry, there is no plane of symmetry to divide the methylene protons, resulting in non-equivalent protons, i.e. diastereotopic protons.

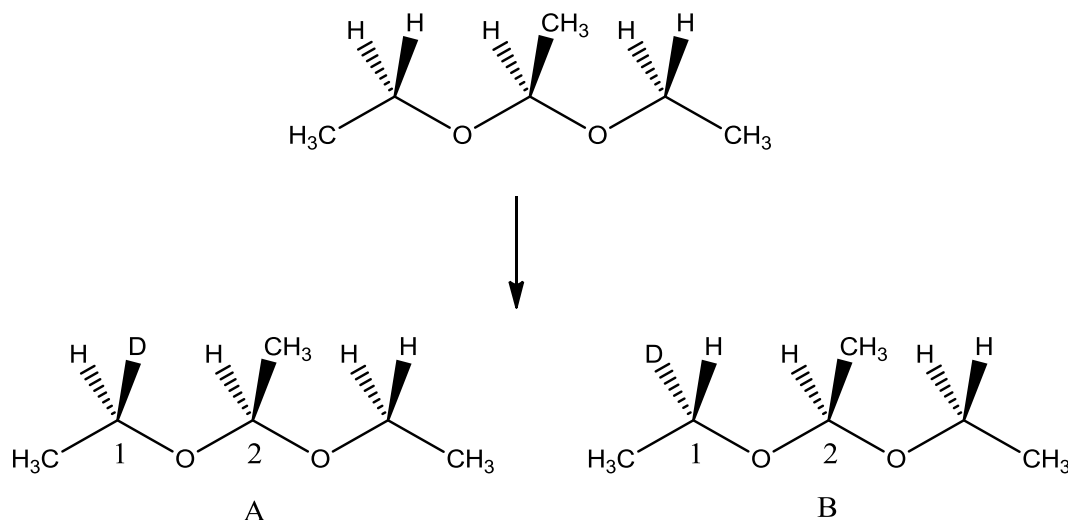


Figure 3.4. A demonstration of diastereotopic protons present in a compound with no asymmetric centers.

This last example is particularly important when justifying the different multiplicity patterns seen for the methylene protons of the tertiary amine of the acylthiourea ligand and the corresponding Co(III) complex, attributed to their diastereotopic environment which causes the protons to become non-equivalent and thus results in different chemical shifts and coupling constants.

Although diastereotopicity is present in both the complex and ligand, the multiplicity seen for the methyl and methylene signals in the respective spectra are very different. Note that no measurable multiplicities or coupling constants can be determined for the free ligand whereas in the complex the diastereotopic effects are more distinct and quantifiable. This can possibly be explained by looking at the dihedral H-C-H angle of the methylene protons in the compound. Upon coordination to the metal ion, the anisotropic field now caused by the newly formed coordination sphere is driving the two C-H orbitals closer together (**Figure 3.5**), decreasing the

Chapter 3 | Spectroscopic results

dihedral angle (α) and consequently increasing interaction between the two non-equivalent protons. Hence the resultant effect of diastereotopicity is more prominent and can be seen more clearly in the ^1H NMR spectrum of the complex than for the free ligand.

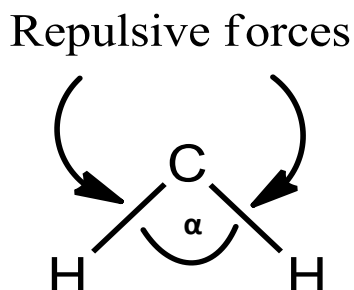


Figure 3.5. A schematic representation of how the dihedral angle (α) between the two methylene protons is decreased as a result of the repulsive forces from the electron density present upon coordination of the ligand to the metal.

Proton decoupled $^{13}\text{C}\{^1\text{H}\}$ NMR spectra of $[\text{Co}(\text{L-S,O})_3]$ complexes

Various comparisons were made between the ^{13}C data of the *fac*- $[\text{Co}(\text{L}^1\text{-S,O})_3]$ complex and the free ligand HL^1 with all relevant chemical shifts summarized in **Table 3.2**. Here the differences are more subtle compared to the ^1H spectra. The two signals with the highest chemical shift values in the ^{13}C spectrum of the ligand correspond to the thiocarbonyl carbon at 179.42 ppm followed by the carbonyl carbon at 163.83 ppm. The reasoning behind these assignments can be attributed to the resonance effect between the carbonyl and secondary amide group, thus the carbonyl is more shielded and hence lower in the spectra.

When the ligand coordinates to the metal center the two carbons of the thiocarbonyl and carbonyl groups are oppositely affected regarding their chemical shifts. The $\text{C}(\text{O})$ group shifts to a higher chemical shift from 163.83 ppm to 175.15 ppm whereas the $\text{C}(\text{S})$ group shifts from 179.42 ppm to 175.61 ppm. These two peaks are consequently seen very close together in the ^{13}C spectra of all the synthesized cobalt complexes. When the two donor atoms coordinate to the metal ion, some of the electron density around these atoms is lost and one would thus expect higher chemical shift values for the thiocarbonyl and carbonyl carbons compared to their corresponding free ligand peaks. This makes sense considering that an increase in the chemical shift of a nucleus comes as a result of the removal of electron density around that

Chapter 3 | Spectroscopic results

atom which occurs upon coordination. How much the peaks shift thus depends on the degree of electron donation of the donor atoms to the metal center.

For the carbonyl carbon, there is a distinct increase in the chemical shift of the signal in the complex when compared to the same peak for the free ligand. Electrons are released from the C(O) bond toward the metal hence the carbon of this particular bond is less shielded when coordinated.

The opposite is the case for the thiocarbonyl carbon. An important concept known as π -backdonation is considered to justify the change in chemical shift. An important criterion for this backbonding is the ligand under consideration needs to be a sufficient π -acceptor. In the case of the thiocarbonyl, electrons from the d-orbital of the cobalt are partly transferred to the antibonding molecular orbitals of the C(S), increasing electron density in this bond. C(S) is also a better π -acceptor than C(O), hence this sort of backdonation being more likely for the thiocarbonyl than the carbonyl. The slight increase in electron density consequently shields the thiocarbonyl carbon in the complex more than in the free ligand since the addition of electrons shields the nucleus, decreasing the chemical shift.

The carbons of the tertiary amine are assigned similarly to the protons, where C9 and C10 have higher chemical shift values than C11 and C12 considering first mentioned are closer in their particular orientation to the sulphur than the latter. The same goes for assignment of the carbon peaks of the phenyl substituent, accept there is a significant decrease in the chemical shift for C1 in the complex compared to the ligand, attributed to added electron density from the coordination sphere.

Table 3.2. 400 MHz ^{13}C chemical shift values from the spectra of the free ligand *N,N*-diethyl-*N'*-benzoylthiourea and its corresponding complex tris(*N,N*-diethyl-*N'*-benzoylthioureaato)cobalt(III) obtained in CDCl_3 at 25 °C.

Compound	^{13}C NMR chemical shifts (ppm)											
	C1	C2	C3	C4	C5	C6	C(O)	C(S)	C9	C10	C11	C12
HL ¹	151	129	128	133	128	129	163	179	48.1	13.4	47.9	12.6
Co(L ¹ -S,O) ₃	139	130	128	131	128	130	175	176	46.1	13.7	45.9	13.4

Chapter 3 | Spectroscopic results

Chapter 3 | Spectroscopic results

Infrared Spectroscopy of $[\text{Co}(\text{L-S,O})_3]$ complexes

In the IR spectra, the disappearance of the prominent N-H band (seen at 3222 cm^{-1} for HL^1) in the spectrum for the complex is the greatest indicator complexation has occurred due to the deprotonation of the ligand prior to coordination (**Figure 3.7**). As mentioned previously, once the ligand coordinates to the cobalt metal there is delocalization in the thioamide fragment (CONCS), which in the case of the IR spectra shifts the C(O) band ($1656\text{--}1630\text{ cm}^{-1}$) to lower values for the metal complex ($1449\text{--}1428\text{ cm}^{-1}$) than for the free ligand. The C(S) band also shifts to slightly lower frequencies for the complex compared to the ligand, where these lower frequencies suggest the coordination of the ligand occurs by means of a thiolate intermediate which leads to the Co-S bond formation.

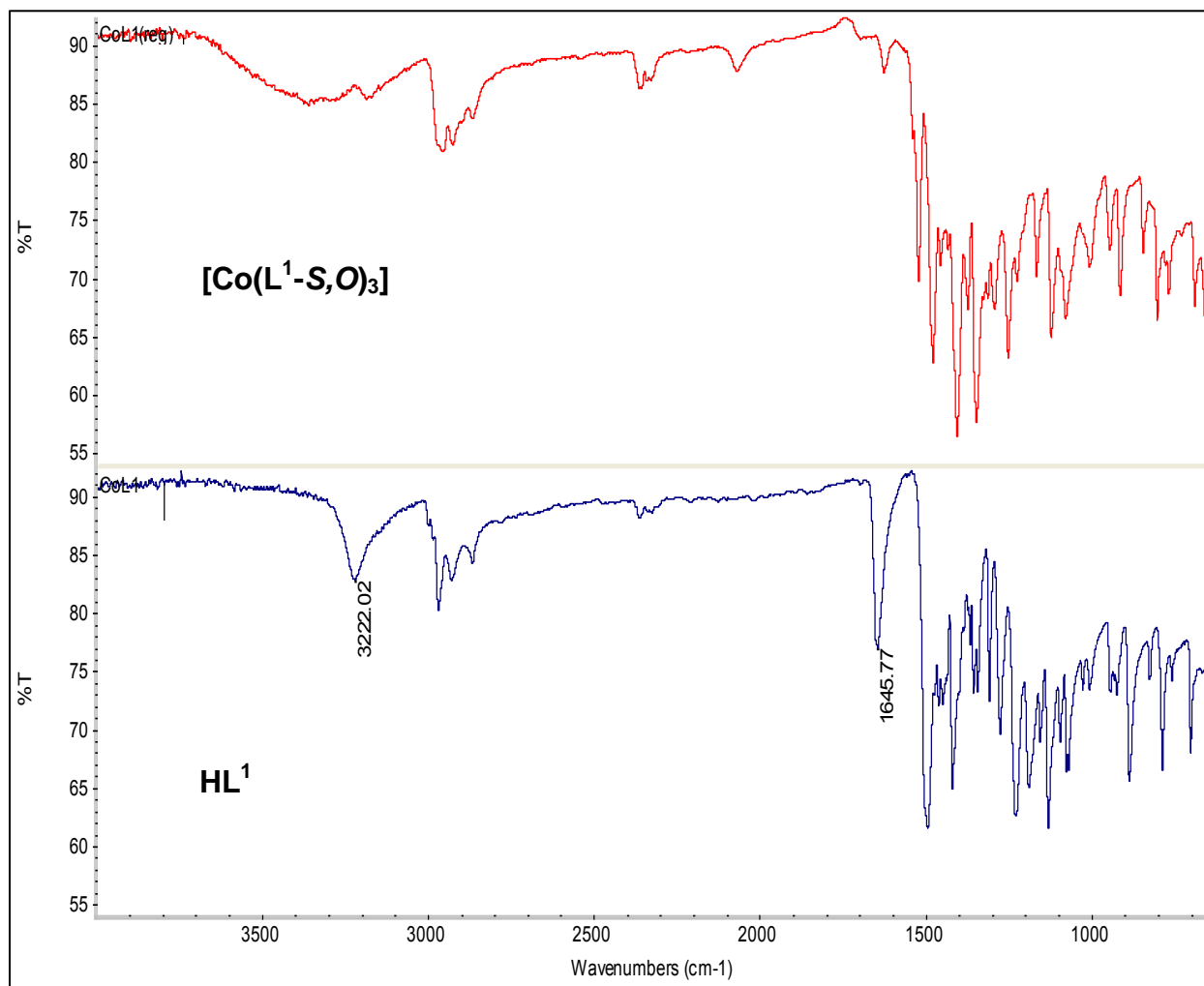


Figure 3.7. The IR spectra of the acylthiourea ligand (HL^1) and its corresponding Co(III) complex.

Chapter 3 | Spectroscopic results

3.1.2. Spectroscopic discussion of the Co(III) complex coordinated to an unsymmetrical acylthiourea ligand

As mentioned in **section 3.1.1**, the alkyl groups of the tertiary amine of symmetrical acylthiourea ligands do not have similar chemical shifts. This comes as a consequence of restricted rotation caused by the partial double bond character about the C-N bond of the thiourea moiety. An interesting phenomenon, briefly considered here, occurs upon coordination of Co(III) to an unsymmetrical acylthiourea ligand, i.e. *N*-methyl-*N*-ethyl-*N'*-benzoylthiourea. When the two alkyl groups of the tertiary amine are different (i.e. $R_2 \neq R_3$), the restricted rotation will give rise to *E,Z* configurational isomers hence two configurations are possible for this particular ligand at any given point.

The *E* isomer is assigned when the groups of highest priority are facing opposite sides of the double bond, thus for the acylthiourea ligand this will be when the alkyl group that is higher in priority is facing the side opposite to the sulphur atom. The *Z* isomer is assigned when the two groups of highest priority are facing the same side, thus the higher priority alkyl group faces the same side as the sulphur atom. Priority is determined by atomic weight, therefore the sulphur atom is of higher priority on the left side of the C-N bond than the nitrogen atom, and on the right side it is determined by considering the alkyl group with the longest chain. Each isomer is illustrated in **Figure 3.8**.

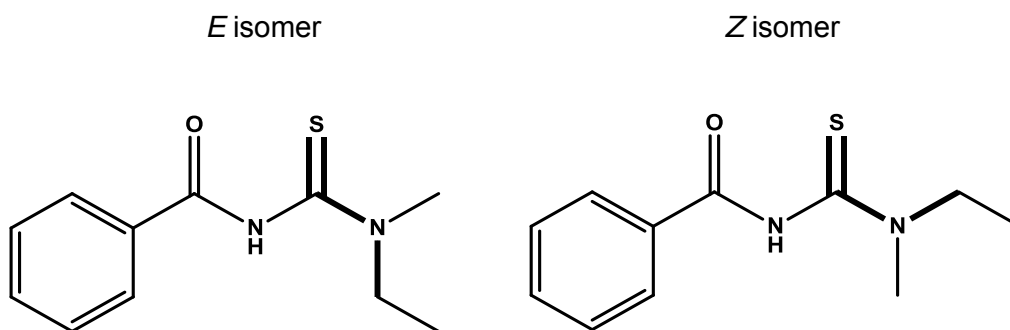


Figure 3.8. Assignment of the two possible configurational isomers of *N*-methyl-*N*-ethyl-*N'*-benzoylthiourea as a result of the restricted rotation about the C-N bond. The sulphur atom and the ethyl groups are assigned as the two highest priority groups on each side of the C-N bond.

Chapter 3 | Spectroscopic results

The configurational isomerism is also observed when the ligand coordinates to Co(III), considering that each of the three ligands could coordinated in either the *E* or *Z* configuration. This gives way to four possible configurational isomers *fac*-[Co(*EEE*-L-S,O)₃], *fac*-[Co(*EZE*-L-S,O)₃], *fac*-[Co(*ZZZ*-L-S,O)₃] and *fac*-[Co(*ZEZ*-L-S,O)₃]. For the *EEE* and *ZZZ* isomers, the ligands in all three chelates are either orientated in the *E* or the *Z* configuration respectively. For the *EZE* and *ZEZ* isomers, only one of the three ligands is orientated in a configuration opposite to the other two ligands. All four possible isomers are illustrated in **Figure 3.9**.

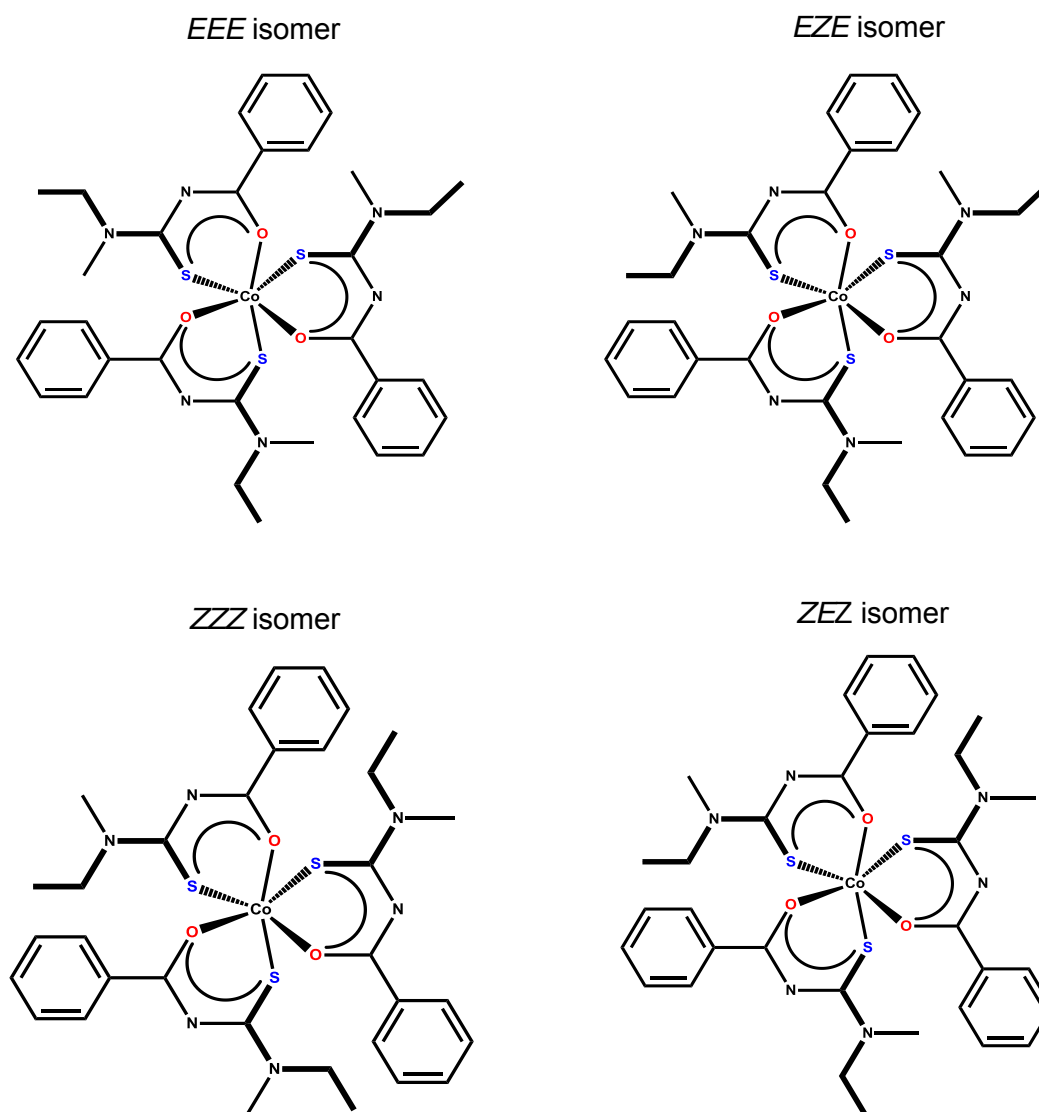


Figure 3.9. The four possible configurational isomers namely *EEE*, *EZE*, *ZZZ*, and *ZEZ* of the complex *fac*-tris(*N*-methyl-*N*-ethyl-*N'*-benzoylthioureato)cobalt(III).

Chapter 3 | Spectroscopic results

Considering the presence of these isomers in solution, the ^1H and ^{13}C NMR results are notably different when compared to the symmetrical acylthiourea derivatives since the *E* and *Z* isomers will resonate at different chemical shifts.

This is demonstrated in **Figure 3.10**, where comparisons were made between the thioamide section of the ^1H spectra of the symmetrical *N,N*-diethyl-*N'*-benzoylthiourea (**Figure 3.10a**) and the unsymmetrical *N*-methyl-*N*-ethyl-*N'*-benzoylthiourea ligand (**Figure 3.10b**). For the first mentioned compound, note there are two separate resonances for the methyl and methylene protons as a result of restricted rotation about the C-N bond, placing these protons in slightly different chemical environments. The protons coplanar to the thiourea group are assigned as the signals with the higher chemical shifts as they are less shielded than those facing the opposite direction.

For the second compound, two resonances are observed for each of the three different methyl and methylene groups. Each resonance represents either the *E* or *Z* isomer of that specific group and each isomer appears at a relative ratio significantly different to the other. Thus assignment of the different isomers considers the same principle mentioned earlier for the symmetrical acylthiourea ligand. Depending on the configuration (i.e. *E* or *Z*), the nuclei coplanar to the sulphur atom will always be slightly less shielded, meaning higher chemical shifts, than the nuclei in the opposite orientation. Therefore in regards to the *N*-CH₂ protons of the ethyl group, the signal with the higher chemical shift can only be due to the *Z* isomer since in this configuration the protons are closer to the sulphur atom than in the *E* isomer, therefore less shielded. It also shows the *Z* isomer to be the major component considering its intensity is almost five times that of the *E* isomer. The same principle is used to assign the resonances of the two other groups, in which case the *N*-CH₃ is now less shielded as the *E* isomer than the *Z* isomer and appears as the minor component. The last group, the methyl protons of the ethyl chain, is shielded in the same way as the *N*-CH₂ group, with the *Z* isomer appearing as the signal with the higher chemical shift than the *E* isomer. The relative distribution of the *E,Z* configurational isomers of the asymmetrical *N*-methyl-*N*-ethyl-*N'*-benzoylthiourea ligand, determined from the ^1H spectra at room temperature (i.e. 25 °C), can be reported as a relative percentage distribution, with the *Z*-isomer appearing at a ratio of 85% relative to the *E*-isomer.

Chapter 3 | Spectroscopic results

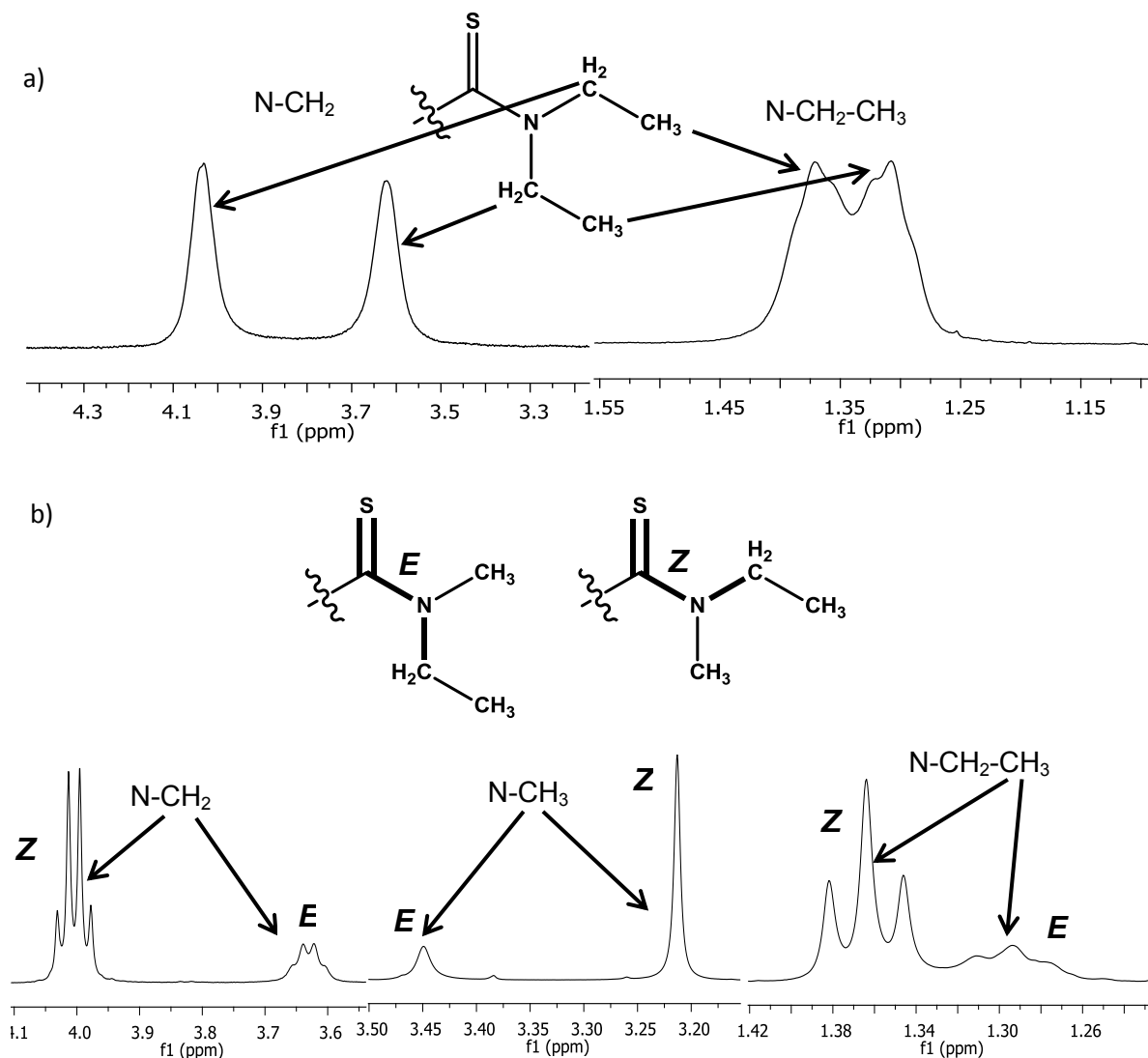


Figure 3.10. A comparison of the 400 MHz ^1H spectra of the *N*-alkyl section of the symmetrical a) *N,N*-diethyl-*N'*-benzoylthiourea ligand and b) *N*-methyl-*N*-ethyl-*N'*-benzoylthiourea ligand showing *E*, *Z* configurational isomers. All spectra were obtained in CDCl_3 at 25 $^\circ\text{C}$.

Assignment of each configurational isomer to the specific signal becomes increasingly complicated upon coordination of the unsymmetrical acylthiourea ligand to the Co(III) metal, considering all the possible configurations as shown in **Figure 3.9**, and is beyond the scope of this study. The spectrum of the complex is available in Addendum A.

Chapter 3 | Spectroscopic results

3.1.3. Spectroscopic discussion of the Co(III) complex coordinated to a chiral acylthiourea ligand

Assignment of the ^1H and ^{13}C NMR spectra of tris(*N,N*-diethyl-*N'*-camphanoylthioureato)cobalt(III) (i.e. $\text{Co}(\text{L}^{12}\text{-S,O})_3$) is somewhat complicated compared to spectra previously discussed for the complexes mentioned in **section 3.1.1** and **section 3.1.2**. It is the only complex where Co(III) is coordinated to an inherently chiral acylthiourea ligand. The presence of chiral center(s) effect magnetic spectra in different ways depending on the specific structure under investigation. Consider for example 2-butanol, which exist as one of two enantiomers *R*- or *S*-2-butanol (**Figure 3.11a**). Since the two enantiomers are physically identical and differ only in their interaction with polarized light, there is consequently no visible difference in their ^1H NMR spectra. The chirality in 2-butanol nonetheless has a unique effect on the chemical equivalence of nearby protons. When looking at the Newman Projection of *R*-2-butanol (**Figure 3.11b**), note that irrespective of how the bonds are rotated around each carbon, the two CH_2 protons (H_a and H_b) remain in separate environments and will thus give rise to second order effects in the ^1H spectra.

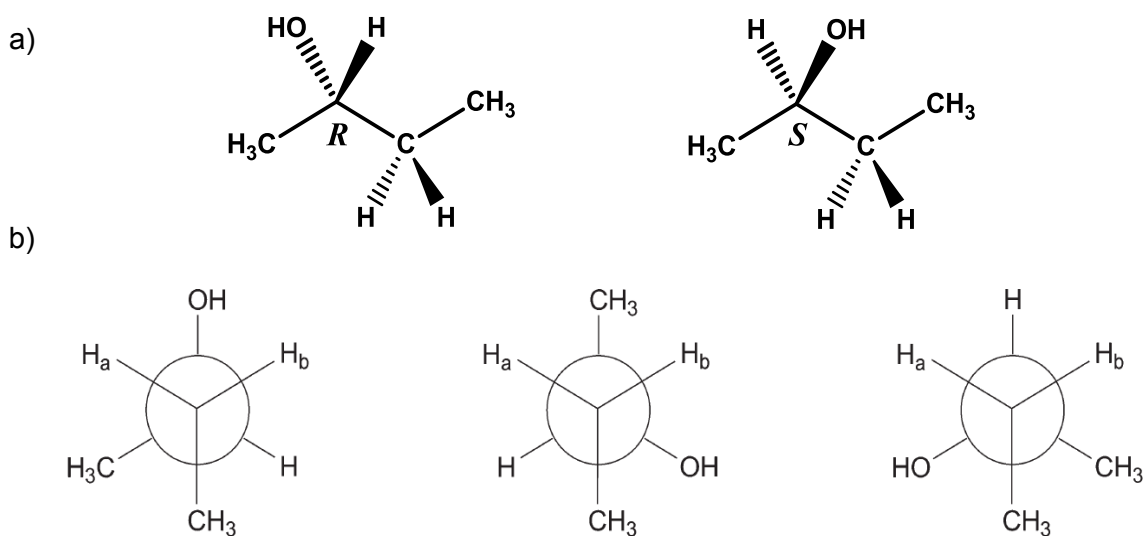


Figure 3.11. a) The two possible enantiomers of 2-butanol and an b) illustration by means of a Newman Projection how the two methylene protons are chemically different.

Chapter 3 | Spectroscopic results

For unequivocal assignment of the $[\text{Co}(\text{L}^{12}\text{-S}, \text{O})_3]$ complex, possible second order effects were considered due to the presence of the chiral center along with general chemical shift considerations. These assignments were substantiated by two-dimensional NMR experiments including COSY and GHSQC.

Assignment of the ^1H NMR spectrum of $[\text{Co}(\text{L}^{12}\text{-S}, \text{O})_3]$, shown in **Figure 3.12**, was based on the same principles previously discussed in **section 3.1.1**. The resonance effect caused by the π -electrons of the thiocarbonyl bond and the lone pair electrons from the tertiary nitrogen, leads to restricted rotation about the C-N bond of the thiourea moiety thereby leaving the methyl and methylene protons (H7-H10) in separate environments, hence different chemical shifts. For the unbound ligand, the methylene groups appear as two broad peaks, whereas fine structure is visible in the spectra of the Co(III) complex. This is attributed to diastereotopicity which is more pronounced in the complex than for the unbound ligand, since the two methylene protons are forced closer together by the electron density of the coordination sphere and therefore able to give measurable coupling constants. The four protons each give rise to a doublet of quartets, observed in the spectrum for the complex as overlapping multiplets between 3.51 – 4.01 ppm. The protons closer to the sulphur will be slightly less shielded as a result of the electron withdrawing ability of this atom, therefore protons H7 and H8 have higher chemical shift values than protons H9 and H10.

Consider henceforth the protons of the camphanic group. Protons adjacent to a chiral center are subject to second order effects since they no longer appear in similar chemical environments (see **Figure 3.11**). Therefore the protons of the camphanic group subject to second-order effects are H15 and H16. They are thus considered separately; hence referred to as H15a and H15b as well as H16a and H16b, respectively. The protons *cis* (H15a and b) relative to the three methyl groups C18, C20 and C21 are more shielded by the induced field caused by the carbon atoms, and therefore have chemical shifts lower than the protons *trans* to these same groups. The four doublet of doublet of doublets observed at 2.42, 1.90, 1.81 and 1.60 ppm could thereby be assigned as H16b, H16a, H15b and H15a respectively.

Chapter 3 | Spectroscopic results

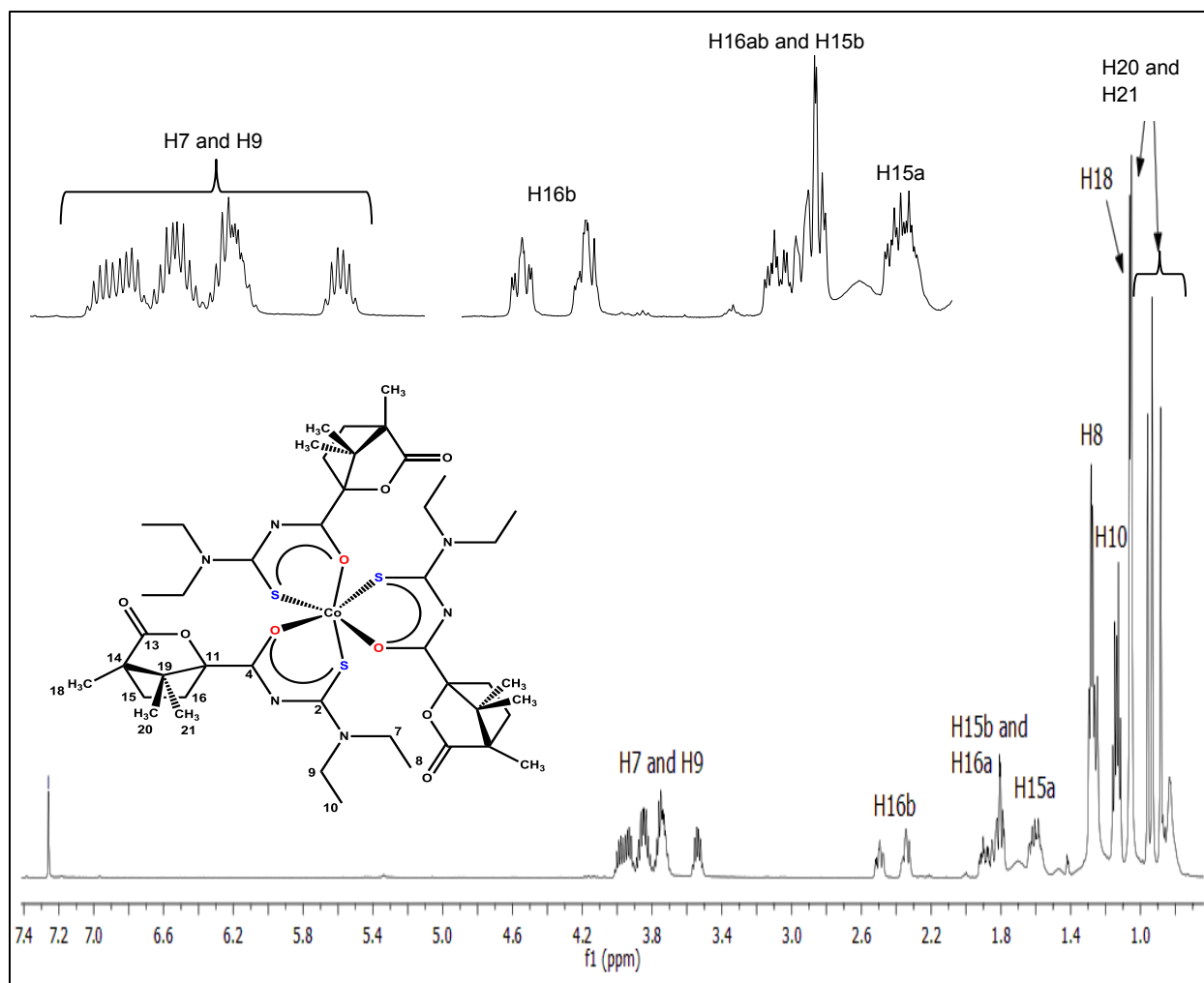


Figure 3.12. The 400 MHz ^1H spectrum in CDCl_3 at 25 $^\circ\text{C}$ of tris(*N,N*-diethyl-*N'*-camphanoylthioureato)cobalt(III).

For the ^{13}C NMR assignment, restricted rotation around the C-N bond of the thiourea moiety causes the primary and secondary carbons of the tertiary amine to resonate at different chemical shifts and therefore separately referred to as C7, C9, C8 and C10. Those carbons nearest to sulphur are less shielded than the carbons orientated in the opposite direction; hence carbons C7, C9, C8 and C10 are assigned as the peaks at 45.73, 45.59, 13.20 and 12.92 ppm respectively. In **section 3.1.1**, the chemical shifts of the carbonyl and thiocarbonyl carbons upon coordination to the Co(III) ion were rationalized. For the $[\text{Co}(\text{L}^{12}\text{-S,O})_3]$ complex, the signal furthest down in the spectrum is assigned as the esteric carbon (C13), followed by the thiocarbonyl and carbonyl carbon at 175.01 and 173.73 ppm respectively. The chemical shift assignments of all carbons are given in **section 2.2.4** and the ^{13}C NMR spectrum is shown in

Chapter 3 | Spectroscopic results

Figure 3.13. Note an important observation in the ^{13}C spectrum, otherwise not clear in the ^1H spectrum, referring to the presence of major and minor signals for some of the carbons. These additional peaks are not present in the ^1H or ^{13}C spectra of the unbound ligand, or any other Co(III) complex previously synthesized in this thesis, therefore suggesting the complex is able to exist as more than one type of isomer. These major and minor signals are indicated in the spectrum shown in **Figure 3.13**. Initial assumptions attempted to relate the presence of the additional peaks to stereoisomerism, suggesting that two isomers are present in solution, each with a different configuration at the equivalent stereocenters present in the ligand (i.e. diastereomers). Assignment of the specific isomer to the relevant signals requires further study beyond the scope of this work.

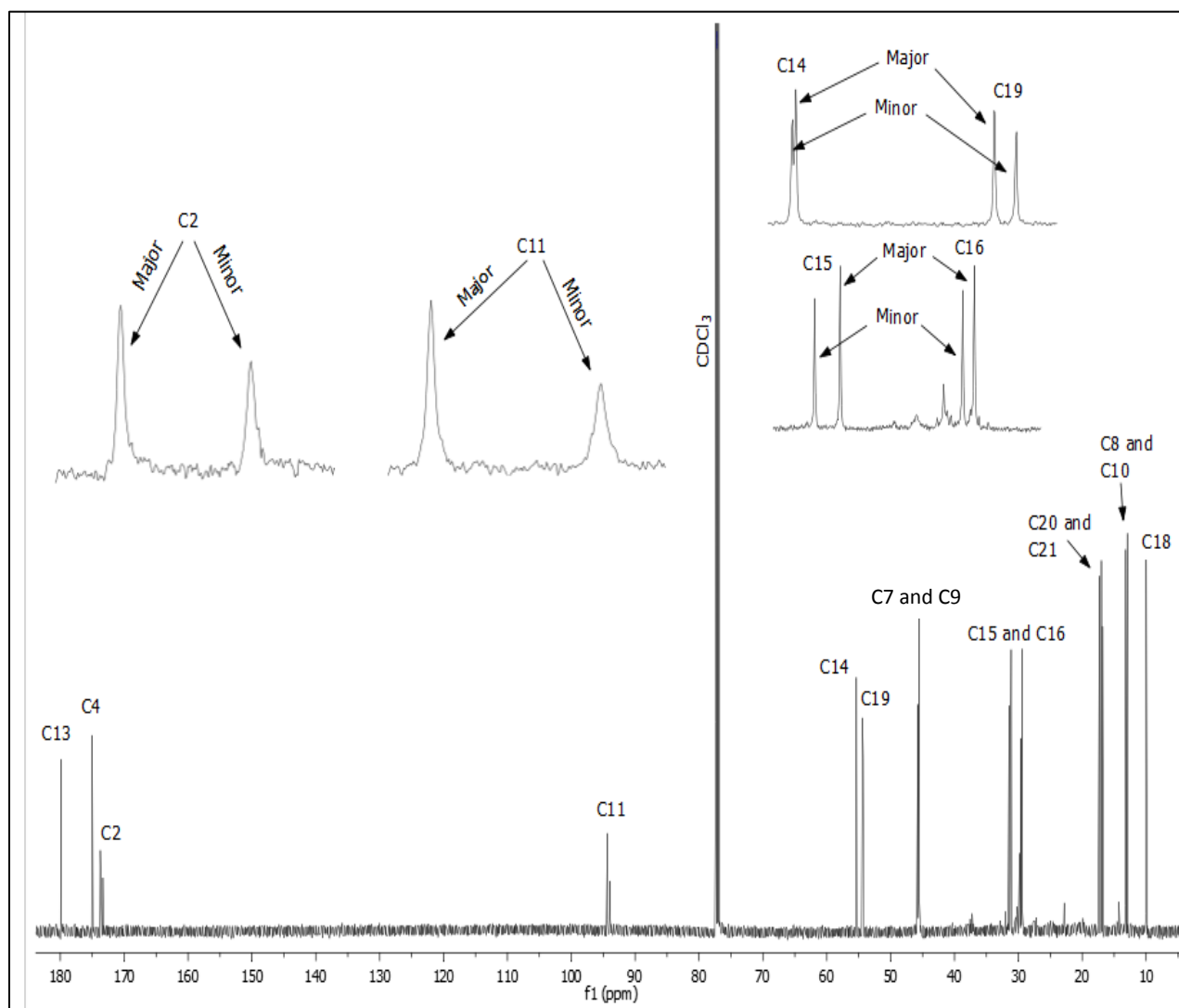


Figure 3.13. The 400 MHz ^{13}C spectrum in CDCl_3 at 25 °C of tris(*N,N*-diethyl-*N'*-camphanoylthioureato)cobalt(III).

Chapter 3 | Spectroscopic results

All ^1H and ^{13}C NMR assignments were confirmed by means of two-dimensional NMR experiments which included H-H Correlation Spectroscopy, i.e. COSY, as well as Gradient Heteronuclear (H-C) Single Quantum Coherence (GHSQC) spectroscopy. The spectra of the two experiments are presented in **Figures 3.14** and **3.15** respectively.

The two-dimensional spectra allowed for identification of coupling partners otherwise difficult to determine, considering the presence of second order effects in the molecule. In the COSY experiment all diagonal peaks correspond to all relevant peaks seen in the one-dimensional spectrum. The peaks cross from the diagonal peak indicate ^1H nuclei that are coupled. To simplify the spectra a solid line is drawn to connect all diagonal peaks. Cross peaks, i.e. coupling partners, are indicated with a dashed line. The first dashed line indicates the coupling between the protons of carbon 10 and carbon 9, whereas the second dashed line indicates the coupling between protons of carbon 8 and carbon 7. The third and fourth dashed lines verified the different types of coupling between the protons of carbon 15 and 16 of the camphanic ring. For instance, the third dashed line reveals ^2J coupling between H15a and H15b as well as ^3J coupling between H15a and H16a, as well as between H15a and H16b. Furthermore, the 4th and 5th dashed lines confirm ^2J and ^3J coupling between the Ha and Hb protons of carbons 16 and 15 respectively.

While the COSY spectrum confirmed the 1D ^1H assignments, GHSQC was used for confirmation of the ^{13}C assignments considering this type of experiment is the result of spin coupling between the carbon and all protons directly attached to it. The various peaks were labelled A-F for simplicity. Peaks A-D subsequently represents the two methylene carbons and their respective protons. Similarly peaks E-G indicate the peaks of carbons 15 and 16 and their protons, where peaks H and I indicate the methyl carbons of the tertiary amine. The last few peaks, J-M, are related to the primary carbons of the camphanic ring.

Chapter 3 | Spectroscopic results

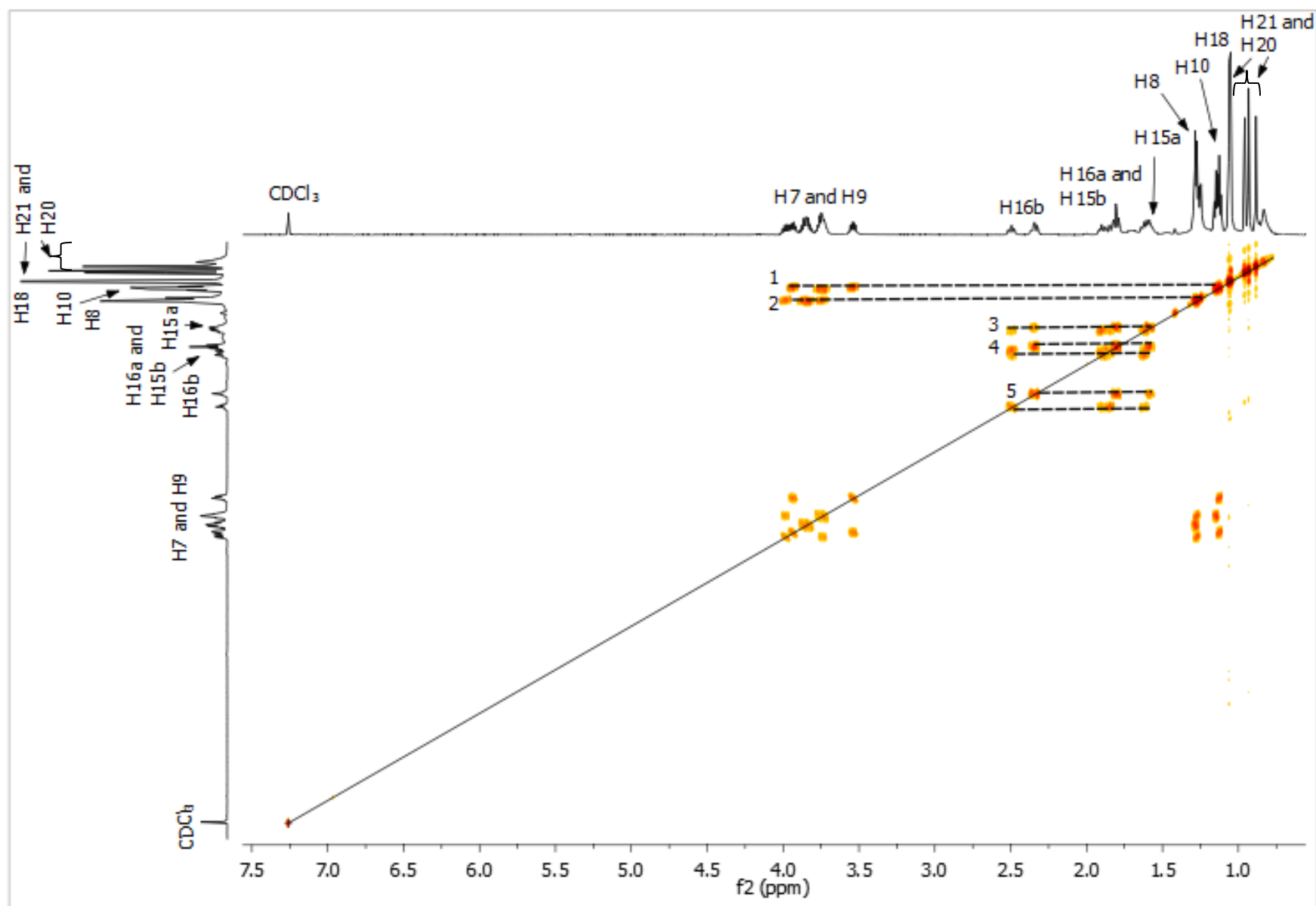


Figure 3.14. The 600 MHz COSY spectrum in CDCl_3 at 25 °C of tris(*N,N*-diethyl-*N'*-camphanoylthioureato)cobalt(III).

Chapter 3 | Spectroscopic results

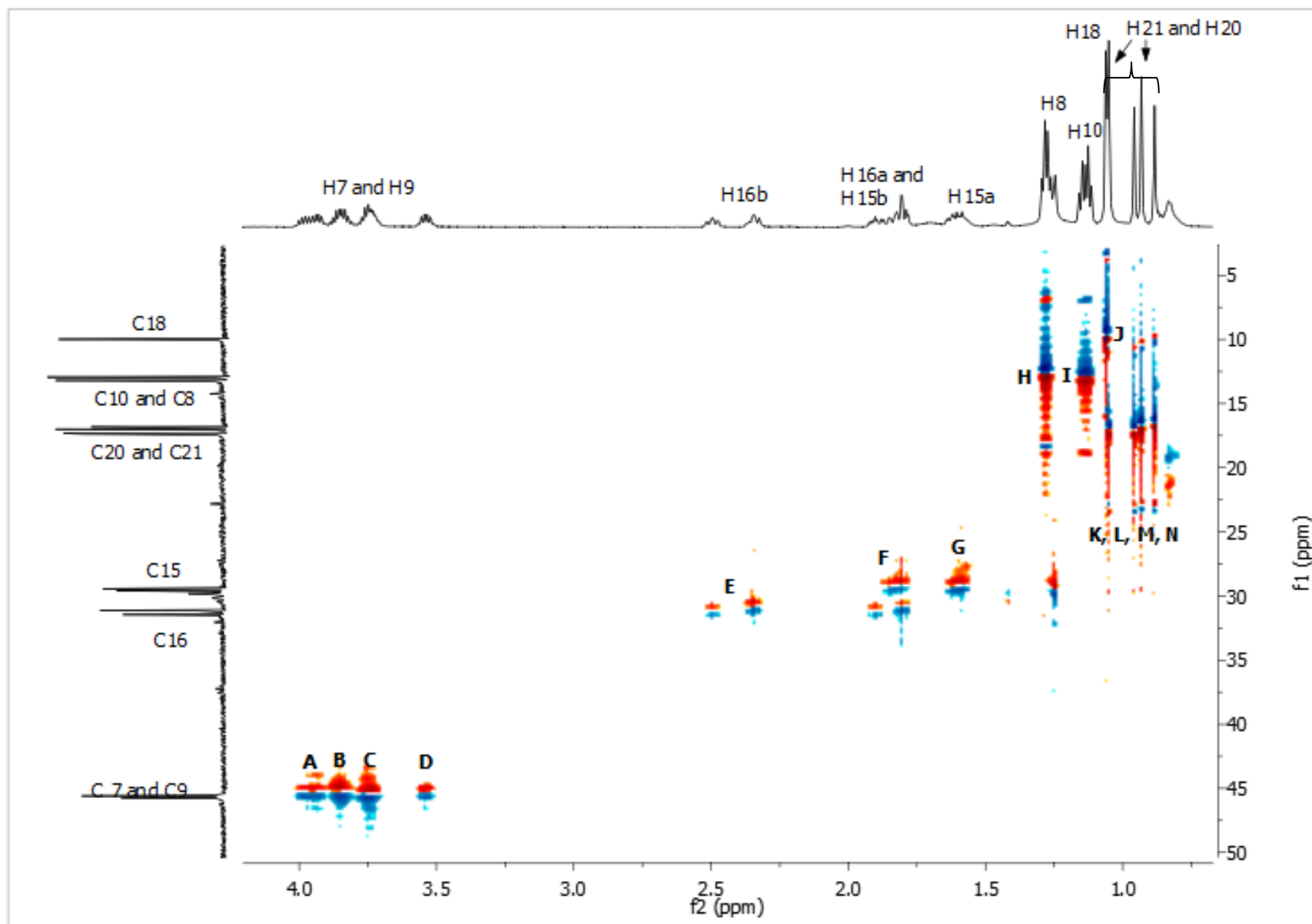


Figure 3.15. The 600 MHz GHSQC spectrum in CDCl_3 at 25 °C of tris(*N,N*-diethyl-*N'*-camphanoylthioureato)cobalt(III).

Chapter 3 | Crystallography

3.2. Molecular structure discussion of selected acylthiourea Co(III) complexes by means of X-ray diffraction analysis

Various crystal structures were obtained during the course of this project and will subsequently be discussed in the current section. All structures were acquired by means of a Bruker-Nonius SMART Apex Area CCD X-ray diffractometer which was fitted with a Mo fine-focus sealed tube as well as a 0.5 mm MonoCap collimator. The software used to solve and refine all of the structures was Mercury 3.5 whereas XSEED was used in order to render molecular graphics. All crystals were obtained by means of slow evaporation, where the compound is dissolved in solvent of choice and slowly evaporated over a period of 3 to 4 weeks or until single crystals appeared. All relevant bond angles and bond lengths are available in Addendum B.

Table 3.3. The crystal data collection and structure refinement parameters for complexes *fac*-[Co(L²-S,O)₃], *fac*-[Co(L¹¹-S,O)₃] and *fac*-[Co(L¹²-S,O)₃].

Compound	<i>fac</i> -[Co(L ² -S,O) ₃]	<i>fac</i> -[Co(L ¹¹ -S,O) ₃]	<i>fac</i> -[Co(L ¹² -S,O) ₃]
Empirical formula	C ₃₉ H ₅₁ N ₆ O ₆ CoS ₃	C ₃₃ H ₃₉ N ₆ O ₃ CoS ₃	C ₄₅ H ₆₉ N ₆ O ₉ CoS ₃
Formula weight	854.98	722.83	993.19
Crystal system	Trigonal	Trigonal	Triclinic
Space group	P-3	P-3	P1
a (Å)	16.231(5)	16.110(17)	11.124(5)
b (Å)	16.231(5)	16.110(17)	13.221(6)
c (Å)	9.791(3)	8.479(9)	17.790(8)
α/°	90.000	90.000	97.612(5)
β/°	90.000	90.000	90.810(5)
γ/°	120.000	120.000	106.127(5)
Volume of cell Å³	2233.8 (18)	1905.6 (5)	2487.56(19)
T/K	100	294	227
μ/mm⁻¹	0.590	4.351	0.529
Independent reflections	3502	1068	20528
R_{int}	0.0436	0.0269	0.0409

Chapter 3 | Crystallography

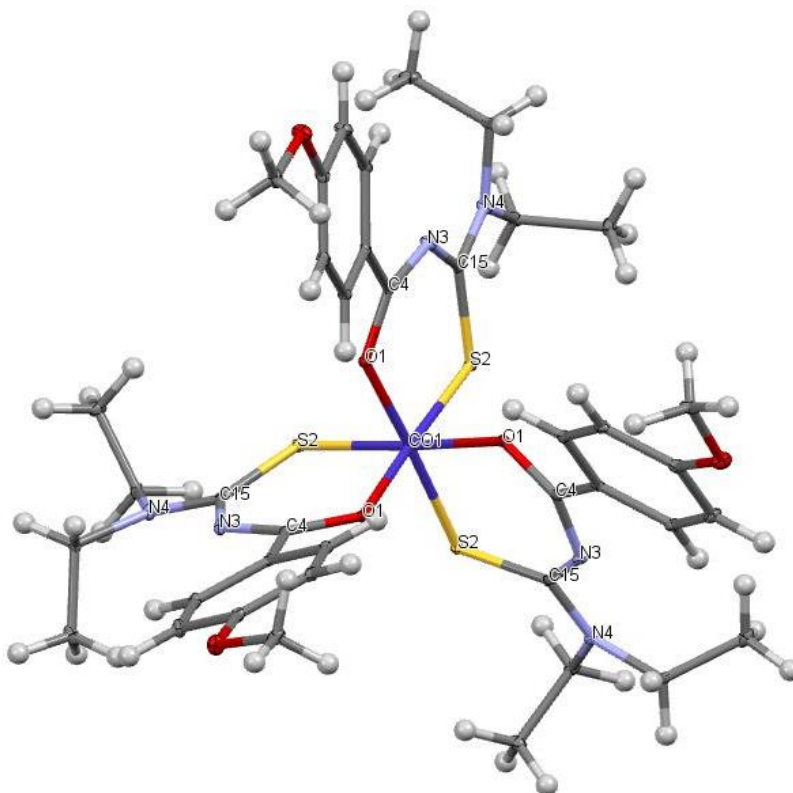
3.2.1. Molecular structure of *fac*-tris(*N,N*-diethyl-*N'*-4-methoxybenzoylthioureato) cobalt(III): *fac*-[Co(L²-S,O)₃]

Figure 3.16. The molecular structure of *fac*-[Co(L²-S,O)₃] with selected bond lengths (Å) and angles (°) as follows; Co-O 1.923(1), Co-S 2.216(1), O(1)-C(4) 1.264(3), C(4)-N(3) 1.329(3), N(3)-C(15) 1.342(3), C(15)-S 1.742(2), O-Co-S 95.24, O-Co-S 176.56, S-Co-S 88.13, O-Co-O 84.48.

All relevant XRD data for the *fac*-[Co(L²-S,O)₃] complex is summarized in **Table 3.3** at the beginning of this section. The crystal structure for this complex is shown in **Figure 3.16** and shows the preference of these complexes to coordinate *via* the *facial* isomer as suggested in chapter 2, considering that all sulphur atoms occupy one face of the octahedron with all oxygen atoms occupying the opposite face.

The complex crystallizes in the P-3 Trigonal space group and it is evident from relevant angles that the complex is slightly distorted from the ideal octahedral geometry. The three O-Co-S angles in each chelate ring is 95.24°, 95.27° and 95.31° respectively, which deviates slightly from the expected 90° angle. The three O-Co-S angles between planes, on the other hand, are

Chapter 3 | Crystallography

176.56°, 176.63° and 176.58° respectively also deviating slightly from the expected 180° angle. The average bond distances for Co-S and Co-O are 2.216 and 1.923 Å respectively, thus the coordination bond between the Co(III) ion and sulphur is longer than the bond between the Co(III) ion and oxygen. The bond distances of C(4)-N(3) and C(15)-N(3) are 1.329 and 1.342 Å respectively, which is shorter than the same two bond lengths for the ligand (1.351 and 1.431 Å respectively). The difference in last mentioned bond lengths for the complex and ligand can be attributed to the delocalised π -electrons in the chelate ring shortening the bond distances between these atoms.

3.2.2. Molecular structure of *fac*-tris(*N*-methyl-*N*-ethyl-*N'*-benzoylthioureato)cobalt(III): *fac*-[Co(L¹¹-S,O)₃]

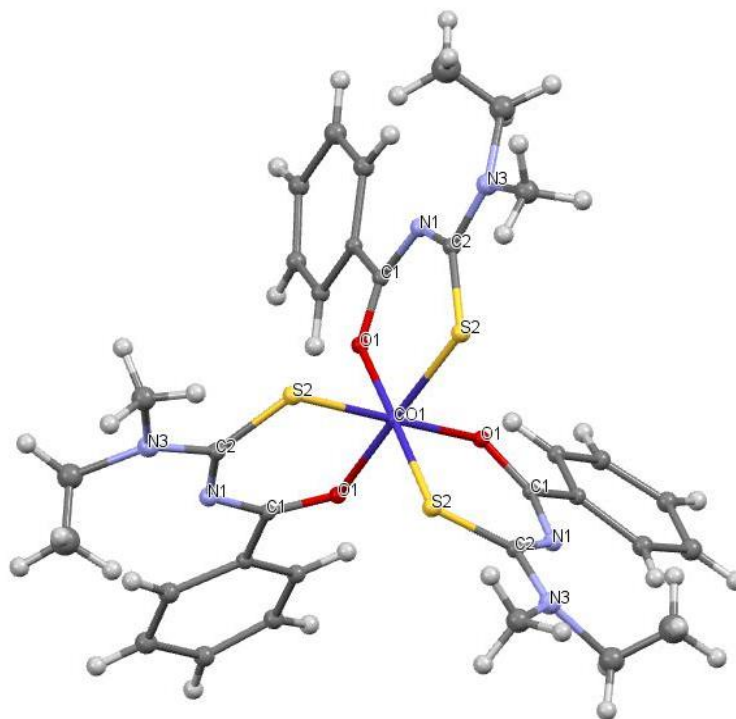


Figure 3.17. Molecular structure of *fac*-[Co(L¹¹-S,O)₃] with selected bond lengths (Å) and angles (°) as follows: Co-O 1.9238(1), Co-S 2.1949(1), O(1)-C(1) 1.2296(1), C(1)-N(1) 1.3473, C(2)-N(1) 1.3473(1), C(2)-S(2) 1.6867(1), S(2)-Co(1)-S(2) 87.79, O(1)-Co(1)-O(1) 85.38, S(2)-Co(1)-O(1) 178.19, O(1)-Co(1)-S(1) 178.19, O(1)-Co(1)-S(2) 93.19.

Chapter 3 | Crystallography

The crystals obtained for the *fac*-[Co(L¹¹-S,O)₃] complex crystallized in the P-3 space group and the molecular structure is shown in **Figure 3.17**. The crystal structure shows the coordination of all three ligands *via* the bidentate mode by means of the sulphur and oxygen donor atoms of the ligand. The orientation of the donor atoms in the coordination plane of the complex is *facial*, hence written as *fac*-[Co(L¹¹-S,O)₃]. All important crystallographic data regarding this complex are summarized in **Table 3.3**.

As mentioned in **section 3.1.2**, Co(III) complexes coordinated to an unsymmetrical acylthiourea ligand, i.e. where R₂ ≠ R₃, are able to exist as *E,Z* configurational isomers. In the crystal diagram, note all of the ethyl groups are facing the opposite direction as the sulphur atom. Consequently, since the *E* isomer is assigned when the groups of highest priority are facing opposite sides of the double bond (in this case the bond between the carbon of the chelate chain and the tertiary nitrogen), the configurational isomer crystallized and shown in **Figure 3.17** can be referred to as the *EEE* configurational isomer, i.e. *fac*-[Co(*EEE*-L¹¹-S,O)₃].

Bond lengths and angles are consistent with what is generally expected for octahedral-d⁶ cobalt(III) complexes of the type [Co(L-S,O)₃]. The average bond lengths for the three carbonyl and thiocarbonyl bonds are 1.2296 and 1.6867 Å respectively, which are slightly longer than the corresponding bond lengths prior to coordination. This supports the notion that coordination occurs by the bidentate mode *via* the sulphur and oxygen donor atoms. The average bond lengths of the various C-N bonds in the chelate ring vary between 1.3090 and 1.3473 Å, which is shorter than an average C-N bond length of 1.472(5) Å. The shortening of these bonds are indicative of delocalisation in the chelate ring. Furthermore, bond angles illustrate the complex is slightly distorted from the angles of an ideal octahedral conformation. For instance the angle of O(1)-Co(1)-S(2) in one of the chelates give a value of 93.19°, which is slightly deviated from the ideal 90° angle. On the other hand the angle between chelates including S(2)-Co(1)-O(1) and O(1)-Co(1)-S(2) are both 178.19° which also deviates slightly from the ideal 180° angle.

Chapter 3 | Crystallography

Chapter 3 | Crystallography

respectively. This deviates from the ideal 90° angle expected for the ideal octahedral geometry. Angles S(4)-Co(2)-O(9), S(1)-Co(2)-O(5), S(5)-Co(2)-O(7) give respective bond angles of 177.53° , 176.54° and 175.26° which also illustrates deviation from the ideal 180° angle of the octahedral geometry. The average bond lengths Co-S and Co-O are 2.215 and 1.911 Å respectively, which show the Co-S coordinate bond to be slightly longer than the Co-O bond. All C-N bond lengths present in each chelate ring which include C(31)-N(10), C(26)-N(10), C(65)-N(21), C(63)-N(21), C(45)-N(11) and C(39)-N(11) give an average bond length of 1.3292 Å which is shorter than the normal C-N bond and strongly suggests the delocalisation of π -electrons in the chelate ring. This is also the case for all C-N bond lengths outside the chelate ring which include bonds C(63)-N(60), C(39)-N(20) and C(26)-N(52) which give an average bond length of 1.3322 Å. This agrees with the notion that this bond has partial double bond character leading to restricted rotation causing the methyl and methylene protons of the tertiary nitrogen to be non-equivalent as mentioned in **section 3.1.1** and evident in the ^1H and ^{13}C NMR spectra for the Co(III) complexes under investigation.

The crystal structure in **Figure 3.18** furthermore shows the complex crystallizing in two different configurations. In **section 1.2.3** it was mentioned that Co(III) octahedral complexes are able to exist as geometric and optical isomers (i.e. enantiomers). Considering the inherent chirality of the acylthiourea ligand, it suggests upon coordination to Co(III) that the complex appears as pairs of stereoisomers which no longer differ at all the relevant stereocenters, and thereby no longer exist as mirror images of one another. This is known as diastereomers which, unlike enantiomers, do not have similar physical properties. This is supported by the ^{13}C NMR results which show two peaks in the spectrum for every carbon signal instead of one. The absolute configuration of the two isomers are determined by the rules of priority and the two crystal structures are thus accordingly given the symbols Lambda Λ (left-handed) and Delta Δ (right-handed).

Chapter 3 | ^{59}Co NMR spectroscopy

3.3. ^{59}Co NMR spectroscopy

3.3.1. Introduction

The ^{59}Co nucleus ($I = 7/2$) has one of the largest NMR chemical shift ranges known spanning more than 18 000 ppm.⁷⁵ Considering the natural abundance, the NMR reception of ^{59}Co relative to ^{13}C is 1572, placing this nucleus in the top six in terms of ease of detection.⁷⁶ Taking into account that almost all Co(III) complexes are six coordinate in an octahedral geometry, the resultant electric field gradient is consequently small or at least lower than in the case of compounds with structures of lower symmetry. This means that relatively narrow NMR signals are obtained for many octahedral Co(III) complexes. Any deviations from the ideal octahedral geometry as a result of ligand variation in this six-fold arrangement consequently means NMR line broadening can occur, which is a sensitive probe for even the smallest distortions in structure. For these reasons and more ^{59}Co NMR is expected to be a sensitive technique for the study of symmetrical and asymmetrical octahedral d^6 *fac*-[Co(L-S,O)₃] complexes.

3.3.2. Referencing in ^{59}Co NMR spectroscopy

One of the objectives of this research project was to determine the effect of varying the *N,N*-dialkyl-*N'*-acylthiourea structure coordinated to the metal, on the chemical shifts of these complexes. To our knowledge the only similar complex previously examined by ^{59}Co NMR is the *fac*-tris(*N,N*-diethyl-*N'*-benzoylthioureato)Co(III), i.e. *fac*-[Co(L¹-S,O)₃], complex studied by Juranic *et al.*⁷⁴ in 1989 showing that a good ^{59}Co NMR could be obtained. These authors reported $\delta(^{59}\text{Co}) \sim 8538$ ppm for this complex (in CDCl_3) relative to the aqueous $\text{K}_3[\text{Co}(\text{CN})_6]$ solution used as an external reference with a $\delta(^{59}\text{Co})$ set to 0 ppm.

This value was substantiated by our own ^{59}Co NMR experiment of the same *fac*-[Co(L¹-S,O)₃] complex by means of a referencing method known as the unified scale as reported by Harris *et al.*¹³. This method removes the need for separate compounds as references and instead allows for reporting the resonance frequencies of all nuclei relative to the ^1H resonance frequency of tetramethylsilane (TMS). It was of interest to determine how the unified scale could be used in a practical sense by relating some common secondary references to the primary reference. Various measurements of secondary references were reported and related to the frequency of the primary standard, defined as the signal of ^1H TMS at exactly 100 MHz. This relationship would eventually be described by the symbol Ξ , defined as the ratio of the secondary frequency

Chapter 3 | ^{59}Co NMR spectroscopy

to the frequency of the ^1H signal in TMS in the same magnetic field and is expressed as a percentage value determined as follows:

$$\Xi I \% = 100 \left(\frac{\nu_X^{obs}}{\nu_{TMS}^{obs}} \right)$$

The value determined above allows, from the absorption frequency of TMS, to calculate the chemical shift of any other nucleus present in the sample where the resultant scale can be set based on secondary references already available in the literature.

Using this referencing method the chemical shift of the *fac*-[Co(L¹-S,O)₃] complex, analysed previously by Juranic⁷⁴, was determined and thus a value of $\delta(^{59}\text{Co}) = 8535$ ppm was reported. The ^{59}Co NMR spectrum for the *fac*-[Co(L¹-S,O)₃] complex is shown in **Figure 3.19**.

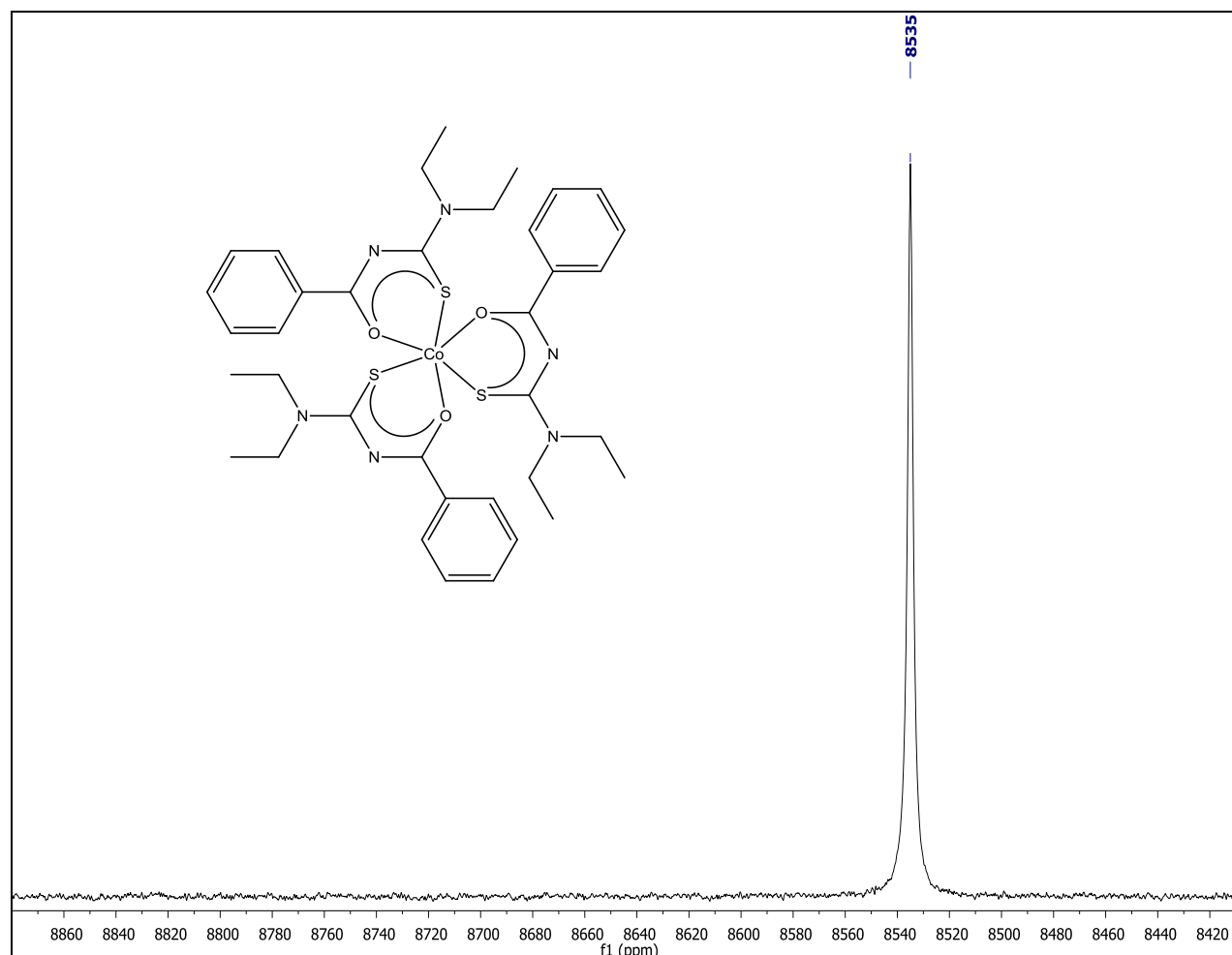


Figure 3.19. The ^{59}Co NMR spectrum of *fac*-tris(*N,N*-diethyl-*N*-benzoylthioureato)Co(III) in CDCl_3 at 25°C .

Chapter 3 | ^{59}Co NMR spectroscopy

Note that the unified scale is not very practical because of the large chemical shift range of ^{59}Co NMR, hence an secondary external reference is required closer to the chemical shift range expected for the complexes of interest in this work. Therefore the complex shown in **Figure 3.19** was used as this secondary external reference axially inserted, **Figure 3.20**, into the NMR tube containing the cobalt complex to be analysed. The complex, $\text{fac}[\text{Co}(\text{L}^1\text{-S,O})_3]$, was used as this secondary reference and can be considered the standard to which the chemical shift of all other complexes analysed could be visibly compared and will be applied as needed to all ^{59}Co NMR spectra obtained in this work.

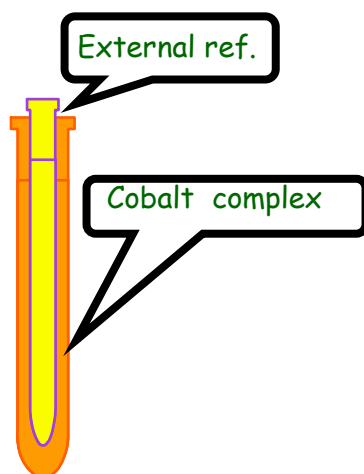


Figure 3.20. A schematic representation of how the external reference, containing the *fac*-tris(*N,N*-diethyl-*N*-benzoylthioureato)Co(III) complex, is axially inserted inside the NMR tube.

3.4. Factors which effect the shielding of the ^{59}Co nucleus

Information obtained from Nuclear Magnetic Resonance spectra is largely used by chemists for the structure elucidation of compounds. Considering the high sensitivity of NMR spectra to even the smallest changes in structure, it consequently makes this a vital piece of equipment in any laboratory. Structure effects on the other hand are not the only factor to consider in terms of NMR sensitivity especially when conducting ^{59}Co NMR experiments. The shielding of an NMR nucleus such as ^{59}Co is reflected by its “chemical shift” as well as line widths and in some cases when scalar spin coupling (J/Hz) takes place. These are all measurable NMR parameters which depend on a variety of factors which include not only the structure but the solvent, temperature and even concentration in some cases of the analyte.

Chapter 3 | ^{59}Co NMR spectroscopy

3.4.1. Effect of concentration on ^{59}Co NMR shielding

In NMR the concentrations of the “analyte” only has a slight effect on the chemical shift, if any, if no chemical exchange takes place. However due to the high chemical shift range of ^{59}Co NMR it was of interest to investigate the effect of concentration on ^{59}Co shielding of the complexes under investigation in this thesis.

A few examples are available in the literature where variations in concentration visibly effected ^{59}Co shielding^{114,115}. These complexes are able to form an outer sphere complex, i.e. the reaction that takes place between a transition metal complex and a solvent molecule. Martin and Fung¹¹⁴ studied this outer sphere complex formation between tris(ethylenediamine)cobalt(III) complexes and phosphate. The authors determined that the complex $[\text{Co}(\text{en})_3]\text{Cl}_3$ is more shielded upon addition of tetramethylammonium phosphate (TMAP), whereas higher concentrations of the complex in the absence of phosphate resulted in a more deshielded ^{59}Co NMR. This indicated some interaction between the complex and chloro anions occurred. This was further substantiated when they observed a gradual increase of the $\delta(^{59}\text{Co})$ upon slow addition of tetramethylammonium chloride, with the change in chemical shift being more pronounced in this instance than the change caused by addition of TMAP. They did not attempt to rationalize the contrasting shielding effect of the phosphate and chloride on the $\delta(^{59}\text{Co})$ of $[\text{Co}(\text{en})_3]^{3+}$, considering the complexity behind this observation, although concentration nonetheless proved here to be an important factor when considering ^{59}Co shielding. In an attempt to account for the effect of concentration in this regard, two important factors were considered; (1) the paramagnetic shielding term (2) as well as the electric field gradient (*efg*) at the cobalt nucleus.⁷⁶ These are both proportional to $\langle 1/r^3 \rangle$, where *r* represents the mean ligand-metal distance. In an octahedral symmetrical environment, the *efg* at the cobalt nucleus needs to be small and comes as a consequence of the interaction with counter-ions in solution. Hence, an increase in concentration will increase the amount of interactions between the $[\text{Co}(\text{en})_3]^{3+}$ complex and the ions in solution which accounts for the resultant change in shielding of cobalt when the concentration is increased.

In an attempt to briefly account for any effect of concentration on the ^{59}Co shielding of the complexes in this study, the ^{59}Co NMR spectra of one of the more soluble complexes, *fac*-tris(*N,N*-diethyl-*N'*-4-tertbutylbenzoylthioureato)Co(III) ($[\text{Co}(\text{L}^5\text{-S,O})_3]$), was obtained at five different concentrations in chloroform. The resultant spectra are overlaid in **Figure 3.20**.

Chapter 3 | ^{59}Co NMR spectroscopy

Although the intensity of each signal, proportional to the molar concentration, decreases as concentration is decreased, the $\delta(^{59}\text{Co})$ remains unchanged. This experiment suggests that the effect of concentration for the complexes under consideration is negligible, since there are no interactions between the solvent and complex which would warrant large differences in shielding, as observed by the study by Martin and Fung.

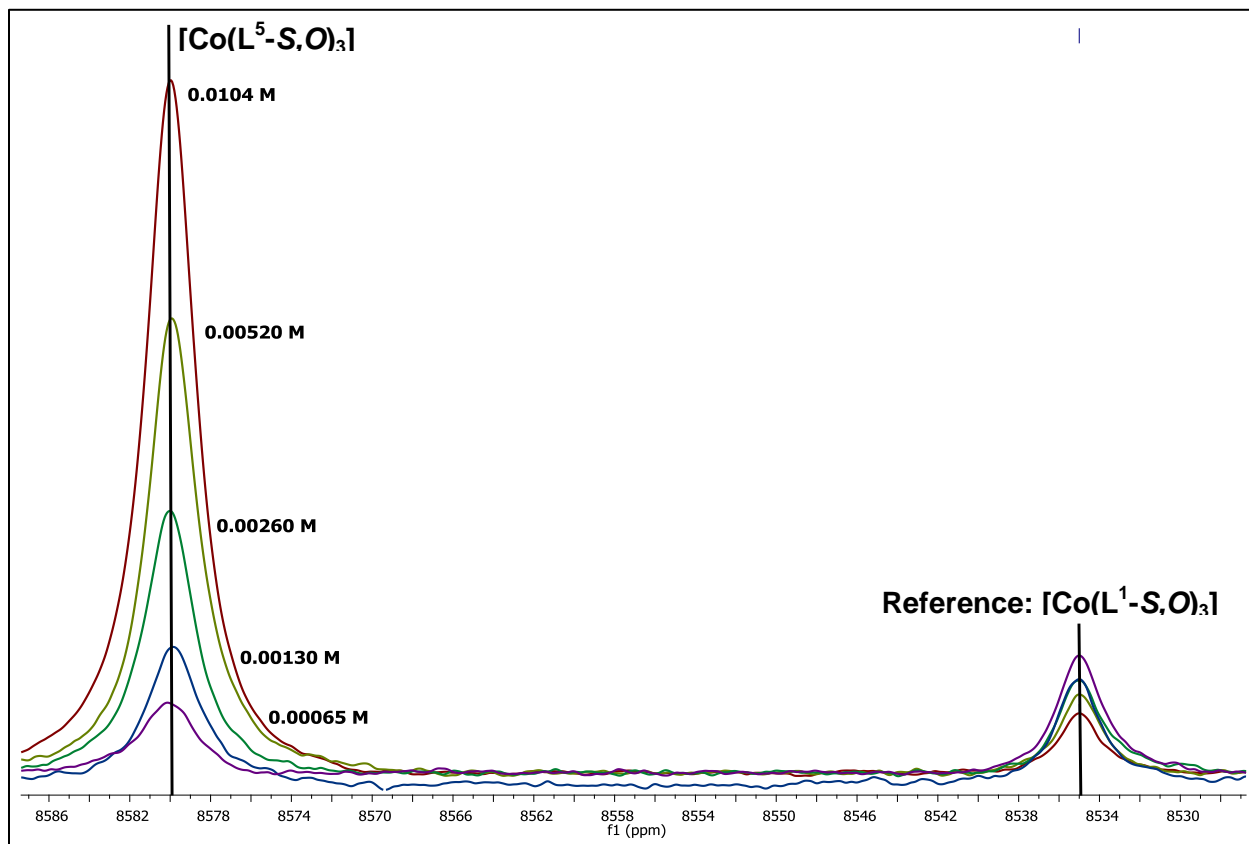


Figure 3.21. A 600 MHz ^{59}Co NMR experiment in which the spectra of *fac*-tris(*N,N*-diethyl-*N'*-4-tertbutylbenzoylthioureato)Co(III) at five different concentrations in CDCl_3 at 25 °C are overlaid and their $\delta(^{59}\text{Co})$ compared.

3.4.2. Effect of temperature on ^{59}Co NMR shielding

Various studies are available in the literature which illustrate the high sensitivity of the ^{59}Co nucleus to changes in temperature. During the 1950's Proctor and Yu¹¹⁶ became the first to recognise this relatively high temperature effect of ^{59}Co chemical shifts in Co(III) complexes. This discovery inspired research in an attempt to understand the implication of such findings. In

Chapter 3 | ^{59}Co NMR spectroscopy

1957 the work of Proctor and Yu was taken further by Freeman, Murray and Richards¹¹⁷ by extending their research to a number of different Co(III) complexes. A detailed examination followed in order to relate their experimental results to the hypothesis given by Orgel¹¹⁸ which states a correlation exists between the temperature dependence of the ^{59}Co chemical shifts and the concept of crystal field theory. This can be explained by considering the large crystal field splitting, $14\,000\text{ cm}^{-1}$, of Co(III) complexes causing almost all molecules at normal temperature to reside in their ground state. Upon raising the temperature, occupation of higher vibrational modes become possible which is expected to reduce the ligand field splitting by lowering the first excitation state relative to the ground state. The consequence being an increase in the resonance frequency with temperature.

In 1963 Benedek *et al.*¹¹⁹ conducted both pressure and temperature dependent experiments on $\delta(^{59}\text{Co})$. The measurements obtained from these pressure dependent experiments showed a correlation between the crystal field splitting and the Co-ligand distance, on condition that the compressibility of the complex is known. They were able to provide a more explicit theory as to the temperature dependence of the ^{59}Co chemical shifts. This theory considers the temperature dependent population of the vibrational levels of the electronic ground state to cause a decrease in the average value of the electronic excitation energy, ΔE , with an increase in temperature. Thus there is a linear increase in σ_p , paramagnetic screening constant, as $(\Delta E)^{-1}$ increases, leading to a higher ^{59}Co frequency shift with higher temperatures.

Although this was considered a reasonable theory, in 1987 Jameson *et al.*¹²⁰ noted that it did not hold for NMR isotope shifts as seen for transition metal complexes. Considering that both the temperature coefficient of the chemical shift and isotopic shift can be seen as measurements of shielding sensitivity to bond lengths and angles, a new theory was developed by Jameson that would ultimately clarify the temperature dependence of both. The author consequently related changes in chemical shift as a result of temperature to bond extension and that any changes in liquid density leading to intermolecular effects could be ignored for transition metals coordinated to ligands. In 1998 Kanakubo *et al.*¹²¹ determined the $\delta(^{59}\text{Co})$ of tris(acetylacetonato)cobalt(III), $[\text{Co}(\text{acac})_3]$, and tris(dipivaloylmethanato)cobalt(III), $[\text{Co}(\text{dpm})_3]$, in 14 different organic solvents at five different temperatures. The temperature coefficient ranged from $2.17\text{--}2.79\text{ ppm K}^{-1}$ in the various solvents for $[\text{Co}(\text{acac})_3]$ and $0.15\text{--}2.06\text{ ppm K}^{-1}$ for $[\text{Co}(\text{dpm})_3]$. The results of these experiments clearly illustrated the chemical shift increase with temperature and this temperature dependence was related to the work found by Jameson *et al.*¹²⁰

Chapter 3 | ^{59}Co NMR spectroscopy

A recent comprehensive study on the temperature and pressure dependence of ^{59}Co NMR, by Gillies *et al.*¹²², was done on the highly symmetrical hexacyanocobaltate(III) ($[\text{Co}(\text{CN})_6]^{3-}$) complex in D_2O . The high symmetry of the complex makes it particularly useful for determining the effect to even the smallest changes in external conditions. A linear relationship was found for the temperature dependence of the complex with a temperature coefficient of $+1.401 \pm 0.003$ ppm K^{-1} , which compared well with the value previously obtained by Levy *et al.*¹²³. Relatively large temperature coefficients such as these require careful temperature control during all experimental measurements.

The temperature coefficient of two relatively soluble Co(III) complexes under investigation namely *fac*-tris(*N,N*-diethyl-*N'*-4-tertbutylbenzoylthioureato)Co(III), i.e. $[\text{Co}(\text{L}^5\text{-S,O})_3]$ and *fac*-tris(*N,N*-diethyl-*N'*-4-chlorobenzoylthioureato)Co(III), i.e. $[\text{Co}(\text{L}^4\text{-S,O})_3]$ were determined. No such values have previously been determined for similar Co(III) complexes of type $[\text{Co}(\text{L-S,O})_3]$. The two complexes investigated are illustrated in **Figure 3.22**.

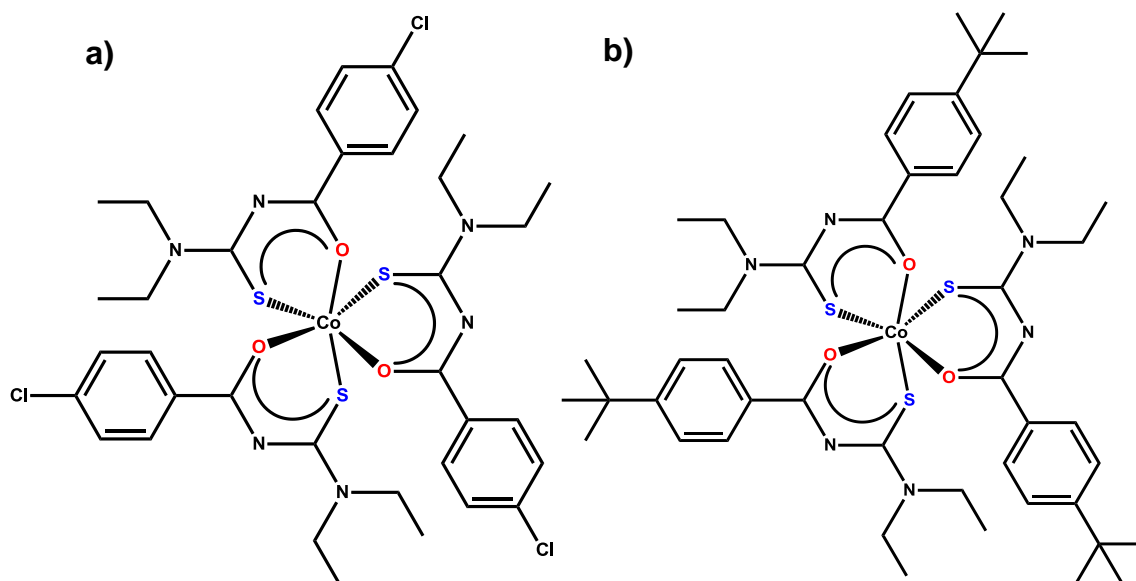


Figure 3.22. The two complexes used for the temperature dependence study namely a) *fac*-tris(*N,N*-diethyl-*N'*-4-chlorobenzoylthioureato)Co(III) and b) *fac*-tris(*N,N*-diethyl-*N'*-4-tertbutylbenzoylthioureato)Co(III).

Chapter 3 | ^{59}Co NMR spectroscopy

The temperature dependent experiment for last mentioned complexes commenced at 298 K in CDCl_3 and concluded after increasing the temperature to 318 K, obtaining a ^{59}Co NMR spectrum after every 5° increment. The results for the first experiment are shown in **Figure 3.23** for the $[\text{Co}(\text{L}^5\text{-S,O})_3]$ complex with a calculated temperature coefficient of 2.4 ppm K^{-1} . The results for the subsequent temperature dependent experiment of $[\text{Co}(\text{L}^4\text{-S,O})_3]$ is shown in **Figure 3.24** and the temperature coefficient for this complex was determined as 3.0 ppm K^{-1} . The results illustrated the same linear relationship found for the temperature dependent study of the highly symmetrical hexacyanocobaltate(III) complex by Gillies *et al.*¹²² The temperature dependent results for complexes under investigation could be justified by considering the work by Benedek *et al.*¹¹⁹ who suggested an increase in the paramagnetic shielding contribution, σ_p , in ^{59}Co NMR, to be inversely related to the average excitation energy gap $(\Delta E)^{-1}$ between the HOMO and LUMO electronic levels as the temperature changes. Line widths are summarized in **Table 3.4** and remain relatively steady in contrast to the $\delta(^{59}\text{Co})$, indicating that overall symmetry in the Co(III) complexes are retained with increase in temperature.

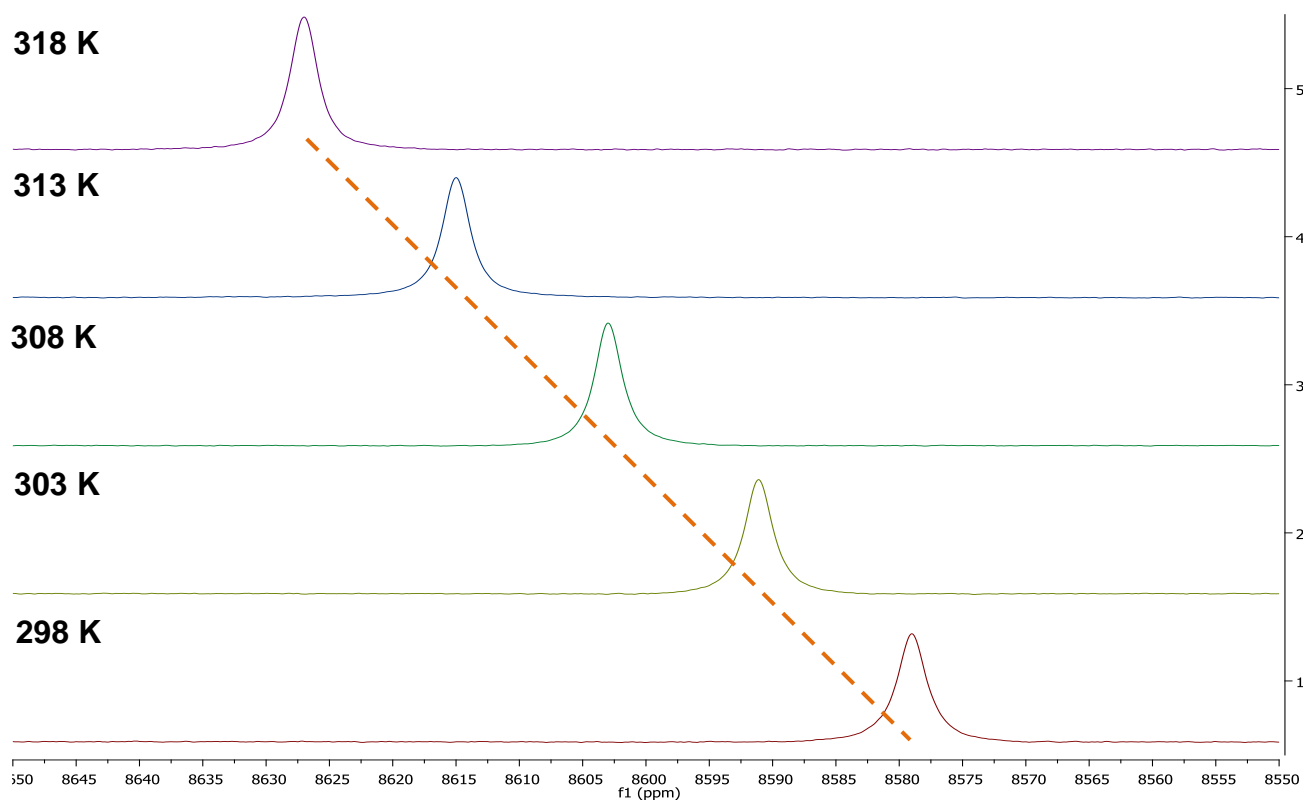


Figure 3.23. The 600 MHz ^{59}Co NMR temperature dependent experiment of *fac-tris*(*N,N*-diethyl-*N'*-4-*tert*butylbenzoylthioureato)Co(III) in CDCl_3 .

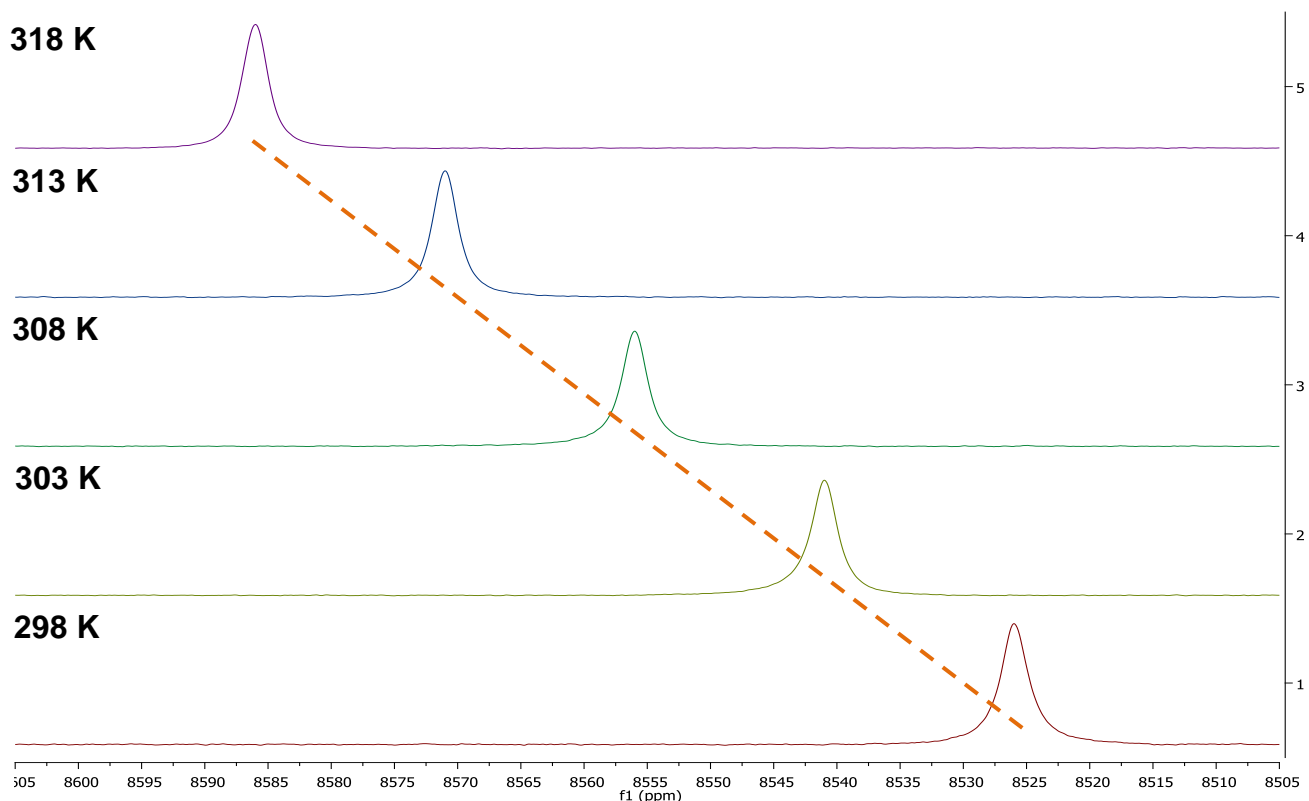
Chapter 3 | ^{59}Co NMR spectroscopy

Figure 3.24. The 600 MHz ^{59}Co NMR temperature dependent experiment of *fac*-tris(*N,N*-diethyl-*N'*-4-chlorobenzoylthioureato)Co(III) in CDCl_3 .

Table 3.4. Temperature dependence of $\delta(^{59}\text{Co})$ and half-height line widths ($\Delta_{1/2}$) from the 600 MHz ^{59}Co NMR spectra of *fac*-tris(*N,N*-diethyl-*N'*-4-tertbutylbenzoylthioureato)Co(III) and *fac*-tris(*N,N*-diethyl-*N'*-4-chlorobenzoylthioureato)Co(III) respectively.

$[\text{Co}(\text{L}^5\text{-S,O})_3] - 2.4 \text{ ppm K}^{-1}$			$[\text{Co}(\text{L}^4\text{-S,O})_3] - 3.0 \text{ ppm K}^{-1}$		
Temperature (K)	$\delta(^{59}\text{Co})/\text{ppm}$	$\Delta_{1/2}$ (Hz)	Temperature (K)	$\delta(^{59}\text{Co})/\text{ppm}$	$\Delta_{1/2}$ (Hz)
298	8579	374	298	8525	366
303	8591	352	303	8540	346
308	8603	350	308	8555	351
313	8615	374	313	8570	348
318	8627	368	318	8585	331

3.4.3. Effect of solvent on ^{59}Co NMR shielding

Another important factor to consider when conducting ^{59}Co NMR experiments is the effect of solvent. Freeman *et al.*¹¹⁷ were the first to implement such a study and conducted an investigation into the effect of solvent on the ^{59}Co chemical shifts of tris(acetylacetonato)cobalt(III). This particular complex was selected for its solubility in a range of different solvents in order to determine to which extent the $\delta(^{59}\text{Co})$ depends on the type of solvent used. The chemical shift values ranged over 200 ppm starting from the most deshielded signal at 12 741 ppm in acetone, changing gradually for every subsequent solvent including (in order of decreasing chemical shift) DMF, benzene, toluene, carbon disulphide, ether, ethanol and finally reaching the lowest chemical shift of 12 565 ppm in chloroform. Although this chemical shift range is small compared to the overall cobalt shielding range, the effect of solvent is nonetheless a necessity to consider especially regarding compounds with similar chemical shift values. Another solvent dependent study of ^{59}Co NMR chemical shifts was done on tris(acetylacetonato)cobalt(III) and tris(dipivaloylmethanato)cobalt(III) by Kanakubo *et al.*¹²¹ in a variety of solvents. The authors noted that the observed $\delta(^{59}\text{Co})$ for tris(dipivaloylmethanato)cobalt(III) appeared over a wider range than the $\delta(^{59}\text{Co})$ observed for tris(acetylacetonato)cobalt(III) in the different solvent. Overall solvent effects were rationalized by referring to the work of Juranic¹²⁴ which related such observations to a change in the d-d electronic excitation energy.

The effect of solvent on the $\delta(^{59}\text{Co})$ of the soluble *fac*-tris(*N,N*-diethyl-*N'*-4-methoxybenzoylthioureato)Co(III), i.e. $[\text{Co}(\text{L}^2\text{-S,O})_3]$, complex was investigated in order to determine effect of solvent on the ^{59}Co NMR shielding of Co(III) complexes of type $[\text{Co}(\text{L-S,O})_3]$. The ^{59}Co NMR spectrum of the complex was obtained at different solvent ratios (% v/v) of chloroform relative to acetonitrile. Each signal is referenced to the same compound as previously mentioned in **section 3.4.1**, i.e. $[\text{Co}(\text{L}^1\text{-S,O})_3]$. The $\delta(^{59}\text{Co})$ as well as half-height line widths ($\Delta_{1/2}$) are summarized in **Table 3.5**. A noteworthy observation from the ^{59}Co NMR spectra shown in **Figure 3.25**, is the increase in the $\delta(^{59}\text{Co})$ upon addition of steady amounts of acetonitrile to the Co(III) complex dissolved in chloroform. The increase in the $\delta(^{59}\text{Co})$ is most prominent for the second and third signals, after which the change in the $\delta(^{59}\text{Co})$ becomes progressively less pronounced as the volume percentage (% v/v) is altered, i.e. increasing amount of acetonitrile relative to chloroform. This trend is clearly evident by the blue line in the graph in **Figure 3.26**. In an attempt to clarify these results, consider the change in half-height

Chapter 3 | ^{59}Co NMR spectroscopy

line widths ($\Delta_{1/2}$) of the Co(III) complex as the solvent ratio is altered, illustrated by the red line in **Figure 3.26**. Note that as the $\delta(^{59}\text{Co})$ increases, the line width of the complex decreases. Line widths depend on the symmetry of the electronic environment surrounding the metal center. Therefore the overall decrease in line width observed upon addition of acetonitrile suggest there is some interaction between the Co(III) complex and acetonitrile subtly altering the octahedral geometry, which in turn effects the shielding experienced by the ^{59}Co nucleus. Another possibility relates the observed changes in the $\delta(^{59}\text{Co})$ and line widths to viscosity effects in mixed solvents, although further work is required to substantiate such assumptions.

Table 3.5. ^{59}Co chemical shift and half-height line widths ($\Delta_{1/2}$) values of *fac*-tris(*N,N*-diethyl-*N'*-4-methoxybenzoylthioureato)Co(III) at different volume ratios of chloroform:acetonitrile (v/v) at 25 °C.

Chloroform: Acetonitrile (v/v)	$\delta(^{59}\text{Co})/\text{ppm}$	$\Delta_{1/2}$ (Hz)
100:0	8564	609
95:5	8589	556
90:10	8598	530
80:20	8603	505
70:30	8607	510
60:40	8609	469
50:50	8612	440
0:100	8619	267

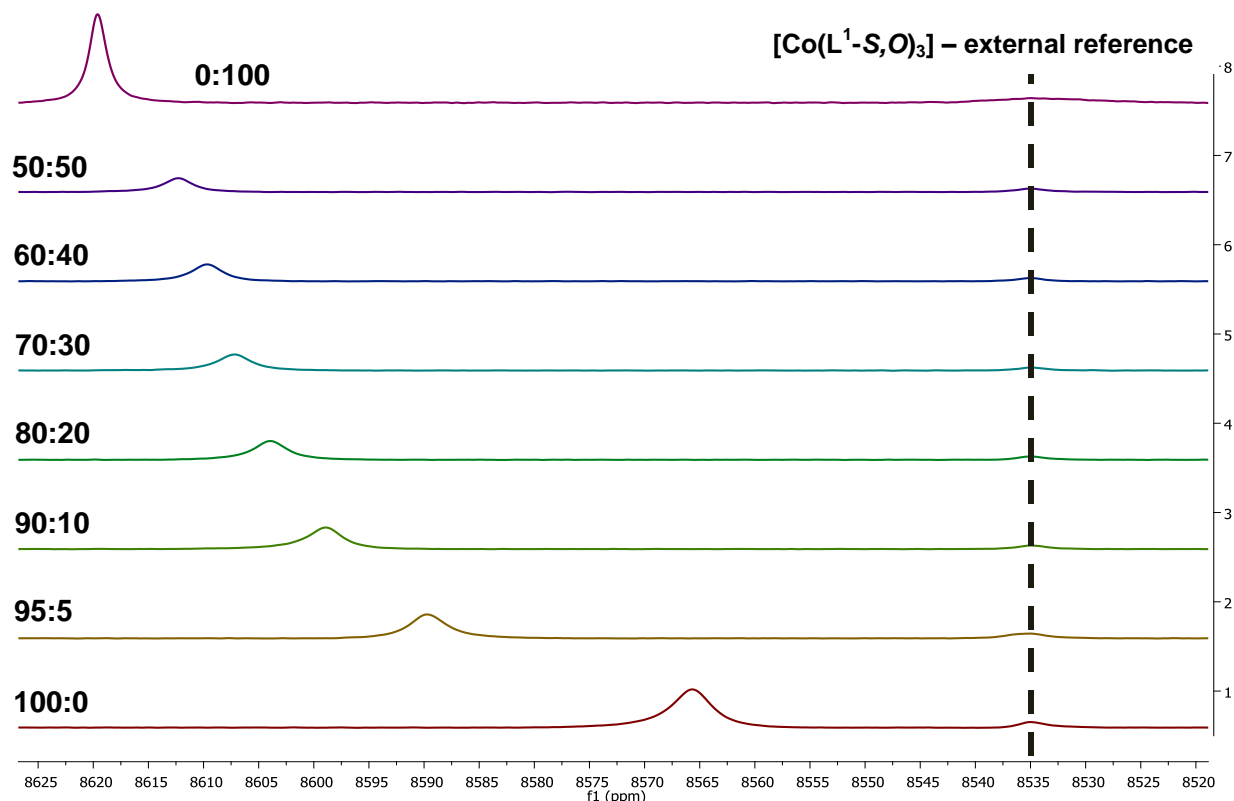
Chapter 3 | ^{59}Co NMR spectroscopy

Figure 3.25. ^{59}Co NMR spectra of *fac*-tris(*N,N*-diethyl-*N'*-4-methoxybenzoylthioureato)Co(III) at different volume ratios of chloroform:acetonitrile (v/v) at 25 °C.

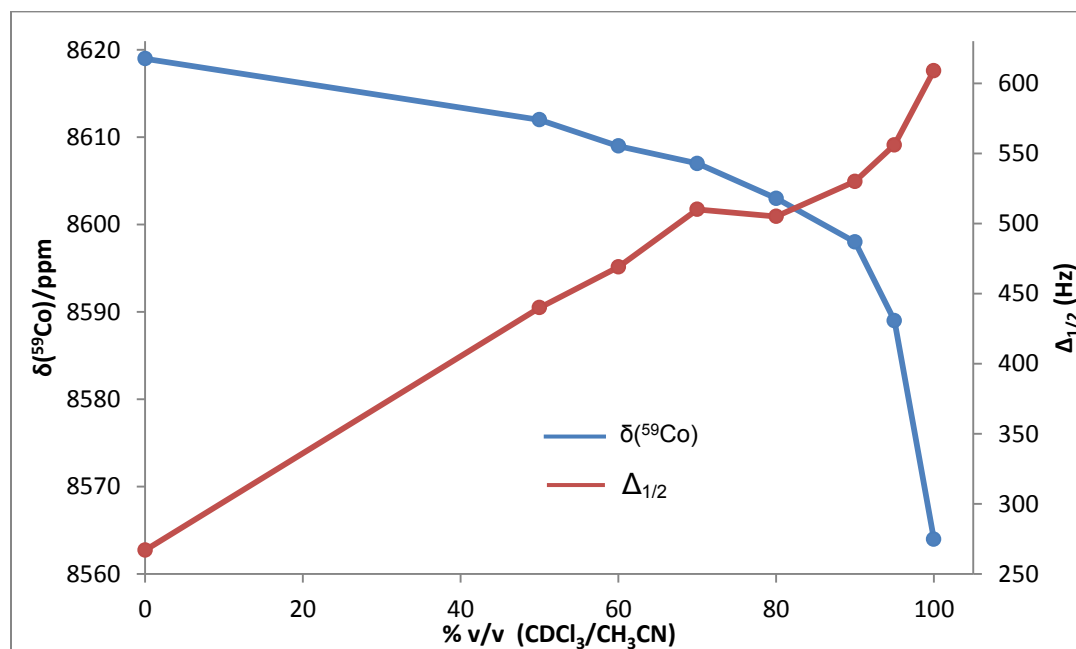


Figure 3.26. Graphic illustration of change in $\delta(^{59}\text{Co})$ and half-height line widths ($\Delta_{1/2}$) of *fac*-tris(*N,N*-diethyl-*N'*-4-methoxybenzoylthioureato)Co(III) with a change in % v/v ($\text{CDCl}_3/\text{CH}_3\text{CN}$).

Chapter 3 | ^{59}Co NMR spectroscopy3.4.4. Effect of ligand structure on ^{59}Co NMR shielding

The $\delta(^{59}\text{Co})$ of complexes $[\text{Co}(\text{L}^1\text{-S},\text{O})_3]$ - $[\text{Co}(\text{L}^{10}\text{-S},\text{O})_3]$ were compared in order to determine the effect of varying the symmetrical *N,N*-dialkyl-*N'*-acylthiourea structure coordinated to Co(III) on the ^{59}Co NMR shielding. The results are summarized in **Table 3.6**. Complex $[\text{Co}(\text{L}^1\text{-S},\text{O})_3]$ was used as the external reference and observed at 8535 ppm, with the $\delta(^{59}\text{Co})$ of every subsequent complex compared relative to this value. The collective ^{59}Co NMR results from this analysis is shown in **Figure 3.27**. In an attempt to justify the results, various factors able to effect the chemical shift of organometallic complexes including either the inductive, resonance or polarisability effects of the ligand substituents were considered.

Initially comparisons were made of the $\delta(^{59}\text{Co})$ of complexes that differ only at the carbonyl moiety. Complexes $[\text{Co}(\text{L}^2\text{-S},\text{O})_3]$, $[\text{Co}(\text{L}^4\text{-S},\text{O})_3]$ and $[\text{Co}(\text{L}^5\text{-S},\text{O})_3]$ are good examples of the role played by the mesomeric effect on the $\delta(^{59}\text{Co})$. The benzene substituents of the acylthiourea ligands coordinated to complexes $[\text{Co}(\text{L}^2\text{-S},\text{O})_3]$ and $[\text{Co}(\text{L}^5\text{-S},\text{O})_3]$ both have electron releasing properties, which shifts the $\delta(^{59}\text{Co})$ to higher values relative to the reference. Complex $[\text{Co}(\text{L}^4\text{-S},\text{O})_3]$ on the other hand has an electron withdrawing group which in contrast shifts the $\delta(^{59}\text{Co})$ to slightly lower values. When the benzene ring of the reference compound is replaced by a tertiary butyl group, as for complex $[\text{Co}(\text{L}^{10}\text{-S},\text{O})_3]$, it is significantly more shielded than the reference, which suggests the inductive effect is diminished by the steric effect caused by the large substituent. Complexes $[\text{Co}(\text{L}^3\text{-S},\text{O})_3]$ and $[\text{Co}(\text{L}^7\text{-S},\text{O})_3]$ have chemical shift values similar to the reference, hence assume their structural differences have effects too subtle to relate to either steric or inductive effects.

Comparisons were made between the three complexes that differ only at the thiocarbonyl moiety. The terminal CH_3 groups of the tertiary amine in the reference compound are replaced in $[\text{Co}(\text{L}^8\text{-S},\text{O})_3]$ by voluminous alkyl groups which causes a very slight shift from the reference compound to a lower $\delta(^{59}\text{Co})$. The $[\text{Co}(\text{L}^9\text{-S},\text{O})_3]$ complex is shielded more than any other complex attributed to steric effects pertaining to the two terminal phenyl groups of the tertiary amine. The $[\text{Co}(\text{L}^6\text{-S},\text{O})_3]$ complex, although structurally very similar to the reference compound, is also considerably more shielded than the reference compound. All ten compounds appear in a range of 137 ppm which suggests the $\delta(^{59}\text{Co})$ is remarkably sensitive to variations in the *N,N*-dialkyl-*N'*-acylthiourea structure, although no clear structure $\delta(^{59}\text{Co})/\text{ppm}$ trend was evident in the data obtained in this study.

Chapter 3 | ^{59}Co NMR spectroscopy

The half-height line widths ($\Delta_{1/2}$), related to the complex symmetry, of the various complexes are reported in **Table 3.6**. The large variations observed for the measured line widths for some complexes illustrate the extent to which some deviate from the ideal octahedral symmetry more than others. Large line widths indicate more distortion whereas smaller line widths indicate less distortion from the ideal geometry. This is evident with some complexes coordinated to bulky substituents such as complexes $[\text{Co}(\text{L}^8\text{-S},\text{O})_3]$ and $[\text{Co}(\text{L}^9\text{-S},\text{O})_3]$ with the two largest half-height line widths equal to 499 and 482 Hz respectively.

Table 3.6. ^{59}Co chemical shifts and half-height line widths ($\Delta_{1/2}$) values of complexes $[\text{Co}(\text{L}^1\text{-S},\text{O})_3]$ - $[\text{Co}(\text{L}^{10}\text{-S},\text{O})_3]$ at 25 °C all measured in CDCl_3 .

Complex	$\delta(^{59}\text{Co})/\text{ppm}$	$\Delta_{1/2}$ (Hz)
$[\text{Co}(\text{L}^1\text{-S},\text{O})_3]$ - external reference	8535	349
$[\text{Co}(\text{L}^2\text{-S},\text{O})_3]$	8564	433
$[\text{Co}(\text{L}^3\text{-S},\text{O})_3]$	8540	321
$[\text{Co}(\text{L}^4\text{-S},\text{O})_3]$	8525	420
$[\text{Co}(\text{L}^5\text{-S},\text{O})_3]$	8579	392
$[\text{Co}(\text{L}^6\text{-S},\text{O})_3]$	8458	166
$[\text{Co}(\text{L}^7\text{-S},\text{O})_3]$	8531	382
$[\text{Co}(\text{L}^8\text{-S},\text{O})_3]$	8534	499
$[\text{Co}(\text{L}^9\text{-S},\text{O})_3]$	8442	482
$[\text{Co}(\text{L}^{10}\text{-S},\text{O})_3]$	8500	238

In **sections 3.1.2** and **3.1.3** the possibility of various isomers, i.e. same molecular formula but different chemical structures, resulting from the coordination of Co(III) to certain acylthiourea ligands were mentioned. It became of significant interest to determine if ^{59}Co NMR spectroscopy could be utilized to identify more than one isomer present in solution, whether configurational or geometrical, and to which extent these isomers could be separated in terms of their ^{59}Co shielding.

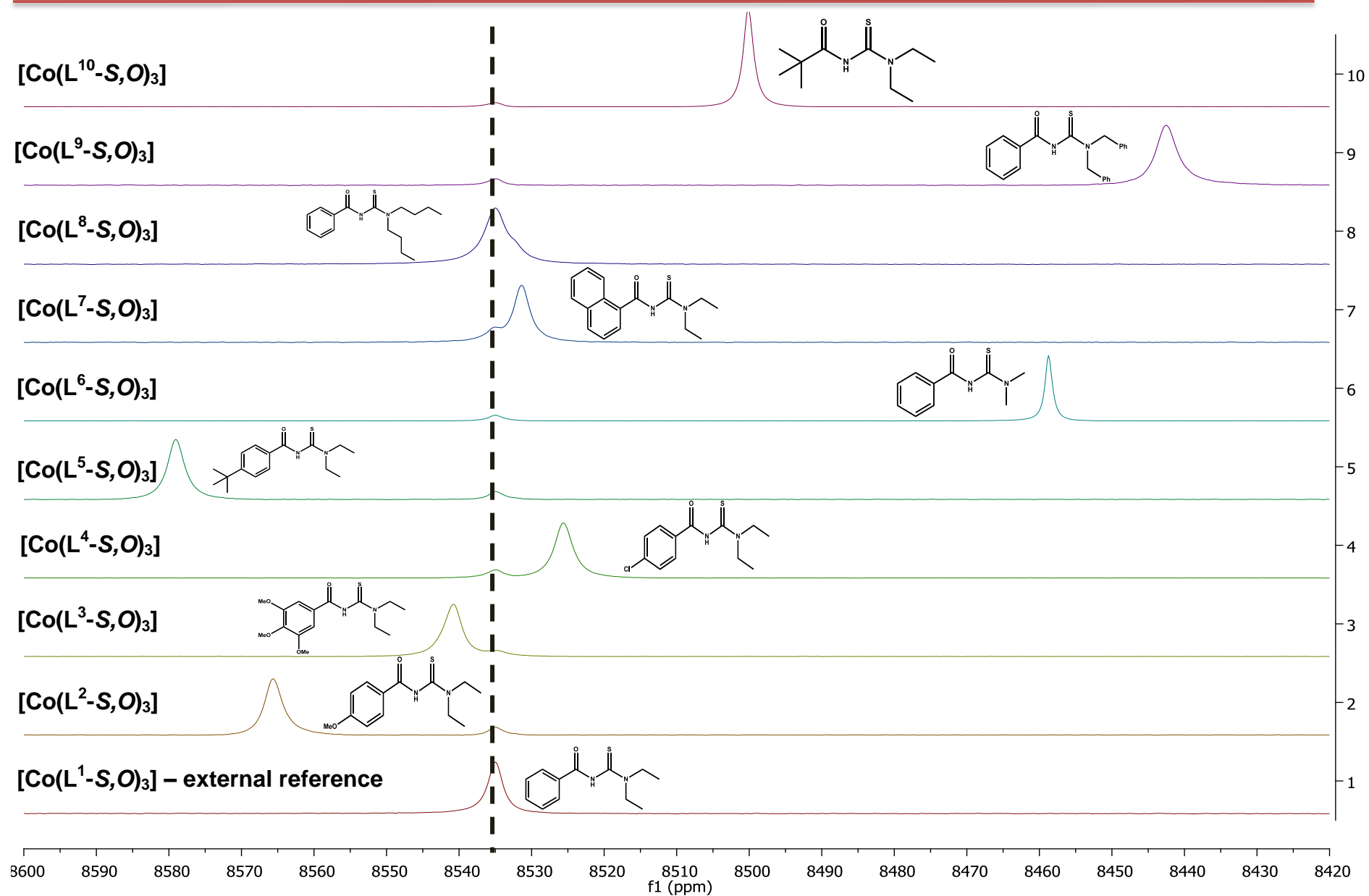
Chapter 3 | ^{59}Co NMR Spectroscopy

Figure 3.27. The 600 MHz ^{59}Co NMR spectra of complexes $[\text{Co}(\text{L}^1\text{-S},\text{O})_3]$ - $[\text{Co}(\text{L}^{10}\text{-S},\text{O})_3]$ at 25 °C in CDCl_3 showing their respective ligands next to every peak, illustrating how ligand structure effects $\delta(^{59}\text{Co})$ upon coordination to Co(III).

Chapter 3 | ^{59}Co NMR Spectroscopy

The complex *fac*-tris(*N*-methyl-*N*-ethyl-*N'*-benzoylthioureato)cobalt(III) has four possible configurational isomers, depending on the orientation of the ligand in each chelate (*i.e.* *E* or *Z*), and the isomers can be referred to as *fac*-[Co(*EEE*-L-S,O)₃], *fac*-[Co(*EZE*-L-S,O)₃], *fac*-[Co(*ZZZ*-L-S,O)₃] or *fac*-[Co(*ZZE*-L-S,O)₃], as discussed in **section 3.1.2**. The ^{59}Co NMR spectrum of this complex is shown in **Figure 3.28**. Note that although only one analytically pure complex is present in solution, four well separated signals can be observed in the spectrum, each present at different ratios. Each signal is suggested to be related to one of the four different isomers as proposed for this complex. Various factors need to be considered in order to assign one isomer to the specific signal and will require an in depth study in its own right, which is beyond the scope of this work.

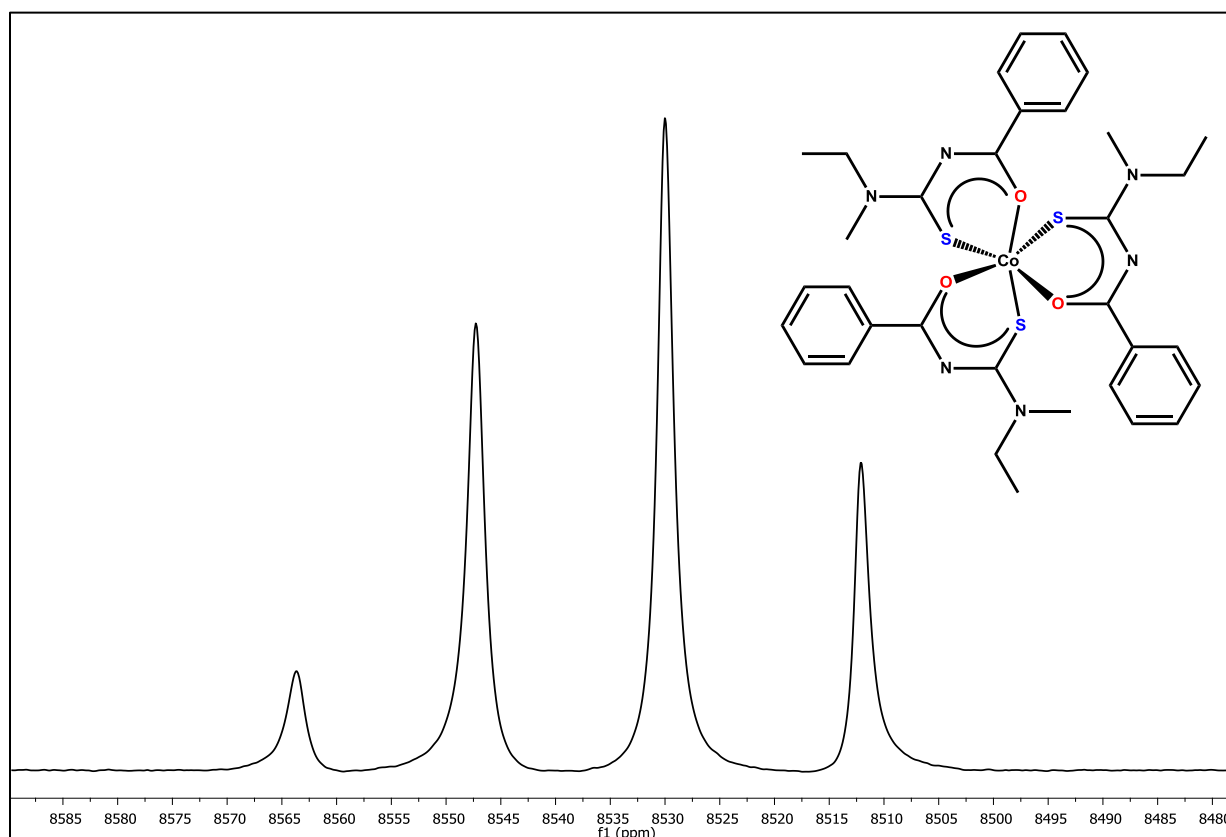


Figure 3.28. 600 MHz ^{59}Co NMR spectrum of *fac*-tris(*N*-methyl-*N*-ethyl-*N'*-benzoylthioureato)cobalt(III) in CDCl_3 at 25 °C, illustrating four peaks representative of four different configurational isomers.

Chapter 3 | ^{59}Co NMR Spectroscopy

In Chapter 1, **section 1.2.3**, we briefly discussed that octahedral complexes are able to exist as optical isomers. Enantiomeric compounds, i.e. non-superimposable mirror images, have the exact same physical properties; hence only one peak is observed in the ^{59}Co NMR spectrum seen for the previously analysed complexes shown in **Figure 3.27**. Upon coordination of a chiral acylthiourea ligand, *N,N*-diethyl-*N'*-camphanoylthiourea, to Co(III), two signals are observed in the ^{59}Co NMR spectrum (**Figure 3.29**). This suggests that the inherent chirality of the ligand upon coordination to Co(III) causes the complex to no longer exist as non-superimposable mirror images and therefore exists as either one of two possible stereoisomers not related by their mirror images, namely diastereomers. Since diastereomers, unlike enantiomers, do not have the exact same physical properties the shielding felt by the ^{59}Co nucleus will differ to an extent for each isomer, depending on the electronic environment, and therefore two separate signals are observed in the spectrum. The integrals also differ for the two signals which indicate some stereoselectivity since one stereoisomer is evidently formed in slight excess to the other. Assignment of the two peaks to the particular diastereomer as well as rationalizing differences in peak ratios have not been discussed in any previous work and will require further investigation beyond the scope of this thesis.

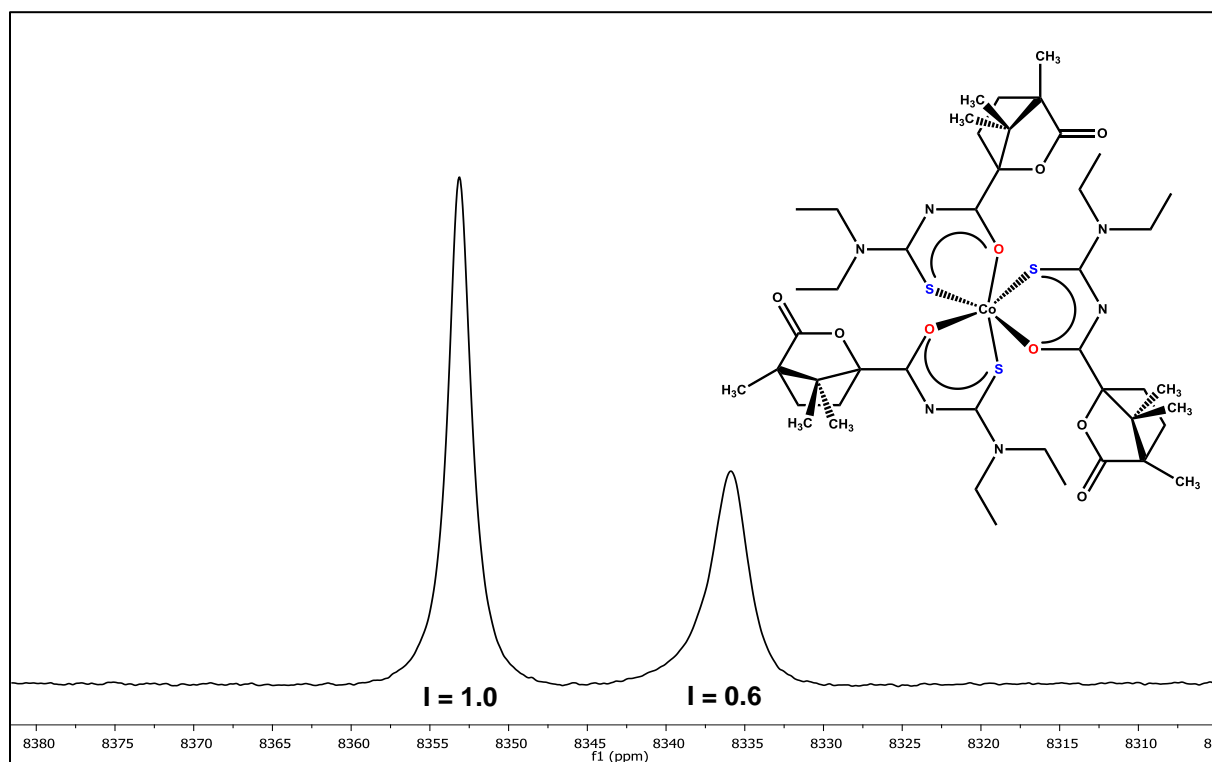


Figure 3.29. 600 MHz ^{59}Co NMR spectra of *fac*-tris(*N,N*-diethyl-*N'*-camphanoylthiourea)cobalt(III) in CDCl_3 at 25 °C.

Chapter 3 | Conclusion

3.5. Conclusion

Various Co(III) complexes coordinated to acylthiourea ligands were characterized by means of ^1H NMR, ^{13}C NMR, infrared spectroscopy, elemental analysis as well as X-ray crystallography. All complexes, substantiated by X-ray crystallography, coordinate preferentially in a distorted *facial* octahedral coordination sphere with ligands binding *via* the bidentate mode by means of the sulphur and oxygen donor atoms.

The spectroscopic, ^1H and ^{13}C NMR, results for all symmetrical complexes, i.e. $[\text{Co}(\text{L}^1\text{-S},\text{O})_3]$ – $[\text{Co}(\text{L}^{10}\text{-S},\text{O})_3]$, are relatively similar to the spectra of their respective unbound ligands, accept for some differences in chemical shift and coupling constants. These differences can be related to a variety of factors including the paramagnetic anisotropy caused by the metal center upon coordination, a decrease in the rotational barrier of the thioamide fragment and diastereotopicity. The otherwise similar ^1H and ^{13}C NMR spectra observed for the symmetrical Co(III) complexes and their unbound ligands, gives a clear indication that only type of isomer is present in solution for these complexes, i.e. the geometrical *fac* isomer. This is not the case for the coordination of Co(III) to either the unsymmetrical, *N*-methyl-*N*-ethyl-*N'*-benzoylthiourea, or chiral, *N,N*-diethyl-*N'*-camphanoylthiourea, ligand, whose ^1H and ^{13}C NMR spectra differed significantly with the spectra of their respective unbound ligands. This was attributed to the presence of more than one isomer formed upon coordination to the metal center, since additional peaks were observed in the spectra of the complexes not otherwise seen in the spectra of the respective unbound ligands.

^{59}Co NMR spectroscopy was furthermore utilized in order to investigate the octahedral- d^6 cobalt(III) complexes of type *fac*- $[\text{Co}(\text{L-S},\text{O})_3]$. The shielding experience by ^{59}Co nucleus is effected by a variety of factors which include not only the structure of the complex but also the solvent, temperature and concentration in some cases of the analyte. It was thus of interest to determine how each of these factors effect the $\delta(^{59}\text{Co})$ of the Co(III) complexes under consideration. The temperature dependence of the $\delta(^{59}\text{Co})$ was determined for complexes *fac*- $[\text{Co}(\text{L}^4\text{-S},\text{O})_3]$ and *fac*- $[\text{Co}(\text{L}^5\text{-S},\text{O})_3]$ with calculated temperature coefficients of 2.4 and 3.0 ppm K^{-1} respectively. An earlier literature study related this temperature dependence to the paramagnetic screening constant which increases as the electronic excitation state increases hence leading to a higher ^{59}Co frequency shift with higher temperatures.¹¹⁹ Solvent composition also proved to strongly influence the $\delta(^{59}\text{Co})$. Various ^{59}Co NMR spectra were obtained of the soluble *fac*- $[\text{Co}(\text{L}^2\text{-S},\text{O})_3]$ complex dissolved in different ratios of chloroform and acetonitrile with

Chapter 3 | Conclusion

the complex becoming less shielded as the percentage acetonitrile relative to chloroform was increased. This was justified by considering the change in line-width which also decreased as the amount of acetonitrile relative to chloroform was increased, which strongly suggests some interaction between the solvent and complex which alters the octahedral geometry in a way that effects the shielding felt by the ^{59}Co nucleus.

The $\delta(^{59}\text{Co})$ of symmetrical complexes, i.e. $[\text{Co}(\text{L}^1\text{-S},\text{O})_3] - [\text{Co}(\text{L}^{10}\text{-S},\text{O})_3]$, were obtained to determine to which extent the ^{59}Co nucleus is effected by alterations in the acylthiourea ligand structure coordinated to Co(III). The factors considered to effect the $\delta(^{59}\text{Co})$ were related to either inductive or steric effects depending on the specific substituents of the acylthiourea ligand coordinated to Co(III). All complexes appeared in a spectral range of 137 ppm. The ^{59}Co NMR spectra obtained for the Co(III) complexes coordinated to a unsymmetrical as well as chiral ligand proved that possible isomerism, whether it be configurational isomerism or stereoisomerism, resulting from coordination to Co(III) could be separated and investigated by means of ^{59}Co NMR spectroscopy.

Considering the limited information available in the literature regarding Co(III) complexes of the type *fac*- $[\text{Co}(\text{L-S},\text{O})_3]$ it brings forth the question as to the lability of said complexes. Low-spin d^6 octahedral complexes are generally considered substitutionally inert, although this depends to some extent on the nature of the ligands coordinated to the metal ion. What follows is a brief study into the lability of the complexes under investigation by considering the possible ligand exchange reaction between pairs of homoleptic complexes of the type *fac*- $[\text{Co}(\text{L-S},\text{O})_3]$.

CHAPTER FOUR

**A STUDY OF THE LIGAND
EXCHANGE REACTION BY ^{59}Co
NMR SPECTROSCOPY AND *RP*-
HPLC**

Chapter 4 | The ligand exchange reaction

4.1. Investigate the ligand exchange reaction by ^{59}Co NMR spectroscopy and *rp*-HPLC

4.1.1. Introduction

From *rp*-HPLC results obtained in honors it was suggested that the unexpected ligand exchange reaction occurs upon addition of two different homoleptic Co(III) complexes under investigation in this work. The chromatogram revealed, after some time, two additional peaks appeared between the peaks corresponding to the two different homoleptic complexes initially added to the same solution. Although the possibility of ligand exchange was only speculated at the time, it was somewhat substantiated when the same results were observed in the ^{59}Co NMR spectra. Again, two additional signals appeared days after two different homoleptic complexes were mixed together in solution with $\delta(^{59}\text{Co})$ between the initial signals. This reaction is surprising, considering that first row d^6 transition metals able to exist in higher oxidation states, such as Co(III), generally form low-spin complexes which are typically considered substitutionally inert. The reason being, according to ligand field theory, low-spin complexes have large Δ splitting of the *d* orbitals and for Co(III) this means the low energy t_{2g} orbitals are filled before the higher energy e_g orbitals. When there are no higher energy electrons, as for low-spin d^6 Co(III), the bond to the ligand is stronger. The degree of Δ splitting is also influenced by the ligand coordinated to the metal where some either increase, i.e. strong field ligands, or decrease, i.e. weak-field ligands, the amount of Δ splitting. Low-spin octahedral Co(III) complexes could therefore, in principal, become more labile depending on the ligands coordinated to the metal center.

Ligand exchange in Co(III) octahedral complexes of the type *tris*(*N,N*-dialkyl-*N'*-aroyl(acyl)thioureato)cobalt(III) ($[\text{Co}(\text{L-S},\text{O})_3]$) have not been reported to date. It was of subsequent interest to elaborate on the results observed in honors by conducting a more detailed study on the relative rate and extent of ligand exchange between two different homoleptic complexes of the type *fac*- $[\text{Co}(\text{L}^{\text{A}}\text{-S},\text{O})_3]$ and *fac*- $[\text{Co}(\text{L}^{\text{B}}\text{-S},\text{O})_3]$. Investigation of ligand exchange reactions were carried out by means of ^{59}Co NMR spectroscopy, *rp*-HPLC and LC-MS.

Chapter 4 | The ligand exchange reaction

4.1.2. Investigate ligand exchange by ^{59}Co NMR spectroscopy

The ligand exchange reaction was initially investigated between two different pairs of homoleptic $[\text{Co}(\text{L}-\text{S},\text{O})_3]$ complexes by means of ^{59}Co NMR spectroscopy. Three complexes were selected for this study based on their solubility in the particular solvent required, i.e. chloroform, considering that the solubility of most complexes considered were too low for attaining reproducible or sensible results. For every experiment that followed, the two different homoleptic complexes were dissolved in separate vials in deuterated chloroform (at a concentration of approximately 5 mM unless stated otherwise) after which equimolar amounts of each were added to the 5 mm NMR tube. All experiments were referenced to the same complex, tris(*N,N*-diethyl-*N'*-benzoylthioureato)Co(III), used for the ^{59}Co NMR spectra obtained in chapter 3.

The first reaction investigated is illustrated in **Figure 4.1** between tris(*N,N*-diethyl-*N'*-4-chlorobenzoylthioureato)Co(III) ($[\text{Co}(\text{L}^4-\text{S},\text{O})_3]$) and tris(*N,N*-diethyl-*N'*-4-tertbutylbenzoylthioureato)Co(III) ($[\text{Co}(\text{L}^5-\text{S},\text{O})_3]$), A and B respectively. The two different homoleptic complexes, as a result of ligand exchange, give rise to two new heteroleptic complexes (C and D).

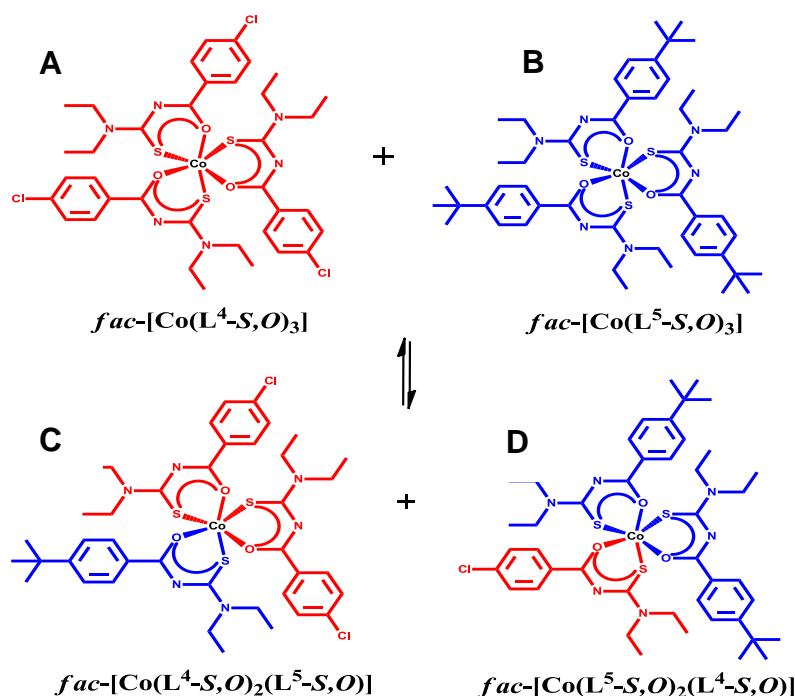


Figure 4.1. The ligand exchange reaction between tris(*N,N*-diethyl-*N'*-4-chlorobenzoylthioureato)Co(III) (**A**) and tris(*N,N*-diethyl-*N'*-4-tertbutylbenzoylthioureato)Co(III) (**B**) resulting in two new heteroleptic complexes **C** and **D**.

Chapter 4 | The ligand exchange reaction

The ^{59}Co NMR spectra of the reaction illustrated in **Figure 4.1** are shown in **Figure 4.2**. The two signals at day 1 correspond to the two complexes initially added in the same solution. Note the ratios for the two complexes are approximately 1:1 when looking at their respective integrals. After a couple of days, the total peak areas of the initial complexes begin to decrease as the total peak area of the new peaks begin to increase, with $\delta(^{59}\text{Co})$ between that of the first mentioned complexes. The change in peak area is the consequence of ligand exchange, where the amount of homoleptic species in solution decrease relative to the increase in heteroleptic species as ligands are interchanged between the two homoleptic species. By the last measurement (day 29) the total peak area ratios for B:D:C:A is approximately 1:2:2:1. After day 29, the total peak area for all species in solution remains unchanged therefore it takes approximately 29 days for the reaction to reach equilibrium from first mixing homoleptic species.

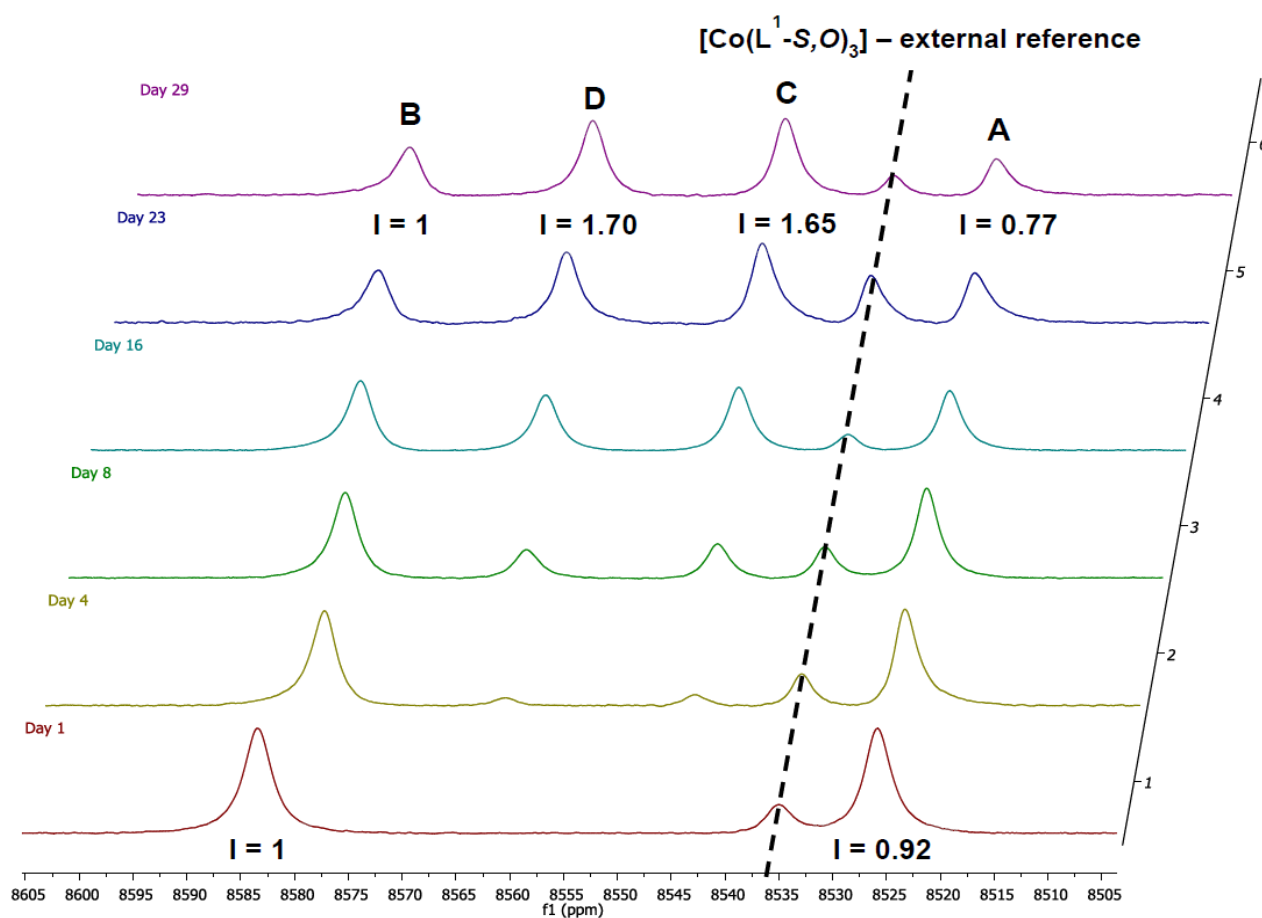


Figure 4.2. 600 MHz ^{59}Co NMR spectra in CDCl_3 at 25 °C of the ligand exchange reaction between tris(*N,N*-diethyl-*N'*-4-chlorobenzoylthioureato)Co(III) (A) and tris(*N,N*-diethyl-*N'*-4-tertbutylbenzoylthioureato)Co(III) (B) resulting in two new heteroleptic complexes C and D.

Chapter 4 | The ligand exchange reaction

The ligand exchange reaction as shown in **Figure 4.2** was repeated using a different pair of homoleptic complexes namely tris(*N,N*-diethyl-*N'*-4-chlorobenzoylthioureato)Co(III) ([Co(L⁴-S,O)₃]) and tris(*N,N*-diethyl-*N'*-4-methoxybenzoylthioureato)Co(III) ([Co(L²-S,O)₃]), noted as A and B respectively in **Figure 4.3**. The same procedure was followed as for the first mentioned ligand exchange reaction. The ⁵⁹Co NMR results are shown in **Figure 4.4**. The results for this reaction follow the same trend as the previous study since a decrease in the peak area of the homoleptic species (A and B) is observed, as the peak area of the newly formed heteroleptic species (D and C) increase. Chemical equilibrium is achieved after approximately 29 days after first mixing the two different homoleptic species.

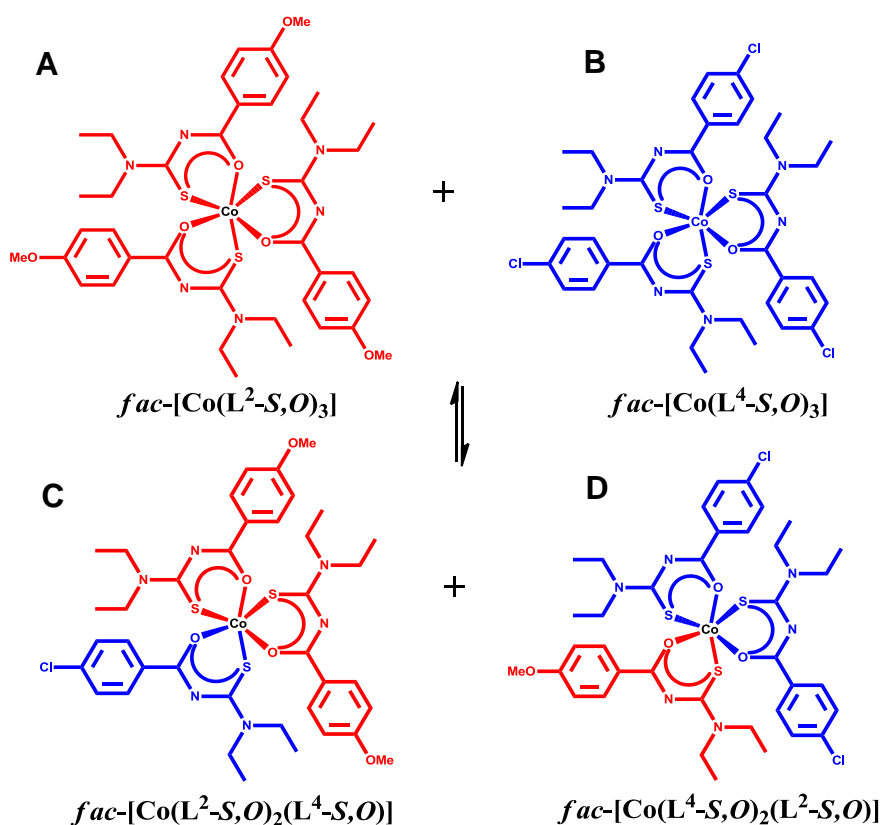


Figure 4.3. The ligand exchange reaction between tris(*N,N*-diethyl-*N'*-4-chlorobenzoylthioureato)Co(III) (**A**) and tris(*N,N*-diethyl-*N'*-4-methoxybenzoylthioureato)Co(III) (**B**) resulting in two new heteroleptic complexes **C** and **D**.

All assignments of homoleptic species as well as newly formed heteroleptic species for the two ligand exchange reactions studied by ⁵⁹Co NMR spectroscopy are summarized in **Table 4.1**.

Chapter 4 | The ligand exchange reaction

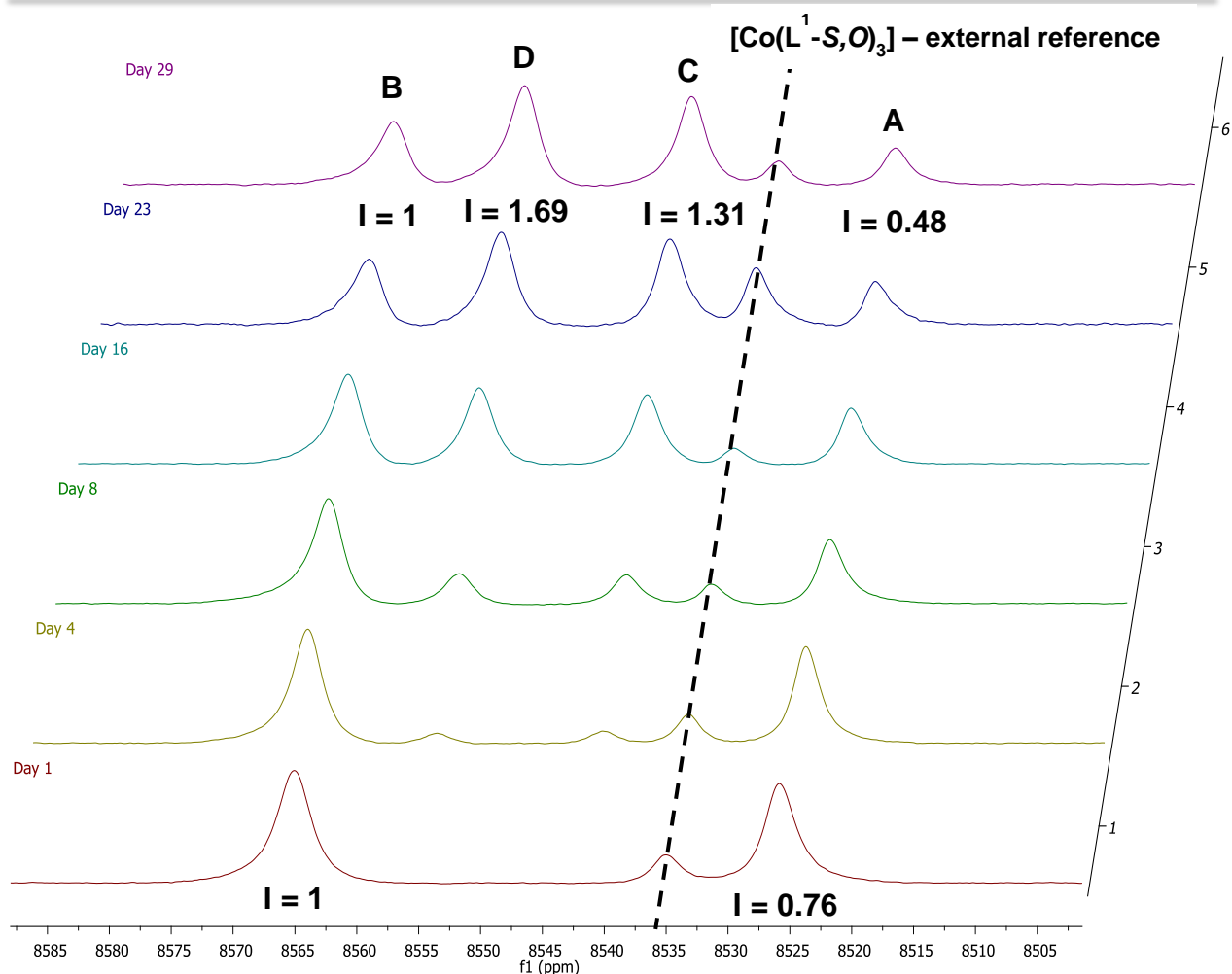


Figure 4.4. 600 MHz ^{59}Co NMR spectra in CDCl_3 at 25°C of the ligand exchange reaction between tris(*N,N*-diethyl-*N'*-4-chlorobenzoylthioureato)Co(III) (A) and tris(*N,N*-diethyl-*N'*-4-methoxybenzoylthioureato)Co(III) (B) resulting in two new heteroleptic complexes C and D.

Table 4.1. Assignment of the four different peaks, at chemical equilibrium, seen from the ligand exchange reactions studied by ^{59}Co NMR in CDCl_3 at 25°C .

[Co(L ⁴ -S,O) ₃] and [Co(L ⁵ -S,O) ₃]			[Co(L ⁴ -S,O) ₃] and [Co(L ² -S,O) ₃]		
Species	$\delta(^{59}\text{Co})/\text{ppm}$	Peak Integral	Species	$\delta(^{59}\text{Co})/\text{ppm}$	Peak Integral
[Co(L ⁴) ₃]	8525	0.77	[Co(L ⁴) ₃]	8525	0.48
[Co(L ⁴) ₂ (L ⁵)]	8544	1.65	[Co(L ⁴) ₂ (L ²)]	8542	1.31
[Co(L ⁴)(L ⁵) ₂]	8562	1.70	[Co(L ⁴)(L ²) ₂]	8555	1.69
[Co(L ⁵) ₃]	8579	1.00	[Co(L ²) ₃]	8565	1.00

Chapter 4 | The ligand exchange reaction

4.1.3 Investigate the ligand exchange reaction by *rp*-HPLC and UV/Vis

Another technique available for studying the ligand exchange reaction is *via* reversed-phase high-performance liquid chromatography (*rp*-HPLC). Where differences in separation between two peaks in ^{59}Co NMR spectroscopy are related to subtle differences in molecular configuration, for HPLC separation is achieved largely by differences in which compounds interact with the stationary and mobile phases selected for a particular column. HPLC is a useful technique considering less amount of sample is required for all experiments and taking into account the low rate at which ligand exchange occurs between the complexes of interest, there is practically no risk of the reaction continuing on-column at a rate that might affect the separation.

A variety of mobile phases were considered for the ligand exchange study by *rp*-HPLC, but only acetonitrile proved suitable considering the low solubility of the Co(III) complexes in most solvents. A number of experiments proved unsuccessful since the solubility of the complexes significantly affected chromatograms and results were inconsistent and could not be used for any detailed examination. The experiments discussed henceforth focused only on successful ligand exchange reactions which include the reaction between homoleptic complexes tris(*N,N*-diethyl-*N'*-4-methoxybenzoylthioureato)Co(III) ($[\text{Co}(\text{L}^2\text{-S}, \text{O})_3]$) and tris(*N,N*-diethyl-*N'*-3,4,5-trimethoxybenzoylthioureato)Co(III) ($[\text{Co}(\text{L}^3\text{-S}, \text{O})_3]$) as well as tris(*N,N*-diethyl-*N'*-benzoylthioureato)Co(III) ($[\text{Co}(\text{L}^1\text{-S}, \text{O})_3]$) and tris(*N,N*-diethyl-*N'*-3,4,5-trimethoxybenzoylthioureato)Co(III) ($[\text{Co}(\text{L}^3\text{-S}, \text{O})_3]$).

Each complex was dissolved in a separate vial in acetonitrile (at a concentration of approximately 200 μM unless stated otherwise), after which equimolar amounts of the two homoleptic complexes were added to a single vial. The sample was then placed directly in the HPLC in order to obtain a chromatogram of the complexes prior to any ligand exchange (**Figure 4.5a**). Considering the slow rate of the reaction, the sample was run every subsequent day and monitored until chemical equilibrium, i.e. the point at which peak area of all solutes in solution remain unchanged (**Figure 4.5b**). It is possible that if the rate of ligand exchange is faster than the elution process, the separation between the different peaks will become disproportionate and will thus require a faster flow rate to improve separation. This is illustrated by the schematic diagram of an HPLC separation in **Figure 4.6a**. The exchange reaction for the various cobalt complexes used during this study were too slow for this to be of any concern, hence the flow rate was kept constant for all reactions, illustrated by **Figure 4.6b**.

Chapter 4 | The ligand exchange reaction

Chapter 4 | The ligand exchange reaction

by the apolar stationary phase. If separation between the two initial homoleptic complexes were not sufficient for observing the newly formed heteroleptic species (those peaks appearing between the two initial complexes), the ratio of acetonitrile relative to water would consequently be decreased. Decreasing the amount of acetonitrile increases the polarity of the mobile phase; hence solutes remain on the column longer in order to provide more opportunity for separation. In some cases the elution time for the complexes were too long, requiring a less polar mobile phase by increasing the ratio of acetonitrile relative to the amount of water. A buffer solution was not required for the chromatographic study considering complexes remained uncharged in the solvent of choice.

The detector used, i.e. Photodiode array UV-Vis detector, has the ability to simultaneously monitor two different wavelengths, which were consequently selected at the point of maximum absorbance for each of the two initial homoleptic complexes. An illustration is given in **Figure 4.7** where the wavelengths of the two individual homoleptic complexes A and B (**Figure 4.8**) were determined by comparing their absorption spectra and finding the points of maximum absorbance for each complex (in this example found to be 220 and 294 nm respectively).

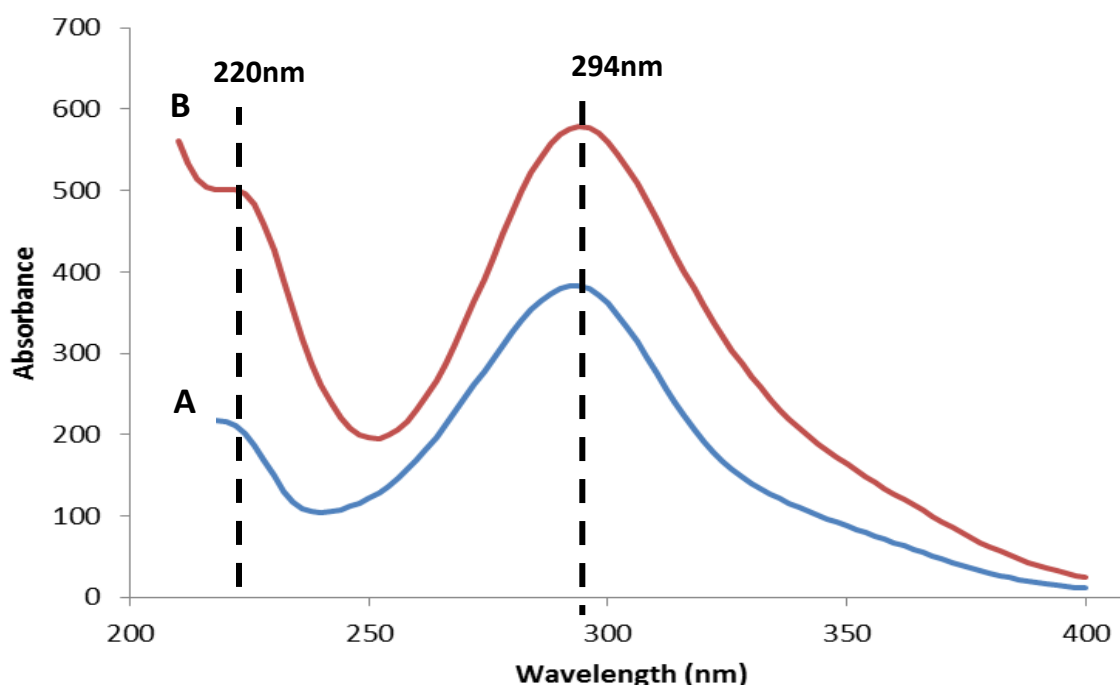


Figure 4.7. UV/Vis absorbance spectra of tris(*N,N*-diethyl-*N'*-4-methoxybenzoylthioureato)Co(III) (A) and tris(*N,N*-diethyl-*N'*-3,4,5-trimethoxybenzoylthioureato)Co(III) (B)

Chapter 4 | The ligand exchange reaction

All of the samples used for the ligand exchange experiments were measured on a Precisa XT 220A to an accuracy of 0.0001g and subsequently dissolved in the specific solvent of choice (Sigma-Aldrich Acetonitrile E Chromasolv® HPLC grade acetonitrile far-UV (34888)).

The first successful ligand exchange reaction studied by *rp*-HPLC was between the two homoleptic complexes tris(*N,N*-diethyl-*N'*-4-methoxybenzoylthioureato)Co(III) and tris(*N,N*-diethyl-*N'*-3,4,5-trimethoxybenzoylthioureato)Co(III), illustrated in **Figure 4.8** as A and B respectively. The two newly formed heteroleptic complexes are given as C and D in the same image.

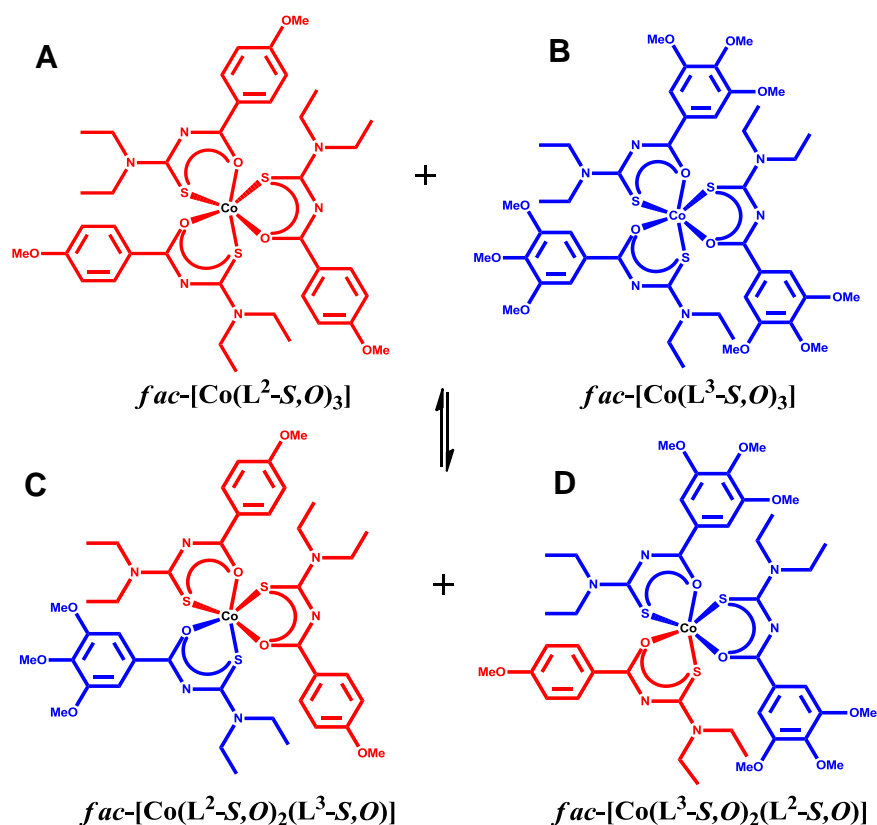


Figure 4.8. The ligand exchange reaction between two homoleptic complexes tris(*N,N*-diethyl-*N'*-4-methoxybenzoylthioureato)Co(III) (**A**) and tris(*N,N*-diethyl-*N'*-3,4,5-trimethoxybenzoylthioureato)Co(III) (**B**) resulting in two new heteroleptic complexes **C** and **D**.

Chapter 4 | The ligand exchange reaction

The *rp*-HPLC chromatograms for the ligand exchange reaction illustrated in **Figure 4.8** are shown in **Figure 4.9**. The first chromatogram (day 1) displayed two peaks corresponding to the two homoleptic complexes initially added in solution, prior to any ligand exchange. Here the elution order is based on polarity with the more polar complex (complex B in **Figure 4.8**) eluting first at 7.36 min, followed by the less polar complex eluting at 9.57 min (complex A in **Figure 4.8**).

On the third day, note two important differences from the results from day 1. The first is the appearance of two new peaks with retention times between that of the two homoleptic complexes initially added in solution. The new peaks appear as a consequence of the formation of heteroleptic species in solution as ligands are interchanged amongst homoleptic species. The second difference is the dramatic decrease in the peak intensity of the two initial complexes in contrast to the increase in intensity of the newly formed species. This trend, with regards to the change in peak intensity for the different species in solution, continues from day 3 until day 15 at which point the intensity remains constant. Therefore the reaction, from first mixing together the two homoleptic complexes together in solution, until equilibrium took approximately 15 days to complete. All additional peaks noticed in the chromatograms, in particular those seen between 2-4 mins t_R , could be attributed to the presence of some unbound ligand. This is supported by comparing the UV-Vis absorption spectra of these additional peaks to the free ligands used for coordination to the two cobalt complexes used in this reaction. The percentage of unbound ligand is on the other hand so small compared to the complexes that any and all contribution to the relative rate or extent of the ligand exchange reaction could be ignored.

Chapter 4 | The ligand exchange reaction

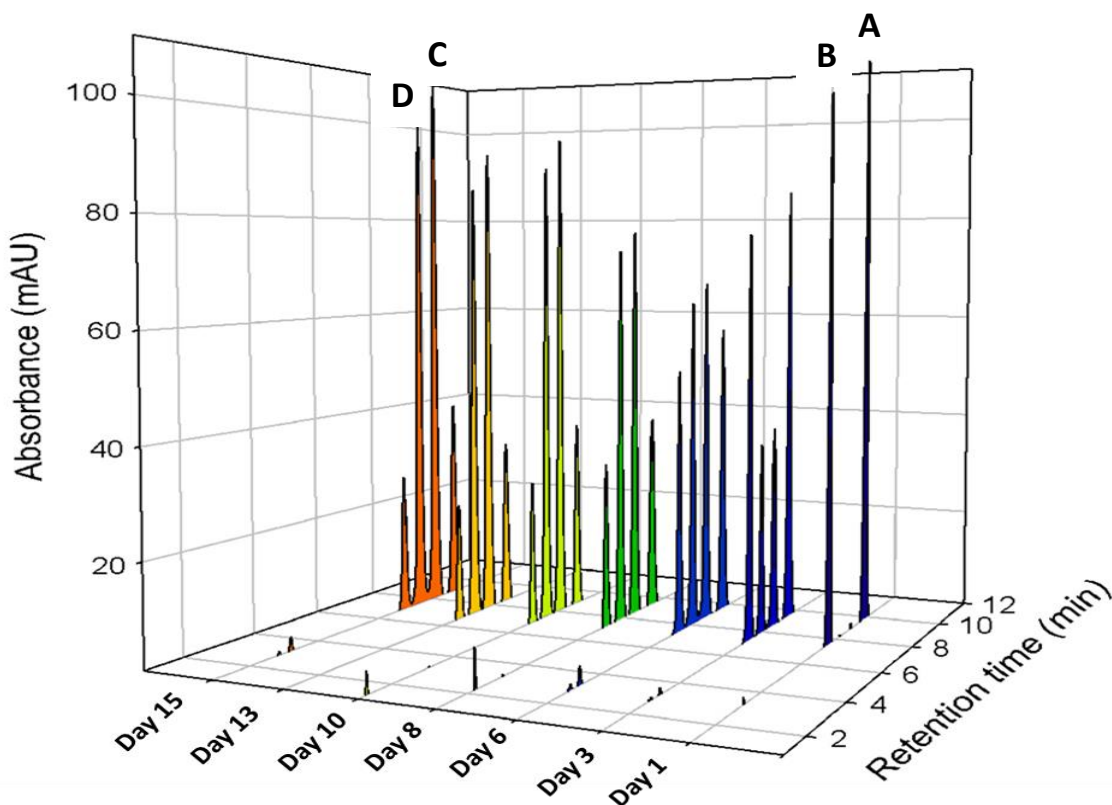


Figure 4.9. A GEMINI C₁₈ ODS (5 μ m, 150 x 4.6 mm) chromatogram at 20 °C, flow rate of 1 ml min⁻¹, and 90:10 (% v/v) acetonitrile:water, of the ligand exchange reaction between a mixture of two homoleptic cobalt complexes tris(*N,N*-diethyl-*N*'-4-methoxybenzoylthioureato)Co(III) (**A**) and tris(*N,N*-diethyl-*N*'-3,4,5-trimethoxybenzoylthioureato)Co(III) (**B**) which results in the formation of the heteroleptic complexes **C** and **D**.

4.1.4. Identification of mixed-ligand species via Liquid-Chromatography Mass-Spectrometry

Identification of the two new peaks observed upon the addition of two different homoleptic cobalt complexes in solution, as seen in the *rp*-HPLC chromatograms, have been largely based on the assumption that ligand exchange takes place between said complexes. Liquid chromatography-mass spectrometry is a good technique for substantiating this assumption. It is able to combine the separation capability of the HPLC with that of the mass analysis ability of the MS, hence allowing for mass determination of each solute as they elute in the chromatogram.

Chapter 4 | The ligand exchange reaction

The LC-MS analysis was done on a Waters Liquid Chromatograph-Waters Synapt G2-Si Mass Spectrometer system which operated in the positive electrospray ionization (ESI) mode. The column specifications were as follows: Waters BEH C18, 2.1 x 100 mm, 1.7 μm at 35 $^{\circ}\text{C}$, flow rate 0.3 ml/min, isocratic, 10% aq. The Cone Voltage used was 15 V. These conditions are similar to those used for the separation of the metal complexes in the *rp*-HPLC study in order to maintain the same degree of separation prior to introduction into the mass spectrometer. Some formic acid was added to the mobile phase in order to prevent the formation of the sodium adduct.

The ligand exchange reaction studied by LC-MS was investigated between a different pair of complexes tris(*N,N*-diethyl-*N'*-benzoylthioureato)Co(III) ($[\text{Co}(\text{L}^1\text{-S},\text{O})_3]$) and tris(*N,N*-diethyl-*N'*-3,4,5-trimethoxybenzoylthioureato)Co(III) ($[\text{Co}(\text{L}^3\text{-S},\text{O})_3]$) and used the same method previously used for the first *rp*-HPLC ligand exchange experiment. After some time, the reaction between these two complexes again produced four distinct peaks. The LC-MS chromatogram shown in **Figure 4.11** was measured at equilibrium, 13 days after first mixing the two homoleptic complexes together. The peaks were initially assumed to correspond to the two homoleptic complexes initially added in solution, as well as the two newly formed heteroleptic complexes with retention times between that of the two homoleptic complexes.

Prior to the MS results, the assignment of the various peaks in **Figure 4.11** was based on the polarity of the various complexes and hence their elution order. As previously mentioned the more polar solutes elute first in a reversed phase column. Therefore, regarding the newly formed heteroleptic complexes, the elution times should follow the order from most polar to least polar in terms of retention time. In other words the heteroleptic complex $[\text{Co}(\text{L}^1\text{-S},\text{O})(\text{L}^3\text{-S},\text{O})_2]$ should in principal elute after the complex closely matching its polarity namely $[\text{Co}(\text{L}^3\text{-S},\text{O})_3]$, followed by the second heteroleptic complex $[\text{Co}(\text{L}^1\text{-S},\text{O})_2(\text{L}^3\text{-S},\text{O})]$ with a polarity closer to the least polar $[\text{Co}(\text{L}^1\text{-S},\text{O})_3]$ complex. These assumptions are substantiated by looking at the mass determination results of the various peaks (**Figure 4.12**) observed in the LC chromatogram.

The results from the mass spectra obtained for the various peaks shown in **Figure 4.12** can be rationalized by carefully considering the process by which these spectra are obtained. The effluent from the Liquid chromatographer, when passing through the electrospray-ionization, is transformed into droplets *via* a high voltage. These droplets are then continuously exploded into smaller droplets until the analyte enters the gas phase as an ion. In the positive ion mode, ionization is accomplished by the loss or gain of a proton where the number of charged species

Chapter 4 | The ligand exchange reaction

that are normally observed in the spectra is reflected by the number of basic sites in a molecule that can be protonated at low pH. ESI is able to transfer the charged species from solution to gas phase, with formally charged compounds able to provide the best results. Neutral compounds, able to readily associate with charged species, are also able to achieve good results and involves protonation in order to provide the $[M + H]^+$ pseudomolecular ions, ultimately observed in the mass spectrum.

The most intense peaks observed in the mass spectra shown in **Figure 4.12a – 4.12d** represents the protonated molecular ion of the respective compounds. Additional, less intense, peaks are observed in the MS spectra and are most prominent for the complex shown in **Figure 4.12d**. Upon further consideration, these peaks are suggested to be the result of some reduction from Co(III) to Co(II) during the ionization process. Consider hereby the spectrum observed for the compound in **Figure 4.12d**, i.e. *fac*-[Co(L¹-S,O)₃]. When one of the Co-O bonds of the protonated complex is broken during the ionization process, the intermediate product formed, stabilized by a solvent molecule, can then either form an adduct with a second complex or could be reduced to Co(II) to form [Co(L¹-S,O)₂], in each case followed by loss of one ligand. The suggested mechanism is illustrated in **Figure 4.10** with m/z values indicated for the respective molecular ions observed in the MS spectrum.

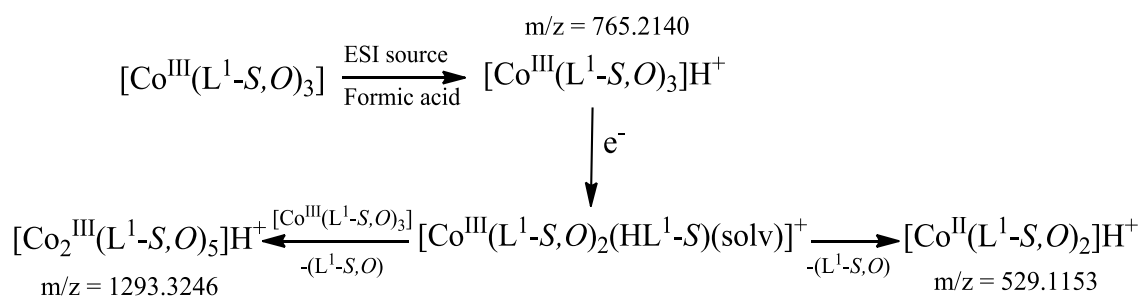


Figure 4.10. Suggested mechanism for the formation of the various molecular ions as observed in the mass spectrum of the [Co(L¹-S,O)₃] complex.

The mechanism suggested in **Figure 4.10** could also be considered in an attempt to justify the additional peaks observed in the mass spectra of the compounds given in **Figure 4.12a – 4.12c**. Note, by the absence of this peak, that these complexes seem less likely to form the corresponding Co(II) ions during the ionization process. The two heteroleptic species (**Figure 4.12b and c**) are able to lose one of the two different ligands when forming the suggested adduct with a second complex, illustrated by the two less intense peaks indicated in the respective MS spectra.

Chapter 4 | The ligand exchange reaction

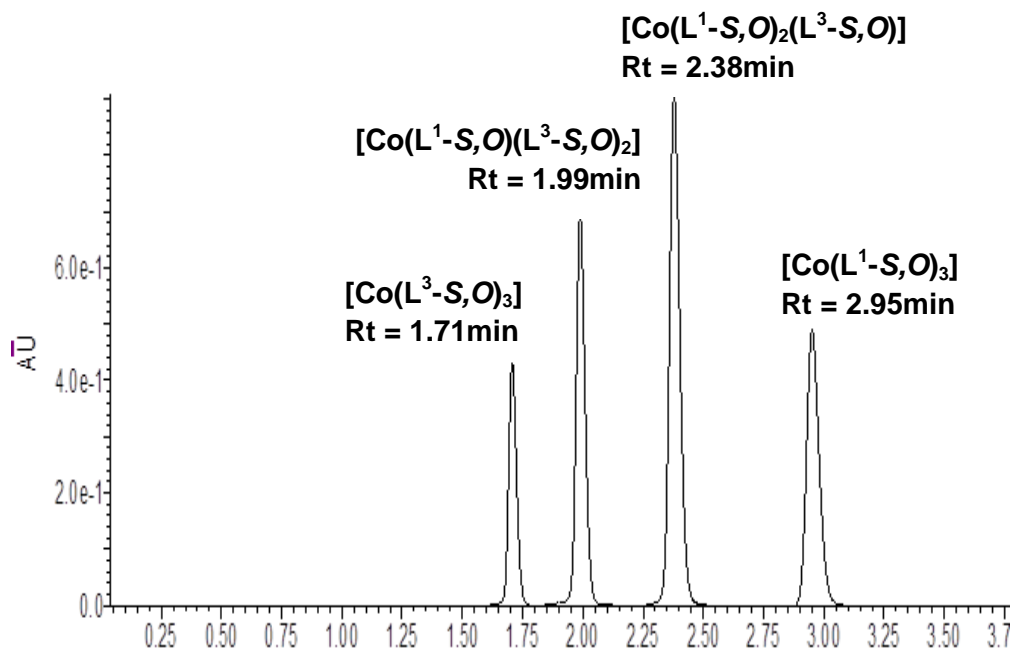
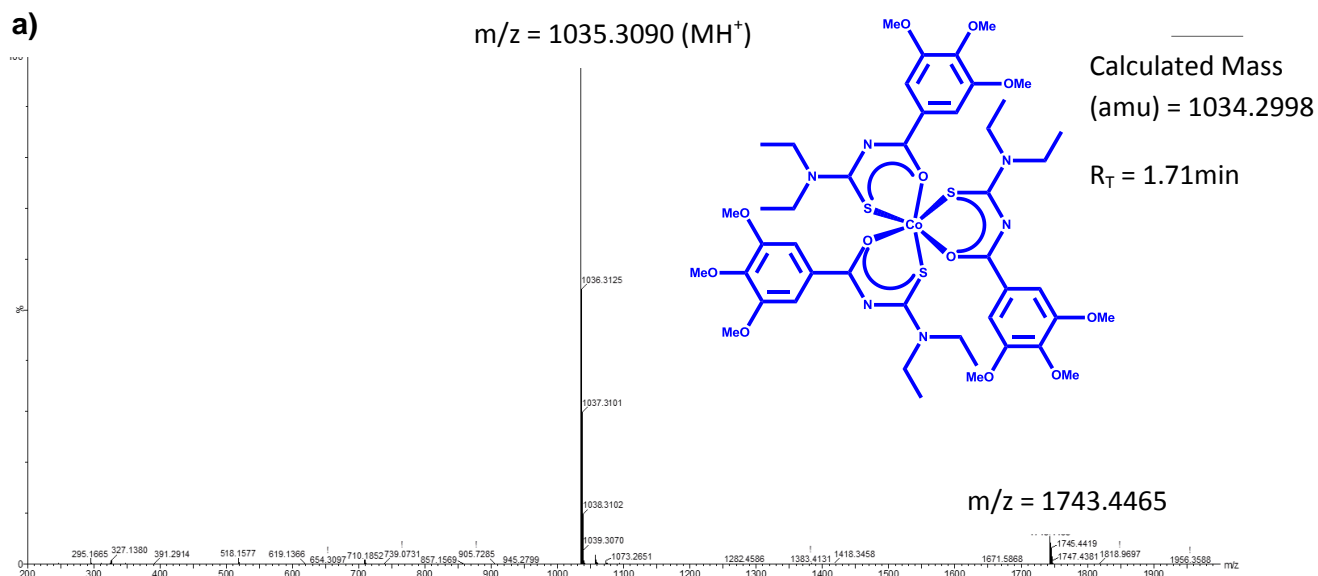


Figure 4.11. LC chromatogram with specifications: Waters BEH C18, 2.1 x 100 mm, 1.7 μm at 35 $^\circ\text{C}$, flow rate 0.3 ml/min, isocratic, 10% aq; illustrating the four species present in the sample as a result of ligand exchange after 13 days between tris(*N,N*-diethyl-*N'*-benzoylthioureato)Co(III) ($[\text{Co}(\text{L}^1\text{-S,O})_3]$) and tris(*N,N*-diethyl-*N'*-3,4,5-trimethoxybenzoylthioureato)Co(III) ($[\text{Co}(\text{L}^3\text{-S,O})_3]$) forming two new heteroleptic complexes $[\text{Co}(\text{L}^3\text{-S,O})(\text{L}^1\text{-S,O})_2]$ and $[\text{Co}(\text{L}^1\text{-S,O})(\text{L}^3\text{-S,O})_2]$.



Chapter 4 | The ligand exchange reaction

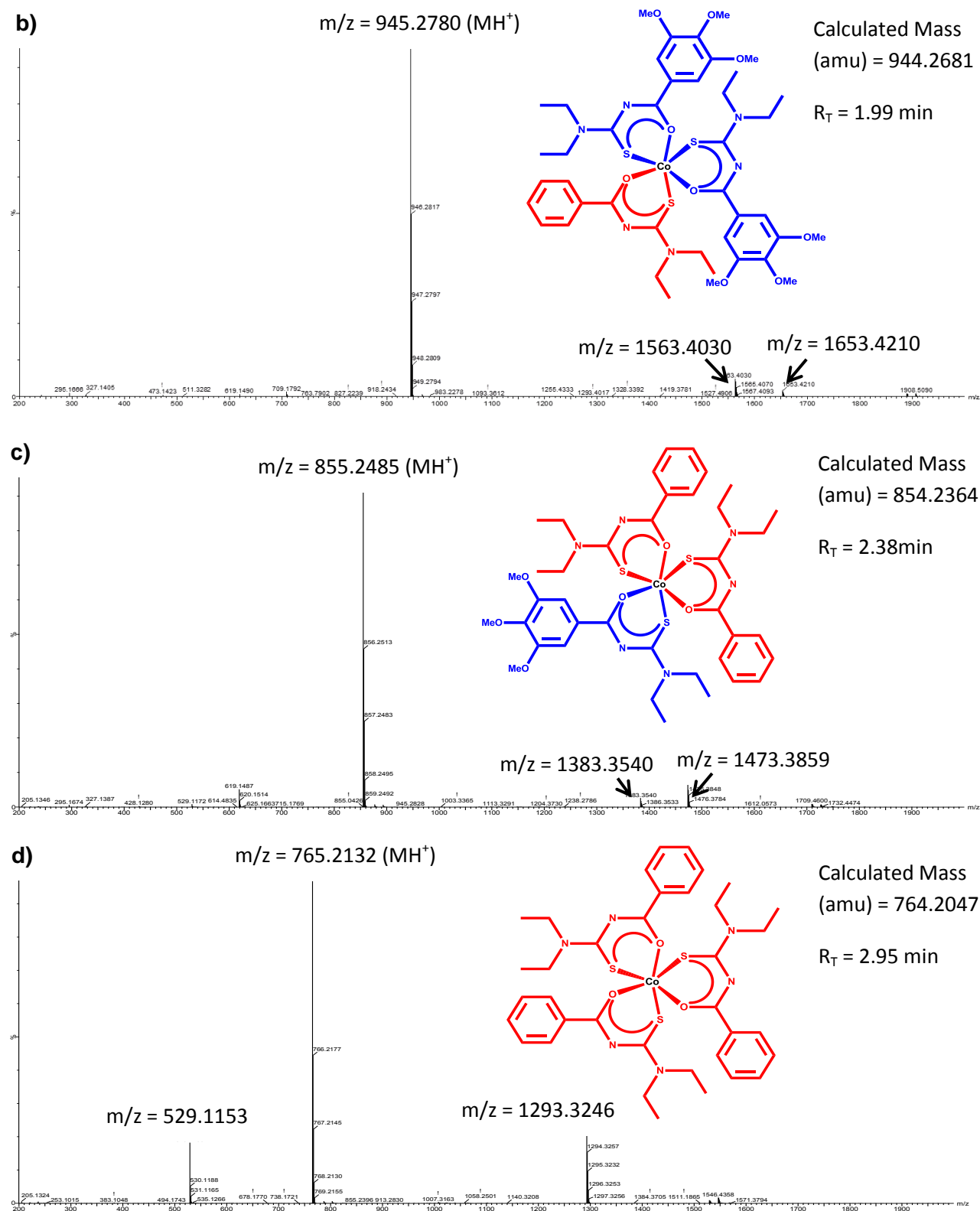


Figure 4.12. Liquid-chromatography mass spectra of homoleptic complexes a) $[Co(L^3-S,O)_3]$ and d) $[Co(L^1-S,O)_3]$ as well as heteroleptic species b) $[Co(L^3-S,O)_2(L^1-S,O)]$ and c) $[Co(L^1-S,O)_2(L^3-S,O)]$.

Chapter 4 | Ligand exchange observations

4.2. Concluding remarks concerning the spontaneous ligand exchange reaction in *fac*-[Co(L-S,O)₃] complexes in solution

It was found by means of ⁵⁹Co NMR and *rp*-HPLC that two different homoleptic complexes of the type *fac*-[Co(L-S,O)₃] undergo spontaneous ligand exchange in solution. All ligand exchange reactions, including technique, reaction conditions and time to reach equilibrium are summarised in **Table 4.2**.

Table 4.2. Summary of techniques, conditions and time to reach equilibrium for all ligand exchange reactions investigated.

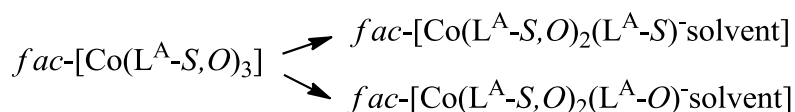
First Complex	Second Complex	Technique	Concentration	Solvent	Days to reach equilibrium
[Co(L ¹ -S,O) ₃]	[Co(L ³ -S,O) ₃]	<i>rp</i> -HPLC	± 200 µM	Acetonitrile	± 13
[Co(L ³ -S,O) ₃]	[Co(L ² -S,O) ₃]	<i>rp</i> -HPLC	± 200 µM	Acetonitrile	± 15
[Co(L ⁴ -S,O) ₃]	[Co(L ² -S,O) ₃]	⁵⁹ Co NMR Spectroscopy	± 5 mM	Chloroform	± 29
[Co(L ⁵ -S,O) ₃]	[Co(L ⁴ -S,O) ₃]	⁵⁹ Co NMR Spectroscopy	± 5 mM	Chloroform	± 29

The relative rate of the ligand exchange reactions were considerably slow in general, although all reactions eventually reached equilibrium where four peaks are observed in the respective spectra/chromatograms, indicative of both homoleptic and heteroleptic species present in solution. This is a remarkable observation considering that the relatively kinetically inert Co(III) complexes of type *fac*-[Co(L-S,O)₃] are far more labile than initially assumed, able to undergo ligand exchange in both chloroform and acetonitrile. Although substitution reactions in general are more likely for low coordination number complexes, since the energy split between the set of degenerate d-orbitals are lower, it is possible for higher coordination number complexes

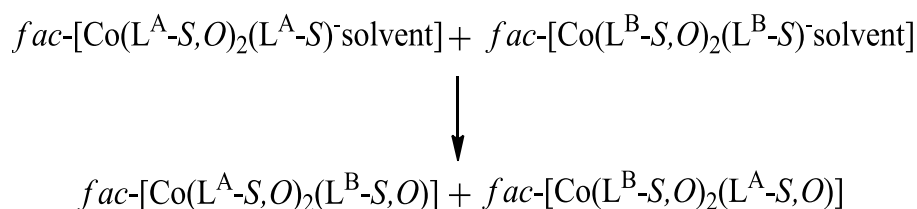
Chapter 4 | Ligand exchange observations

depending on the nature of the specific ligand coordinated. Therefore the ligands under investigation in this thesis could be considered as somewhat weaker-field ligands since they do not cause a large enough splitting of the d-orbitals to warrant strong enough interactions with the metal which could decrease overall lability.

This implies, when considering a possible mechanism, that ligand exchange reactions occur upon breakage of one of the coordinate Co-S or Co-O bonds, which is similarly observed for *cis*-[Pd(L^A-S,O)₂] and *cis*-[Pd(L^B-S,O)₂] complexes as described by van der Molen and Koch⁹². Considering the relative rate of ligand exchange in acetonitrile is almost half that in chloroform, regardless of the vastly different concentrations used in each solution, it does suggest that the ligand exchange reaction is rather complicated and could happen by either one of two possible mechanisms. Since breaking of one of the Co-S or Co-O coordinate bonds is required for ligand exchange to happen, one imagines a collision of the two different homoleptic *fac*-[Co(L^A-S,O)₃] and *fac*-[Co(L^B-S,O)₃] complexes followed by the exchange of ligands in order to form the heteroleptic complexes. This could happen either simultaneously by partial ligand dissociation or by formation of a cluster of the two homoleptic complexes upon collision, followed by ligand rearrangement. This can be illustrated by first looking at the two possible intermediates which could be formed when either one of the coordinate bonds of a homoleptic complex is broken, as illustrated by the following equation:



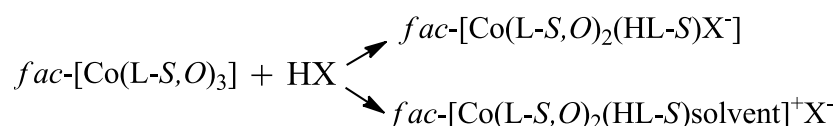
The above equation illustrates partial ligand dissociation of a homoleptic complex, with a solvent molecule occupying the vacant coordination site, whereby ligand exchange is imagined to now easily occur for two homoleptic complexes which undergo either full or partial dissociation in solution, illustrated below.



Chapter 4 | Ligand exchange observations

Acetonitrile has a reasonable donor number, i.e. the ability of the donor atoms of the solvent to donate a lone pair of electrons in order to form a coordinate bond, therefore the last mentioned mechanism is plausible in such solutions. The suggested mechanism could thereby also account for the slow rate of the ligand exchange reaction, since the formation of a solvent stabilized intermediate would be a rate limiting step.

The ligand exchange reaction is also observed in chloroform, which has practically no Lewis basicity (i.e. very small donor number) which is consistent with the even slower relative rate of ligand exchange observed in this solution. It is remarkable that ligand exchange in general is able to happen in this solvent and suggests that the exchange reaction in the two solvents, although occurring at different relative rates, should have something in common. Since the mechanism of the ligand exchange reaction is still currently unknown, it is speculated that some trace amount of acid, i.e. HX, or free ligand present in a solution of *fac*-[Co(L-S,O)₃] could play a role in the ligand exchange reaction. The presence of some trace amount of acid or free ligand may result in protonation of one of the ligands coordinated in a *fac*-[Co(L-S,O)₃] complex and so promoting partial ligand dissociation. This is illustrated below.



The reactive species as shown in this last equation may well be short lived and depend on the relative amount of traces of acid or free ligand in solution, they are nonetheless considered as possible important intermediate complexes that could lead to the ligand exchange reaction and therefore the formation of heteroleptic complexes in solution. There is currently no credible evidence to support this mechanism and will require further future work. The alternative mechanism of ligand exchange, as a result of the formation of some kind of two complex aggregate formed in solution, is a much more complicated mechanism to envision and therefore not further discussed here.

In conclusion, the proposal discussed above is supported qualitatively by the relatively higher ligand exchange rate in acetonitrile compared to chloroform. Since solvent molecules are involved in the suggested mechanism, acetonitrile is thereby expected to readily stabilize partial or full dissociation into a low concentration of *fac*-[Co(L-S,O)₂(L-S)CH₃CN] at room temperature or even the *fac*-[Co(L-S,O)₂(HL-S)CH₃CN]⁺X⁻, formed by protonation of trace amount of HX or free ligand in solution.

CHAPTER FIVE

GENERAL DISCUSSION AND CONCLUSION

Chapter 5 | Conclusion

5.1. Conclusion

A series of ligands of the type *N,N*-dialkyl-*N'*-acyl(aryl)thiourea were coordinated to Co(III) in order to study the subsequent complexes of type *fac*-tris(*N,N*-dialkyl-*N'*-acyl(aryl)thioureato)Co(III). These complexes were synthesized in relatively good yield and characterised by means of ^1H , $^{13}\text{C}\{^1\text{H}\}$ and ^{59}Co NMR spectroscopy, mass spectrometry, infrared spectroscopy, elemental analysis as well as X-ray crystallography.

5.1.1. Spectroscopic findings

One of the more important findings from the NMR spectroscopic results indicate without question the manner in which the acylthiourea ligands coordinates to the Co(III) metal ion. Two important events occur upon coordination of the ligands to the metal ion. This includes the deprotonation of the amidic proton, illustrated by the disappearance of the N-H peak in the ^1H NMR spectra as well as the IR spectra. Then upon reacting the Co(II) precursor salts, when stoichiometry of Co(II) relative to HL is 1:3, presumed oxidation of Co(II) to Co(III) by atmospheric oxygen finally results in the formation of $[\text{Co}(\text{L-S,O})_3]$ type complexes. Three techniques can be used to verify the mode of coordination for these complexes. The shift of the carbonyl and thiocarbonyl bands in the IR spectra towards lower frequencies in the complex in respect to the free ligand can be used as an indication that coordination has occurred *via* the sulphur and oxygen donor atoms. There is also a clear shift visible for the same peaks in the ^{13}C NMR spectra, since coordination causes some change in electron density brought on by the metal ion. The X-ray diffraction results could unequivocally show the coordination of the acylthiourea ligands to Co(III) occurs *via* the bidentate mode by means of the S and O donor atoms. This is further substantiated by X-ray diffraction showing the elongation of the C=S and C=O bonds in the complex compared to the free ligand. This particular mode of coordination results in a distorted *facial* octahedral coordination sphere considering that all angles deviate slightly from the ideal octahedral conformation.

Spectroscopic, i.e. ^1H and ^{13}C NMR, results of symmetrical C(III) complexes (the alkyl groups attached to the tertiary amine of the ligand are identical) were briefly compared with that of the spectra of Co(III) coordinated to an unsymmetrical, *N*-methyl-*N*-ethyl-*N'*-benzoylthiourea, as well as an chiral acylthiourea ligand, *N,N*-diethyl-*N'*-camphanoylthiourea. The consequence of restricted rotation, caused by the partial double bond character about the C-N bond of the

Chapter 5 | Conclusion

thiourea moiety, on the ^1H NMR signals of the acylthiourea ligands and corresponding Co(III) complexes were previously discussed (see **section 3.1.1**). For the unsymmetrical acylthiourea ligand, i.e. when the two alkyl groups of the tertiary amine are not the same, the restricted rotation now show *E*, *Z* configurational isomerism hence two configurations are possible for this particular ligand. The isomers result in multiple signals in the ^1H and ^{13}C NMR spectra. Thus, for *N*-methyl-*N*-ethyl-*N'*-benzoylthiourea, the result is two signals for each methyl and methylene group of the tertiary amine related to either the *E* or *Z* isomer. This isomerism is carried over to the Co(III) chelates upon coordination and thereby able to form one of four possible configurational isomers (**Figure 3.9**). Moreover, coordination of a chiral acylthiourea ligand (*N,N*-diethyl-*N'*-camphanoylthiourea) to Co(III) also gives rise to complicated spectra attributed to stereoisomerism, considering coordination of the chiral ligand suggests the formation of diastereomeric Co(III) complexes, observed as two separate signals in the ^{13}C NMR spectrum.

5.1.2. ^{59}Co NMR spectroscopy studies

Considering ^{59}Co NMR spectroscopy has one of the largest chemical shift ranges known it was utilized to establish the effect of a variety of factors on the shielding of the ^{59}Co nucleus in d^6 Co(III) complexes of type $[\text{Co}(\text{L}-\text{S},\text{O})_3]$. The only complex similar in structure previously studied by means of ^{59}Co NMR spectroscopy was *fac*-tris(*N,N*-diethyl-*N'*-benzoylthioureaato)Co(III), $[\text{Co}(\text{L}^1-\text{S},\text{O})_3]$, with a $\delta(^{59}\text{Co}) \sim 8538$ ppm determined by Juranic *et al.*¹¹⁷ These authors showed that a good ^{59}Co NMR could be obtained, suggesting that ^{59}Co NMR may be a good technique for the study of *fac*- $[\text{Co}(\text{L}-\text{S},\text{O})_3]$ complexes. The chemical shift of $\delta(^{59}\text{Co}) = 8535$ ppm of a freshly prepared *fac*- $[\text{Co}(\text{L}^1-\text{S},\text{O})_3]$ complex, relative to the conventionally used external reference signal of $\text{K}_3[\text{Co}(\text{CN})_6]$ in D_2O at 0.00 ppm, is in good agreement with the value obtained by Juranic *et al.* Due to the large chemical shift $\delta(^{59}\text{Co})/\text{ppm}$ range expected for ^{59}Co NMR, we chose to use the complex *fac*- $[\text{Co}(\text{L}^1-\text{S},\text{O})_3]$ in CDCl_3 as our external reference against which all $\delta(^{59}\text{Co})$ of other complexes synthesized are reported, to minimize errors in such measurements. This work established that factors such as the concentration of *fac*- $[\text{Co}(\text{L}-\text{S},\text{O})_3]$, the solvent (CDCl_3 and mixtures of CDCl_3 with acetonitrile), the recording temperature, as well as the ligand structure affect ^{59}Co shielding (as measured by the $\delta(^{59}\text{Co})/\text{ppm}$) of the series of *fac*- $[\text{Co}(\text{L}-\text{S},\text{O})_3]$ complexes under investigation.

The temperature dependence was noted for two complexes *fac*- $[\text{Co}(\text{L}^4-\text{S},\text{O})_3]$ and *fac*- $[\text{Co}(\text{L}^5-\text{S},\text{O})_3]$, in CDCl_3 , with calculated temperature coefficient values of 2.4 and 3.0 ppm K^{-1}

Chapter 5 | Conclusion

respectively. These results were related to theoretical studies available in the literature stating an increase in the paramagnetic screening constant as $(\Delta E)^{-1}$ increases and therefore higher chemical shifts are observed at higher temperatures. The interesting effect of the solvent on the $\delta(^{59}\text{Co})/\text{ppm}$ of *fac*-[Co(L²-S,O)₃] was examined by mixtures of CDCl₃ and acetonitrile in various volume ratios (limited by the solubility of the complex). The ⁵⁹Co NMR spectra show a significant solvent dependence, resulting in an increase in the $\delta(^{59}\text{Co})/\text{ppm}$ chemical shift to more positive values with increasing the amount of acetonitrile relative to chloroform. The results were related to changes in line-widths, which decrease in a higher ratio of acetonitrile to CDCl₃, possibly indicative of some degree of interaction between complexes and solvent which subtly alters the octahedral geometry, or simply viscosity effects in mixed solvents. This is in need of further study, but confirms the high sensitivity of the ⁵⁹Co shielding as a sensitive probe for such subtle effects in these *fac*-[Co(L-S,O)₃] complexes.

The $\delta(^{59}\text{Co})$ of the symmetrical Co(III) complexes synthesized were obtained in order to investigate the differences in ⁵⁹Co shielding brought on by differences in ligand structure. All complexes appeared in the range of 137 ppm where differences in chemical shifts were attributed to either inductive or steric effects pertaining to the substituents of the various acylthiourea ligands coordinated to Co(III). No clear structure $\delta(^{59}\text{Co})/\text{ppm}$ trend was evident in the data obtained in this study and more work in this regard is necessary. Note that although these complexes exist as two pairs of enantiomers, i.e. the Lambda Λ or Delta Δ absolute configuration, they appear as only one peak in the ⁵⁹Co NMR spectra, since enantiomers are considered physically identical. It is for this reason that the ⁵⁹Co NMR spectrum obtained for the analytically pure Co(III) complex coordinated to the chiral ligand, *N,N*-diethyl-*N'*-camphanoylthiourea, seemed remarkable since it illustrated two well resolved signals (**Figure 3.29**) instead of the expected one single, as seen for the symmetrical complexes. These results could be clarified by considering the single crystal X-ray results which, although showing only one geometrical *fac* isomer, clearly indicated two stereoisomers crystallizing in the particular space group which are not mirror images in any conformation and thereby strongly suggests that two diastereomers are formed upon coordination of the Co(III) to the chiral ligand. This could thereby account for the two peaks observed in the ¹³C and ⁵⁹Co NMR spectra, whereby last mentioned show sufficiently different $\delta(^{59}\text{Co})$ for the two stereoisomers and could therefore be used to resolve chiral complexes by NMR, which is to be confirmed by future work. Lastly, the Co(III) complex made by the acylthiourea derivative derived from an unsymmetrical amine, i.e. *N*-methyl-*N*-ethyl-*N'*-benzoylthiourea, showed four peaks in the ⁵⁹Co NMR spectrum for the

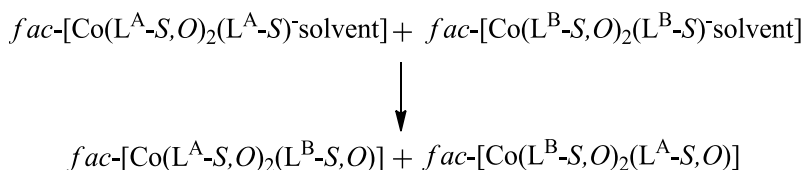
Chapter 5 | Conclusion

analytically pure complex (**Figure 3.28**). Both the ligand and complex show configurational *E,Z* isomers, where the geometrical *fac* isomer of the complex can have *EEE*, *EZE*, *ZEZ* and *ZZZ* configurational isomers. The different possible isomers are remarkably well resolved in the ^{59}Co NMR spectrum whereby the relationship between chemical shift and specific configuration could be determined in some further studies.

5.1.3. The ligand exchange study between homoleptic complexes of type *fac*-[Co(L-S,O)₃]

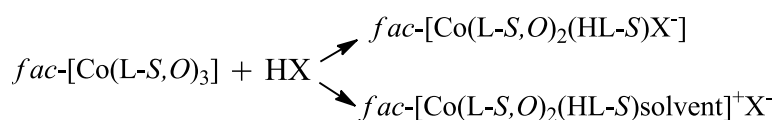
The substitutional inertness of the Co(III) complexes under investigation was also considered followed by a number of ligand exchange reactions studied by ^{59}Co NMR spectroscopy as well as *rp*-HPLC. Relatively similar results were observed for all subsequent experiments, with the only significant difference being the relative rate of ligand exchange in the two different solvents used. Upon addition of two different homoleptic complexes of the type *fac*-[Co(L^A-S,O)₃] and *fac*-[Co(L^B-S,O)₃] in the same solution, two new heteroleptic complexes were formed in the reaction mixture as a result of ligand exchange between the two first mentioned complexes given as *fac*-[Co(L^A-S,O)₂(L^B-S,O)] and *fac*-[Co(L^A-S,O)(L^B-S,O)₂]. This is a remarkable observation considering that no such exchange reaction, to our knowledge, have previously been observed for such low spin Co(III) complexes of type *fac*-[Co(L-S,O)₃]. The heteroleptic complexes formed in solution were furthermore identified by LC-MS.

A noteworthy difference between the ligand exchange reactions studied by ^{59}Co NMR spectroscopy and *rp*-HPLC was the solvent used, namely chloroform and acetonitrile respectively. The ligand exchange reaction in acetonitrile was almost half the relative rate than in chloroform. This observation could be clarified by considering one of two possible mechanisms. The first mechanism considers partial ligand dissociation when one of the coordinate Co-O or Co-S bonds of the Co(III) complex is broken, stabilized by a solvent molecule able to form a coordinate bond, i.e. acetonitrile, in the vacant coordination site. This partial or complete dissociation of the ligands is suggested to be the driving force behind the ligand exchange reaction between two homoleptic Co(III) complexes, illustrated below.



Chapter 5 | Conclusion

For a solvent far less likely to form a coordinate bond, such as chloroform, trace amount of acid, i.e. HX, or free ligand present in solution is now suggested to be the governing factor for partial ligand dissociation, since these are able to protonate the ligands coordinated to Co(III). This happens at a relative rate much lower than for acetonitrile considering the short lived intermediate species formed as well as relative amounts of the trace species. After this partial ligand dissociation, as suggested in chloroform, the reaction then follows the same route as shown by last mentioned equation, upon reacting with a second partially dissociated complex, and the formation of the intermediate species is illustrated below.



The second mechanism suggested for the ligand exchange reaction involves the formation of a two complex aggregate, although at this stage too complicated a mechanism to describe in any certain detail.

5.2. Remarks and Future work

- All *fac*-[Co(L-S,O)₃] complexes were synthesized by reaction of a cobalt(II) salt with a *N,N*-dialkyl-*N'*-acyl(aryl)thiourea ligand, resulting in Co(III) complexes which implies fast oxidation of Co(II) to Co(III) by atmospheric O₂ during synthesis. Attempts to synthesize and so characterize Co(II) complexes of type [Co(L-S,O)₂], with either square planar or tetrahedral geometry, is suggested for future work to understand the coordination chemistry and spectroscopic aspects of such presumably paramagnetic complexes
- The Co(III) complex *fac*-[Co(L¹¹-S,O)₃] generated complicated spectra attributed to *E*, *Z* configurational isomerism, **section 3.1.2**. Further work is required for the unequivocal assignment of the various possible isomers in the spectra whereby a variety of factors could be considered in an attempt to rationalize the relative stability of each isomer in solution.

Chapter 5 | Conclusion

- The inherent chirality of *fac*-[Co(L-S,O)₃] complexes, into the possible optical Δ and Λ isomers (enantiomers) is of interest. In normal solvents this study showed a single ⁵⁹Co NMR resonance is obtained. However in chiral solvents, it may be that the Λ and Δ enantiomers of *fac*-[Co(L-S,O)₃] may be resolved into two peaks, given the sensitivity of the ⁵⁹Co NMR shielding to the various factors described here. This would be a novel and interesting finding.
- The remarkable and initially unexpected ligand exchange reaction observed between two homoleptic *fac*-[Co(L-S,O)₃] complexes is interesting and requires further investigation of the slow reaction kinetics and other factors which influence this metathesis, with a view to establishing a possible mechanism of how two coordinatively saturated and crowded Co(III) complexes can undergo such ligand exchange, which has never been reported for tris(*N,N*-diethyl-*N'*-benzoylthioureato)cobalt(III) complexes in the literature.

References

References

1. Young, R. S. *Cobalt*; New York, Reinhold Pub. Corp. **1948**.
2. Kostakis, G. E.; Perlepes, S. P.; Blatov, V. A.; Proserpio, D. M.; Powell, A. K. *Coord. Chem. Rev.* **2012**, 256 (11-12), 1246.
3. Walton, R. *Cobalt Market report*; The Crucible, July **2013**, p. 6-9.
4. Drury, C. W. *Cobalt – Its occurrence, metallurgy, uses and alloys*; A. T. Willgress: Toronto, **1919**, No. 4, p. 84.
5. Nocera, D. G. *Acc. Chem. Res.* **2012**, 45 (5), 767.
6. Fisher, K. G. *Cobalt Processing Developments*, The Southern African Institute of Mining and Metallurgy, **2011**, 237.
7. Sole, K. C.; Feather, A. M.; Cole, P. M. *Hydrometallurgy* **2005**, 78, 52.
8. Ashraf-Khorassani, M.; Combs, M. T.; Taylor, L. T. *J. Chromatogr. A.* **1997**, 774, 37.
9. Wai, C. M.; Wang, S. *J. Chromatogr. A.* **1997**, 785, 369.
10. Murphy, J. M.; Erkey, C. *Environ. Sci. Technol.* **1997**, 31, 1674.
11. Beyer, L.; Hoyer, E.; Hartman, H. *J. Liebscher. Z. Chem.* **1981**, 81, 21.
12. El Aamrani, F. Z.; Kumar, A.; Cortina, J. L.; Sastre, A. M. *Anal. Chim. Acta.* **1999**, 382, 205.
13. El Aamrani, F. Z.; Kumar, A.; Beyer, L.; Cortina, J. L.; Sastre, A. M. *Solv. Extr. Ion Exch.* **1998**, 16 (6), 1389.
14. Luckay, R. C.; Mebrahtu, F.; Esterhuysen, C.; Koch, K. R. *Inorg. Chem. Commun.* **2010**, 13 (4), 468.
15. Domínguez, M.; Anticó, E.; Beyer, L.; Aguirre, A.; García-Granda, S.; Salvadó, V. *Polyhedron* **2002**, 21, 1429.
16. Neucki, E.; *Ber. Dtsch. Chem. Ges.* **1873**, 6, 598.
17. Atiş, M.; Karipcin, F.; Sariboga, B.; Taş, M.; Çelik, H. *Spectrochim. Acta - Part A Mol. Biomol. Spectrosc.* **2012**, 98, 290.
18. Cunha, S.; MacEdo, F. C.; Costa, G. A. N.; Rodrigues, M. T.; Verde, R. B. V.; De Souza Neta, L. C.; Vencato, I.; Lariucci, C.; Sá, F. P. *Monatshefte fur Chemie* **2007**, 138 (5), 511.
19. Saeed, A.; Rafique, H.; Hameed, A.; Rasheed, S. *Pharm. Chem. J.* **2008**, 42 (4), 191.
20. Zhang, J. F.; Xu, J. Y.; Wang, B. L.; Li, Y. X.; Xiong, L. X.; Li, Y. Q.; Ma, Y.; Li, Z. M. *J. Agric. Food Chem.* **2012**, 60 (31), 7565.
21. Duan, L. P.; Xue, J.; Xu, L. L.; Zhang, H. B. *Molecules* **2010**, 15 (10), 6941.
22. Ke, S. Y.; Xue, S. Y. *Arkivoc* **2006**, 10, 1-6.
23. Kurt, G.; Sevgi, F.; Mercimek, B. *Chem. Pap.* **2009**, 63 (5), 548.
24. Huheey, J. E. *Inorganic chemistry, principles of structure and reactivity*; Harper and Row publishers, New York, **1983**, 3rd ed, p. 312-315, 387-428.
25. Saeed, A.; Flörke, U.; Erben, M. F. *J. Sulfur. Chem.* **2014**, 35 (3), 318.
26. Woldu, M. G.; Dillen, J. *Theor. Chem. Acc.* **2008**, 121, 71.
27. Banerjee, S. N.; Sukthankar, A. C. *J. Ind. Chem. Soc.* **1962**, 39, 197.
28. Livingstone, A. *Q. Rev.* **1965**, 19, 4.
29. Koch, K. R.; Sacht, C.; Bourne, S. *Inorg. Chem. Acta.* **1995**, 232, 109.
30. Koch, K. R.; Coetzee, A.; Wang, Y. *J. Chem. Soc., Dalton Trans.* **1999**, 1013.
31. Arslan, H.; Külçü, N. *Trans. Metal. Chem.* **2003**, 28, 816-819.

References

32. Mautjana, A. N.; Miller, J. D. S.; Gie, A.; Bourne, S. A.; Koch, K. R. *Dalt. Trans.* **2003**, 10 (5), 1952.
33. König, K. H.; Schuster, M.; Steinbrech, B.; Schneeweiss, R.; Schlodder, R. *Fresenius' Z. Anal. Chem.* **1985**, 321, 457.
34. Matoetoe, M. *M.Sc. Thesis*, University Of Cape Town, **1989**.
35. Merdivan, M.; Güngör, A.; Savaşci, Ş.; Aygün, R. S. *Talanta* **2000**, 53 (1), 141.
36. Koch, K. R. *Coord. Chem. Rev.* **2001**, 473, 216-217.
37. Zhang, Y.; Qin, J.; Wei, T. *J. Fluorine. Chem.* **2006**, 127, 1222-1227.
38. Zhang, Y. M.; Cao, C.; Wei, W.; Xie, T. B. *Chin. J. Chem.* **2007**, 25, 709-713.
39. Boiocchi, M.; Del Boca, L.; Gomez, D. E.; Fabbrizzi, L.; Licchelli, M.; Monzani, E. *J. Am. Chem. Soc.* **2004**, 126, 16507-16514.
40. Bonizzoni, M.; Fabbrizzi, L.; Taglietti A.; Tiengo, F. *Eur. J. Org. Chem.* **2006**, 3567-3574.
41. Otazo-Sanchez, E.; Perez-Marin, L.; Estevez-Hernandez, O.; Rojas-Lima, S.; Alonso-Chamarro, J. *J. Chem. Soc.* **2001**, 2211-2218.
42. Wilson, D.; Arada, M. A.; Alegret, S.; del Valle, M. *J. Hazard. Mater.* **2010**, 181, 140-146.
43. Gunasekaran, N.; Remya, N.; Radhakrishnan, S.; Karvembu, R. *J. Coord. Chem.* **2011**, 64, 491-501.
44. Gunasekaran, N.; Karvembu, R. *Inorg. Chem. Commun.* **2010**, 13, 952-955.
45. Gunasekaran, N.; Jerome, P.; Ng, S. W.; Tiekink, E. R. T.; Karvembu, R. *J. Mol. Catal. A.* **2012**, 353-354, 156-162.
46. Gunasekaran, N.; Ramesh, P.; Ponnuswamy, M. N. G.; Karvembu, R. *Dalton Trans.* **2011**, 40, 12519.
47. Bailey, R. A.; Rothaupt, K. L.; Kullnig, R. K. *Inorg. Chim. Acta.* **1988**, 147, 233-236.
48. Bensch, W.; Schuster, M. *Z. Anorg. Allg. Chem.* **1992**, 611, 99-102.
49. Che, D. J.; Li, G.; Yao, X. L.; Wu, Q. J.; Wang, W. L.; Zhu, Y. *J. Organomet. Chem.* **1999**, 584, 190-196.
50. Hanekom, D.; McKenzie, J. M.; Derix, N. M.; Koch, K. R. *Chem. Commun. (Camb).* **2005**, No. 6, 767.
51. Koch, K. R.; Grimmbacher, T.; Sacht, C. *Polyhedron* **1998**, 17, 267.
52. O'Reilly, B.; Plutín, A. M.; Pérez, H.; Calderón, O.; Ramos, R.; Martínez, R.; Toscano, R. A.; Duque, J.; Rodríguez-Solla, H.; Martínez-Alvarez, R.; Suárez, M.; Martín, N. *Polyhedron* **2012**, 36 (1), 133.
53. Pérez, H.; Da Silva, C. C. P.; Plutín, A. M.; Simone, C. A. de; Ellena, J. *Acta. Crystallogr. Sect. E Struct. Reports Online* **2011**, 67 (4), m504.
54. Cîrcu, V.; Ilie, M.; Iliş, M.; Dumitraşcu, F.; Neagoe, I.; Păsculescu, S. *Polyhedron* **2009**, 28 (17), 3739.
55. Pisiewicz, S.; Rust, J.; Lehmann, C. W.; Mohr, F. *Polyhedron* **2010**, 29 (8), 1968.
56. Selvakumaran, N.; Ng, S. W.; Tiekink, E. R. T.; Karvembu, R. *Inorganica. Chim. Acta.* **2011**, 376 (1), 278.
57. Sacconi, L. *J. Chem. Soc.* **1970**, 248.
58. Carlin, R. L. *Trans. Metal. Chem.* **1965**, 1, 1.
59. King, R. B. *Encyclopedia of inorganic chemistry*, Chichester, New York: Wiley, **1994**, p. 712-731.
60. Wood, D. L.; Remeika, J. P. *J. Chem. Phys.* **1967**, 46, 3595.

References

61. Baker, L. C. W.; Simmons, V. E. *J. Amer. Chem. Soc.* **1959**, 81, 4744.
62. Pratt, J. M.; Thorpe, R. G. *Adv. Inorg. Chem. Radiochem.* **1969**.
63. Weiqun, Z.; Wen, Y.; Liqun, X.; Xianchen, C. *J. Inorg. Biochem.* **2005**, 99 (6), 1314.
64. Pérez, H.; Mascarenhas, Y.; Plutín, A. M.; De Souza Corrêa, R.; Duque, J. *Acta. Cryst.* **2008**, E64, m503.
65. Pérez, H.; Corrêa, R. S.; Plutín, A. M.; O'Reilly, B.; Duque, J. *Acta. Cryst.* **2008**, E64, m733.
66. Yang, W.; Liu, H.; Li, M.; Wang, F.; Zhou, W.; Fan, J. *J. Inorg. Biochem.* **2012**, 116, 97.
67. Tan, S. S.; Al-Abbasi, A. A.; Mohamed Tahir, M. I.; Kassim, M. B. *Polyhedron* **2014**, 68, 287.
68. Thompson, H. W. *Nomenclature of Inorganic Chemistry*, Weedon, B. C.; International Union of Pure and Applied Chemistry, **1970**, 2nd edition, 75-81.
69. Cahn, R. S.; Ingold, C.; Prelog, V. *Angew. Chem. Intern.* **1966**, 5, 385.
70. Fay, C.; Piper, T. S. *Inorg. Chem.* **1963**, 85 (5), 500.
71. Mohamadou, A.; Déchamps-Olivier, I.; Barbier, J. P. *Polyhedron* **1994**, 13, 1363.
72. Déchamps-Olivier, I.; Guillon, E.; Mohamadou, A.; Barbier, J. P. *Polyhedron* **1996**, 15 (20), 3617.
73. Campo, R. Del; Criado, J. J.; Gheorghe, R.; González, F. J.; Hermosa, M. R.; Sanz, F.; Manzano, J. L.; Monte, E.; Rodríguez-Fernández, E. *J. Inorg. Biochem.* **2004**, 98 (8), 1307.
74. Juranic, N.; Hoyer, E.; Dietze, F.; Beyer, L. *Inorg. Chim. Acta.* **1989**, 162, 161.
75. Annual reports on NMR Spectroscopy, Webb, G. A., Academic Press: New York, **1980**, Vol. 10, 29.
76. Kidd, R. G.; Goodfellow, R. J. *NMR and the Periodic Table*, Harris, R. K., Mann, B. E., Academic Press: New York, **1978**, Chapter 8, 225-244.
77. Kopfermann, H.; Rasmussen, E. *Naturwiss.* **1934**, 22, 291.
78. More, K. R. *Phys. Rev.* **1935**, 47, 256.
79. Kanakubo, M.; Uda, T. Ikeuchi, H.; Satô, G. P. *J. Solution Chem.* **1998**, 27 (7), 645.
80. Ajam, M. *M.Sc. Thesis*, University of Johannesburg, **2005**.
81. Schneider, V. Frolich, P. K. *Ind. Eng. Chem.* **1931**, 23, 1405-1410.
82. Banks, R. L.; Bailey, G. C. *Ind. Eng. Chem. Prod. Res. Dev.* **1964**, 3, 170-173.
83. Calderon, N.; Chen, H. Y.; Scott, K. W. *Tetrahedron* **1967**, 34, 3327-3329.
84. Chauvin, Y.; Herisson, J. L. *Makromol. Chem.* **1971**, 141, 161-176.
85. Ahlberg, P. *Development metathesis method Org. Synth. Adv. Inf. Nobel Prize Chem. 2005*, R. Swedish Acad. Sci. Stock. 2005; http://nobelprize.org/nobel_prizes/chemistry/laureates/2005/chemad **2005**, No. October, 1.
86. Lockhart, J. C.; Mossop, W. J. *J. Chem. Soc. Dalton Trans.* **1973**, 19.
87. Lockhart, J. C.; Mossop, W. J. *J. Chem. Soc. Dalton Trans.* **1973**, 662.
88. Moriyasu, M.; Hashimoto, Y. *Bull. Chem. Soc. Jpn.* **1980**, 53, 3590-3595.
89. Ohya, T.; Iwamoto, K.; Sato, M. *J. Chem. Soc. Dalton Trans.* **1985**, 987.
90. Olk, R.; Dietzsch, W.; Kahlmeier, J.; Jörcchel, P.; Kirmse, R.; Sieler, J. *Inorg. Chim. Acta.* **1997**, 254, 375.
91. Yordanov, N. D.; Dimitrova, A. *Inorg. Chem. Commun.* **2005**, 8 (1), 113.
92. van der Molen, L. *M.Sc. Thesis*, University of Stellenbosch, **2008**.
93. Davison, A.; McCleverty, A.; Shawl, E. T.; Wharton, E. J. *J. Am. Chem. Soc.* **1967**, 830.
94. Balch, A. L. *Inorg. Chem.* **1971**, 10, 388.

References

95. Huber, J. F. L.; Kraak, J. C. *Anal. Chem.* **1972**, 44 (9), 1554-1559.
96. Liška, O.; Guiochon, G.; Colin, H. *J. Chromatogr.* **1979**, 171, 145.
97. Liška, O.; Lehotay, J.; Brandšteterová, E.; Guiochon, G. *J. Chromatogr.* **1979**, 171, 153.
98. Moriyasu, M.; Hashimoto, Y. *Chem. Lett.* **1980**, 117-120.
99. Uden, P. C.; Wang, T. *J. Anal. Atom. Spectr.* **1988**, 3, 919.
100. Wang, T.; Uden, P. C. *J. Chromatogr.* **1990**, 517, 185.
101. Ellis, P.; Wilkins, R. G.; Williams, M. J. G. *J.* **1957**, 4456-4461.
102. Lehotay, J.; Liška, O.; Brandšteterová, E.; Guiochon, G. *J. Chromatogr.* **1979**, 172, 379.
103. Cardwell, T. J.; Caridi, D. *J. Chromatogr.* **1984**, 288, 357-364.
104. Cardwell, T. J.; Caridi, D.; Ming, S. L. *J. Chromatogr.* **1986**, 351, 331-336.
105. Douglass, I. B.; Dains, F. B. *J. Am. Chem. Soc.* **1934**, 56, 719.
106. March, J. *Advanced organic chemistry*, John Wiley and Sons, United States and Canada, **1992**, 4th edition, p. 429.
107. Stewart, W. E.; Siddall, T. H. III, *Chem. Rev.* **1970**, 70, 517.
108. Wiberg, K. B.; Rablen, P. R.; Rush, D. J.; Keith, T. A. *J. Am. Chem. Soc.* **1995**, 117, 4261.
109. Laidig, K. E.; Cameron, L. M. *J. Am. Chem. Soc.* **1996**, 118, 1737.
110. Lauvergnat, D.; Hiberty, P. C. *J. Am. Chem. Soc.* **1997**, 119, 9478.
111. Crawford, S. M. N.; Taha, A. N.; True, N. S.; LeMaster, C. B. *J. Phys. Chem. A.* **1997**, 101, 4699.
112. Nair, P. M.; Roberts; J. D. *J. Am. Chem. Soc.* **1957**, 79, 4565.
113. Harris, R. K.; Becker, E. D.; Cabral de Menezes, S. M.; Goodfellow, R.; Granger, P. *J. Pure Appl. Chem.* **2001**, 73 (11), 1795.
114. Martin, T. H.; Fung, B. M. *J. Phys. Chem.* **1973**, 77, 637.
115. Ader, R.; Loewenstein, A. *J. Magn. Reson.* **1971**, 5, 248.
116. Proctor, W. G.; Yu, F. C. *Phys. Rev.* **1951**, 81 (1), 20.
117. Freeman, R.; Murray, G. R.; Richards, R. E. *Proc. Roy. Soc.* **1957**, A242, 455.
118. Griffith, J. S.; Orgel, L. E. *Trans. Faraday Soc.* **1957**, 53, 601.
119. Benedek, G. B.; Englman, R.; Armstrong, J. A. *J. Chem. Phys.* **1963**, 39, 3349.
120. Jameson, C. J.; Rehder, D.; Hoch, M. *J. Am. Chem. Soc.* **1987**, 109, 2589.
121. Kanakubo, M.; Uda, T.; Ikeuchi, H.; Satô, G. P. *J. Sol. Chem.* **1998**, 27(7), 645.
122. Gillies, D. G.; Sutcliffe, L. H.; Williams, A. J. *Magn. Reson. Chem.* **2002**, 40 (1), 57.
123. Levy, G. C.; Bailey J. T.; Wright, D. A. *J. Magn. Reson.* **1980**, 37, 353.
124. Juranic, N. *Coord. Chem. Rev.* **1989**, 96, 253.

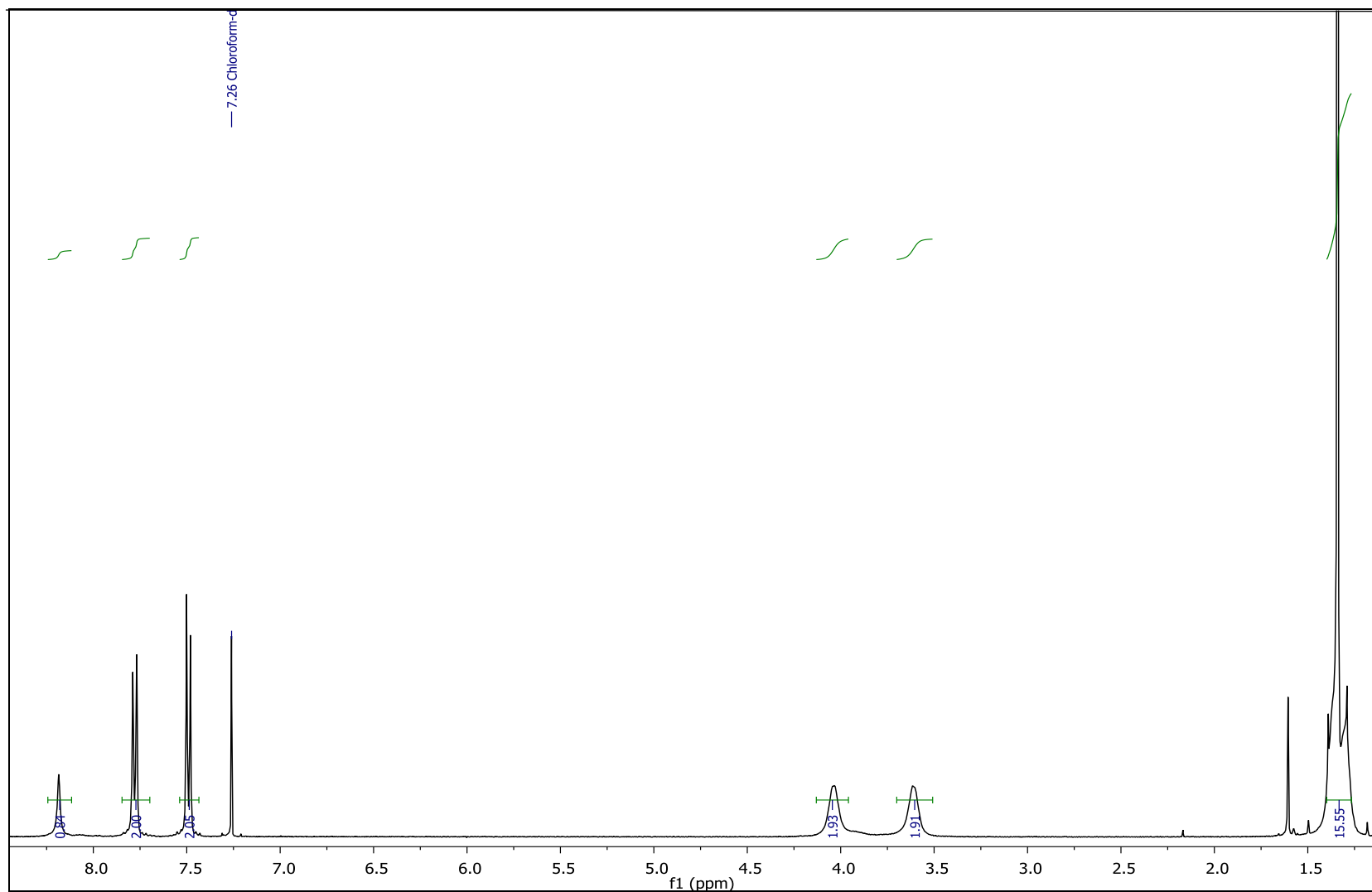
Addendum A | ^1H spectra of selected ligands and complexes

Figure 1. ^1H Spectrum of *N,N*-diethyl-*N'*-4-*tert*butylbenzoylthiourea

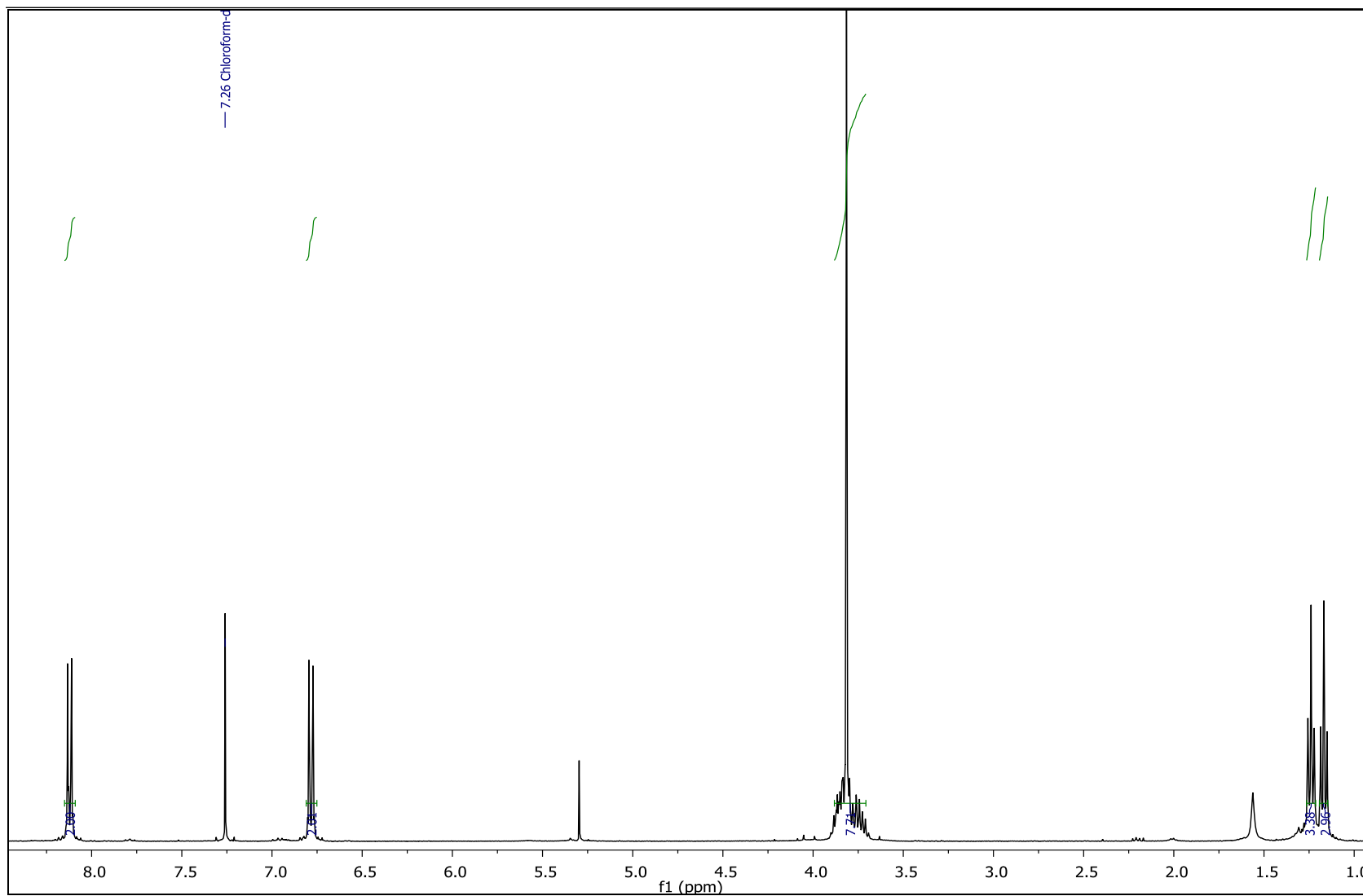
Addendum A | ^1H spectra of selected ligands and complexes

Figure 3. ^1H Spectrum of *fac*-tris(*N,N*-diethyl-*N'*-4-methoxybenzoylthioureato)cobalt(III)

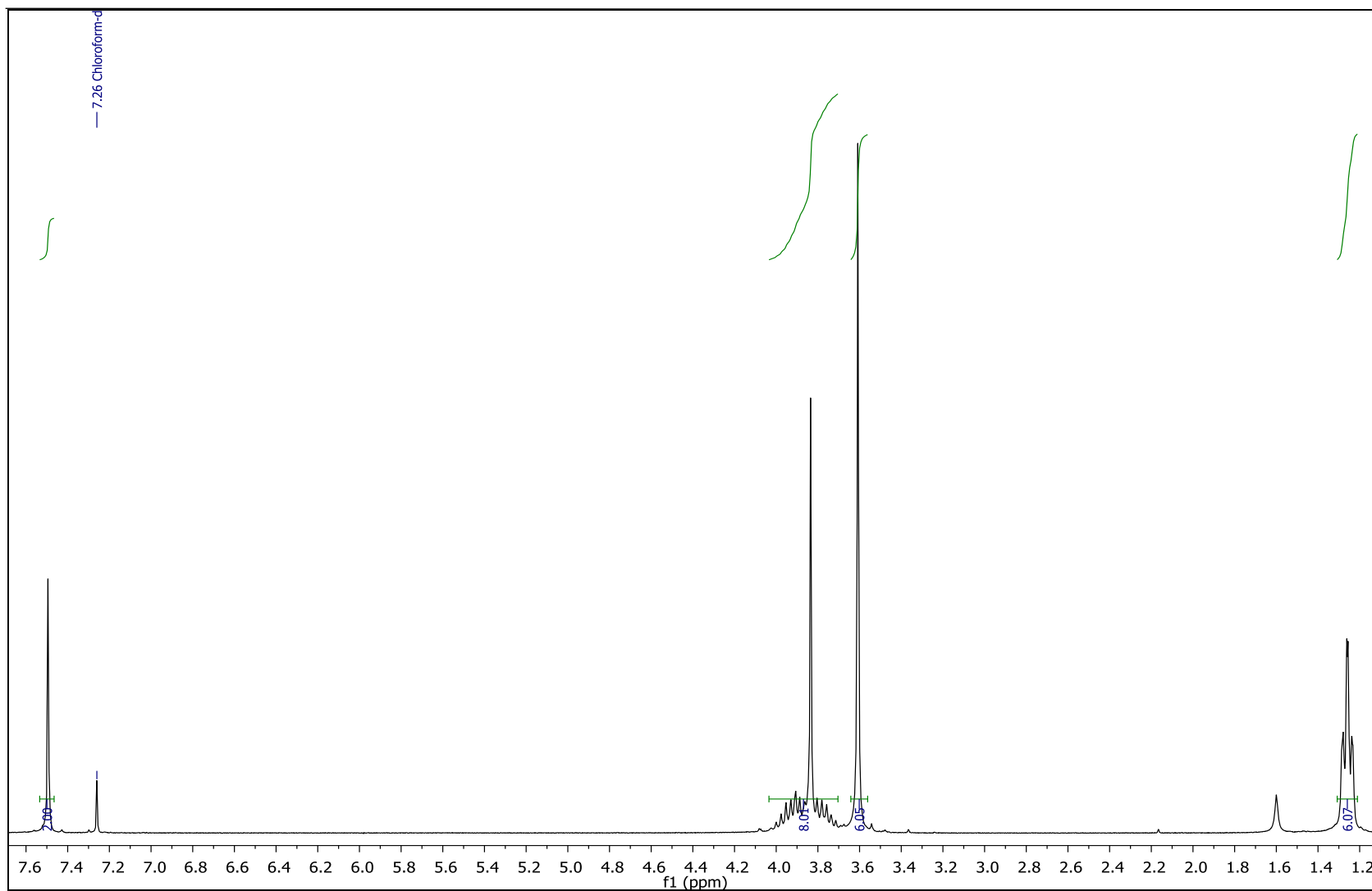
Addendum A | ^1H spectra of selected ligands and complexes

Figure 4. ^1H Spectrum of *fac*-tris(*N,N*-diethyl-*N'*-3,4,5-trimethoxybenzoylthioureato)cobalt(III)

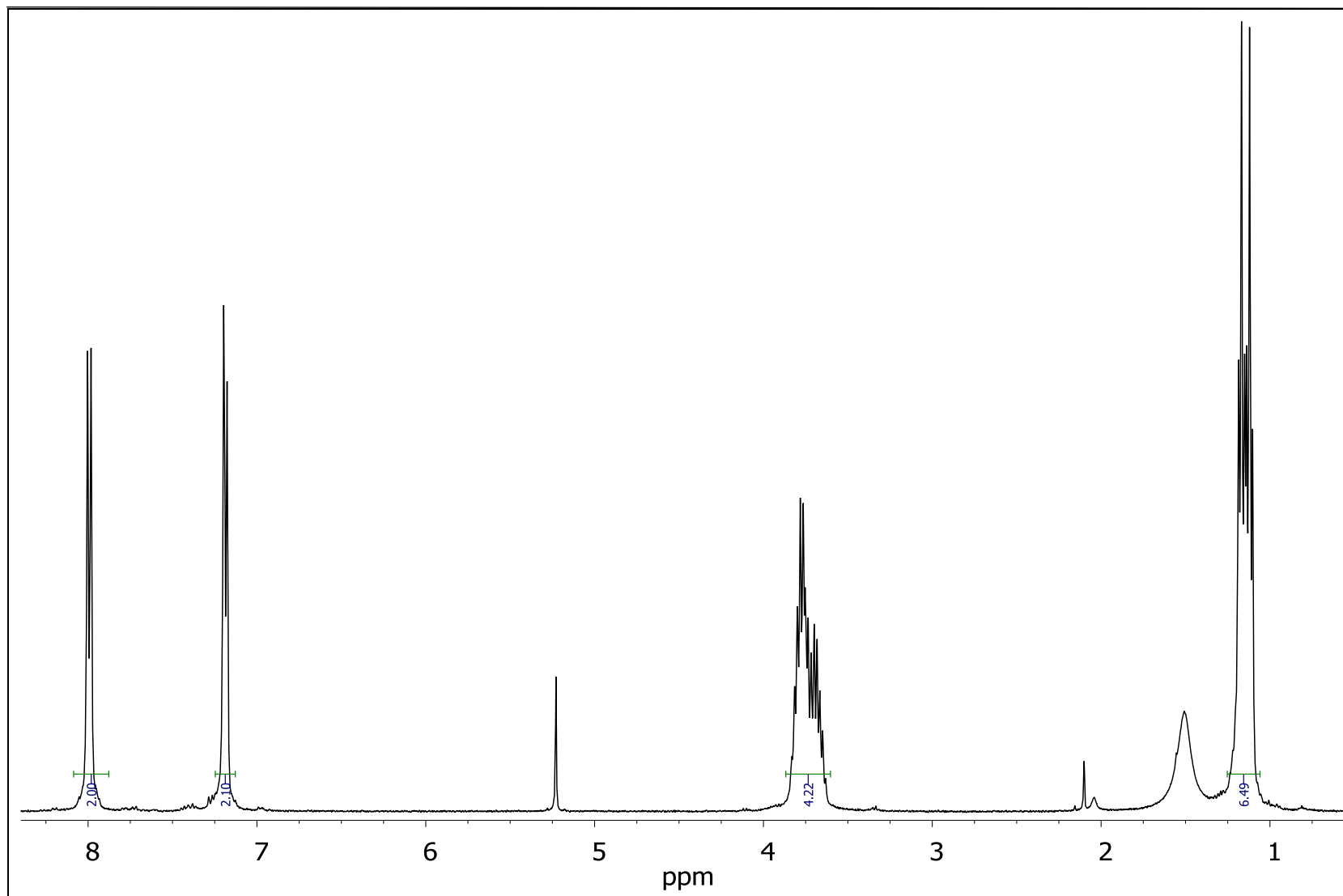
Addendum A | ^1H spectra of selected ligands and complexes

Figure 5. ^1H Spectrum of *fac*-tris(*N,N*-diethyl-*N'*-4-chlorobenzoylthioureato)cobalt(III)

Addendum A | ^1H spectra of selected ligands and complexes

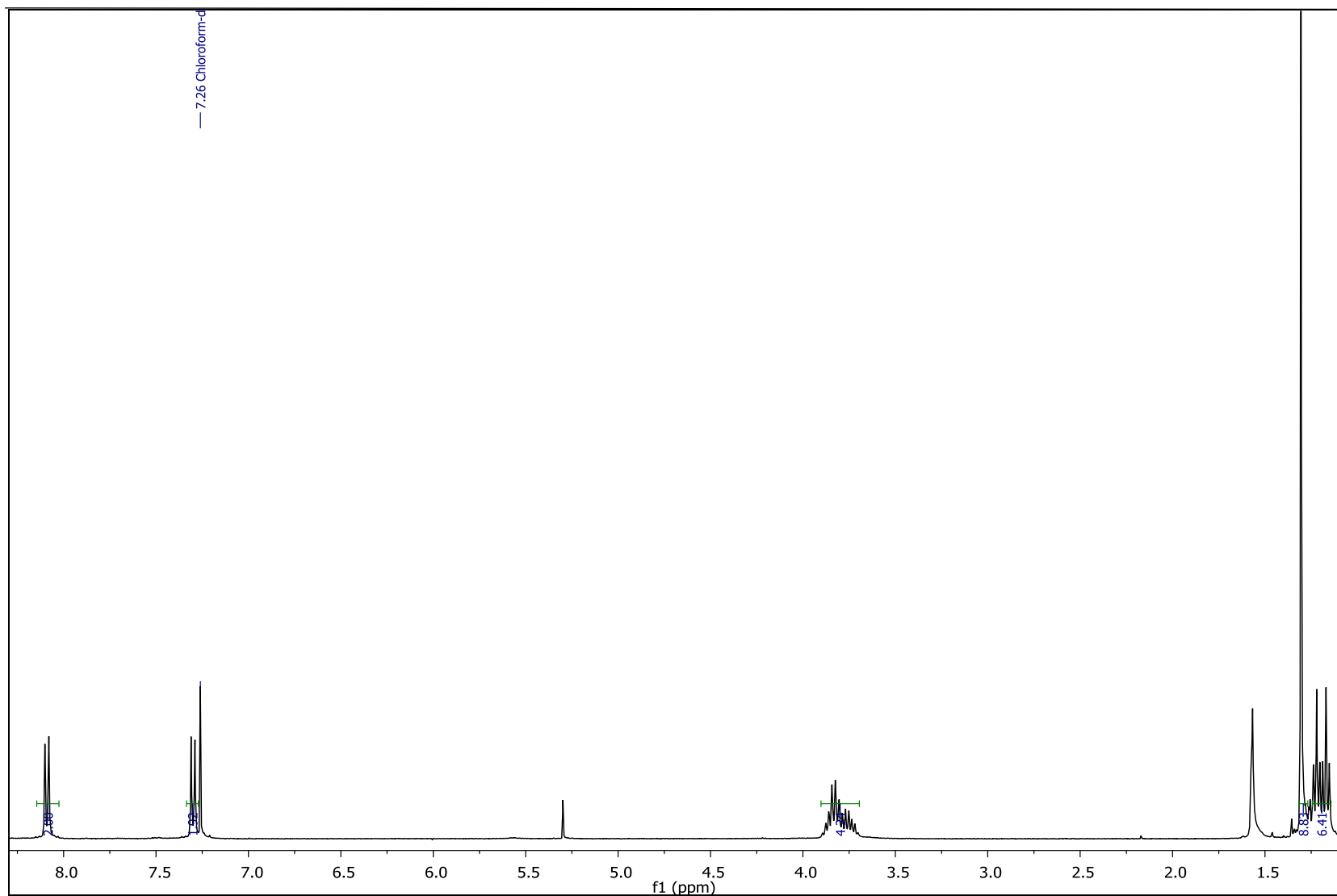
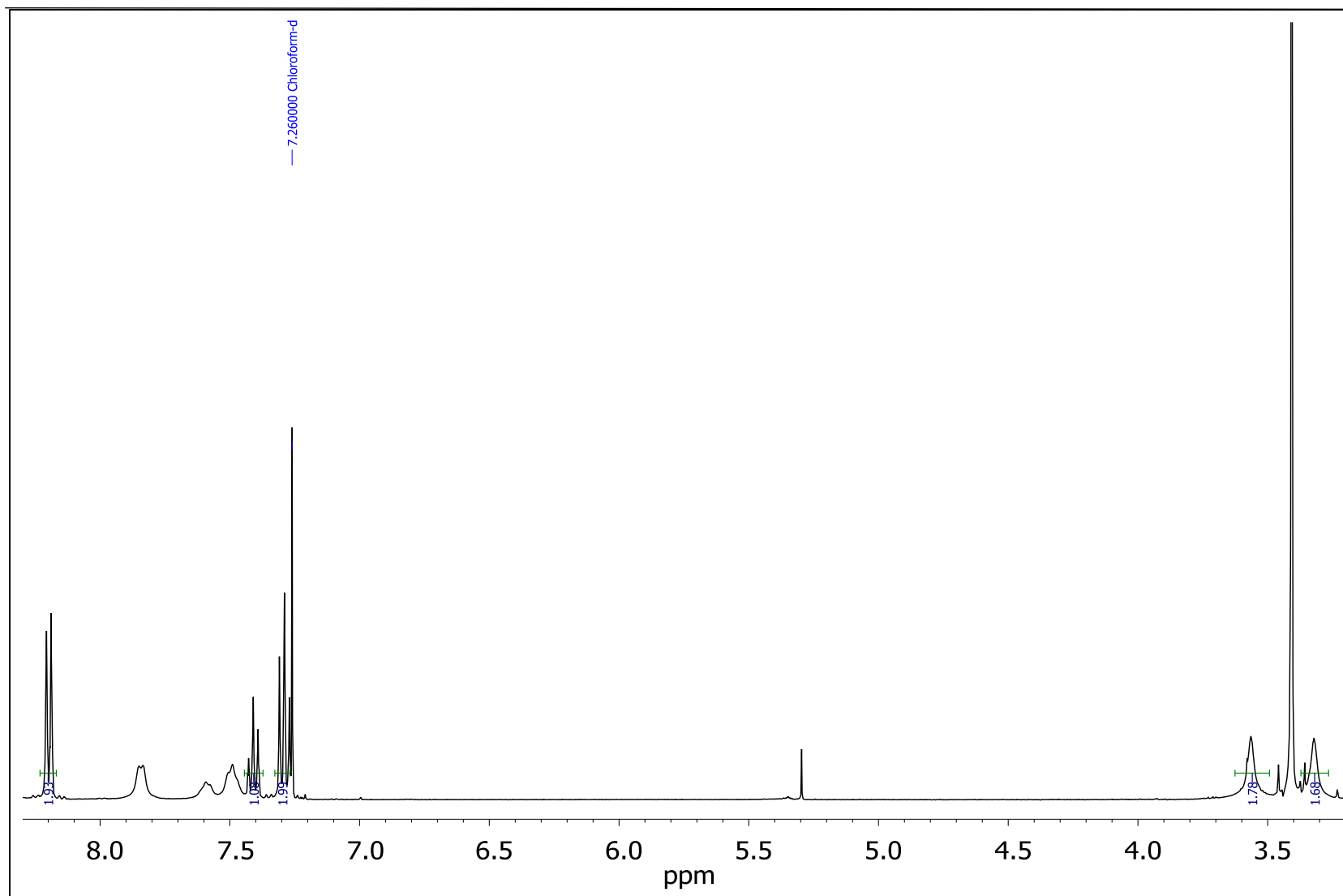


Figure 6. ^1H Spectrum of *fac*-tris(*N,N*-diethyl-*N'*-4-*tert*butylbenzoylthioureato)cobalt(III)

Addendum A | ^1H spectra of selected ligands and complexes**Figure 7.** ^1H Spectrum of *fac*-tris(*N,N*-dimethyl-*N'*-benzoylthioureato)cobalt(III)

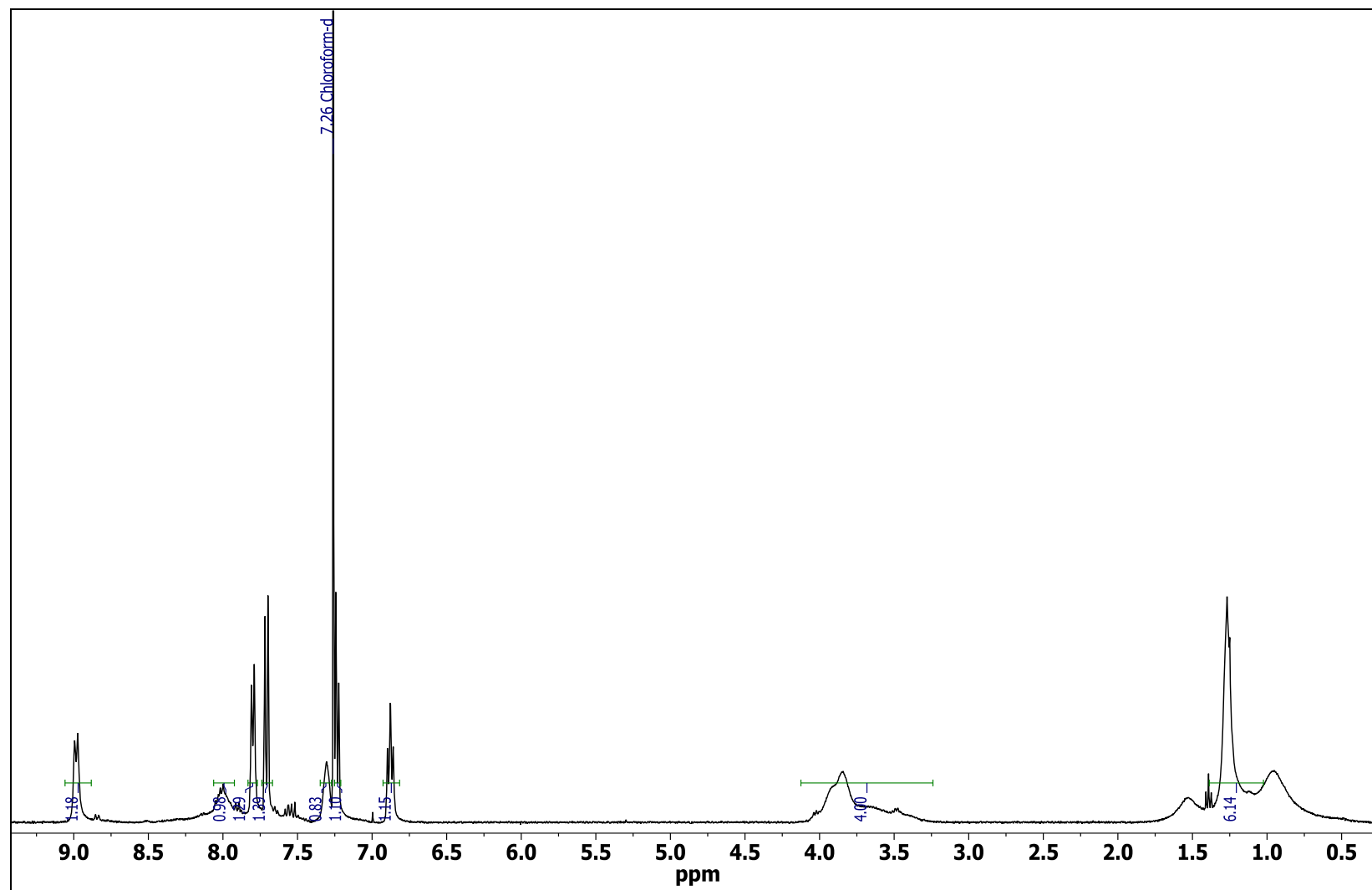
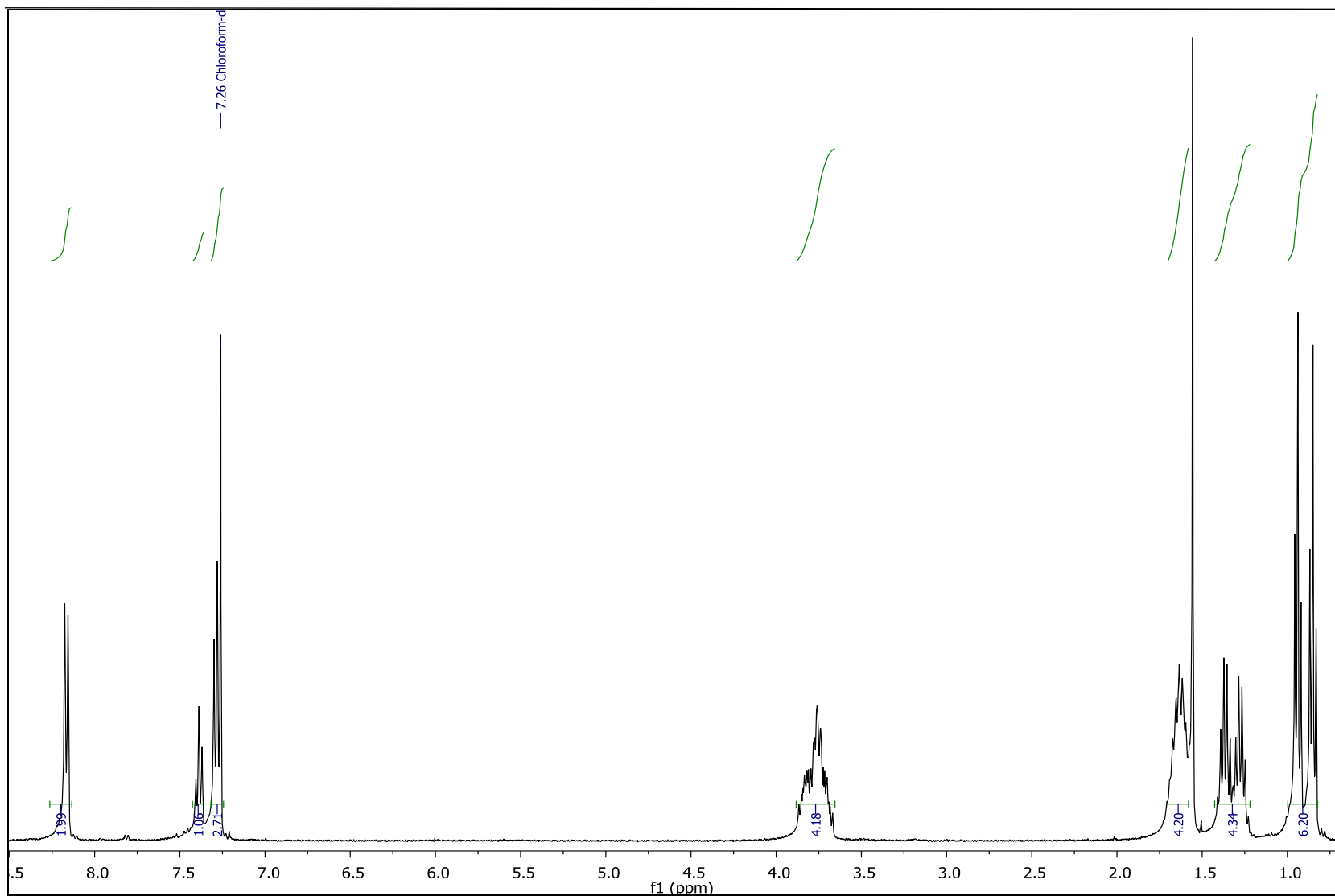
Addendum A | ^1H spectra of selected ligands and complexes

Figure 8. ^1H Spectrum of *fac*-tris(*N,N*-diethyl-*N'*-naphthoylthioureato)cobalt(III)

Addendum A | ^1H spectra of selected ligands and complexes**Figure 9.** ^1H Spectrum of *fac*-tris(*N,N*-dibutyl-*N'*-benzoylthioureato)cobalt(III)

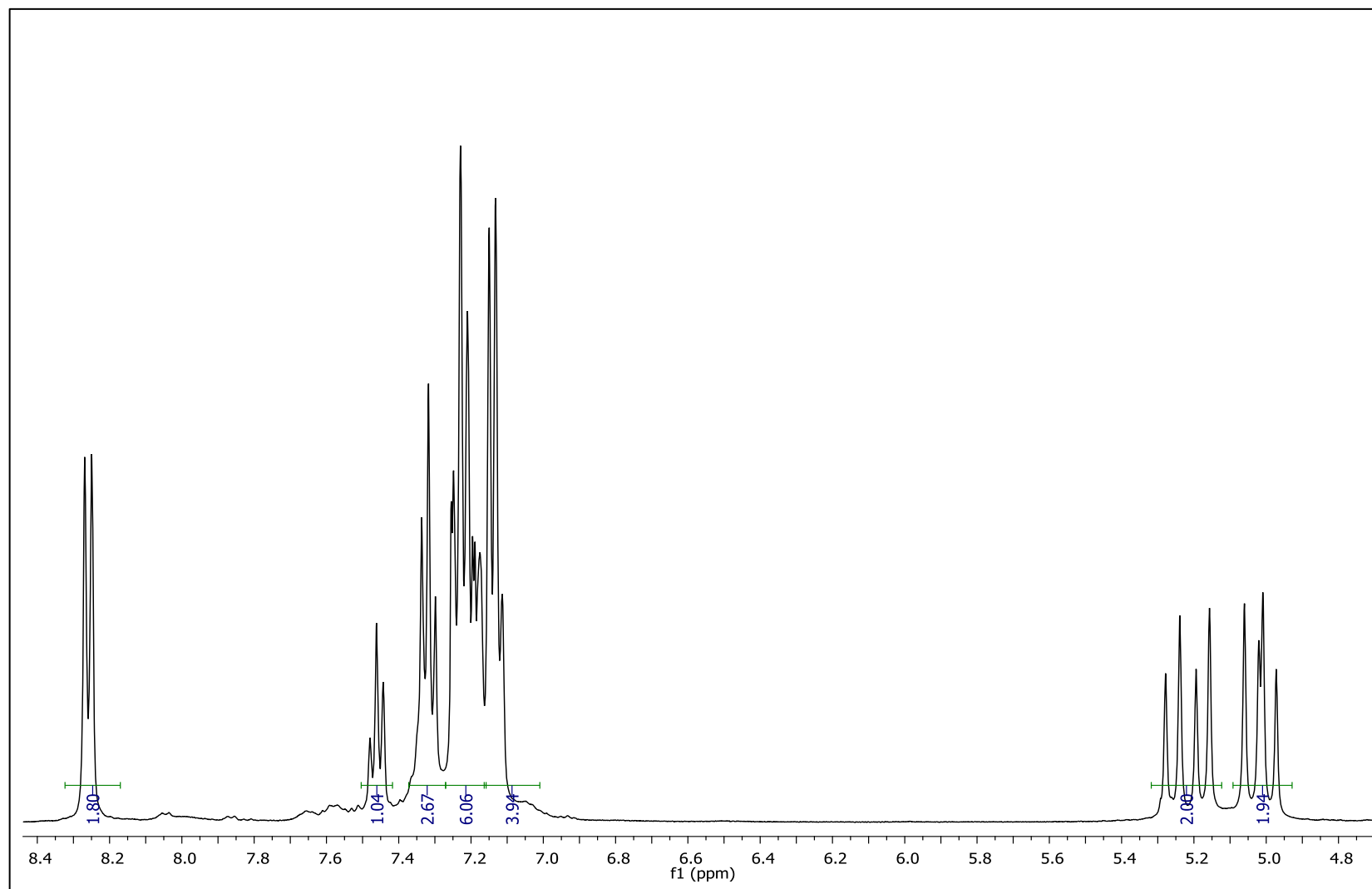
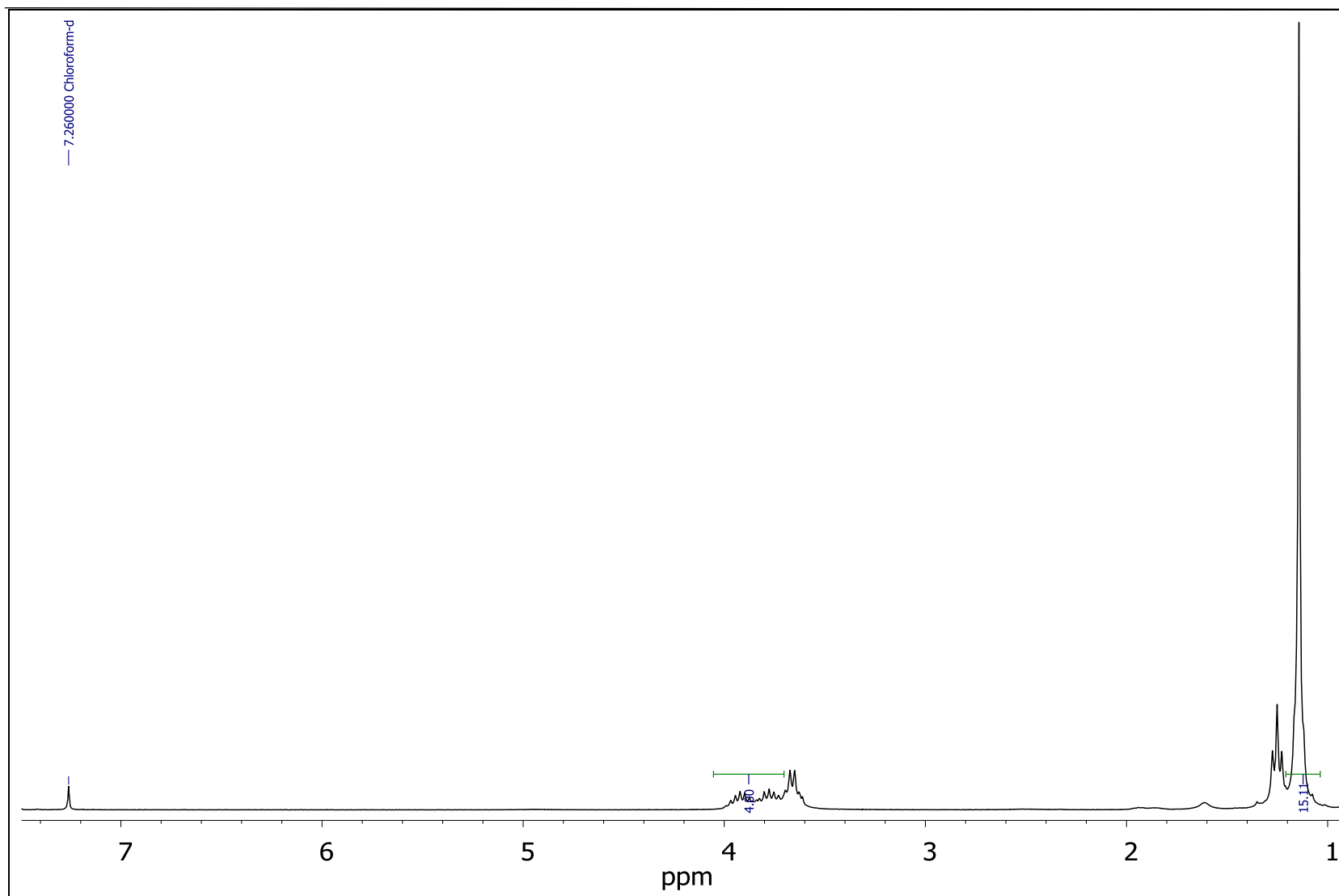
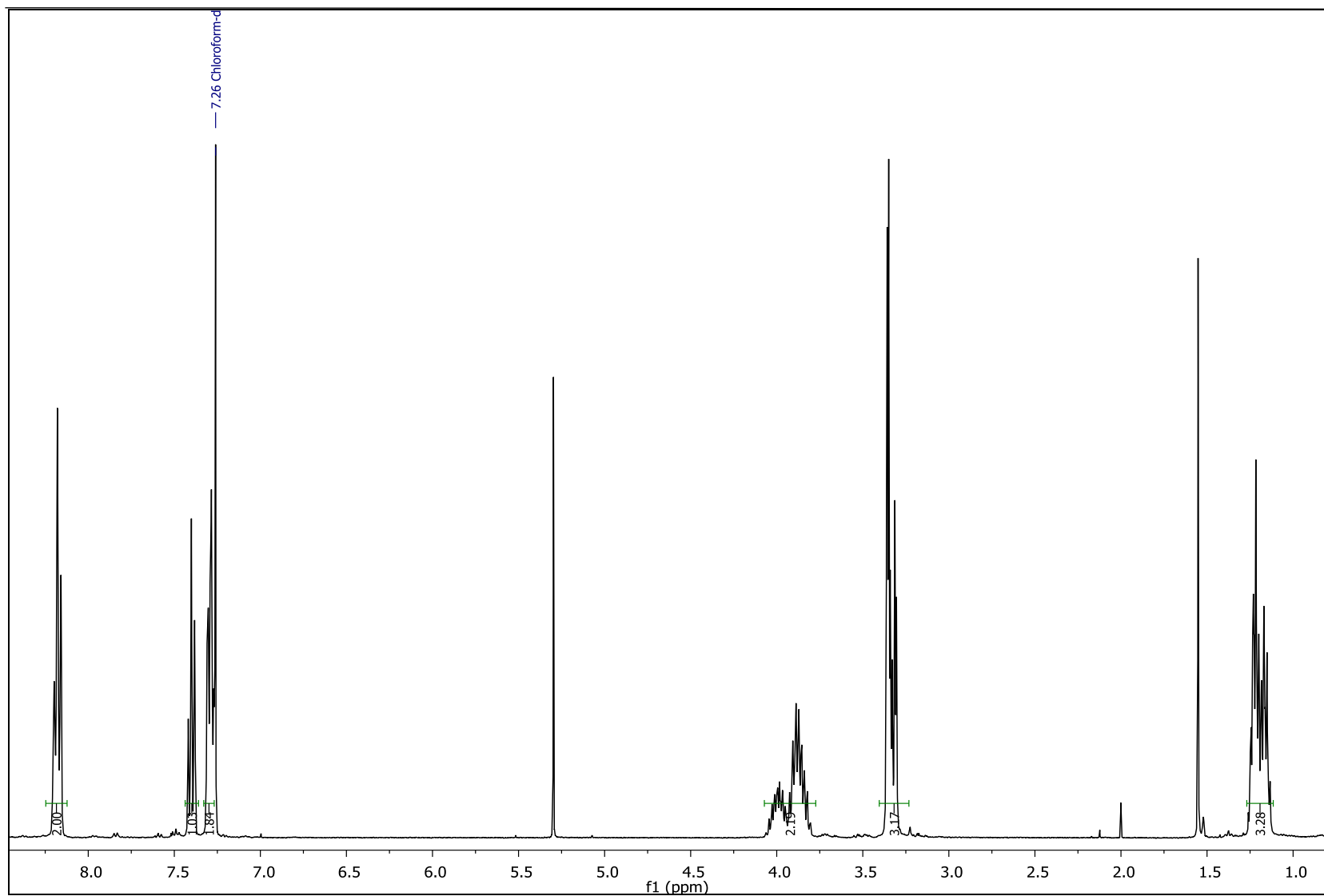
Addendum A | ^1H spectra of selected ligands and complexes

Figure 10. ^1H Spectrum of *fac*-tris(*N,N*-dimethylphenyl-*N'*-benzoylthioureato)cobalt(III)

Addendum A | ^1H spectra of selected ligands and complexes**Figure 11.** ^1H Spectrum of *fac*-tris(*N,N*-diethyl-*N'*-pivaloylthioureato)cobalt(III)

Addendum A | ^1H spectra of selected ligands and complexes**Figure 12.** ^1H Spectrum of *fac*-tris(*N*-methyl-*N*-ethyl-*N'*-benzoylthioureato)cobalt(III)

Addendum B | Bond lengths and angles

Table 1: Bond lengths of *fac*-tris(*N,N*-diethyl-*N'*-4-methoxybenzoylthioureato) cobalt(III) in Å

Number	Atom1	Atom2	Length
1	CO1	S2	2.2164
2	CO1	O1	1.9224
3	CO1	S2	2.2164
4	CO1	O1	1.9224
5	CO1	S2	2.2164
6	CO1	O1	1.9224
7	S2	C15	1.7414
8	O1	C4	1.2641
9	N3	C15	1.3423
10	N3	C4	1.3293
11	N4	C15	1.3414
12	S2	C15	1.7414
13	O1	C4	1.2641
14	N3	C15	1.3423
15	N3	C4	1.3293
16	N4	C15	1.3414
17	N4	C12	1.4655
17	S2	C15	1.7414
18	O1	C4	1.2641
19	N3	C15	1.3423
20	N3	C4	1.3293
21	N4	C15	1.3414
22	N4	C12	1.4655

Table 2: Bond angles of *fac*-tris(*N,N*-diethyl-*N'*-4-methoxybenzoylthioureato) cobalt(III) in degrees

Number	Atom1	Atom2	Atom3	Angle
1	S2	CO1	O1	95.27
2	S2	CO1	S2	88.14
3	S2	CO1	O1	92.1
4	S2	CO1	S2	88.14
5	S2	CO1	O1	176.59
6	O1	CO1	S2	176.59
7	O1	CO1	O1	84.49
8	O1	CO1	S2	92.1
9	O1	CO1	O1	84.49
10	S2	CO1	O1	95.27

Addendum B | Bond lengths and angles

11	S2	CO1	S2	88.14
12	S2	CO1	O1	92.1
13	O1	CO1	S2	176.59
14	O1	CO1	O1	84.49
15	S2	CO1	O1	95.27

Table 3: Bond lengths of *fac*-tris(*N*-methyl-*N*-ethyl-*N'*-benzoylthioureato)cobalt(III) in Å

Number	Atom1	Atom2	Length
1	CO1	S2	2.1949
2	CO1	O1	1.9238
3	CO1	S2	2.1949
4	CO1	O1	1.9238
5	CO1	S2	2.1948
6	CO1	O1	1.9238
7	S2	C2	1.6867
8	O1	C1	1.3889
9	C1	N1	1.4006
10	C2	N3	1.4493
11	C2	N1	1.3090
12	S2	C2	1.6867
13	O1	C1	1.2296
14	C1	N1	1.3473
15	C2	N3	1.3739
16	C2	N1	1.309
17	S2	C2	1.6867
18	O1	C1	1.2296
19	C1	N1	1.3473
20	C2	N3	1.3739
21	C2	N1	1.309

Addendum B | Bond lengths and angles

Table 4: Bond angles of *fac*-tris(*N*-methyl-*N*-ethyl-*N'*-benzoylthioureato)cobalt(III) in degrees

Number	Atom1	Atom2	Atom3	Angle
1	S2	CO1	O1	93.91
2	S2	CO1	S2	87.79
3	S2	CO1	O1	92.9
4	S2	CO1	S2	87.79
5	S2	CO1	O1	178.19
6	O1	CO1	S2	178.19
7	O1	CO1	O1	85.38
8	O1	CO1	S2	92.9
9	O1	CO1	O1	85.38
10	S2	CO1	O1	93.91
11	S2	CO1	S2	87.79
12	S2	CO1	O1	92.9
13	O1	CO1	S2	178.19
14	O1	CO1	O1	85.38
15	S2	CO1	O1	93.91

Table 5: Bond lengths of *fac*-tris(*N,N*-diethyl-*N'*-camphanoylthioureato)cobalt(III) in Å

Number	Atom1	Atom2	Length
1	CO1	S3	2.2165
2	CO1	S2	2.2017
3	CO1	S6	2.2115
4	CO1	O4	1.9001
5	CO1	O6	1.9079
6	CO1	O8	1.9022
7	S3	C4	1.7179
8	S2	C2	1.7194
9	S6	C6	1.7178
10	O4	C1	1.2566
11	O6	C3	1.2608
12	O8	C5	1.2667
13	N13	C1	1.3335
14	N13	C2	1.353
15	N15	C2	1.3441
16	N16	C4	1.3493
17	N16	C3	1.3315
18	N17	C6	1.3524
19	N17	C5	1.3102
20	C4	N54	1.3413
21	C6	N64	1.332

Addendum B | Bond lengths and angles

22	CO2	S4	2.2103
23	CO2	S5	2.2088
24	CO2	S1	2.2255
25	CO2	O5	1.8974
26	CO2	O7	1.9197
27	CO2	O9	1.9147
28	S4	C39	1.7306
29	S5	C63	1.7384
30	S1	C26	1.7372
31	O5	C45	1.2804
32	O7	C31	1.2632
33	O9	C65	1.2577
34	N10	C26	1.3511
35	N10	C31	1.3158
36	N11	C39	1.3523
37	N11	C45	1.3083
38	N20	C39	1.326
39	N21	C63	1.3373
40	N21	C65	1.3104
41	C26	N52	1.353

Table 6: Bond angles of *fac*-tris(*N,N*-diethyl-*N'*-camphanoylthioureato)cobalt(III) in degrees

Number	Atom1	Atom2	Atom3	Angle
1	S3	CO1	S2	88.37
2	S3	CO1	S6	91.24
3	S3	CO1	O4	174.8
4	S3	CO1	O6	95
5	S3	CO1	O8	88.91
6	S2	CO1	S6	88.32
7	S2	CO1	O4	96.81
8	S2	CO1	O6	89.81
9	S2	CO1	O8	175.5
10	S6	CO1	O4	89.39
11	S6	CO1	O6	173.43
12	S6	CO1	O8	95.33
13	O4	CO1	O6	84.58
14	O4	CO1	O8	85.89
15	O6	CO1	O8	86.85
16	S4	CO2	S5	87.29

Addendum B | Bond lengths and angles

17	S4	CO2	S1	88
18	S4	CO2	O5	95.43
19	S4	CO2	O7	90.74
20	S4	CO2	O9	177.53
21	S5	CO2	S1	89.05
22	S5	CO2	O5	91.55
23	S5	CO2	O7	175.26
24	S5	CO2	O9	95.07
25	S1	CO2	O5	176.54
26	S1	CO2	O7	95.19
27	S1	CO2	O9	91.3
28	O5	CO2	O7	84.35
29	O5	CO2	O9	85.26
30	O7	CO2	O9	86.97